Characterisation of Novel Cofactors in Myc-dependent Transcription Regulation

Dissertation

zur

Erlangung der naturwissenschaftlichen Doktorwürde
(Dr. sc. nat.)

vorgelegt der

Mathematisch-naturwissenschaftlichen Fakultät

der

Universität Zürich

von

Michael Furrer

von

Unterbäch VS

Promotionskomitee

Dr. Peter Gallant (Leitung der Dissertation)
Prof. Dr. Alex Hajnal (Vorsitz)
Prof. Dr. Konrad Basler
Prof. Dr. Bernhard Lüscher
Prof. Dr. Matthias Peter

Zürich, 2008

Table of contents

Abbreviations

>	FRT (abbreviation in genotype annotations, e.g. *ey>dm^{P0}*)
α	antibody against indicated protein
Δ	deletion
aa	amino acid
bHLHzip	basic helix-loop-helix leucine zipper
bp	base pairs
cDNA	complementary DNA
DNA	deoxyribonucleic acid
dsRNA	double stranded RNA
flp	flipase
FRT	flipase recombination target
GFP	green fluorescent protein
GST	glutathione-S-transferase
HA	hemagglutinin
HAT	histone acetyltransferase
HDAC	histone deacetylase
HMT	histone methyltransferase
IP	immunoprecipitation
IVT	*in vitro* translation
kb	kilo base pairs
kDa	kilo Dalton
mRNA	messenger RNA
nt	nucleotide
ORF	open reading frame
PCR	polymerase chain reaction
qRTPCR	quantitative real-time PCR
RNA	ribonucleic acid
RNA*i*	RNA interference
RNAP I, II & III	RNA polymerase I, II & III
RT	reverse transcription
UAS	upstream activating sequence
WB	Western blot

Zusammenfassung

Die Myc Proto-Onkogene sind Transkriptionsfaktoren, die eine wichtige Rolle in unterschiedlichen zellulären Prozessen spielen. Mutationen in Myc-Genen, oder deren Fehlregulierung, können zur Entstehung verschiedenster Krebsarten beitragen. Besonders wichtig sind die Myc-Proteine für die Kontrolle des Wachstums auf zellulärer und organismischer Ebene. Im Gegensatz zu Säugetieren besitzt *Drosophila* nur ein Myc-Ortholog. Die Funktionen, welche die Myc-Proteine in der Zelle übernehmen, sind zumindest teilweise konserviert. *Drosophila* Myc ist in Säugerzellen teilweise funktionell, und umgekehrt kann menschliches c-Myc letale Myc-Mutationen in der Fruchtfliege retten. Das Verständnis über die molekularen Mechanismen, durch welche Myc die Expression seiner Zielgene kontrolliert ist in den letzen Jahren stark angewachsen, und etliche neue Myc-Cofaktoren sind entdeckt worden. Überraschenderweise ist jedoch wenig über die physiologische Relevanz von Myc-Cofaktoren bekannt.

In dieser Arbeit wird die Entwicklung und die Durchführung eines Myc-abhängigen RNA-Interferenz-Screens beschrieben. Mithilfe dieses Systems konnten wir mehrere bis anhin unbekannte Myc-Cofaktoren identifizieren. Zudem beschreiben wir die genauere Analyse zweier Gruppen dieser identifizierten Myc-Interaktoren. Dabei handelt sich einerseits um den PAF-Komplex und andererseits um das Protein HCF. Der RNA Polymerase II-associated factor1 (PAF) Komplex wurde in Hefe als Transkriptions-Elongationsfaktor identifiziert. Im hier beschriebenen RNA-Interferenz-Screen erwiesen sich drei Komponenten des PAF-Komplexes als Repressoren des Myc-abhängigen Reportersystems. *In vivo* Experimente haben hingegen gezeigt, dass einige PAF-Komplexkomponenten auch aktivierende Funktionen im Zusammenhang mit Myc haben. Zwischen den PAF-Komplexkomponenten Atms, Atu und Rtf1 und Myc besteht eine genetische Interaktion, und eine Reduktion der Proteinmenge dieser Komponenten führt zu verringertem Wachstumspotential in verschiedenen Geweben. Wir stellten auch fest, dass der PAF-Komplex für die korrekte Expression von Myc-Zielgenen benötigt wird und dass er mittels seiner Untereinheit Atu direkt an Myc bindet.

Im Gegensatz zum PAF-Komplex, wurde im Screen das Protein Host cell factor (HCF) als Aktivator identifiziert. Wir konnten zeigen, dass HCF zusammen mit Myc im *Drosophila*-Auge wachstumsfördernd wirkt. Myc-Überexpression in Flügeln führt zu erhöhtem Wachstum und verursacht verschiedenste Defekte. Eine Reduktion der HCF-Menge in Flügeln hemmt die Entstehung solcher Myc-Überexpressionsdefekte, was dafür spricht, dass Myc HCF benötigt, um seine volle Aktivität zu erreichen. Ein weiteres Indiz für diese Annahme lieferten qRTPCR-Messungen, die zeigten, dass HCF die Expression von Myc-Zielgenen beeinflusst. Schliesslich stellten wir mittels Coimmunopräzipitationen aus Embryolysaten eine direkte Bindung zwischen Myc und HCF fest. Diese Daten zeigen schlüssig auf, dass es sich bei HCF um einen essentiellen Cofaktoren von Myc handelt, der zu dessen vollen Aktivität beiträgt. Bis anhin ist es jedoch unbekannt, wie diese Interaktion auf molekularer Basis abläuft. Mit dieser Arbeit konnten wir zeigen, dass sowohl der PAF-Komplex als auch HCF genetisch mit Myc interagieren und dass beide Faktoren direkt an Myc binden. Diese Resultate weisen sehr stark darauf hin, dass es sich bei beiden Faktoren um physiologisch wichtige Cofaktoren von Myc handelt.

Summary

The *myc* proto-oncogenes, which encode transcription factors of the bHLHzip superfamily, play an important role in a wide variety of cellular processes. Most prominent is their involvement in the control of cellular and organismal growth. In contrast to the situation in vertebrates, where several members of the Myc protein family are present, there is one sole *Drosophila* orthologue. *Drosophila* Myc and its human homologue c-Myc can partially substitute for each other in several assays. This suggests that the Myc functions between *Drosophila* and humans are conserved. In recent years, the knowledge of the molecular mechanisms how Myc regulates the expression of its many targets has been significantly expanded and a considerable number of putative cofactors involved in these processes have been identified; still the physiological relevance of these proteins is far less well understood.

In this study, we describe the setup and performance of a Myc-dependent RNA interference (RNA*i*) screen and we report the characterisation of novel Myc cofactors identified in the screen.

The generation of a reporter system that reliably monitors Myc activity made it possible to perform a screen for novel cofactors of Myc involved in transcription control. Using Myc-dependent luciferase reporters, we have identified the multisubunit PAF complex and HCF as potential Myc cofactors and have analysed them further. The RNA Polymerase II-associated factor1 (PAF) complex, which is required for several steps during transcription elongation, was identified as a repressor of the Myc-dependent reporter system. However, *in vivo* experiments have revealed that several PAF complex components exert coactivating functions. We could show that the PAF complex interacts genetically with Myc, since depletion of Atms, Atu and Rtf1 reduces the growth potential in a variety of tissues *in vivo*, especially in the presence of elevated Myc levels. Interestingly, we also found evidence that the PAF complex component Hyx acts as a repressor of Myc in some contexts. Furthermore, the PAF complex subunits Atu, Atms, Hyx and Rtf1 are required for the proper expression of RNA polymerase II-transcribed target genes of Myc. We also revealed a physical interaction between Myc and the PAF complex mediated by the direct binding of Myc to the Atu subunit of PAF.

The Host cell factor (HCF) was identified as an activator of the Myc-dependent reporter system. *In vivo* HCF synergises with Myc to promote growth in the eye. Conversely, depletion of HCF by RNA*i* potently reverts Myc overexpression phenotypes in the wing, and to a lesser extent also in the eye. Moreover, expression of Myc target genes in S2 cells is influenced by HCF. We could also show that the endogenous HCF and Myc proteins physically interact in *Drosophila* embryos. These data coherently indicate that Myc requires HCF to attain its full transcriptional activity. The molecular mechanism behind the Myc:HCF interaction remains to be elucidated. However, there is preliminary evidence for a possible involvement of Ash2-containing HMT complexes. Taken together, we present evidence that both the PAF complex and HCF genetically and physically interact with Myc, which identifies them as physiologically relevant cofactors of Myc.

Introduction

1. The proto-oncogene *myc*

myc is one of the most widely studied and medically relevant human proto-oncogenes. *myc* gene expression is estimated to be deregulated in 20% of all human cancers, resulting in elevated levels of Myc protein (Nesbit et al., 1999). Three decades ago, variants of the viral oncogene *v-myc* were isolated from four separate avian retroviruses (Sheiness et al., 1978). Several years later, it became clear that the *v-myc* variants were virally captured forms of the cellular homologue (*c-myc*) and were shown to confer the oncogenic potential to the myelocytomatosis virus (Vennstrom et al., 1982). The observation that retroviruses lacking oncogenes become tumorigenic when they integrate adjacent to the cellular *myc* locus (*c-myc*), and the discovery that Burkitt's lymphoma is caused by a chromosomal translocation of *c-myc* in B cells (Hollis et al., 1984) have further established *myc's* role as a potent oncogene. In humans *myc* is a multigene family including c-*myc* and two distinct paralogues that are frequently mutated in neuroblastomas and retinoblastomas (*N-myc*) (Kohl et al., 1983) and small cell lung carcinomas (*L-myc*) (Nau et al., 1985). In addition, there are two paralogues *S-myc* and *B-myc*, which so far have only been characterised in rodents. Both variants do not possess neoplastic potential (Henriksson and Luscher, 1996).

The *myc* genes encode transcription regulators of the basic region/helix-loop-helix/leucine zipper (bHLHzip) superfamily, which play an important role in the control of a variety of cell behaviours, including cellular growth, cell-cycle progression, metabolism, differentiation and apoptosis (reviewed in Dang et al., 2006). The importance of the *myc* genes in controlling cell growth and proliferation (amongst others), and their involvement in diverse cellular disorders, is demonstrated by the essentiality of *c-myc* and *N-myc* during development. A null mutation in *c-myc* leads to lethality of mouse zygotes after 10.5 days of gestation (Davis et al., 1993), *N-myc* null mutants die after 11.5 days (Sawai et al., 1991; Sawai et al., 1993), while *L-myc* mutants are fully viable (Hatton et al., 1996).

1.1. Biological functions of Myc

The expression of Myc is tightly controlled by the availability of growth factors, cytokines and mitogens (Kelly et al., 1983; Shibuya et al., 1992; Armelin et al., 1984). Consistent with its role as one of the classical "immediate early genes" Myc activity is required for cell cycle entry (Johnston et al., 1999; Amati, 1998). Ectopic expression of *c-myc* from a retroviral vector can drive quiescent cells into the cell cycle and has been shown to promote S phase entry and shorten G1 phase in cycling cells (Karn et al., 1989). Furthermore, the requirements for growth factors are reduced upon Myc overexpression and cell cycle exit is prevented (Sorrentino et al., 1986; Stern et al., 1986). Conversely, reduced Myc levels prevent quiescent cells from entering the cell cycle in the presence of mitogenic signals (Roussel et al., 1991; Barone and Courtneidge, 1995). Several cell cycle regulators, including cyclins D1, D2 and cdk4, were found to be direct targets of *myc* (Bouchard et al., 2001; Menssen and Hermeking, 2002). Moreover, Myc has been shown to collaborate with Ras in the accumulation of active cyclin E/cdk2 and E2F, therefore inducing cell-cycle entry (Leone et al., 1997). Not only the induction of cell cycle promoting genes, but also suppression of inhibitory factors, contribute to Myc's

activating role of the cell cycle. Both CDK inhibitors *p21CIP* and *p15INK4B* are repressed by Myc (Staller et al., 2001; Wu et al., 2003).

Overexpression of c-Myc in the absence of survival factors does not only promote proliferation, but also leads to both ARF-Mdm2-p53-pathway-dependent and p53-independent apoptosis (reviewed in Meyer et al., 2006; Askew et al., 1991; Evan et al., 1992; Zindy et al., 1998). This observation initially stood in marked contrast to the view of *myc's* role as an oncogene. However, other oncogenes such as *E1A* and *E2F1* were identified to induce apoptosis in a similar manner. The recent view states that in addition to mutations in oncogenes, pro-apoptotic pathways must be disabled in order to promote transformation (Nilsson and Cleveland, 2003). In addition to inducing apoptosis, Myc overexpression was shown to prevent terminal differentiation. Consistently, endogenous *myc* expression decreases rapidly during the terminal differentiation of many cell types (Freytag, 1988; Henriksson and Luscher, 1996).

Myc not only regulates proliferation but also heavily impacts on cell growth (accumulation of cell mass). It has been shown, both in murine and human cell lines, that overexpressed Myc induces cell growth independently of the cell cycle phase and that this increased growth correlates with higher protein synthesis rates (Schuhmacher et al., 1999; Iritani and Eisenman, 1999). Also in *Drosophila* Myc plays a crucial role in the regulation of cell growth, since growth is accelerated and cell size is inreased upon overexpression of Myc (Johnston et al., 1999). Conversely, partial loss of Myc function (as in the hypomorphic *myc* mutation dm^{P0}) results in a prolongation of G1 phase and a substantial reduction of cellular size, irrespective of the cell cycle phase (Johnston et al., 1999). In accordance with the observation that Myc drives protein synthesis, transcriptome profiling techniques (such as SAGE and microarrays) identified a considerable number of genes involved in ribosome biosynthesis and protein biosynthesis as direct target genes of Myc (Boon et al., 2001; Hulf et al., 2005; Zeller et al., 2003). Myc's role as an important integrator of cell growth became even more apparent when it was found not only to regulate RNA polymerase II-transcribed protein-coding genes. In mammals and *Drosophila* Myc controls both the transcription of RNA polymerase III-dependent small RNA genes (Steiger et al., 2008; Gomez-Roman et al., 2003) and of polymerase I-dependent ribosomal RNA (Grandori et al., 2005; Grewal et al., 2005). Additionally to the broad influence on transcription, Myc is proposed to play a direct non-transcriptional role in the initiation of DNA replication. It has recently been shown that c-Myc interacts with the pre-replicative complex and localises to early sites of DNA synthesis (Dominguez-Sola et al., 2007). Moreover, Myc also influences DNA replication in *Drosophila*, as it was shown to drive endoreplication (Maines et al., 2004).

1.2. Molecular functions of Myc

Myc proteins belong to the basic region/helix-loop-helix/leucine zipper (bHLHzip) superfamily of transcription regulators. Analysis of the primary sequence and structure-function analysis of the c-Myc protein identified an N-terminal transactivation domain (TAD) (Kato et al., 1990), containing the two highly conserved motifs termed Myc Box 1 (MB1) and Myc Box 2 (MB2), and a C-terminally located bHLHzip domain. The bHLHzip mediates interaction with Myc's heterodimerisation partner, the small bHLHzip protein Max (Blackwood and Eisenman, 1991; Prendergast et al., 1991) and is required for DNA binding. Upon interaction with Max, Myc/Max heterodimers are able to bind to hexameric DNA sequences with the canonical sequence CACGTG, called E-Boxes (Blackwood and Eisenman, 1991). Additionally, non-canonical E-Box variants of the general sequence CANNTG are bound (Blackwell et al., 1993; Grandori et al., 1996). Binding of the Myc/Max heterodimers to E-Box sequences is required for the transactivation effects of Myc (Amati et al., 1992) and Max was thought to be an essential cofactor for all biological activities of Myc, including cell cycle progression, apoptotic and oncogenic effects (Amati et al., 1993a; Amati et al., 1993b). However, observations made in rat PC12 cells presented evidence for Max-independent functions of Myc, since overexpression of Myc induced apoptosis in the complete absence of Max (Wert et al., 2001). Such Max-independent functions of Myc were indeed demonstrated by Steiger et al., who could show that control of endoreplication and cell competition in *Drosophila* does not, or only partly, require the association with Max (Steiger et al., 2008).

The Myc N-terminus was found to function as a transcription regulation domain. More recent studies have provided insight how transactivation by Myc is mediated (reviewed in Cowling and Cole, 2006). Association of the transactivation domain with chromatin remodelling (nucleosome movement/displacement) and chromatin modifying (histone modification) factors was shown to be crucial for biological Myc activity. One factor that was found to bind to the Myc-Box 2 (MB2) sequence in the Myc N-terminus is TRRAP (Transformation/tRanscription Domain Associated Protein), whose function is required for Myc-mediated transformation (McMahon et al., 1998). TRRAP, homologous to the *Saccharomyces cerevisiae* protein Tra1p, is a component of several histone acetyltransferase complexes, including the SAGA (SPT/ADA/GCN5/Acetyltransferase) (Grant et al., 1998) and Tip60 complexes (Frank et al., 2003). At least part of the transcription activation function of Myc is mediated by the recruitment of the HAT GCN5 through TRRAP (McMahon et al., 2000; Liu et al., 2003). Furthermore, Myc has been shown to associate with two distinct subunits of the Tip60 complex (Shen et al., 2000) independently of TRRAP, the two DNA-helicase/ATPases Tip48 and Tip49 (Wood et al., 2000). Homologues of Tip48 and Tip49 (Reptin and Pontin) have been shown to interact genetically with Myc both in *Drosophila* (Bellosta et al., 2005) and *Xenopus* (Etard et al., 2005). In addition to their role in HAT complexes, both RVBL1p and RVBL2p (the yeast homologues of Tip49 and Tip48) are subunits of the chromatin remodelling complex Ino80 (Shen et al., 2000), while TRRAP is a member of the SWI/SNF-related p400 chromatin remodelling complex (Fuchs et al., 2001). This involvement for TRRAP, Tip49 and Tip48 in both HAT as well as chromatin remodelling complexes suggests that either of these complexes (or both) could have a role in Myc-dependent transcription. Additionally, the SWI/SNF subunit INI1/hSNF5 was found to physically interact with c-Myc (Cheng et al., 1999). Moreover, overexpression of dominant-negative forms of BRG1, a SWI/SNF complex component, and

RUVBL1 (Tip49) block c-Myc-mediated transactivation (Cheng et al., 1999) and transformation, respectively (Dugan et al., 2002). Another mechanism of transactivation exerted by Myc works independently of chromatin modification or nucleosome displacement, as it was shown in the cases of the *cad* and *TERT* promoters. At these promoters Myc binding regulates promoter clearance by RNA polymerase II directly. Myc was found to directly bind both subunits of the RNA polymerase-associated factor P-TEFb (positive transcription elongation factor b), cyclin T1 and CDK9 (Eberhardy and Farnham, 2002, 2001; Bouchard et al., 2001).

In addition, Myc also has the potential to repress certain target genes without binding to E-Boxes. Many of the repressed targets encode proteins involved in cell cycle arrest and contain TATA-less promoters, featuring a specific initiator element (Inr) that recruits the basal transcription machinery to TATA-lacking promoters. Included in this subset of repressed targets are cyclin-dependent kinase inhibitors (e.g., $p21^{CIP1}$, $p15^{INK4B}$), differentiation inducers, and proteins linked to growth arrest in response to stress (Kleine-Kohlbrecher et al., 2006). In the best characterised examples, Myc causes trans-repression by associating with the transcriptional activator Miz-1 and thereby preventing it from associating with the coactivator protein p300 (reviewed in Wanzel et al., 2003).

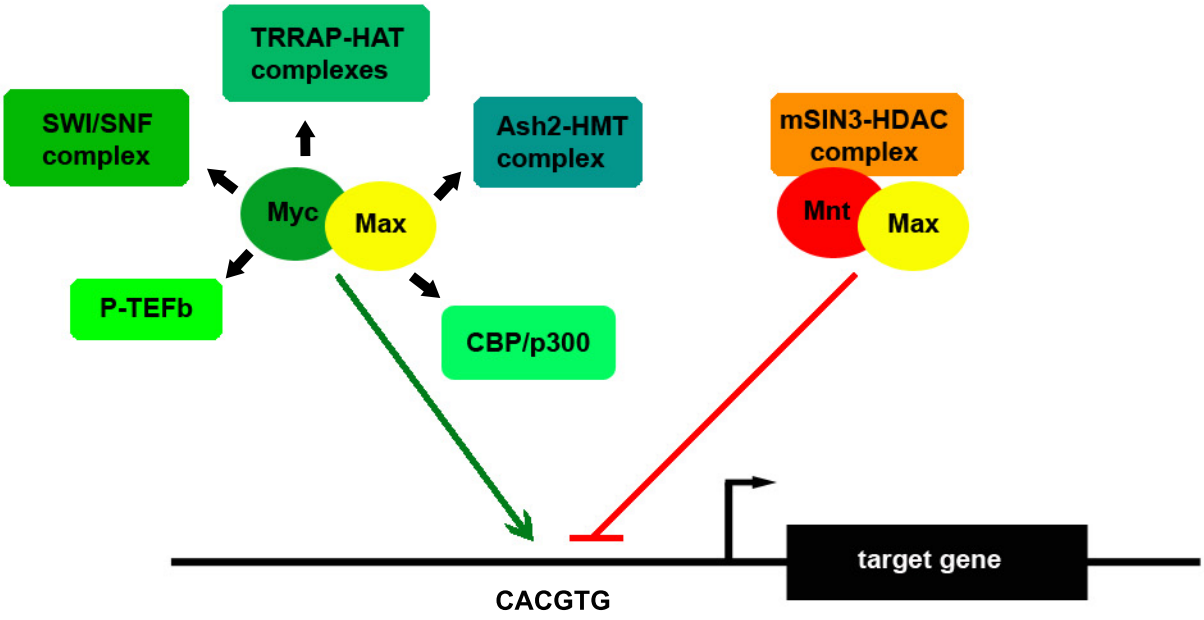

Figure 1

The diagram depicts the Max-network and various associated cofactors. Upon binding to Max, the Myc/Max heterodimers activate transcription of a hypothetical target through the E-Box element 5'-CACGTG-3'.The Myc/Max heterodimer activates transcription through recruitment of transcriptional coactivators. Some of these factors affect chromatin through chromatin acetylation (TRRAP-HAT complexes), chromatin methylation (Ash2-HMT complexes), and chromatin remodelling activities (SWI/SNF complexes). Others influence the activity of additional regulators by acetylation (CBP/p300) or mediate association with the polymerase complex (P-TEFb). Mnt/Max complexes act antagonistically to Myc/Max heterodimers and repress transcription fromE-Box containing promoters by recruiting histone deacetylases via SIN3.

2. The Max network

The fact that Myc is unable to homodimerise, or specifically bind DNA at physiological protein concentrations, prompted the search for Myc interacting factors. This led to the identification of the small bHLHzip protein Max (Grandori et al., 2000). Max has no transactivation domain on its own and is transcriptionally inert in reporter assays (Kato et al., 1992). Still, Max is able to form homodimers which bind to the same E-Boxes *in vitro* that are recognised by Myc/Max heterodimers (Blackwood and Eisenman, 1991; Prendergast et al., 1991) and repress transcription from E-Box reporters (Kretzner et al., 1992). However, the biological relevance of this observation seems to be limited, since this repression is only confined to artificial reporter genes as Max homodimers do not repress Myc-responsive genes *in vivo* (Yin et al., 1998). Moreover, Max is limiting under normal physiological condititons and therefore the Max protein pool in a given cell is bound by other bHLHzip proteins (Walker et al., 2005).

Apart from its role as a cofactor of Myc, Max was shown to dimerise with other bHLHzip proteins that function as transcriptional repressors (reviewed in Hurlin and Huang, 2006). Various assays using Max protein as a probe, led to the discovery of the four closely related bHLHzip proteins Mad1, Mxi1, Mad3 and Mad4 (also called MXD1-4) (Ayer et al., 1993; Zervos et al., 1993; Hurlin et al., 1995) and of the proteins Mnt (also termed Rox) (Hurlin et al., 1997) and Mga (Hurlin et al., 1999). The five proteins MXD1-4 and Mnt were shown to interact with Sin3 corepressor complexes via their SID (Sin3-interaction domains). Sin3, in turn, mediates active repression by recruitment of the class I histone deacetylases HDAC1 and HDAC2 which leads to subsequent deacetylation of histone tails, and formation of repressive chromatin structure (Hassig et al., 1997). Consistent with their role as transcriptional repressors, the Mad and Mnt proteins block Myc-dependent cell transformation in cell culture assays (Ayer and Eisenman, 1993; Hurlin et al., 1995; Koskinen et al., 1995; Schreiber-Agus et al., 1995; Hurlin et al., 1997; Ayer et al., 1993), as well as the expression of synthetic reporters in an E-Box dependent manner (Ayer et al., 1993; Hurlin et al., 1997). Increased expression of the Mad proteins is associated with the onset of cellular differentiation and growth arrest (Ayer and Eisenman, 1993; Chin et al., 1995). Moreover, for both Mxi and Mnt tumour suppressor activity could be shown (Hurlin and Huang, 2006).

Recent studies have provided evidence that Mnt is the crucial antagonist of Myc function. While the expression of Mad proteins is highly regulated and generally restricted to terminal differentiation in a range of cell types (Hurlin et al., 1995; Queva et al., 1998), *mnt* is ubiquitously expressed and readily detected as Mnt/Max heterodimers along with Myc/Max in proliferating cells (Zhou and Hurlin, 2001). In accordance with this expression pattern *mnt* knockout mice display the severest phenotype. They die shortly after birth, whereas *mad1*, *mxi1* and *mad3* single-mutant mice are viable and display rather subtle phenotypes. In addition, cells that are mutant for *mnt* show many characteristics of Myc overexpression (Hurlin et al., 2003; Nilsson et al., 2004; Dezfouli et al., 2006; Toyo-oka et al., 2006). Furthermore, Myc and Mnt have been shown to control similar sets of target genes (Toyo-oka et al., 2006). Taken together, these data show that Mnt directly antagonises Myc function *in vivo*.

The biological functions of Mga are less well understood (Hurlin et al., 1999). Mga is a large protein with two DNA binding domains: the bHLHzip domain and a T-Box, a domain involved in the control of a wide range of developmental processes (Papaioannou and Silver, 1998). Mga might function as a

dual-specificity transcription factor that regulates the expression of both Max-network and T-box family target genes in a Max-dependent manner. Interestingly, Mga and Max are also found in an E2F6 repression complex. This complex occupies E2F- and Brachyury- (i.e. T-box-) binding sites as well as E-Boxes in G0 phase, which suggests that these chromatin modifiers contribute to silencing of E2F- and Myc-responsive genes in quiescent cells (Ogawa et al., 2002).

3. The Max network in *Drosophila*

Drosophila contains single orthologs of the mammalian *myc*, *max* and *mad/mnt* genes (Gallant et al., 1996; Loo et al., 2005), called *dmyc*, *dmax* and *dmnt* (hereafter the terms *myc, max* and *mnt* will refer to the *Drosophila* orthologues). In addition to the advantages of *Drosophila* as a genetically well characterised animal model, the lack of redundancy made it possible to overcome many problems associated with studying Myc genes in mammalian model organisms. Moreover, there is conservation of many of the important Myc interactors and cofactors that were characterised in mammalian systems, including TRRAP, Tip48, Tip49 and other components of histone modifying and chromatin remodelling complexes.

3.1. *myc*

The *Drosophila* Myc protein is encoded by the gene *diminutive (dm)*, a gene that was described based on the mutation dm^1 in the 1930s (Bridges, 1935). The official gene designation is *dm* but the synonym *myc* (or *dmyc*) is widely used in the literature. As in vertebrates, heterodimers between *Drosophila* Myc and Max bind to canonical E-Box sequences, thereby activating target genes (Gallant et al., 1996). While the overall conservation of Myc compared to its vertebrate orthologues is rather limited, the bHLHzip domain is highly conserved, as is the MB2 domain in the N-terminus, and the central acidic region (Gallant, 2006). Importantly, Myc and c-Myc can functionally substitute for each other. Myc can transform rat embryo fibroblasts when coexpressed with oncongenic RasV12 (Schreiber-Agus et al., 1997). Myc also functionally substitutes for c-Myc in transactivation assays (Gallant et al., 1996), and rescues proliferation defects of mouse embryonic fibroblasts from *c-myc* conditional knockouts (Trumpp et al., 2001). Conversely, the lethality of a strong hypomorphic *myc* mutant can be rescued by expressing an isoform of c-Myc (Benassayag et al., 2005). The interchangeability of the *Drosophila* and vertebrate Myc proteins demonstrates a high degree of functional conservation between the Myc homologues.

In general, loss of Myc function is associated with growth defects. Hypomorphic *myc* mutants can reach adulthood, are normally patterned, but they are reduced in body size and weight. Additionally, they also display a thin bristle phenotype and prolonged development. The small body size of *myc* mutants is caused by a reduction in cell size and not a reduced number of cells (Johnston et al., 1999), as opposed to mice with hypomorphic or null mutations in *c-myc*, where both cell number and cell size are reduced. Strong hypomorphic or null mutations cause larval lethality (Maines et al., 2004; Pierce et al., 2004). Clonal analyses revealed growth defects of *myc* mutant clones both in diploid and polyploid tissues (Pierce et al., 2004; Maines et al., 2004; Johnston et al., 1999). Conversely, Myc-

overexpression leads to size increases in diploid cells and, to an even larger extent, in polyploid endoreplicating cells.

Myc impacts both on cellular growth and the cell cycle. Hypomorphic mutant imaginal wing disc cells remain small and show a slight prolongation in G1 phase, whereas overexpression of Myc leads to a size increase and a strong acceleration of the G1-S transition. However, the cycling rates of the cells are not accelerated, since the shorter G1 phases are compensated with a prolonged duration of the S and G2 phases. Therefore, only cell size but not cell number is increased (Johnston et al., 1999).

Several of the hallmark characteristics of *myc* mutants, like developmental delay, or slender bristles are reminiscent of the phenotypes seen with *Minute* mutants. *Minute* genes encode ribosomal proteins; therefore *Minute* mutants are partially impaired in biosynthesis. These similarities, the increase of nucleolar size in Myc-overexpressing animals (Grewal et al., 2005), and the fact that a large number of direct Myc target genes is involved in rRNA processing and ribosome biosynthesis (Orian et al., 2003; Hulf et al., 2005) suggest an important role for Myc in the regulation of these processes. Moreover, Myc has been shown to regulate RNA polymerase I-dependent transcription (Grandori et al., 2005; Grewal et al., 2005).

Another striking resemblance between *Minute* and *myc* mutations comes from the observation of clonal growth in wing imaginal discs. In both *myc* and *Minute* mutant situations cells with lower biosynthesis rates are eliminated and replaced by their fitter neighbouring cells, a phenomenon that was discovered for *Minute* mutations in the 1980s and which was termed cell competition (Simpson and Morata, 1981). Similarly, clones mutant for the weak hypomorphic allele dm^{P0} are eliminated by the heterozygous dm^{P0}/+ tissue (Johnston et al., 1999). More recently, it has been demonstrated that upon juxtaposition of cells with differing *myc* levels, apoptosis is induced in the cell with lower *myc* levels (De La Cova et al., 2004; Moreno and Basler, 2004). This competition also holds true in a situation where cells with physiological *myc* levels are outcompeted by neighbours containing (even moderately) enhanced *myc* levels. So far, cell competition has not been described for mammalian systems. However, if it existed, the process of field cancerogenesis might play an important role in the formation of tumours (Braakhuis et al., 2005).

3.2. *max*

Like its mammalian orthologues, Max is an essential cofactor for the regulation of E-Box dependent transcription. It forms transcription-activating Myc/Max heterodimers as well as the repressive Max/Mnt counterparts that regulate the expression of target genes upon binding to E-Box sequences (Gallant et al., 1996; Loo et al., 2005). The observation that phenotypes of *max* null mutations are less severe than lesions in *myc*, led to the identification of Max-independent functions of Myc (Steiger et al., 2008). In contradiction to the present notion, several biological functions of Myc, like cell competition, endoreplication and the regulation of RNA polymerase III-transcribed small RNA genes do not, or at least not fully, depend on Max.

3.3. *mnt*

The sole *Drosophila* ortholog of the *mad/mxi/mnt* family has been termed *mnt*, as it is most similar to the vertebrate *mnt* gene regarding its size and structure (Loo et al., 2005). Together with Max, Mnt binds to canonical E-Box sequences and acts as a transcriptional repressor by recruiting Sin3 corepressors, which subsequently cause deacetylation of surrounding chromatin by HDACs. Unlike the *mnt* mutant knockout mice, which die at birth, *mnt* mutant flies are fully viable. Compared to wild type animals, *mnt* mutants have larger individual cells and a higher body weight (Loo et al., 2005).

4. Identification of Myc target genes

The development of large scale screening technologies like microarry expression profiling, ChIP on chip assays, or serial analysis of gene expression (SAGE) has greatly facilitated the identification of potential Myc targets (reviewed in Dang et al., 2006). Recent estimates suggest that Myc could regulate as many as 15% of genes in genomes from flies to humans (Orian et al., 2003; Fernandez et al., 2003; O'Connell et al., 2003). Despite the fact that a large number of target genes have been identified in recent years, the data from various studies only show a limited overlap, which can be attributed to several factors: First of all, data compilation is dependent on the technique and biological system of choice. Furthermore, Myc is a short-lived protein, whose transcriptional regulatory effects only ranges from 2 to 5 fold. Thus, targets can be difficult to identify against the background of the strong global effects on cell behaviour.

Recently, a long list of putative Myc target genes has been compiled by using methods such as microarrays, ChIP-on-chip, or in silico bioinformatic searches. Most studies have relied on responses to changes in Myc protein levels as their primary screening approach. Methods like the inducible MycER system (Eilers et al., 1989) have been extensively used. The MycER method relies on a chimeric Myc-estrogen receptor fusion protein that is being sequestered in the cytoplasm by chaperones and upon induction with estrogenic compounds travels to the nucleus to induce target gene expression. In order to identify primary targets, the MycER method is preferably applied in the presence of cycloheximide to block translation. However, the MycER system does not fully reflect the physiological conditions in the cell. Therefore, it is crucial to identify endogenous target genes of Myc in the presence of physiological Myc levels. Chromatin immunoprecipitation (ChIP) experiments are suitable to detect Myc binding *in vivo* at cognate genomic sites (Eberhardy and Farnham, 2001). ChIP experiments in human cell lines overexpressing Myc showed that an extremely large number of loci were bound by Myc. These loci can be roughly divided into two classes of genes that are bound in a Myc titre dependent manner (Fernandez et al., 2003): A “high-affinity” group of targets that is being bound independently of the Myc-expression level and invariably at the E-Box sequence(s), and a set of “low-affnity” target genes that are bound by Myc with increased frequency upon Myc overexpression and, at extreme Myc levels, also at sequences other than E-Boxes. This finding might be interpreted to indicate that overexpression of Myc leads to widespread unspecific association with sites that are not bound in cells with lower Myc expression, which definitely holds true for unphysiologically high Myc concentrations upon strong overexpression. But how does Myc recognise the subset of targets amongst the huge number of potential Myc binding sites present throughout the genome? Recent data

from Guccione and coworkers (Guccione et al., 2006) prove that binding-site recognition by Myc is determined by the chromatin context. Myc was shown to cluster with euchromatin sites that are characterised by elevated levels of histone H3 trimethylated on residue K4 or histone H3 trimethylated on K79 (abbreviated as H3K4me3 or H3K79me3) and acetylated H3, whereby H3K4me3 showed the strongest correlation with Myc binding. Moreover, these euchromatin marks are present independently of Myc binding, and they are not affected by changes in Myc levels. This suggests that Myc binding to specific sites is a consequence of the chromatin structure and that sequence recognition by Myc is important, but comes second to chromatin recognition. Thus, E-Boxes outside euchromatic islands are not normally bound in a physiological context, but might possibly be bound in the presence of supraphysiological Myc levels, which might account for the large number of loci that were only identified in Myc overexpression studies. The correlation between distinctive histone marks and preferential recruitment of Myc to these sites may well constitute a mechanism of target selection. In such cases, Myc would be associated with cofactors that recognise – perhaps redundantly - acetylated or methylated histone residues with their chromo- or bromo-domains and therefore are able to selectively “read” the histone code. Such a tethering of Myc to restricted chromatin domains would greatly reduce the portion of the genome accessible to physiological Myc binding. Once bound to DNA, Myc locally enhances histone acetylation, but not methylation (Guccione et al., 2006). Other adaptor proteins, such as β-catenin, induce trimethylation of histone H3 on K4 (Sierra et al., 2006) and may regulate the access of Myc to a subset of promoters.

With Myc target genes approaching a total of about 3000-4000 in humans, it is critical to further decode regulatory modules (i.e. the protein complexes that are required for Myc-dependent expression of certain subsets or all target genes) that associate with Myc and to determine the contribution of individual Myc binding sites to the regulation of target genes.

4.1. Myc target genes

Even though overexpression studies suggest that c-Myc might control up to 15% of all loci in a genome, this is likely to be an overestimate, and Myc is probably influences less than 5% of all genes under physiological conditions (Hulf et al., 2005). Within this group of c-Myc targets, certain classes of genes are greatly overrepresented. These targets are involved in protein biosynthesis, metabolism, cell cycle regulation, cell adhesion and the cytoskeleton. The deregulated expression of c-Myc also induces genes that contribute to apoptosis under nutrient or growth factor deprivation. In addition to protein coding genes, microRNAs were identified to be regulated by Myc proteins in vertebrates (O'Donnell et al., 2005; reviewed in Dang et al., 2006; Chang et al., 2008). microRNAs are small regulatory molecules that regulate the stability or translational efficiency of target mRNAs. They are transcribed as long transcripts, which subsequently undergo processing and maturation to form microRNA duplexes. One of the mature miRNA strands is incorporated into the RNA-induced silencing complex (RISC) and guides target mRNA silencing. Recently, c-Myc and Myc were also discovered to control RNA polymerase I and III-transcribed targets (Grewal et al., 2005; Grandori et al., 2005; Gomez-Roman et al., 2003; Steiger et al., 2008). By regulating transcriptional activity of all three RNA polymerases, Myc even has greater influence on ribosome biogenesis and protein synthesis. Despite significant advances in the knowledge of Myc target genes, it is to date unknown whether Myc

promotes tumorigenesis by altering the expression levels of physiological Myc targets, by controlling non-physiological targets, or by a combination of both mechanisms.

5. RNA interference

The discovery of the RNA interference (RNA*i*) phenomenon has radically changed the field of experimental genetics in recent years. Not surprisingly, Andrew Fire and Craig Mello, the researchers who discovered RNA*i* gene silencing, were awarded the Nobel Prize for Physiology or Medicine in 2006. Because of RNA*i* reverse genetic approaches to globally or selectively dissect genetic pathways by specific knockdown of gene expression became feasible in many model organisms. Moreover, the reduction of expression without fully abrogating gene function makes it possible to assess hypomorphic phenotypes of essential genes.

The phenomenon RNA*i*, also known as post-transcriptional gene silencing (PTGS), was discovered by chance in the late 1980s. Attempts to increase the colouration of petunia flowers by inserting extra copies of the pigmentation gene surprisingly led to variegating petal colouration or even complete absence of colour, due to degradation of pigmentation mRNAs from both the endogenous locus and the transgene (Napoli et al., 1990). The injection of antisense RNA complementary to the gene *par-1* in *Caenorhabditis elegans* resulted in the expected embryonic lethality, but surprisingly also control sense RNA gave a similar phenotype (Guo and Kemphues, 1995). Experiments performed in following years revealed, that a mixture of sense and antisense RNA resultet in 10-fold greater reduction of endogenous transcript levels than either strand alone (Fire et al., 1998). In retrospective, the initial *par-1* single-strand RNAs were most probably contaminated with complementary strands.

RNA interference plays an important part in regulating the expression of cellular RNAs. On one hand, RNA*i* is involved in the innate immune surveillance system. Double stranded RNAs, which can be produced by invasive genetic elements but is not supposed to arise from tightly regulated cellular genes, are detected and the corresponding target genes are post-transcriptionally silenced. On the other hand the same mechanism is important in production of microRNAs (miRNAs). These small RNAs, which are cellularly expressed, regulate the translation efficiency of partially complementary target mRNAs, many of which code for crucial developmental genes that are often also involved in the genesis of neoplastic diseases. The RNA*i* mechanism is activated when dsRNA recruits an RNase III type enzyme called Dicer, which cleaves the dsRNA – either long transcripts of invasive elements or pre-miRNA – into 21- and 22-nucleotide double stranded fragments (Bernstein et al., 2001; Sontheimer, 2005). The 21 and 22 nt fragments, termed short interfering RNAs (siRNAs), are subsequently loaded into the large multiprotein nuclease RNA-induced silencing complex (RISC). The antisense strand of the siRNAs is used as a template to find homologous mRNA molecules, which are then degraded by the complex (siRNAs, miRNAs) or translationally silenced (miRNAs).

Since the the discovery of the RNA*i* phenomenon and the unravelling of its mechanism, the technique has successfully been used in a variety of model systems. In conjuction with the still expanding genomic sequence data, it has become an immensely powerful genetic tool to study biological processes.

6. Project overview

Even though the knowledge about the molecular mechanism how Myc regulates the expression of its targets has been significantly expanded, and many proteins that interact physically with Myc have been identified in vertebrate tissue culture systems in recent years, the physiological relevance of only a handful of these putative cofactors has fully been demonstrated. Many studies have relied on Myc overexpression to elucidate its transactivation properties or they have examined - the potentially indirect - effects of putative cofactors on the transformation potential of Myc in immortalised cell lines. A great deal less is known about the physiological effects of putative cofactors *in vivo*, e.g. on the expression of endogenous Myc target genes or their localisation to target promoters in a Myc-dependent fashion. Furthermore, the association of putative cofactors with Myc is not exclusively influencing initial transcription activation but also other Myc-dependent processes, such as re-initiation of transcription or repression of certain targets. Moreover, candidate cofactors might impact on Myc's involvement in DNA replication. This lack of data concerning the physiological regulation of Myc targets prompted us to carry out an RNA interference screen in *Drosophila* Schneider 2 cells in order to identify physiologically relevant novel cofactors involved in Myc-dependent transcription regulation. The fact that the Max network and many essential cofactors are functionally conserved but present in a simpler form in *Drosophila* - with only single orthologues of *myc* and *mnt* families present - makes it an ideal model to study Myc function.

In the course of the RNA*i* screen, gene products of roughly 750 transcription-associated factors were downregulated, and the effect on a Myc-dependent luciferase reporter was assayed. About four percent of the candidates tested showed a specific influence on the reporter construct driven by the promoter of the Myc target gene *CG5033*. These were considered to be specific Myc-dependent transcription regulators. Subsequently, we focussed on two groups of candidates to further characterise their molecular and genetic interaction with Myc. The *Drosophila* Host cell factor protein (HCF) and the components of the RNA polymerase-associated factor 1 complex (PAF complex) were confirmed as specific Myc cofactors, which are required for the correct expression of Myc target genes. Both HCF and the *Drosophila* orthologue of Leo1, which is termed Atu, directly interact with Myc. While HCF clearly acts as a coactivator of Myc function *in vivo*, experiments with PAF complex mutants provided evidence for converse activities of individual subunits. Originally identified as repressors of Myc activity in the RNA*i* screen, *in vivo* experiments suggest that several PAF complex components exert coactivating functions. We could show that the PAF complex subunits Atu, Atms and Rtf1 are required for the proper expression of RNA polymerase II-transcribed target genes of Myc. Moreover depletion of Atms, Atu and Rtf1 reduces the growth potential in a variety of tissues *in vivo*, especially in the presence of ectopic Myc levels. In contrast the PAF complex component Hyrax (Hyx) can also act as a repressor of Myc in a context dependent manner.

As mentioned above HCF was identified as a positive cofactor of Myc-dependent transcription control. In addition to the interaction of overexpressed proteins, we have shown a direct physical interaction between endogenous HCF and Myc. Furthermore, HCF impacts on the expression of Myc target genes in S2 cells. *In vivo* HCF synergises with Myc in the promotion of growth in the eye and of imaginal wing disc clones. HCF depletion by RNA*i* has the potential to revert Myc overexpression phenotypes in the wing and, to a lesser extent, also in the eye. These data show that Myc requires

HCF to reach its full transcriptional activity during proliferation and differentiation. In order to activate Myc-dependent transcription, HCF has to recruit additional complexes with enzymatic activity. The molecular nature of such a mechanism has to be elucidated, but it might depend on Ash2-containing HMT complexes.

Taken together, we present clear evidence that both the PAF complex and HCF are physiologically relevant cofactors of Myc in transcription control.

7. Introduction of RNA*i* screen candidates

7.1. Proteasome components

The 26S proteasome is the major non-lysosomal proteolytic manchinery in eukaryotes, by which polyubiquitylated proteins are degraded in an ATP-dependent manner (Ciechanover, 1998). Polyubiquitylation is known to be responsible for the degradation of many short lived growth-regulating proteins, and more than 80% of the proteins in mammalian cells are degraded in the proteasome. More recently it became evident that the ubiquitin-proteasome system is implicated in transcriptional control, and is used in controlling the distribution, abundance and activity of components of the transcriptional machinery (Muratani and Tansey, 2003). It was shown that the activity of many transcriptional activators, including Myc, is enhanced by ubiquitylation (Kim et al., 2003; von der Lehr et al., 2003). For example the E3 ubiquitin ligase Skp2 not only regulates the stability of Myc *in vivo* but is also required for full activity of Myc (Muratani and Tansey, 2003). Both the “timer” and “black widow” mechanism (Kodadek et al., 2006) propose that transcriptional activators have to be designated for subsequent destruction in order to obtain their full activation potential. While the timer model focusses on a window of activity, during which the activator drives target gene expression, the “black widow” model states that activator polyubiquitination and subsequent destruction are a necessary consequence of physical interaction with the RNA polymerase holoenzyme. Both models stipulate that full activation of transcription factors depends on their ubiquitination. However, it is not clear how depletion of proteasome components in the RNA*i* screen should lead to reduced transactivation potential of Myc and hence decreased Myc activity reporter expression.

The 26S proteasome is assembled from two large macromolecular complexes. The 20S proteolytic particle and the 19S regulatory complex (RC). The 20S proteasome is composed of four seven-membered rings that form a barrel-like structure. Within this chamber, which can be accessed through axial pores, the six protease catalytic sites are contained. The 900kDa 19S RC caps one or both ends of the 20S particle, and can be functionally subdivided into base and lid components. The base complex consists of six homologous AAA ATPases (Rpt1-6: regulatory particle ATPases) and three non-ATPase components, whereas the lid of the RC is made of an additional eight non-ATPase subunits (Rpns: regulatory particle non-ATPases). The 19S ATPases regulate the assembly of the 26S proteasome, they unfold substrate proteins targeted for degradation, and they gate protein translocation into the central chamber of the 20S proteasome (Ciechanover, 1998; Pickart and Cohen, 2004). A proteasome complex that consists of the 20S particle and the RC base still performs ATP-dependent degradation of unfolded proteins, but it can no longer degrade ubiquitin-tagged substrates. Therefore the lid subcomplex of the RC recognises polyubiquitin signals. Six components of the 19S RC were found in the Myc-dependent RNA*i* screen as modulators of the luciferase reporter system. Five non-ATPase subunits of the lid subcomplex (Rpn5, Rpn6, Rpn7, Rpn11, Rpn12) and Rpn2, which forms part of the base subcomplex, were identified. Rpn11, a de-ubiquitylase of whole ubiquitin-chains, is the only protein of the lid complex with a known enzymatic activity (Verma et al., 2002).

7.2. Host cell factor (HCF)

7.2.1. Vertebrate HCF-1

The Host cell factor 1, a highly conserved and abundant chromatin-associated protein, was initially identified as a component of the VP16-induced transcriptional regulatory complex (Kristie and Sharp, 1990). HCF-1, one of the two human paralogues, is a broadly expressed nuclear protein, which is involved in the regulation of cellular and viral gene expression (Wilson et al., 1993). Upon infection with Herpes simplex virus (HSV) the virion transactivator protein VP16 is a key player in the decision whether the virus enters the lytic or latent life cycle. To initiate the lytic state, VP16 induces the expression of the first set of viral proteins by associating with HCF-1, and subsequently with another cellular protein, Oct-1, on regulatory elements in each immediate early gene promoter (Wysocka and Herr, 2003).

HCF-1 is synthesised as a large 2035 amino acid long precursor protein that is subsequently cleaved at six central HCF-1_{PRO} repeats (Figure 2). However, the two resulting subunits (HCF-1_N and HCF-1_C) remain non-covalently associated through their self-association sequences SAS1 and SAS2. The interaction between HCF-1 and transactivator proteins, including VP16, is mediated by the N-terminal Kelch domain, named because of its similarity to the *Drosophila* protein Kelch. Additionally, HCF-1 contains centrally located basic and acidic regions, two Fibronectin type 3 (Fn3) repeats that make up the SAS2 element, and a C-terminal nuclear localisation signal (NLS). Sequence analyses of the HCF-1 interacting proteins VP16 and LZIP (cellular leucine zipper protein) identified a conserved four amino acid sequence D/EHxY, termed HCF-binding motif (HBM). This particular sequence was shown to be indispensable for their binding to HCF (Freiman and Herr, 1997).

In addition to its role as a cotransactivator in viral infection, HCF-1 emerged as an important regulator of the cell cycle. It controls exit from mitosis, where it ensures proper cytokinesis, as well as passage through G1 phase (Julien and Herr, 2003). In keeping with these two functions, depletion of HCF-1 causes cell cycle arrest in G1 phase with a population of multinucleated cells. Interestingly, expression of the N-terminal subunit HCF-1_N is sufficient to promote G1 phase progression and S phase entry. This activating effect of HCF-1 on cell cycle progression is, at least partially, due to inactivation of the Myc-interacting protein Miz-1. Miz-1 stimulates the expression of the CDK inhibitor *p15INK4b*, and is thereby inhibiting retinablastoma protein (pRb) inactivation (Piluso et al., 2002). HCF-1 binds to Miz-1 and interferes with p300 recruitment and the activation of cell cycle repressors. However, recent studies have revealed a much broader impact of HCF-1 on cell growth and division. HCF-1 proteins exert the cell-cycle control through temporally regulated association with various effector proteins. For example, HCF-1 was found to interact with a trithorax-related Set1/Ash2 H3K4 methyltransferase complex (Wysocka et al., 2003), and concomitant association with E2F transcription factors and the MLL family of histone H3K4 methyltransferases is crucial for HCF-1 dependent activation of S phase promoters (Tyagi et al., 2007). MLL (mixed lineage leukemia) was identified as the human homologue of the *Drosophila* Trx protein, and was characterised as a proto-oncogene. It is found in complex with hAsh2, the tumour suppressor Menin, and both human host cell factor orthologues HCF-1 and HCF-2 (Yokoyama et al., 2004). The same mechanism seems to be applied by HCF-1 in the activation of HSV immediate early genes, since both Set1 and MLL1 H3K4 methyltransferases are found in

complex with HCF-1 at IE enhancers (Narayanan et al., 2007). Moreover, HCF-1 was found to interact with several core components of the Sin3 histone deacetylase complex (Wysocka et al., 2003). Taken together HCF-1 interacts with several histone modifying complexes and tethers the Sin3 HDAC complex to the Set1/Ash2 HMT complex. Since these two complexes exert opposite transcriptional activities – repression in the case of Sin3 and activation for Set1/Ash2 – HCF-1 might constitute a switch between both positive and negative chromatin modifications. Intriguingly, the tethering of different complexes via HCF-1 is context-dependent. The transcriptional coactivator VP16 was only found in complex with Ash2 HMT-bound HCF-1 but not with repressive Sin3 HDAC–HCF-1 complexes (Wysocka and Herr, 2003). As mentioned above, HCF-1 was shown to interact with activator E2F1 proteins to drive G1-to-S phase progression by recruiting H3K4 HMT complexes to E2F-responsive promoters (Tyagi et al., 2007). In a cell cycle-dependent manner HCF-1 also binds repressive E2F4 proteins to switch off S phase genes in a mechanism dependent on Sin3A HDAC complexes. This selective interaction with both activating and repressive E2Fs is conserved in insect cells and constitutes another example for context dependent interaction of HCF-1 with transcription modulators.

7.2.2. *Drosophila* HCF

The sole *Drosophila* HCF orthologue (HCF) is expressed from the *hcf* gene located on the 4th chromosome at the cytological location 102B5. The whole gene spans 15 kb and comprises 13 exons. HCF displays high sequence conservation with vertebrate HCF proteins within the Kelch and Fn3 domains but not in the intervening stretches. Despite the lack of sequence identity in the central portion of the protein, HCF contains corresponding basic- and acidic-residue enriched regions but the HCF-1_{PRO} repeats are absent. Nevertheless, the HCF protein undergoes proteolytic processing. Like the vertebrate counterparts the mature HCF protein consists of two cleavage products that remain associated with each other (Figure 2) (Mahajan et al., 2003).

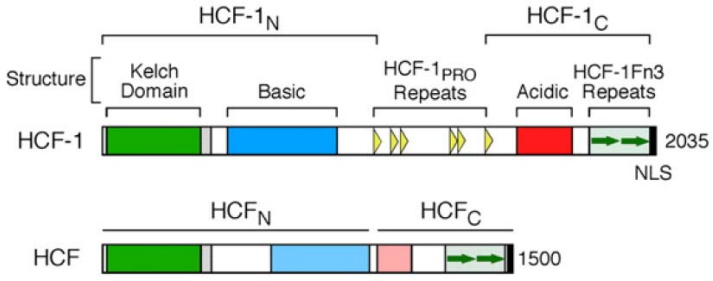

Figure 2

Schematic depiction of human HCF-1 and *Drosophila* HCF.
Structural elements are labelled above HCF-1 and related elements are shown similarly for HCF. HCF-1_{PRO}, HCF-1 proteolytic processing repeats; HCF-1Fn3, fibronectin type 3 repeats; NLS, nucelar localisation signal

(Adapted from Tyagi et al 2007).

Although HSV infection is restricted to mammalian cells, a VP16-induced HCF-complex can be formed in invertebrate cell extracts, including *Drosophila* cells (Mahajan et al., 2003). This led to the assumption that the *Drosophila* homologue HCF applies the same or similar molecular mechanisms as HCF-1. Indeed, coimmunoprecipitation studies and immunolocalisation on polytene chromosomes demonstrated that HCF interacts with the *Drosophila* homologue of human Sin3A, dSin3A, which is also a subunit of a class 1 HDAC complex (Beltran et al., 2007; Cho et al., 2005), as well as with Ash2 (Beltran et al., 2007). These data suggest that HCF tethers both HDAC and HMT activities as it was reported in mammals. Experiments on the histone acetyltransferase (HAT) dGcn5 and its associated complexes led to the identification of another HCF-associated complex. dGcn5 is a conserved HAT found in a number of multisubunit complexes in yeast, mammals, and flies. In the *Drosophila* version of the SAGA complex (dSAGA), dGcn5 is associated with dAda3, dAda2B, dSpt3 and dTra1, the homologue of TRRAP. The analysis of proteins interacting with the novel Ada2 orthologue dAda2A, led to the identfication of the previously unknown HAT complex ATAC (Guelman et al., 2006). In addition to the subunits common with dSAGA (dGcn5 and dAda3), ATAC contains dAda2A, Atac1 and HCF. Taken together, HCF is found in association with the Sin3a HDAC complex, the Ash2-containing HMT complex, and the novel HAT complex ATAC. However, reports of a linkage between specific transcription factors and the chromatin modifying machinery via HCF are still missing in *Drosophila*.

7.3. RNA Polymerase II-associated factor complex (PAF complex)

7.3.1. Yeast PAF complex

The PAF complex was first identified in yeast (yPAF) as an RNA polymerase II-associated factor that interacts with TATA Binding Protein (TBP), the elongation factors Spt4–Spt5, and FACT during transcription elongation (reviewed in Shilatifard, 2006). The yPAF complex comprises the five components Paf1, Cdc73, Leo1, Ctr9, and Rtf1 (Krogan et al., 2002). During RNAP II-mediated transcription the PAF complex is associated with both the promoter and coding regions of transcriptionally active genes. Furthermore, it was found to interact with the non-phosphorylated and both the Ser2- and Ser5-phosphorylated forms of the RNAP II large subunit (Rozenblatt-Rosen et al., 2005). The C-terminal domain (CTD) of the RNA polymerase II large subunit contains two important serine residues, Ser2 and Ser5, which are phosphorylated during transcription. Phosphorylation of Ser5 is required during transcription initiation and the early phase of elongation, while phosphorylation of Ser2 is linked to elongation (Komarnitsky et al., 2000). The association with all three forms of RNAP II and the distribution throughout the coding regions of transcribed genes indicate an involvement for the PAF complex in both transcription initiation and elongation. Indeed, the PAF complex mediates the successive recruitment of various stage-specific factors required for the formation of the mature elongation complex. It was shown that the PAF complex stimulates the Rad6-mediated monoubiquitination of the core histone H2B (Wood et al., 2003, 2005), the Set1-mediated histone H3-K4 methylation (Dover et al., 2002; Krogan et al., 2003b; Ng et al., 2003), and the Dot1-mediated histone H3-K79 methylation (Krogan et al., 2003b; Krogan et al., 2003a). Also, the recruitment of the elongation factor FACT is dependent on the presence of the PAF complex. FACT is a dimeric protein that plays a major role in displacing the H2A/H2B dimer from the core nucleosome and thus allowing elongation to proceed over chromatin (Belotserkovskaya et al., 2003). Surprisingly, considering their broad function in transcription, components of the PAF complex are nonessential in yeast. Losses of individual components display differences in phenotypic severity. While *paf1Δ* and *ctr9Δ* strains show severe and nearly identical growth defects, *Cdc73* and *Rtf1* mutants are less strongly affected - nevertheless they cause disruption of the PAF complex chromatin association -, and the *Leo1Δ* strains exhibited few detectable deficiencies (Betz et al., 2002). However, mutations of all the components show defects in transcription elongation. While the overall chromatin distribution of RNAP II is not affected upon loss of PAF components, RNAP II Ser2 phosphorylation is strongly reduced and poly(A) tails are shortenend. This indicates an essential additional role of the PAF complex in the linkage of transcriptional and posttranscriptional events (Mueller et al., 2004; Penheiter et al., 2005). Most likely the influence of the PAF complex on pre-mRNA processing and maturation is exerted by recruiting factors involved in 3' end formation. Sheldon and colleagues revealed a functional interaction between the PAF complex and the Nab3 and Nrd1 proteins in the 3' end formation of nonpolyadenylated RNAP II transcripts like snoRNAs (Sheldon et al., 2005).

7.3.2. The PAF complex in humans (hPAF)

Like the yPAF complex, the human counterpart hPAF contains five subunits. However it differs from yPAF in having an additional eukaryote specific component hSki8, which is involved in mRNA quality control (Zhu et al., 2005), and lacking the human homologue of yRtf1. The hPAF complex interacts with the non-phosphorylated and Ser2- and Ser5-phosphorylated forms of the RNAP II large subunit (Rozenblatt-Rosen et al., 2005), which indicates an involvement in both transcription initiation and -elongation. Also the regulation of transcription-associated histone monoubiquitination of H2B, a prerequisite for transcription elongation, as well as trimethylation of histone H3-K4 and dimethylation of histone H3-K79 are conserved functions between yeast and human PAF complexes (Pavri et al., 2006; Zhu et al., 2005). This suggests that the PAF complex in humans affects gene expression through a mechanism similar to that in yeast.

Various studies to identify genes which may play a role in progression of cancer found several hPAF complex subunits to be dysregulated in tumours. Like its yeast homologue Cdc73, the human PAF complex component Parafibromin induces cell-cycle arrest in the G1 phase by blocking expression of cyclin D1 (Zhang et al., 2006). Parafibromin is encoded by the *HRPT2* gene and indeed was characterised as a tumour suppressor associated with the suppression of the hyperparathyroidism-jaw tumour (HPT-JT) syndrome (reviewed in Wang et al., 2005). Interestingly, *HRPT2* is amplified in liver carcinomas (Parada et al., 1998) and breast cancers (Stange et al., 2006), which points to opposing functions of Parafibromin in different tissues. hPaf1/PD2, the human homologue of yPaf1, in contrast, was identified as a potential oncogene, since it is overexpressed in pancreatic cancer cell lines (Chaudhary et al., 2007), and it was shown to synergise with *AKT2* in the development of cancers (Cheng et al., 1996; Moniaux et al., 2006). Also, a third hPAF complex component hLeo1 was implicated in the etiology of cancers. In *Drosophila* the hLeo1 homologue Atu interacts with β-catenin in the Wnt/Wg-signalling cascade (Mosimann et al., 2006) and is amplified in human colorectal cancers – which often display dysregulation of Wnt-signalling - (Camps et al., 2006) and malignant bone tumours (Tarkkanen et al., 2006). Taken together, various human PAF complex components play a role in the development of cancers. Strikingly, the hPaf1 and hLeo1 subunits were characterised as oncogenes, whereas Parafibromin is a potential tumour suppressor.

7.3.3. *Drosophila* PAF complex

A comparison between yPAF and its metazoan homologue in *Drosophila* has revealed extensive functional conservation but also striking differences. Like yPAF, the *Drosophila* PAF complex globally associates with actively elongating RNAP II and is required for the activation of target genes (Adelman et al., 2006). However, the nature of the Polymerase II association and the composition of the complex are markedly different between the two species.

In contrast to the situation in yeast, loss of PAF complex in *Drosophila* does not cause changes in the levels of Ser2 phosphorylated RNAP II, however, the level of the chromatin associated elongation factors Spt6 and the FACT component SSRP1 are strongly reduced (Adelman et al., 2006). Moreover, depletion of Paf1 results in a loss of histone H3-K4 trimethylation within actively transcribed regions, while the levels of histone H3-K79 trimethylation remain unaffected (Adelman et al., 2006; Tenney et

al., 2006). Despite these considerable differences between yPAF and its homologue in *Drosophila*, there is evidence that the molecular mechanisms used by the PAF complex are conserved between the two species. Induction of histone H3-K4 methylation at the *Hsp70* promoter through PAF complex action was shown to involve Trithorax, the *Drosophila* homolog of the yeast Set1 histone methyltrasferase of the COMPASS (Complex Proteins Associated with Set1) complex (Smith et al., 2004). In turn, Histone H2B ubiquitination activity by the Rad6 and Bre1 proteins is a prerequisite for Histone H3 methylation at lysine 4 in yeast (Krogan et al., 2003a; Wood et al., 2003). As discussed previously, the PAF complex is required to activate Rad6 and Bre1 histone ubiquitination activity in yeast. Tenney et al. (2006) determined that the *Drosophila* Rtf1 subunit of the PAF complex facilitates *Notch* signalling, providing a link between histone ubiquitination and methylation to gene activation by the *Notch* pathway, since Bre1 is also required for *Notch* target gene expression in *Drosophila* (Bray et al., 2005). Therefore, the important functional links between the PAF complex, Rad6/Bre1 and histone methylation seen in yeast seem to be conserved in *Drosophila*.

While Rtf1 is an integral part of the yPAF complex, the *Drosophila* and human homologues do not appear to be a stable part of the PAF complex. The *Drosophila* Rtf1 protein neither stably associates with Paf1 nor Hyrax, the homologue of Cdc73. However, Rtf1 colocalises broadly with actively transcribing RNAP II and with Paf1 in the context of active transcription (Adelman et al., 2006). Rtf1 also plays an important role in histone methylation (Tenney et al., 2006). Thus, the function of this protein is conserved in yeast and *Drosophila*, suggesting that Rtf1 functions in association with the PAF complex *in vivo*.

In contrast to the situation in yeast, where PAF components are nonessential, mutations of the *Drosophila* PAF subunits Hyx, Paf1, which is also called Antimeros, or RNA*i*-mediated depletion of Rtf1 are lethal (Adelman et al., 2006; Tenney et al., 2006). Presumably the metazoan PAF components have acquired additional functions as compared to their yeast homologues. Indeed, Adelman et al. (2006) provide evidence for a nucleolar function for both Paf1 and Rtf1 in *Drosophila*. Moreover several PAF components in *Drosophila* have been implicated in complex signalling cascades. As discussed above, Rtf1 is involved in Notch signalling, while the Cdc73 homologue Hyrax plays an important role in the activation of Wg signalling targets (Mosimann et al., 2006). While the yPAF complex plays a broad, almost genome-wide role in transcription (i.e. it is found in association with RNAP II at most gene loci) without needing sequence-specific transcription factors, there is evidence for PAF complex recruitment by specific signalling pathways in *Drosophila* (Mosimann et al., 2006; Bray et al., 2005).

Results

1. RNA*i* screen for Myc cofactors

One strategy to characterise the function and specificity of a transcription factor is through the identification of its target genes. A long and still growing list of putative targets of Myc has been compiled during recent years in humans and *Drosophila* (Dang et al., 2006; Hulf et al., 2005; Fernandez et al., 2003; Orian et al., 2003; Oster et al., 2002). This process was greatly assisted by the availability of technologies suitable for large-scale assays such as genome-wide location of Myc/Max binding sites, or transcriptome profiling techniques (SAGE, microarrays). A subset of these potential targets was further characterised and the dependence on Myc binding for their transactivation was verified (McMahon et al., 1998; Nikiforov et al., 2002a).

To add another level of complexity, transcription factors depend on a number of cofactors to elicit their full activation potential. Even though several cofactors that are involved in Myc-dependent transcription control have been identified, (e.g. McMahon et al., 1998; Cheng et al., 1999; Wood et al., 2000; Bellosta et al., 2005), both in vertebrates and *Drosophila*, still comparatively little is known about the mechanistic aspects of transcription modulation by Myc.

In order to identify novel physiologically relevant cofactors of Myc, we performed an RNA interference (RNA*i*) screen in embryonic hematopoietic Schneider 2 (S2) cells. The screen was based on a directly Myc-dependent Dual luciferase reporter system and 752 *in silico* preselected transcription-associated genes were tested for their influence on Myc-dependent regulation of reporter expression.

1.1. Myc-dependent luciferase reporter system

In order to identify physiological Myc targets and to further characterise Myc-responsive regulatory sequences, T. Hulf significantly down-regulated Myc in exponentially proliferating S2 cells by RNA interference during the course of his PhD thesis (Hulf, 2004). Based on this microarray analysis, a set of direct Myc targets was established. The majority of the 30 genes that were significantly downregulated at all the timepoints tested (6, 12, and 48 hours after addition of *myc* dsRNA) play a role in in ribosome biogenesis, protein synthesis, and metabolism. Screening for common nucleotide sequences within 1000 bp of the predicted transcription start site of all these genes displaying expression differences, revealed the E-box to be significantly enriched (27 of 30 genes contained at least one E-box, 13 of them two). A clear positional bias of E-boxes to the first 100 bp following the predicted transcription start was also discovered. The genes containing such a downstream E-box potentially constitute a distinct subset of Myc targets (Hulf et al., 2005).

To demonstrate the importance of the sequence and position of the E-box for the regulation of Myc target genes, the promoter of the Myc responsive gene *nnp-1* (a sequence homolog of the nucleolar protein Nnp1/Nop52 (in vertebrates) and Rrp1 (in *Saccharomyces cerevisae*)) was chosen to control the expression of the firefly luciferase open reading frame (Hulf et al., 2005). The *nnp-1* gene is significantly downregulated at all time-points after *myc* RNA*i* in S2 cells and upregulated after Myc overexpression in wing discs. Its regulatory region also contains one E-box at position +29 relative to

the transcription start site. This E-box conforms to the consensus of the general sequence CANN(N)TG (Blackwell et al., 1993), and furthermore, it is bound by Myc in S2 cells as demonstrated by ChIP experiments. To analyse the function of the E-Box a 386 bp fragment of the *nnp-1* promoter, including 108 bp downstream of the transcription start site, was fused to the luciferase ORF, with translation of the luciferase starting at the ATG of Nnp-1. Additionally to the wild type *nnp-1* promoter a mutated form lacking the E-box (ΔE-Box) was created. The reporter constructs were transiently transfected into S2 cells, together with *myc* dsRNA and a control plasmid expressing the *Renilla* luciferase gene under the control of the constitutive α-tubulin promoter. The ability of *myc*-RNA*i* to inhibit wild type *nnp-1* driven luciferase expression to a similar extent as *nnp-1* mRNA confirmed *nnp-1* to be a direct target of Myc.

Based on these *nnp-1* model reporters for Myc activity we proceeded to create additional constructs. Analogous to the *nnp-1* reporters, a 390 bp promoter sequence of the directly Myc activated target *CG5033* (a sequence homolog of the vertebrate protein Bop-1, which is involved in rRNA processing and ribosome biogenesis) was fused to the *Renilla* luciferase ORF. This reporter showed a qualitatively similar, but quantitatively stronger response to *myc*-RNA*i* than the *nnp-1* reporter (Figure 3b). In contrast to the original reporter system, in which we used an α-tubulin driven luciferase as control plasmid, a ΔE-Box firefly reporter served as an internal control to monitor basal expression level of the promoter. Since the regulatory sequences driving the reporter genes are identical, except for the presence or absence of the single E-Box sequence at position +21 relative to the transcription start, the readout of the system directly reflects Myc's activation potential (Figure 4b). Hereafter, we refer to the wild type/ΔE-Box luciferase reporter pairs as Myc activity reporter.

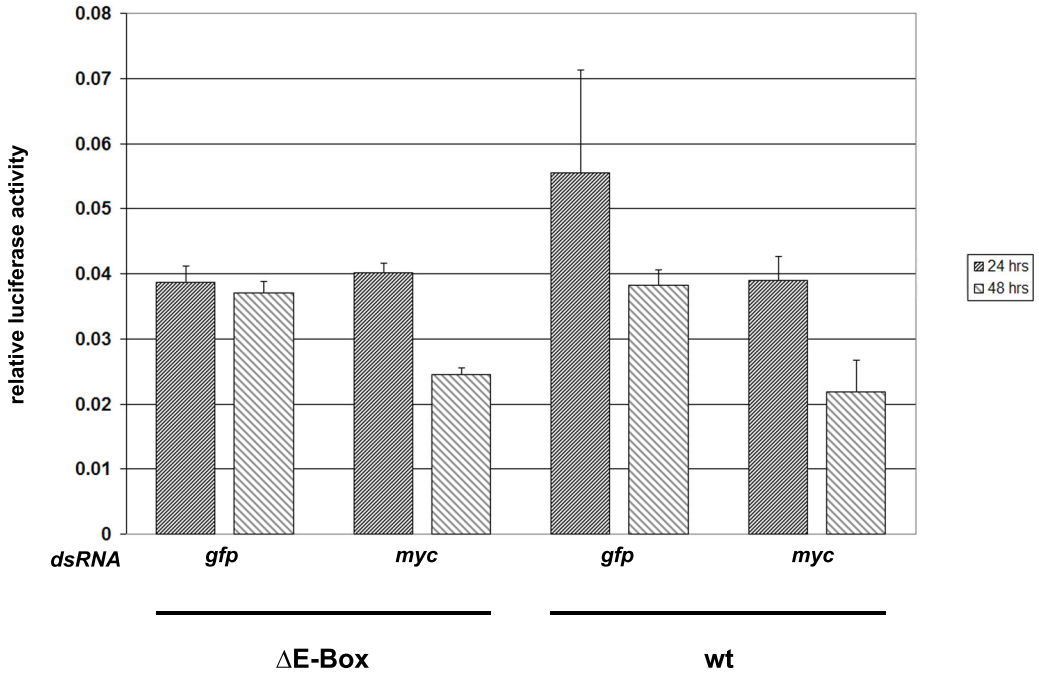

Figure 3a

***nnp-1*-luciferase reporter activity** 24 and 48 hours after RNA*i* against *myc* or *gfp* as a control. All values are calculated relative to an α–tubulin-*Renilla* luciferase reference. Error bars indicate standard deviations from three independent experiments. The wild type reporter (wt) is slightly downregulated by *myc* RNA*i*. This downregulation is more pronounced after 48 hours. The reporter with a mutated E-Box sequence (ΔE-Box), is completely unresponsive to *myc* RNA*i*.

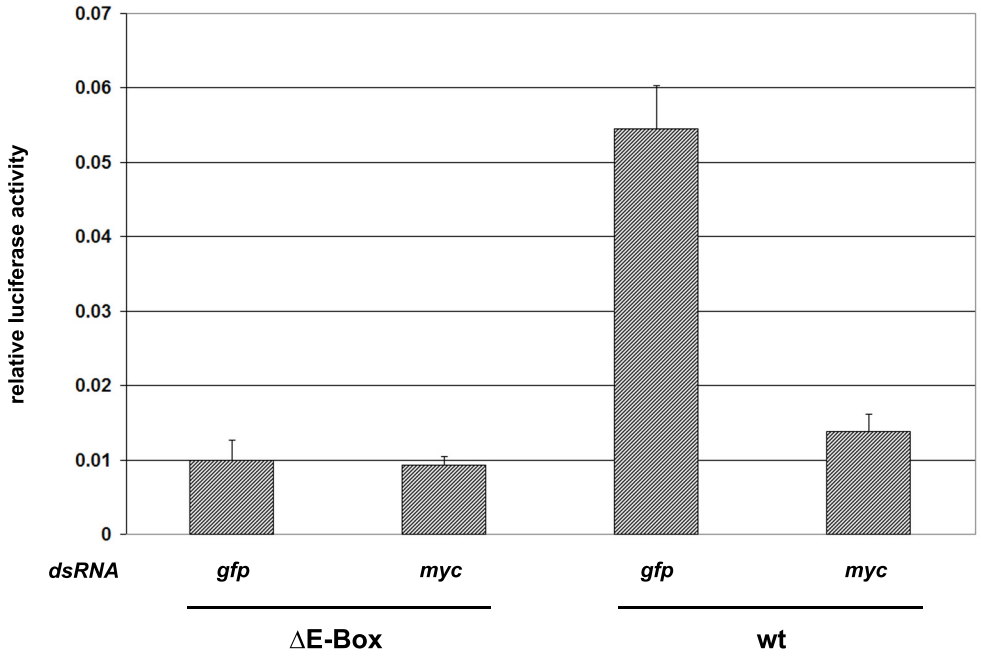

Figure 3b

***CG5033*-luciferase reporter activity** 24 hours after RNA*i* against *myc* or *gfp* as a control. All values are calculated relative to an α–tubulin-*Renilla* luciferase reference. Error bars indicate standard deviations from three independent transfections. The wild type variant is downregulated by 4-fold in response to *myc* RNA*i*. The mutated luciferase reporter without E-Box (ΔE-Box) is rendered unresponsive to *myc* RNA*i* and is expressed at comparable levels to *myc* RNA*i* treated wild type (wt) samples.

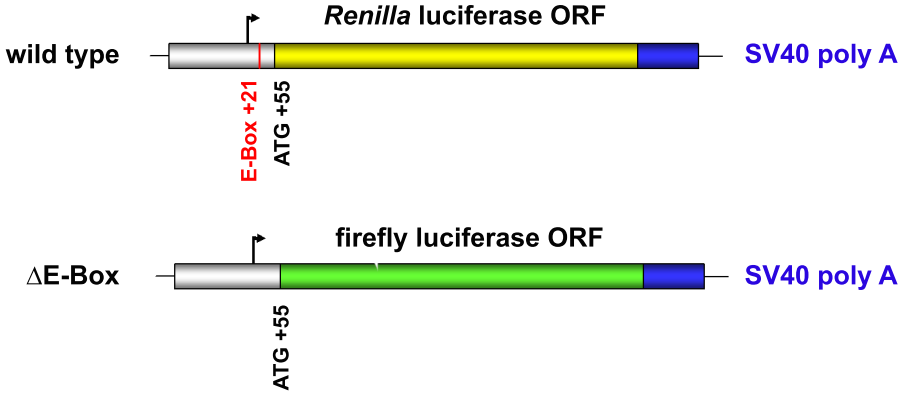

Figure 4

Schematic representation of the *CG5033*-Myc activity reporter constructs
A 390 bp fragment of the wild type promoter from the Myc-activated target gene *CG5033*, including 55 bp downstream of the transcription start site, was fused to the *Renilla* luciferase ORF, with translation of the luciferase starting at the ATG of CG5033. The single E-Box within the promoter is located 21 bp downstream of the transcription start site. The ΔE-Box firefly luciferase variant serves as an internal control to monitor basal activity of the promoter. The regulatory sequences of the two reporters are identical except for the absence of the E-Box in the ΔE-Box firefly reporter. The schematic is not drawn to scale.

In addition to the two Myc activity reporters mentioned above (*nnp-1* and *CG5033*), which both contain a single E-Box in their promoter region downstream of the transcription start site, we also tested another Myc activity reporter with a different E-Box pattern. *CG4364*, whose vertebrate homologue *pescadillo* is also involved in rRNA processing, does not possess a downstream E-Box in its regulatory region but a putative Myc binding site at position -421 relative to the transcription start. After site-directed mutagenesis of the E-Box the reporter was still responsive to changes in Myc levels, possibly due to redundantly acting variant Myc binding sites at position -261 (of the sequence CATGCG) and at position +15 (CACGCG) which both retained their function. It was shown for c-Myc that not only the core E-Box sequence CACGTG but also variants thereof (CANNTG) are bound by Myc/Max dimers (Luscher and Larsson, 1999). We refrained from mutating these E-Boxes, as the wildtype *CG4364* reporter could only be repressed about two-fold by *myc*-RNA*i*; a readout we deemed not sensitive enough for our purposes (Figure 5a). In contrast to the functional luciferase reporters containing the regulatory region of either one of the positive Myc target genes *nnp-1*, *CG5033* or *CG4364*, a construct carrying regulatory sequences of *mfas* (midline fasciclin; a gene involved in axonogenesis that is repressed by Myc (Bellosta et al., 2005; Orian et al., 2003)) was unresponsive to changing Myc levels (Figure 5b).

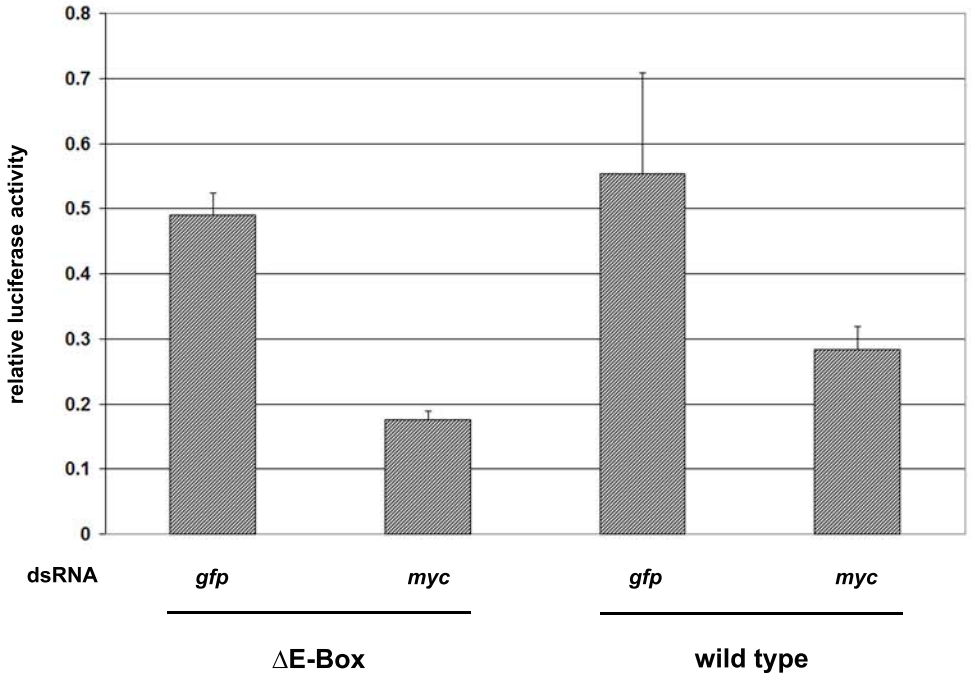

Figure 5a

***CG4364*-luciferase reporter activity** 24 hours after RNA*i* against *myc* or *gfp* as a control. All values are calculated relative to an α–tubulin-*Renilla* luciferase reference. Error bars indicate standard deviations from three independent experiments. Both the wild type and mutant luciferase reporter variants are responsive to *myc* RNA*i* treatment. The responsiveness of the ΔE-Box variant is most probably due to redundantly acting non-canonical E-Box variants at positions -261 and +15 relative to the transcription start site.

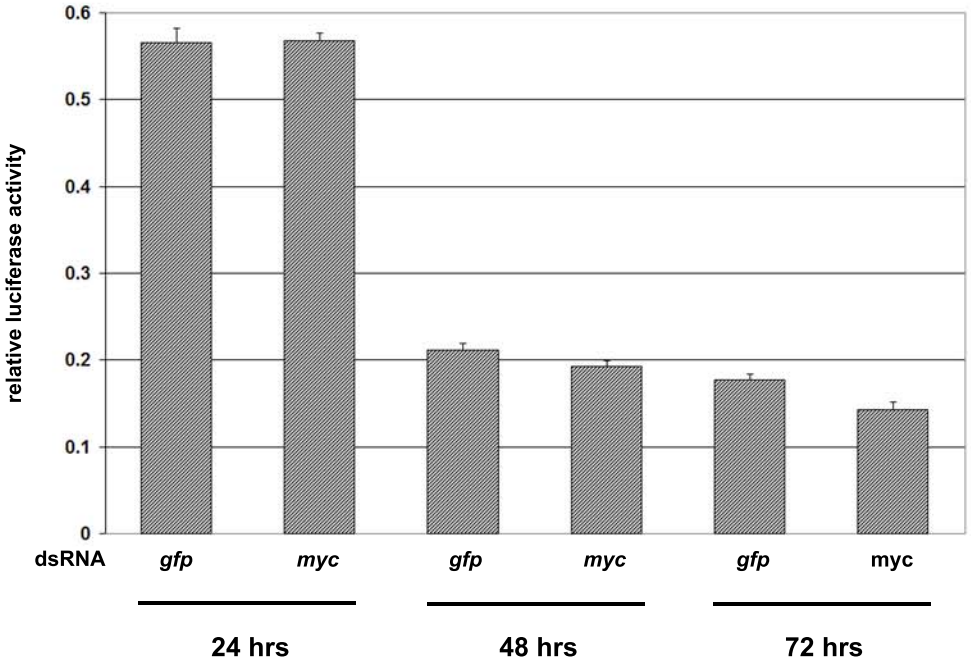

Figure 5b

***mfas*-luciferase reporter activity.** The activity of a luciferase reporter gene under the control of the promoter of the Myc-repressed gene midline fascicline *(mfas)* was measured 24, 48 and 72 hours after RNA*i* against *myc* or *gfp* as a control. The promoter sequences ranges position -861 to +503 relative to the transcription start site. All values are calculated relative to an α–tubulin-*Renilla* luciferase reference. Error bars indicate standard deviations from three independent experiments.

1.2. Screening of a preselected candidate pool using a Myc-dependent reporter system

Based on the previous experiments with the constructed Myc activity reporters, in which we compared the expression levels of wildtype promoter containing vs. ΔE-Box luciferase constructs (at various timepoints 24, 48 and 72 hours after addition of dsRNA), we chose to use the *CG5033* reporter pair over the *nnp-1* constructs for the initial screen of the selection of double-stranded RNAs. While the *CG4364* ΔE-Box reporter still responded to changing *myc* levels and therefore was not suitable for our purposes, both the *CG5033* ΔE-Box and *nnp-1* ΔE-Box constructs are unresponsive to *myc*-RNA*i*. However, the *CG5033* Myc activity reporter constituted a more sensitive system as the wild type variant could be downregulated 3 to 4 fold upon RNA interference (RNA*i*) against *myc* as compared to 1.5 to 2.5 fold in the case of *nnp-1* (Figures 6a & 6b).

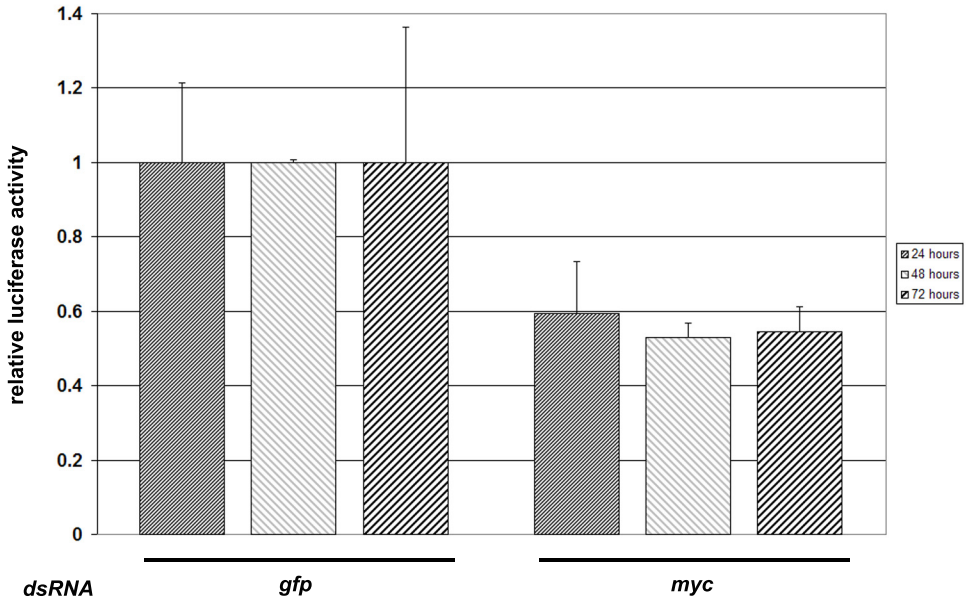

Figure 6a

Relative luciferase reporter expression of the *nnp-1*-Myc activity reporter
The relative luciferase activity of the nnp-1 luciferase reporter pair was measured 24, 48 and 72 hours after RNA*i* induction against *myc* or *gfp* as a control. All values are calculated relative to the ΔE-Box luciferase reporter reference. Error bars indicate standard deviations from three independent experiments. Upon *myc* depletion the luciferase activity is reduced by roughly 1.5 fold for all three timepoints.

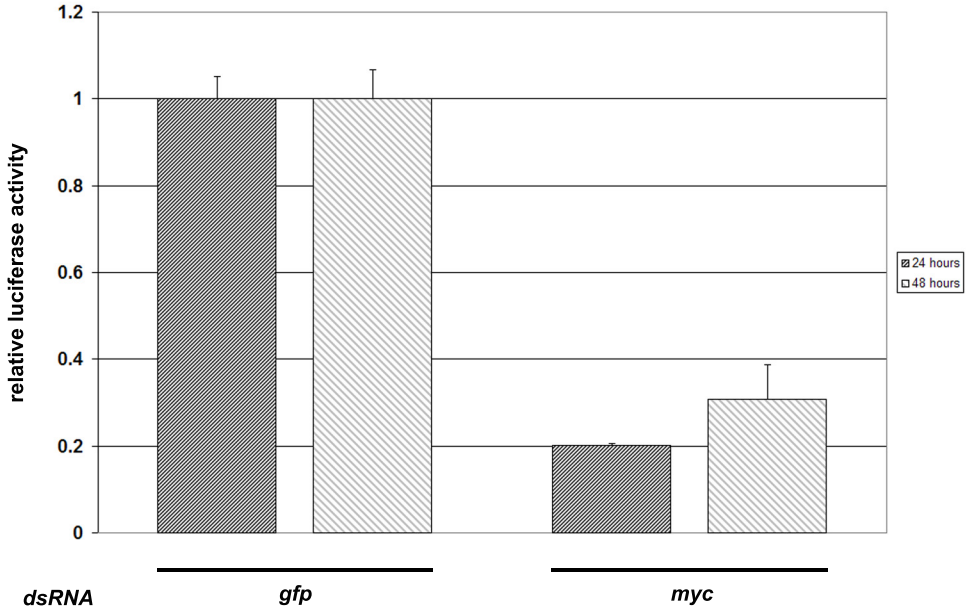

Figure 6b

The *CG5033*-Myc activity reporter is more sensitive to myc RNA*i* than the *nnp-1* reporter
The relative luciferase activity of the *CG5033* luciferase reporter pair was measured 24 and 48 hours after RNA*i* induction against *myc* or *gfp* as a control. All values are calculated relative to the ΔE-Box luciferase reporter reference. Error bars indicate standard deviations from three independent transfections. Depletion of *myc* leads to a repression of luciferase activity of 4 to 5-fold.

As we were interested in identifying physiological cofactors of Myc involved in transcription control and to minimise the scale of the screen, we chose not to carry out a genome-wide RNA*i* screen but rather focused on a subset of 752 preselected candidates. The selection was compiled of proteins that are known to be associated with transcription because of earlier reports, or because their gene ontology (GO) annotation placed them into transcription-related processes. Furthermore, the list contained a number of factors that were known to be involved in Myc-dependent processes in various model organisms and/or to interact with Myc genetically or physically. Examples of factors in this subset are Gcn5 (Grant et al., 1997; McMahon et al., 2000; Patel et al., 2004) a histone acetyltransferase known to be the catalytic subunit of both the SAGA and ATAC1 histone acetyltransferase (HAT) complexes (Grant et al., 1997; Guelman et al., 2006), and TRRAP (**TR**ansactivation/ t**R**ansformation **A**ssociated **P**rotein), a component of several histone acetyltransferase (HAT) complexes (McMahon et al., 1998; McMahon et al., 2000; Bouchard et al., 2001). Both proteins were identified to interact with the transactivation domain of the Myc protein. Additionally, the Tip60 DNA-helicase/ATPases Tip48/Reptin and Tip49/Pontin, which had been identified as c-Myc interacting proteins in vertebrate tissue culture cells (Wood et al., 2000), and were later shown to interact genetically with Myc in *Drosophila* (Bellosta et al., 2005) and *Xenopus* (Etard et al., 2005), the elongation factor p-TEFb (Eberhardy and Farnham, 2001; Kanazawa et al., 2003), or components of the BRM chromatin-remodellling complex (Cheng et al., 1999) were included. In addition to this group of "characterised" putative cofactors, a second tier of candidates containing known components of "transcription-associated" complexes like transcription initiation or elongation factors, histone-modifiers like acetyltransferases or methylases, chromatin remodellers or enzymes of the ubiquitination-machinery was included in the list (e.g. trx, Iswi, or Taf2). A third subset of poorly characterised or uncharacterised proteins was added based on their gene ontology (GO) annotation. Within this group fall a large number of the computed genes (CGs), which have not been fully characterised and were predicted to be involved in transcription. Finally a number of handpicked candidates were also included in the list. One example for a handpicked candidate is the sequence-specific transcription factor E2F. It was included in the list because it was shown that activating E2F proteins and Myc share common target genes (Grandori et al., 2000), which might indicate a concerted control of certain targets. However, in general we omitted sequence-specific transcription factors from the screen, since the use of the E-Box/ΔE-Box system ensured a strictly Myc-dependent readout. Furthermore, an inclusion would have significantly increased the number of candidate factors. Since there is no significant sequence conservation among Myc target gene promoters (except for E-Boxes) we would expect sequence-specific transcription factors to affect only the expression of a limited number of targets, whereas the screen was designed to identify general cofactors of Myc.

For all of the 752 selected candidates sequence specific primer pairs, which allow for the amplification of gene-specific amplicons of an average length of 400 base pairs, were ordered from Eurogentec. The design of the oligonucleotides was based on the BDGP annotation of the *Drosophila melanogaster* genomic sequence v2.0 and excluded predicted homology regions between individual *Drosophila* proteins (e.g. of a related protein family). Primary PCR products were amplified using genomic *Drosophila* DNA as template. Furthermore, universal sequences were added to the primers

that permitted re-amplification of the primary products. All 3'-primers contained the same tag sequence, while 5'-primers contained 9 different sequences. Therefore, the whole set of sequence-specific amplicons could be re-amplified using only 9 primer pairs. The secondary primers used for re-amplification also contained a 5' 23bp T7 promoter sequence, resulting in PCR products with T7 promoter sequences added to both ends of the amplicons. These were subsequently used as templates for the generation of dsRNA by phage T7 RNA polymerase. The whole amplification procedure was carried out by P. Zipperlen (Group of Prof. K. Basler) and was done in an automated fashion in 96-well plates using a pipetting robot.

1.3. Screening procedure and candidate selection

dsRNA against all the 752 candidates was transferred to 96-well plates and transiently transfected into *Drosophila* S2 cells together with the two *CG5033*-Myc activity reporters. After an incubation period of 60 hours, individual luciferase values were measured. This screen procedure was carried out twice for the whole set of candidate genes. Individual plates were selected for a second repetition, since they showed a slight but systematic regional bias across the plate. Within every single sample plate *myc* dsRNA was plated into 8 sample wells as a positive control for the functionality of the transfection procedure. Furthermore, this also provided an estimate of the variation of transfection efficiency between the individual plates. Subseqently, the ratio between the firefly and *Renilla* luciferase expression levels for each transfected dsRNA sample was calculated. For the initial screen runs we determined the ratios by dividing ΔE-Box by wild type reporter values. Later on, the reporter ratios were determined reciprocally since they then directly reflect Myc activity, rather than being inversely proportional to Myc activity. To determine the RNA*i* samples that lead to a significant change in luciferase expression ratio, we first calculated the difference between the ratio of each experimental well and the average ratio of all the samples within the same sample plate. Next, we assessed the z-score for each sample by dividing the resulting values by the standard deviation of all experimental values of a single plate; this revealed 80 genes to have an influence on the Myc activity reporter system. Forty-five of the 80 dsRNAs included in this second candidate list lead to an upregulation of the wildtype reporter, while the ΔE-Box reporter remained unaffected, (this results in a decrease of luciferase ratio), and 35 lead to a repression of the wild type reporter gene (increase of the luciferase ratio). In the list we included candidate dsRNAs that either had a considerable effect in both screen runs (for some samples all the 3 runs) or that showed a large change in expression ratios in one single screen run.

For the secondary screen, all the 80 dsRNA species were freshly replated, and 8 *myc* dsRNA samples (positive control) and 8 *gfp* dsRNA samples (negative control) were included per 96 well plate. After screening the subset, the difference between each experimental luciferase ratio and the average *gfp* ratio per plate was determined. Out of these 80 dsRNAs 33 changed the reporter activity by at least 1.5 fold as compared to *gfp*-RNA*i*: 19 dsRNAs had a Myc-like effect, 14 lead to an activation of the reporter (Table 1).

A number of 33 significant modulators of the Myc activity reporter out of a total number of 752 candidates tested corresponds to 4.5 % specific "hits", which suggests high specificity of the screen,

even more so as a biased preselection of candidates was used. Further evidence that the screen allowed us to find specific Myc-interactors came from the rescreen of the last 33 candidates with *nnp-1* luciferase reporters which gave a considerable overlap of the upregulating factors with the screen. Most prominently three components of the Polymerase-associated factor 1 complex (PAF), the PAF-associated factor Spt6, and the deacetylase Sin3A were positively identified with both reporter variants. The Myc-activating factors (i.e. the downregulators of the Myc activity reporter), however, were not picked up with the significance criteria used in the screen, which is due probably to the reduced sensitivity of the *nnp-1* reporter compared to *CG5033*. However the strongest downregulators of the screen (i.e. several components of the 19S proteasome regulatory complex) reduced the reporter activity to about the same extent as Myc itself.

Finally, 7 candidates influence both the wildtype and ΔE-Box luciferase expression levels and therefore they might affect transcription in a manner that is not strictly Myc-dependent.

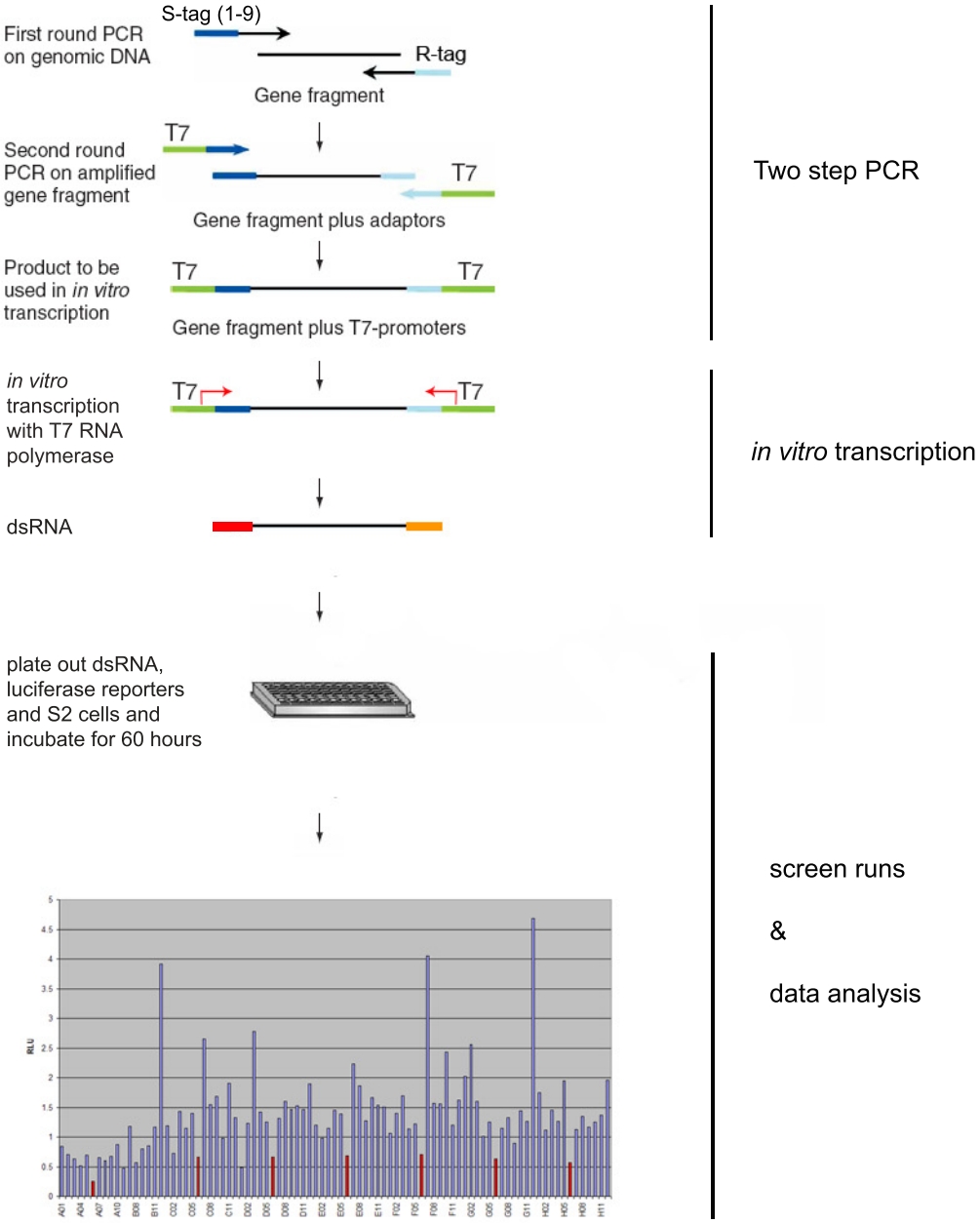

Figure 7

Schematic overview of the RNA interference screening procedure.
Gene-specific amplicons of an average length of 400 base pairs were generated in a first PCR round. Resulting products were reamplified in a second PCR step, using oligonucleotides with complementary sequences to the R- and S-tags of the primary PCR. In addition, primers for the second PCR step contained T7 polymerase promoters, allowing for *in vitro* transcription with T7 RNA polymerase. 1μg of dsRNA per screen candidate was transferred to 96 well plates and cotransfected into S2 cells together with Myc-dependent luciferase reporter constructs. Cells were incubated for 60 hours, lysed, and luciferase activity was measured.

Table 1

Final screen candidate List

Gene	wild type	mutant	Ratio (wt/mutant)	fold change (GFP)	impact on mutant	nnp-1
su(s)	92.7	14.9	6.2	6.4	1.5	+
hyrax	12.1	3.6	3.4	3.5	0.4	+
His4	3.7	1.1	3.3	3.4	0.1	+
His3	2.8	0.9	3.0	3.1	0.1	-
Sin3A	7.5	2.9	2.5	2.6	0.3	+
Trf2	14.2	5.9	2.4	2.5	0.6	+
D19A	7.7	3.4	2.3	2.3	0.3	+
Spt6	11.0	5.2	2.1	2.2	0.5	+
Ctr9	12.6	6.4	2.0	2.0	0.7	+
Atms	13.9	7.5	1.9	1.9	0.8	+
su(z)2	1.1	0.6	1.8	1.9	0.1	-
E2f	17.5	10.2	1.7	1.8	1.0	-
sima	1.5	0.9	1.6	1.6	0.1	+
Med21	0.5	0.3	1.6	1.6	0.1	+

A Repressors of the Myc activity reporter

Gene	wild type	mutant	Ratio (wt/mutant)	fold change (GFP)	impact on mutant	nnp-1
CG17181	4.7	18.2	0.3	0.3	1.8	-
Rpn2	3.4	12.4	0.3	0.3	1.3	-
Rpn5	6.4	19.4	0.3	0.3	2.0	-
Rpn7	3.6	10.0	0.4	0.4	1.0	-
Rpn12	6.7	18.5	0.4	0.4	1.9	-
Rpn6	1.5	4.1	0.4	0.4	0.4	-
symplekin	8.4	23.3	0.4	0.4	2.4	-
cdk8	12.0	32.7	0.4	0.4	3.3	-
myc	**1.5**	**3.8**	**0.4**	**0.4**	**0.3**	-
Rpn11	2.4	5.8	0.4	0.4	0.6	-
Snr1	7.1	16.5	0.4	0.4	1.7	-
ro	2.1	4.1	0.5	0.5	0.4	-
Prosβ3	1.2	2.4	0.5	0.5	0.2	-
vnd	7.4	14.6	0.5	0.5	1.5	-
Hcf	9.4	17.7	0.5	0.5	1.8	-
Asx	8.4	15.0	0.6	0.6	1.5	-
Neu2	7.7	12.8	0.6	0.6	1.3	-
tgo	7.7	12.5	0.6	0.6	1.3	-
CrebB-17A	11.7	18.8	0.6	0.6	1.9	-
zfh1	6.3	10.1	0.6	0.6	1.0	-

B Activators of the Myc activity reporter

Table 1
Final candidate list of the RNA*i* screen with the *CG5033*-driven Myc activity reporter. Panel A shows the 14 dsRNA repressors of the Myc activity reporter, Panel B the 19 dsRNA activators identified in the screen. Expression levels of the wild type *Renilla* luciferase and the ΔE-Box firefly luciferase are given in arbitrary units. Columns 3 and 4 depict the ratios between the wild type and mutant luciferase reporters and the comparison to the *gfp* control dsRNA. The 5 column gives an estimateof the influence of the RNA*i* on the mutant ΔE-Box reporter (ratio between the individual ΔE-Box reporter expression compared to the average firefly expression). The candidates highlighted in redwere further characterised in the course of this study. The factors highlighted in grey also significantlyinfluence the expression of the mutant reporter construct. The last column summarises the findings from a tertiary screen, in which the candidates were retested with the *nnp-1* Myc activity reporter. Candidates also identified with this reporter are marked with (+), factors that were not identified are marked with (-).

2. Candidate overview

Of the 752 dsRNAs against transcription-associated factors tested, we identified 33 as significant modulators of the Myc activity reporter system. RNA*i* against 14 of these factors lead to an increase in the ratio between the expressions of the two experimental reporter genes. In five cases (histone 4, histone 3, Su(z)2, sima, Med21) this shift of the ratio was mostly due to their influence on the Myc-unresponsive ΔE-Box reporter. These five factors might therefore act, at least partially, in a Myc-independent manner. This leaves nine candidates which act as specific repressors of the reporter system (Table 1). Within this group of nine significant repressors of the Myc activity reporter are three homologues of PAF complex subunits in yeast and vertebrates and one PAF-complex associated factor. This suggests that the Drosophila version of the PAF complex as a whole plays a role in controlling the Myc activity reporter. This finding prompted us to focus on the characterisation of the PAF complex. The three PAF complex components identified in the RNA*i* screen are the following: Hyrax (Hyx) (which corresponds to CG11990; homologous to the yeast protein Cdc73), Ctr9 (also termed CG2469), and Antimeros (Atms) (also called dPaf1 or CG2503). Furthermore, another Paf complex associated factor Spt6 was identified in the screen.

In addition to the 14 repressing factors we also identified 19 positive regulators of the system. RNA*i* against these factors leads to a downregulation of the reporter expression. Two of the positive factors (cdk8 and CG2097, which is also termed Symplekin) have a considerable influence on the ΔE-Box reporter, suggesting that they (partly) influence the reporter expression independently of Myc, analogous to the situation observed with histone 3 and 4. Of the remaining 17 factors, 6 of the most potent regulators are components of the 19S regulatory subunit of the 26S proteasome. Another factor within the list of downregulators we concentrated on, is HCF (Host cell factor), an abundant chromatin-associated protein, whose mammalian homologue was originally identified for its role in the propagation of Herpes simplex virus upon infection. The characterisation of HCF was largely carried by Mirjam Balbi during her master thesis.

3. Proteasome components

Of the 10 known eukaryotic non-ATPase subunits that are comprised in the 19S regulatory complex of the proteasome (Pickart and Cohen, 2004; Holzl et al., 2000) eight were included in the original RNA*i* screen candidate list (Rpn1, Rpn2, Rpn5-7, Rpn9, Rpn11 & Rpn12; **r**egulatory **p**article **n**on-ATPase). Six of these eight (75%; all except Rpn1 and Rpn9, which is also known as Rpn4) were found to belong to the strongest modulators of the *CG5033*-Myc activity reporter. Downregulation of the Rpns led to significant repression of the reporter activity to 28-42% of the average reporter activity upon *gfp* control RNA*i* (see final candidate list Table 1 and Figure 8). This finding was unexpected as downregulation of proteasome components decreases protein turnover and therefore might increase the level of active Myc protein in a cell, as Myc has been shown to be a target of the ubiquitin-mediated proteolysis machinery (Gregory and Hann, 2000; von der Lehr et al., 2003). On the other hand it has been reported that poly-ubiquitination, and thereby priming for later destruction, is one of the necessary steps for the full activation of several transcription factors, including Myc (reviewed both in Muratani and Tansey, 2003; Weake and Workman, 2008). To determine whether the effect on the luciferase expression caused by *rpn*-RNA*i* is due to influences on Myc protein levels, we treated Schneider 2 (S2) cells with dsRNA against *gfp*, and the various *rpns* found to be modulators of the reporters and assessed if Myc protein levels were changed. The corresponding Western blot in Figure 9 was probed with anti-dMyc hybridoma supernatant and anti-α-tubulin as a loading control. No obvious changes in the abundance of endogenous Myc protein in response to RNA*i* against the proteasome components are seen as compared to treatment with *gfp* control dsRNA. Therefore, the reduced expression of the luciferase reporter genes is not due to reduced Myc protein levels.

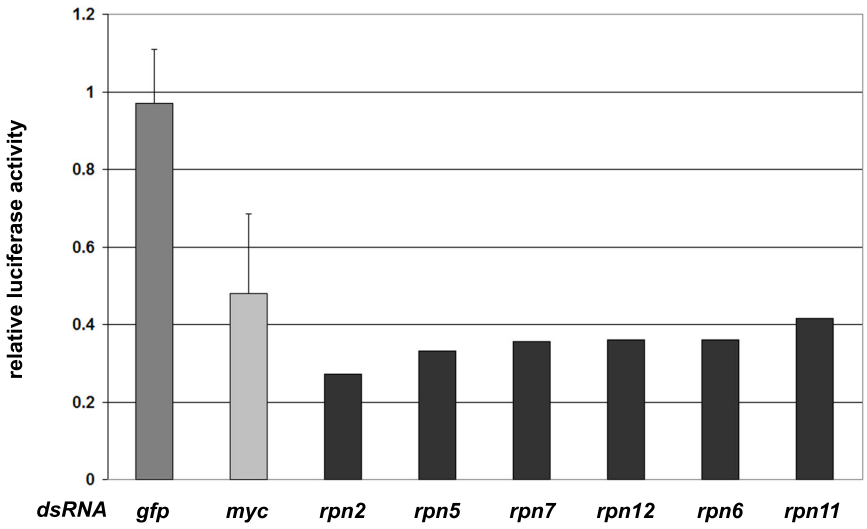

Figure 8

Luciferase assay upon downregulation of components of the 19S proteasome regulatory complex. Recapitulation of the RNA*i* screen results. Depicted are the effects of RNA*i*-mediated downregulation of the 6 non-ATPase 19S RC subunits identified in the screen. Values represent single measurements and were taken from the rescreen with the *CG5033*-driven Myc activity reporter. Luciferase measurements were performed 48 hours after induction of RNA*i*. Error bars for the *gfp* and *myc* samples indicate standard deviations from 8 independent samples.

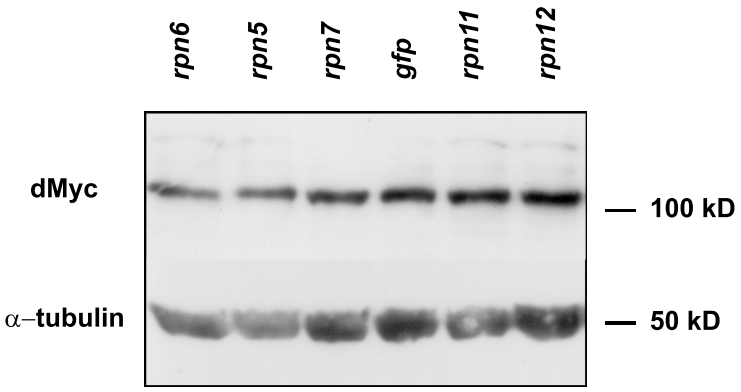

Figure 9

Myc protein levels are not affected by RNA*i* against components of the 19S regulatory complex. Western blot of S2 whole cell lysates treated with dsRNA against 19S RC components; Incubation time 48 hours. One lane corresponds to the cell lysate of roughly 2.5 million cells. The levels of α–tubulin were taken as a loading control. Antibodies used: mouse anti-dMyc; mouse anti-α-tubulin.

3.1. The *Drosophila* eye is sensitive to downregulation of 19S proteasome components

Since RNA*i* against the majority of the 19S proteasome components included in the screen (75%) led to a significant downregulation of the Myc activity reporter, we tested whether reduction of *rpn* levels also caused specific phenotypes *in vivo*. For this purpose we examined if reduction of Rpn proteins resulted in dominant genetic interactions with the hypomorphic myc allele dm^{P0}. The dm^{P0} allele is caused by a P-element insertion into the *myc* promoter, which results in reduced *myc* expression. dm^{P0} had been found to show a strong genetic interaction with the essential Myc cofactor Tip49/Pontin (Pont) (Bellosta et al., 2005). The interaction of *myc* with *pont* is essential for tissue growth *in vivo* and it is manifested by a prolonged duration of development, reduced survival rates, and decreased size of adult animals in flies that are hypomorphic for *myc* and heterozygous for *pont* (Bellosta et al., 2005). Most strikingly, these animals have small, irregularly shaped, and slightly rough eyes (Bellosta et al., 2005). Interestingly, the same eye defect occurs in dm^{P0}/Y males at a very low frequency, but its prevalence is enhanced upon mutation of one *pont* allele (Bellosta et al., 2005). Based on these observations, we examined the eye phenotype of dm^{P0} flies with reduced *rpn* levels, as the eye seems to be particularly sensitive to a reduction of Myc activity. To analyse a potential interaction between *myc* and the proteasome components (and also other interactors found in the screen) we used flies of the following genotype: *w* dm^{P0} *tub>myc>GAL4 ey-flp*. These animals carry the hypomorphic allele dm^{P0} but the mutant phenotypes are rescued by the ubiquitously expressed *myc* cDNA under the control of the *tubulin*-promoter. The *myc* cDNA-transgene is flanked by FRT sites, which allow for recombination with each other when FLP-recombinase is expressed. Since the *eyeless* promoter is used to drive the FLP-recombinase expression, the *myc* cDNA will be eliminated in the whole head capsule, including the eyes. Thus, the hypomorphic dm^{P0} phenotype will only be revealed in these tissues. This line will be called *ey>*dm^{P0} for simplification.

Four classical alleles of the Rpn genes identified in the screen were available from the Bloomington stock collection. Three alleles of *Rpn6/proteasome subunit p44.5* and one allele of *Rpn11/p37B*, which codes for a de-ubiquitinating enzyme (Holzl et al., 2000). $Rpn6^{2F}$ (loss of function; recessive lethal 1901 bp deletion that removes putative upstream regulatory sequences, the complete 5' UTR and the first 145 codons) and $Rpn6^{20F}$ (hypomorph; recessive lethal; imprecise excision, leaving P-element sequences at the insertion site; *Rpn6* coding sequences intact), which are both imprecise excisions of the original insertion $Rpn6^{k00103}$, had no effect on the eye phenotype of *ey>*dm^{P0} animals. However, $Rpn6^{k00103}$ itself led to eye defects that resemble the ones observed in dm^{P0}*/Y;* $pont^{-/+}$ in 33.3% of the males tested (3/9). In contrary, the only available *Rpn11* allele $Rpn11^{BG01694}$ (a recessive lethal P-element insertion generated by the Gene Disruption project) showed no interaction with dm^{P0}. In addition to their ability to interact with *ey>*dm^{P0} we also tested whether the *Rpn* mutants modulated the eye phenotype of Myc overexpressing *y w; GMR-GAL4 UAS-*myc^{132}*/+; UAS-*myc^{132} *UAS-*myc^{42}*/+* flies. Flies of this genotype highly overexpress Myc in the eye. This leads to an increase of ommatidial size by more than 20% and disruption of the regular ommatidial pattern, which results in a rough eye phenotype. In only two (out of 30-50 animals examined), the P-element insertions $Rpn6^{k00103}$ and $Rpn11^{BG01694}$ led to a suppression of the Myc overexpression phenotype, where the eyes resembled wild type control eyes, concerning size, texture and pigmentation.

We also tested whether RNA*i* lines against the Rpn proteins, available from the Vienna *Drosophila* RNA*i* Center (VDRC), interact genetically with *myc* in a hypomorphic situation. This allows us to assess the effect of potentially stronger reduction-of-function mutants than observed with heterozygosity for *Rpns*. Indeed, six of the seven lines tested showed a strong interaction in the *ey>dm*^{P0} background. RNA*i* against *Rpn5* only had a moderate effect. Taken together, downregulation of the proteasome components by RNA*i* caused severe defects of the eye structure. With a penetrance of almost 100% the eyes became smaller, showed an irregular shape due to loss of a large number of ommatidia, or were completely missing. As a comparison, RNA*i* in a *myc* wildtype background caused only mild defects. The eyes were slightly reduced in size (as judged by inspection under the dissecting microscope) and had a mild rough eye phenotype.

While 6 of the 19S regulatory complex subunits belonged to the strongest interactors in the RNA*i* screen (knockdown of the reporter by about 3-4 fold), the classical mutants of *Rpn6* and *Rpn11* interacted very moderately in *myc* hypomorphic and overexpression backgrounds. Conversely, six of seven RNA*i* lines tested, lead to eye defects with almost complete penetrance. The most obvious explanation is that even in the case of complete loss of function, still 50% of the gene product are present in a heterozyous mutant *rpn6* or *rpn11* fly, whereas downregulation by RNA interference, although it is never complete, probably leads to a larger reduction. Concluding from the few results obtained, there seems to be a considerable genetic interaction between these factors and *myc*. Since we focussed our investigations on other Myc interactors found in the screen, we only scratched the surface of the potential interaction between the 19S proteasome components and *myc*. For a thorough characterisation more *in vivo* interaction data and biochemical analyses are necessary.

4. *Drosophila* Host cell factor (HCF)

4.1. Overview

The following part of the project concerning the interaction between Myc and HCF was mainly carried out by Mirjam Balbi, a Master Student, under my supervision. In her Master thesis (Balbi, 2007), an in depth characterisation of the interaction between Myc and *Drosophila* host cell factor (HCF) has been described. This section gives a brief summary of the performed experiments, and some more recent results are included at the end.

Found as a negative regulator in the initial RNA*i* screen, HCF seems to be required for full transcriptional activity of Myc in S2 cells. Experiments with two additional independent dsRNAs against HCF ruled out that RNA*i* off-target effects are responsible for the observed reporter knock-down to approximately 60% compared to *gfp* control RNA*i*, and thereby corroborated HCF's role as a putative cofactor of Myc (Figure 10). It was also shown that RNA interference with all the dsRNA variants efficiently induced *hcf* degradation for HCF protein levels were undetectable on Western blots at 48 hours after dsRNA addition (Figure 11). Myc protein levels however, remain unchanged by *hcf*-RNA*i* (see Results section 4.2.). This fact suggests that HCF modulates Myc activity, rather than its abundance. Ectopic expression of HCF under the control of an *actin*-promoter highly activated reporter gene expression (Figure 10). This boost of luciferase expression to approximately 300% is well above the effect observed upon Myc overexpression, which is indicative of the limiting nature of HCF under physiological conditions. Moreover, the influence of HCF overexpression is dependent on Myc as it can be suppressed by either *myc* (or *hcf*) –RNA*i* (data not shown). The effect of *hcf*-RNA*i* was not restricted to the used artificial reporter system since qRTPCR measurements revealed that HCF is also required for the correct expression of selected endogenous Myc target genes transcribed by RNA Polymerase II (see Results section 4.2.). Taken together Myc requires HCF for proper transcactivation of its targets in S2 cells.

Coimmunoprecipitations between overexpressed HCF and Myc revealed a physical interaction of the two proteins (Figure 12). The *Drosophila* Myc protein was found to contain a conserved four amino acid HCF-binding motif (HBM) of the sequence DHSY (consensus sequence D/EHxY). The HBM was identified in VP16 and its cellular counterpart LZIP (Freiman and Herr, 1997), and was also shown to be of importance in the E2F-family of transcription factors (Tyagi et al., 2007). The HBM motif is located in the central part of the Myc protein (aa 387-390). Surprisingly, the HCF binding motif (HBM) present in Myc is dispensable for the physical association with HCF, since a mutant form lacking the HBM also interacts with HCF (data not shown). This contrasts with several other HCF-associated proteins that require the HBM for interaction. In order to map the HCF interaction site(s) within the Myc protein, various Myc truncations were generated and examined for their ability to associate with HCF. None of the known conserved domains in Myc, neither Myc-Boxes 1-3 (MB1-3), nor the C-terminal basic helix-loop-helix zipper region are required for stable association between Myc and HCF. Since these experiments revealed a central stretch of Myc (from amino acids 179 to 403) to interact most strongly with HCF, it is therefore likely to contain an interaction site. Furthermore, coimmunoprecipitations and GST-pulldown experiments suggest that additional regions in Myc can

provide contact to HCF. These weaker interaction sites are located between aa 176-295 and in the C-terminal part of Myc between aa 523-626 respectively (data not shown).

All experiments described above suggest that HCF is an essential cofactor of Myc. To examine the physiological importance of the observed interaction *in vivo* experiments were carried out. Induction of *hcf*-RNA*i* in the dorsal compartment of the wing by expressing *hcf*-dsRNA under the control of *apterous*-Gal4 led to a moderate aberrance of the wing morphology as additional vein tissue was present between longitudinal veins L1 and L2. Far more pronounced was the ability of *hcf*-RNA*i* to revert the wing defects caused by Myc overexpression. Elevated Myc levels in the *apterous* expression domain result in overgrowth of the dorsal wing compartment. This is manifested by a slight bent-down phenotype. Additionally, the majority of the animals display severely disturbed wings. The two wing blade epithelia do not adhere to each other anymore. As a consequence fluid-filled bubbles between the epithelial sheets are formed. In older flies the affected wings become necrotic. Strikingly, both the overgrowth phenotype and the severe defects caused by Myc overexpression are strongly suppressed by *hcf*-RNA*i* (Figure 13). A similar suppression of the Myc overexpression phenotype was also observed after RNA-mediated knock-down of Ash2 and Gcn5, which are both published cofactors of Myc. In addition to its effect on Myc activity in adult wings, HCF also restricts the size of Myc overexpressing clones in imaginal wing discs as well as the nuclear size in polyploid salivary gland tissue. In both tissues *hcf*-RNA*i* significantly decreases the size of Myc overexpressing clones without strongly affecting control clones (data not shown). More evidence that HCF is indeed a physiologically relevant cofactor of Myc's, comes from experiments in which the size of ommatidia in the *Drosophila* eye were measured. As in the other tissues examined, *hcf*-RNA*i* led to a significant size reduction in ommatidia in which Myc is overexpressed and to a lesser extent in eyes with endogenous Myc levels (Figure 14). Consistent with these observations, co-overexpression of HCF and Myc has a synergistic effect on ommatidial size, whereas overexpression of HCF alone has no effect on ommatidial size (Figure 15)

Since neither Myc nor HCF possesses intrinsic enzymatic activities, other coactivators have to provide the enzymatic function in order to achieve transcriptional modulation. Therefore, we tried to identify the enzyme [complexes] responsible for the observed activation. We focussed on complexes that were already known to play a role in transcription and that associate with HCF, as these were likely to be recruited to Myc. The three complexes examined were the ATAC histone-acetyltransferase complex, the Sin3A histone-deacetylase complex, and the Set1/Ash2 histone methyltransferase complex. By performing coimmunoprecipitations Mirjam Balbi could confirm interactions between the two ATAC components ATAC-1 and dAda2A and HCF but not between those two and Myc – which could be due to general technical problems and does not rule out an association between Myc and ATAC. RNA*i*-mediated downregulation of both ATAC complex proteins in S2 cells did not alter expression of the Myc activity reporter. Furthermore, *in vivo* interactions with Myc could not be assessed as *atac1* dsRNA fly lines were not available and *dada2*-RNA*i* caused lethality at the pupal stage when expressed under the control of *apterous*-GAL4. The only ATAC component that showed interaction in the assays tested was the acetyltransferase Gcn5. Like the other ATAC components *gcn5*-RNA*i* had no impact on the Myc activity reporter in S2 cells, but knockdown of Gcn5 in the dorsal compartment of the adult wing almost completely suppressed defects caused by ectopic Myc expression. However,

expression of a second Gcn5-RNA*i* transgene (Gcn5-T2-IR), which targets the same sequence as Gcn5-T1-IR, yielded contradictory results as it led to severe wing defects when expressed alone, but showed no suppression of the Myc overexpression phenotypes. This discrepancy is presumably due to insertion effects of the individual transgenes. Gcn5 is a shared subunit of the ATAC and dSAGA HAT complexes which makes it possible that dSAGA, and not ATAC, is the complex involved in transcription control by Myc. However, RNA*i* against the dSAGA protein Spt3 had neither an effect on luciferase expression in S2 cells nor on the Myc overexpression phentype in wings.

Second, knockdown of the histone-deacetylase associated corepressor Sin3A led to a strong activation of the Myc activity reporter and to severe defects when expressed in the adult wing. The dorsal wing compartment show marked overgrowth phenotypes when *sin3A*-dsRNA is being expressed by *apterous*-GAL4. The wings are clearly bent downwards and the attachment of the two wing epithelia is disrupted. This disruption is manifested by the formation of fluid-filled bubbles between the epithelial layers and necrotic patches on the wing. In contrast, *myc*-RNA*i* causes a bent-up wing phenotype when expressed by *apterous*-GAL4, due to reduced growth in the dorsal wing compartment. Since Sin3A-associated histone-deacetylases have been shown to be recruited to regulatory regions by the Myc antagonist Mnt, the overgrowth phenotype of the dorsal wing blade and the increase in luciferase expression most probably reflect the loss of Mnt-dependent growth gene repression upon *sin3A*-RNA*i*, which is mediated by Sin3A.

The third complex tested for its interaction with HCF and Myc looks most promising. Even though *ash2* RNA*i* only leads to a slight reduction of the Myc activity reporter in S2 cells, *ash2*-RNA*i* in the wing led to an almost complete suppression of the Myc overexpression phenotype. On the other hand overexpression of Ash2 in the wing, which has barely an effect on its own, synergises with co-overexpressed Myc, i.e. leads to most strongly affected wings.In contrast to the situation in the wing, neither effects of Ash2 up- or downregulation nor a genetic interaction with Myc could be observed in the eye. Taken together, the experiments performed to identify the cofactors of HCF involved in modulating Mc-dependent transcription control have revealed that all tested complexes had some influence on Myc-dependent processes with the Ash2/Set1 HMT being the most promising of the candidates.

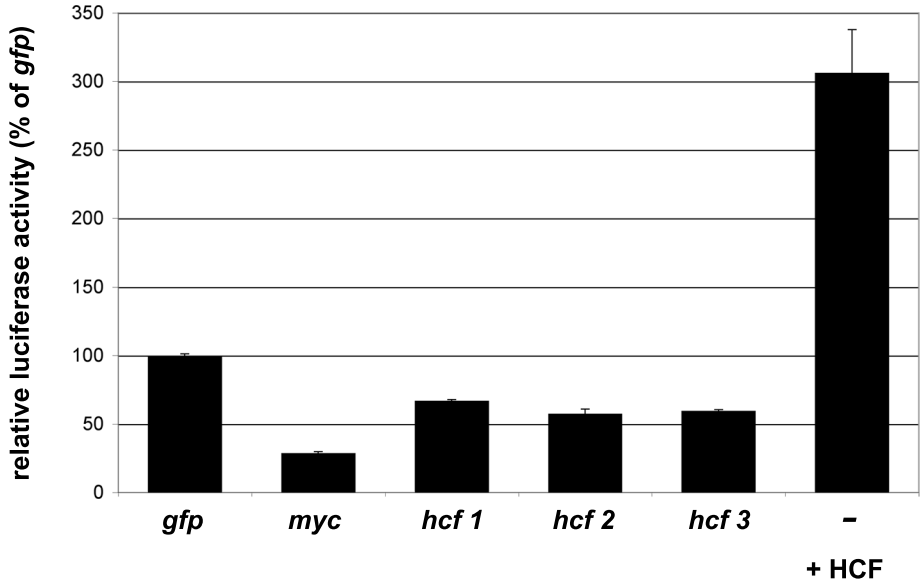

Figure 10

***CG5033*-driven Myc activity reporter is reponsive to changes in HCF levels.** Relative luciferase activities were measured 48 hours after induction of RNA*i*, and normalised to *gfp* control samples. *hcf 1-3* correspond to three independent dsRNA sequences targeting *hcf*. Error bars depict standard deviations of two independent experiments. The last column (+HCF) shows the effect of HCF-overexpression on the Myc activity reporter.

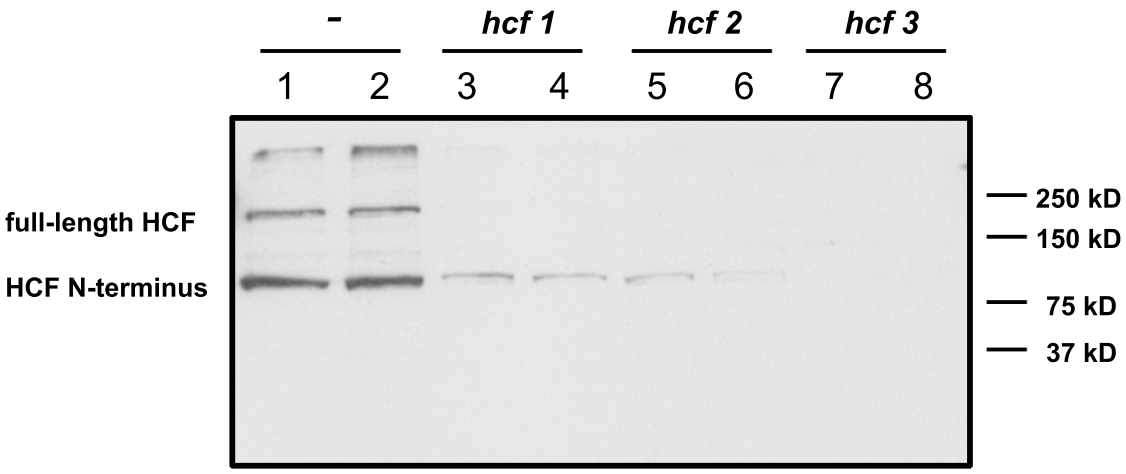

Figure 11

***Drosophila* HCF protein levels are efficiently depleted by *hcf*-RNA*i*.**
S2 cells were either transfected with a T7-tagged-HCF-overexpression plasmid alone (lanes 1 & 2), or together with one of three independent dsRNAs targeting *hcf* (lanes 3-8). After incubation of 48 hours, HCF levels are efficiently depleted by all three dsRNAs. One lane corresponds to the lysate of roughly one million cells. Overexpressed T7-HCF was detected by a mouse anti-T7 antibody. The band of roughly 120kD corresponds to the N-terminal subunit of HCF, while the 180kD signal corresponds to the unprocessed precursor protein.

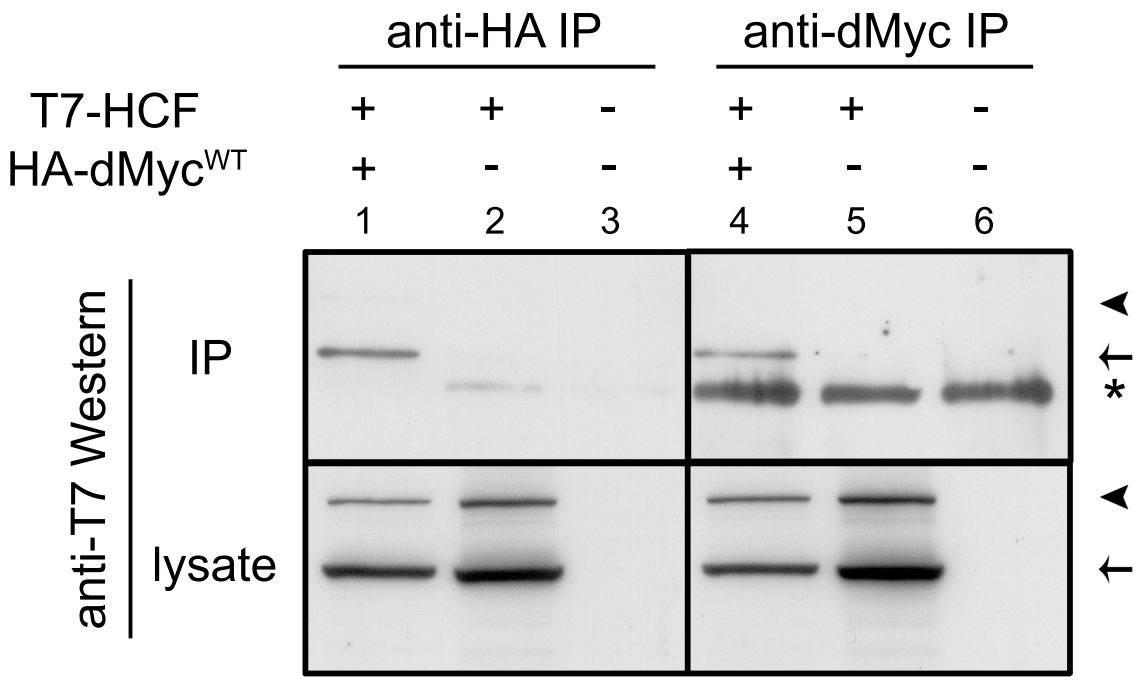

Figure 12

Coimmunoprecipitations of overexpressed HCF and Myc from S2 cells.
S2 cells were transiently transfected with HCF- and Myc-overexpression constructs. Myc was either immunoprecipitated using a mouse anti-Myc or a rabbit anti-HA antibody. Western blots were probed with mouse anti-T7 antibody (upper panel). One lane corresponds to the lysate of 2.5 million cells. HCF is specifically pulled down (with both antibodies) in the presence of overexpressed Myc. The lower panel depicts input controls, corresponding to 5% of the whole sample. Arrowheads show the unprocessed HCF precursor protein, while the arrows depict the T7-tagged N-terminal subunit of *Drosophila* HCF. Asterisk: IgG heavy chain.

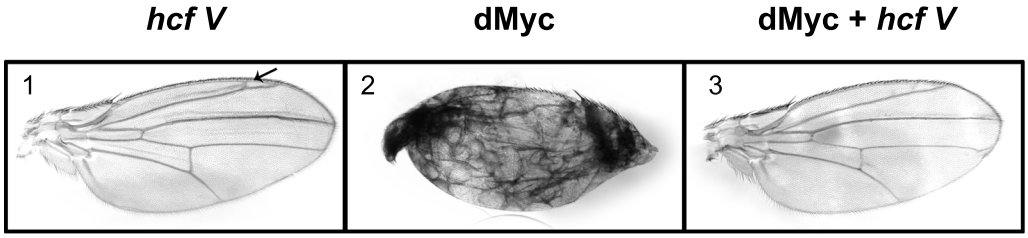

Figure 13

***hcf*-RNA*i* suppresses Myc-overexpression defects in the wing.**
A UAS-*hcf*-RNA*i* hairpin construct (*UAS-hcfV-IR*) is driven by *apterous*-GAL4 in the dorsal compartment of the wing. Panel 1: *hcf*-RNA*i* has mild effects in wings with endogenous Myc levels. The arrow points to excess vein material characteristic for wings expressing *hcf*-RNA*i* hairpin constructs. Panel 2: Myc-overexpression defects in the wing. Epithelial layers are partly detached and fluid-filled bubbles form; often wings become necrotic. Panel 3: suppression of the Myc-overexpression defects by coexpression of *hcf*-RNA*i*. Genotypes: Panel 1: *yw; ap-GAL4/+; UAS-hcf V-IR/+* Panel 2: *yw; ap-GAL4 UAS-Myc/+*; *lacZ-IR/+* Panel 3: *yw; ap-GAL4 UAS-Myc/+; UAS-hcf V-IR/+*

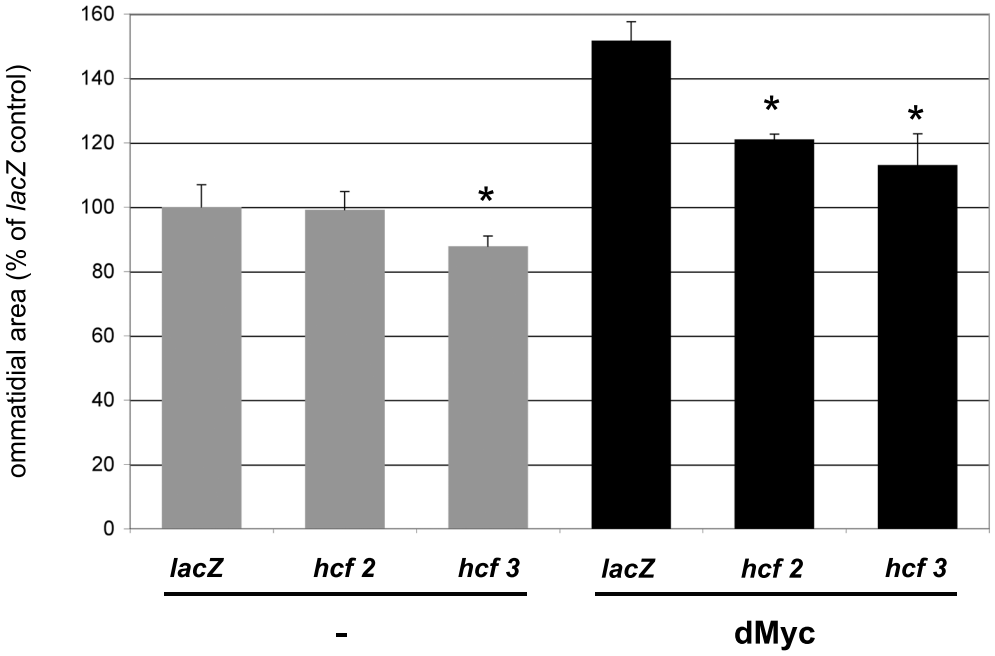

Figure 14

***hcf*-RNA*i* decreases ommatidial size specifically in a Myc-overexpression background.**
Two independent *hcf*-RNA*i* hairpin transgenes (*hcf2*, *hcf3*) or a *lacZ*-hairpin control construct were expressed in the eye by *GMR*-GAL4, either in eyes with endogenous Myc levels (columns 1-3; "**-**") or in a strong Myc-overexpression situation, in flies carrying three UAS-Myc transgenes (columns 4-6; "Myc"). Average ommatidial area (± standard deviation) was calculated from 20 centrally located ommatidia from 5 independent eyes per genotype and normalised to the size of to *GMR-GAL4; UAS-lacZ-IR* control eyes. Ommatidial size is significantly reduced when *hcf*-RNA*i* is induced in a Myc-overexpression background, and upon expression of *hcf3* in flies with endogenous Myc levels. Asterisks indicate significance of difference to the corresponding lacZ genotype, with $p<0.05$.

Genotypes (columns)

1-3: *yw/Y; GMR-GAL4/+; UAS-lacZ-IR* or *UAS-hcf-IR/+*
4-6: *yw/Y; GMR-GAL4 UAS-Myc^{132}/+; UAS-Myc^{132} UAS-Myc^{42}/UAS-lacZ-IR* or *UAS-hcf-IR/+*

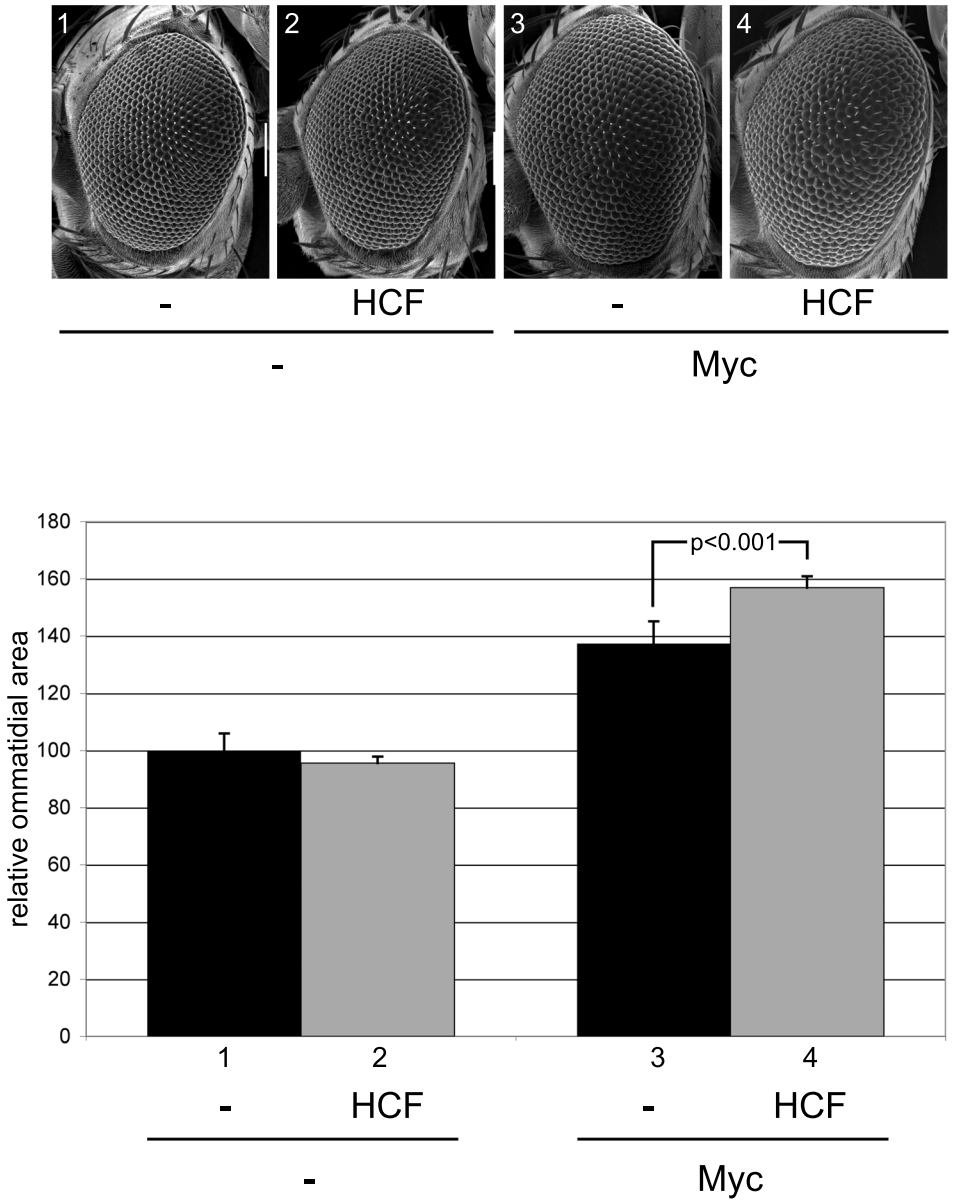

Figure 15

HCF synergises with Myc in promoting ommatidial growth.
A UAS-HCF transgene was expressed by GMR-GAL4 in the eye in the absence or presence of ectopic Myc (panel/column 2 compared to panel/column 4). As a control for the unspecific UAS-titration effects a neutral UAS-lacZ construct was expressed (panel/column 1 & 3). The top panel shows scanning electron micrographs of *Drosophila* compound eyes of the genotypes indicated below. When *hcf* is co-overexpressed with *myc*, ommatidia are increased in size compared to controls. Pictures were taken at a magnification of 180x. The bottom panel depicts the relative ommatidial area of the corresponding genotypes. The areas of 20 centrally located ommatidia in five individual eyes were measured and the sizes are normalised to column 1. Error bars indicate standard deviations. Ommatidial size of column 4 is significantly increased compared to column 3 ($p<0.001$, Student's t-test)

Genotypes (columns/panels)

1: *+; GMR-GAL4/ UAS-lacZ*
2: *+; GMR-GAL4/UAS-T7-HCF-Flag*
3: *+; GMR-GAL4 UAS-Myc^{132}/UAS-lacZ*
4: *+; GMR-GAL4 UAS-Myc^{132}/UAS-T7-HCF-Flag*

4.2. Additional experiments

4.2.1. Downregulation of HCF influences expression of Pol II transcribed Myc target genes

The initial screen runs and numerous luciferase assays performed subsequently showed that downregulation of *hcf* consistently and significantly reduced the activity of the Myc-dependent reporter system. We wanted to examine whether the levels of endogenous Myc target genes were also changed in response to *hcf*-RNA*i,* or whether this downregulation was confined to the artificial reporter system. For this purpose S2 cells were plated out at a density of 5×10^6 cells/ml and incubated with 10µg of dsRNA for 30 minutes in serum-free medium. After addition of full medium, the cells were incubated for 48 hours and then harvested. By choosing an incubation time of 48 hours we sought to ensure comparable downregulation of putative targets as in the screen runs and luciferase assays, which were always performed with the same time frame. After the lysis of the cells, total RNA was extracted, the integrity of the extracted total RNA was confirmed on bioanalyzer chips, and cDNA was generated. Subsequently, we analysed the expression of the selected genes with qRTPCR assays. Based on microarray analysis, a set of direct Myc targets had been established previously (Hulf et al., 2005). In this study, most of the genes found to be regulated by Myc contained E-boxes, with a strong preference for a localisation of the E-box downstream of the promoter (see Results section 1.1.). We included both of the Myc-regulated genes whose regulatory regions were used for the cloning of the luciferase reporters: *nnp-1* and *CG5033* (see Results section 1.1.). As mentioned above both of these genes contain a downstream E-box, and for both of the genes it had been shown that their expression depends on the presence of the E-box (Hulf et al., 2005). The ability of these genes to be reliably upregulated by Myc overexpression and downregulated by loss of *myc* had been confirmed by qRTPCR assays and luciferase reporter transgenes. In addition, two other direct targets of *myc* were included: *CG12295* (also termed *straightjacket* (*stj*); homologous to the human voltage-dependent calcium channel subunit α2/δ3), which contains an E-Box 627 bp upstream of the transcription start site and *fibrillarin (fib)*, a gene involved in 35S RNA primary transcript processing, which contains an E-Box 26 nt downstream of the transcription start.

The microarrays used in the analysis mentioned above, only included RNA polymerase II-transcribed protein-coding genes but not RNA polymerase I and RNA polymerase III-transcribed RNA genes. Since Myc was shown to control the transcription of RNA polymerase III-dependent small RNA genes in mammals (Gomez-Roman et al., 2003; Grewal et al., 2005) and in *Drosophila* (Steiger et al., 2008), we included the previously characterised Myc target genes *5sRNA*, *tRNA(Leu)* and *snoRNA U3* in the analysis.

Figure 16 shows the epxression levels of *myc*, *hcf*, *nnp-1*, *CG5033*, *CG12295*, *fibrillarin*, *5sRNA*, *snoRNA U3* and *tRNA(Leu)* in S2 cells in which HCF or Myc levels were reduced by RNA*i*. For every dsRNA species two independent RNA extractions were performed. For the assays *myc*, *CG5033* and *CG12295* data from two independent experiments are depicted. The levels were normalised against the average of the reference genes *actin5C* and *sec24* and charted relative to their expression levels in samples treated with *gfp* control RNA*i*. The downregulation of *hcf* was efficient since mRNA levels were reduced to 18 ± 5%. On the other hand *myc* levels fluctuate in response to *hcf*-RNA*i*. While they remained unchanged in one experiment, they are reduced by almost 30% in a second measurement.

The efficiency of *myc*-RNA*i* also varied between the two individual experiments. Whereas it did not work as efficiently in one case, as about 60% *myc* mRNA compared to the *gfp* control sample still persisted after 48 hours, downregulation to roughly 30% was achieved in the second experiment. Despite rather high persistence of *myc* mRNA the levels of the four direct RNA polymerase II-transcribed targets (*nnp-1*, *CG5033*, *CG12295*, and *fibrillarin*) consistently dropped to under 40%. This downregulation of the direct targets is even more pronounced in other experiments where *myc* reduction is stronger (data not shown). The levels of the two Pol III-transcribed targets *snoRNA U3* and *tRNA(Leu)* were also reduced by *myc*-RNA*i*, however to a lesser extent than the Pol II-transcribed targets. Similarly, *hcf*-RNA*i* has a clear but moderate effect on the levels of the direct Pol II targets of Myc, even though *myc* mRNA levels remain high. In contrast, the levels of the small RNAs do not decrease in response to hcf-RNA*i*. Possible reasons might be that the Pol III targets are less sensitive to reduction of Myc activity or that HCF is not involved in the transcactivation of RNA polymerase III-transcribed targets of Myc. Taken together, these data consistently show that HCF is involved in the transcriptional regulation of physiological and direct Myc targets. Moreover the observed repression of the Myc target genes to about 60-70% by *hcf*-RNA*i* is not indirectly caused by fluctuations of *myc* levels, since significant downregulation can also be observed in cases where *myc* levels remain high. To address the question whether downregulation of HCF in S2 cells significantly changed the levels of Myc protein itself, we examined Myc protein levels in *hcf*-RNA*i* treated S2 cells by standard Western blotting procedures. Figure 17 depicts a Western Blot of whole cell lysates treated with dsRNA. The picture shows that downregulation of *hcf* by two independent dsRNA species has no obvious influence on the endogenous Myc protein levels, despite the fact that *myc* mRNA levels are fluctuating as a consequence of *hcf*-RNA*i*. This could mean that fluctuations of mRNA levels are “evened out” on the protein level by some sort of Myc auto-regulation. Alternatively, small changes in protein abundance of roughly 30% (as comparable to the mRNA levels) might not be detectable with standard Western blot procedures.

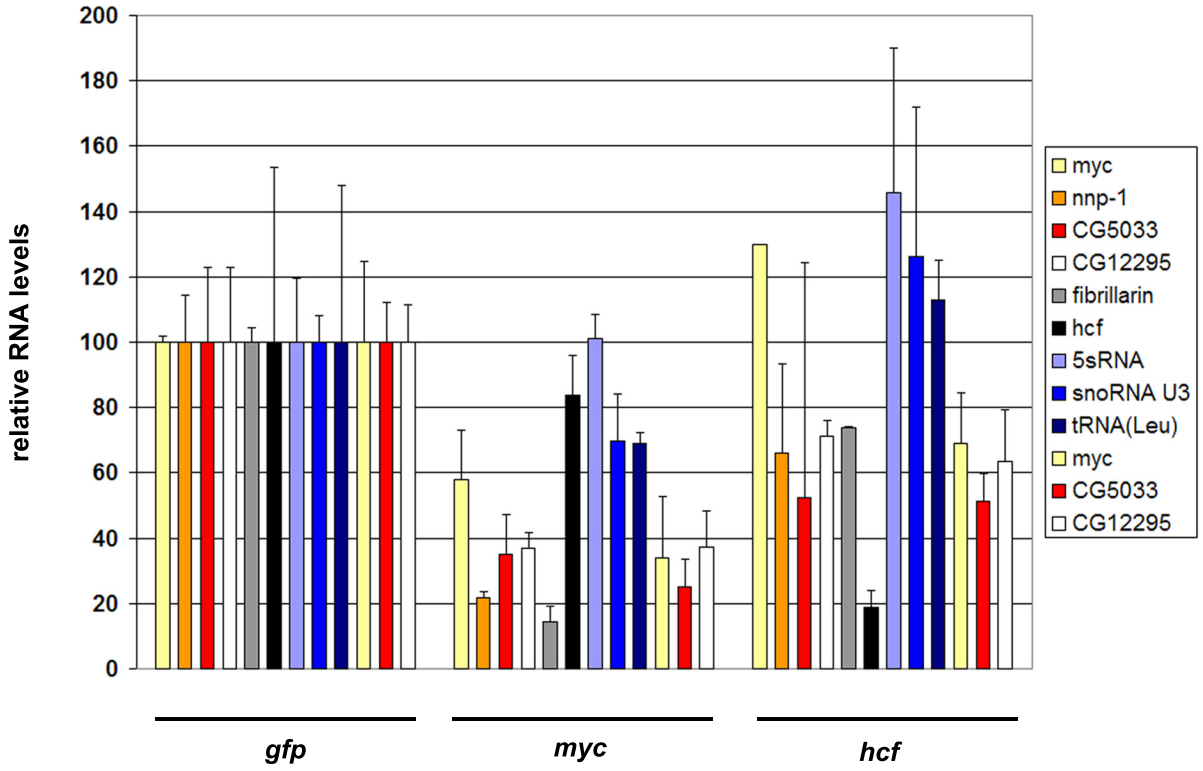

Figure 16

Depletion of HCF influences the expression of RNAP II-transcribed Myc targets. Transcript levels of *myc*, *nnp-1*, *CG5033*, *CG12295*, *fibrillarin*, *hcf*, *5sRNA*, *snoRNA U3* and *tRNA(Leu)* were determined with qRTPCR in S2 cells upon RNA*i*- mediated depletion of *myc* or *hcf* (48 hour incubation with dsRNA). The chart shows average values and the standard deviations for the indicated transcripts, relative to the reference genes *actin5C* and *sec24*. The values are normalised to *gfp* control RNA*i* samples. Two RNA samples were used per RNA*i* and three PCR reactions were performed per assayed transcript. Two independent experiments are shown for the targets *myc*, *CG5033*, and *CG12295*.

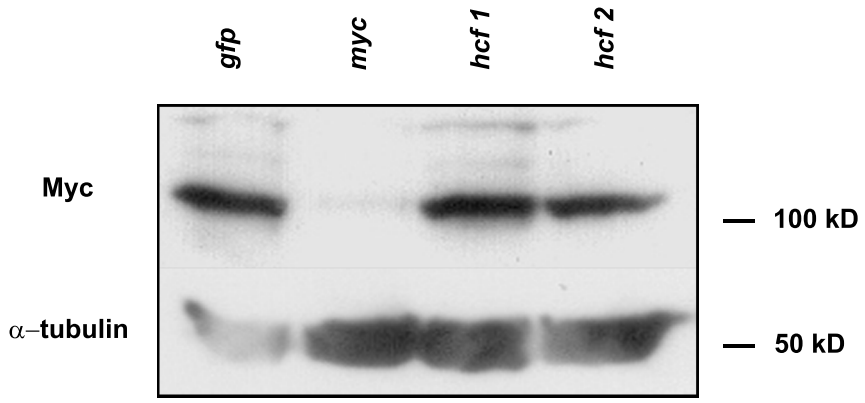

Figure 17

Myc protein levels are not affected by RNA*i*-mediated depletion of HCF
S2 cells were incubated for 48 hours with two independent dsRNAS directed against *hcf*. Depletion of hcf levels does not influence Myc protein abundance. One lane corresponds to the cell lysate of roughly 2.5 million cells.The levels of α–tubulin were taken as a loading control. Antibodies used: mouse anti-dMyc; mouse anti-α-tubulin.

4.2.2. Endogenous Myc and HCF interact physically

After having shown that co-overexpressed HA-tagged Myc and and T7-tagged HCF interact physically in S2 cells, we wanted to confirm this specific interaction by coimmunoprecipitation of the endogenous proteins. We tried to coimmunoprecipitate HCF and Myc from S2 cell lysates, however we were unsuccessful even with large amounts of starting material (2.5×10^8 cells per sample). Therefore, we chose embryonic lysates of 0-18 hour-old *yw* embryos. This long collection time was selected for two reasons. First, our experiences with S2 cells prompted us to use as large an amount of starting material as possible (which precluded the use of closely timed embryos), and second, Myc expression fluctuates strongly during embryogenesis. Upon collection, the embryos were dechorionated and homogenised. Typically 0.5 ml packed embryos was used for one immunoprecipitation, also for the mock IP control. The lysate was split into equal halves and precleared. Then the precleared lysate was incubated for 3 hours at 4°C with the rabbit anti-dMyc antibody or rabbit non-immune serum before adding the protein G-sepharose beads. After SDS-PAGE and Western blotting, the membrane was probed with an antibody directed against the C-terminal HCF subunit. A faint HCF band of 62 kDa was detected specifically in the Myc immunoprecipitation (Figure 18, lane 1), but not in the control sample (lane 2). Reprobing of the membrane with mouse anti-Myc hybridoma supernatant confirmed that Myc had been successfully and specifically pulled down by our rabbit anti-dMyc antibody. However, Myc was undetectable in the total lysate, most probably because the Myc content is below the detection level (about 3% of the total lysate was loaded in lane 3). In summary, these experiments demonstrate the physical interaction between endogenous Myc and HCF proteins.

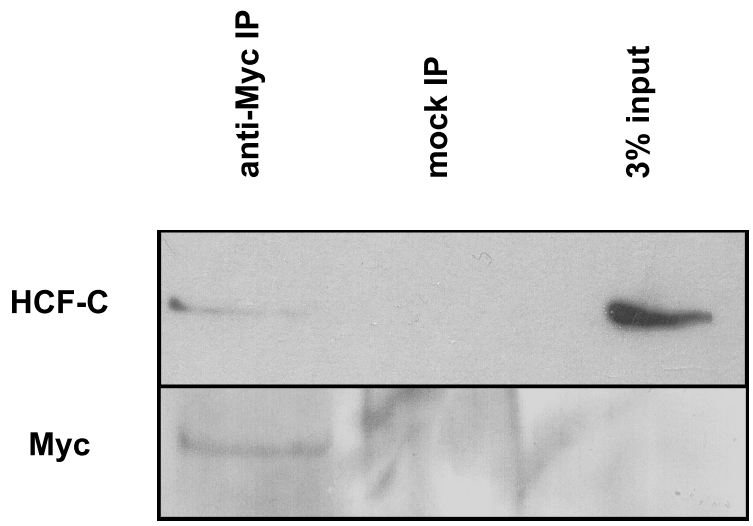

Figure 18

Endogenous Myc and HCF proteins interact physically.
Endogenous Myc and HCF proteins were coimmunoprecipitated from extracts of 0-18 hour-old *yw* embryos. For one immunoprecipitation reaction 0.5ml packed embryos were used. Myc was precipitated using a rabbit anti-Myc antibody. As a control for the specificity of the IP rabbit non-immune serum was used. Endogenous HCF protein was detected with a rat anti-HCF antibody, directed against the C-terminal subunit (upper panel). Membranes were stripped and reprobed with a mouse anti-Myc antibody. Myc protein was not detected in the input control, presumably because the amount was below detection.

4.2.3. The physical interaction between Myc and HCF is direct

Since we had been able to demonstrate a physical association between the endogenous HCF and Myc proteins in embryos, as well as the overexpressed protein variants in a tissue culture cells, we turned to the *in vitro* translation system to further characterise their physical interaction. By expressing recombinant GST-Myc fusion protein variants in *Escherichia coli* and testing their ability to bind an *in vitro* translated ^{35}S-labelled HCF fragment we addressed the question whether the physical interaction observed in coimmunoprecipitations was direct or bridged by other proteins. Furthermore we wanted to test whether the HCF-binding domains identified in Myc were all mediating a direct HCF:Myc interaction or whether there was a single "direct interaction domain". Because HCF is a very large protein with a length of 1500 amino acids, we chose not to clone the full length sequence into the *in vitro* expression vector (pRSet-C). Instead, we only used an N-terminal fragment of 442 amino acids. This stretch comprises the conserved Kelch domain (aa 85-375), which was shown to be required for interactions with the viral transcriptional coactivator VP16 and various cellular transcription factors (Wysocka and Herr, 2003), and the N-terminal self-association sequence SAS1N (aa 401-442)(Mahajan et al., 2003). As baits for the *in vitro* translated HCF$^{1-442}$ fragment various GST-Myc fusion proteins were used. First, we could show that the N-terminal part of HCF is being bound by a GST-Myc variant that contains amino acids 46 to 507 of Myc (Gallant et al., 1996) (Figure 19). This large part of the Myc protein contains the conserved regions Myc-Boxes 1-3 and the HCF-binding motif (HBM) (which has been shown to be dispensable for the interaction between HCF and Myc in S2 cells) but lacks the very C-terminal basic region and the helix-loop-helix leucine zipper (bHLHzip) sequences, that are required for heterodimerisation with Max and DNA binding. To narrow down the interaction site within the Myc protein, we also tested ten additional smaller Myc fragments for their ability to associate with HCF. Figure 20a depicts a schematic drawing of the interactions between HCF$^{1-442}$ and the GST-Myc fragments. These data suggest that there are three independent interaction sites for HCF$^{1-442}$ in Myc. One weakly interacting region is located in the N-terminus, within the first 176 amino acids, while the strongest interacting region maps to the central portion of the Myc protein. This is reflected by the highest affinities of the Myc fragments that contain the MB3 sequence (aa 404 to 417). Probably a longer sequence is responsible for mediating the interaction, as fragments that are truncated at the beginning of MB3 still retain considerable binding to HCF (fragments aa 177-403 and aa 295-403). A third weaker interaction site is contained in the C-terminus after amino acid 523, as the fragment consisting of the last 200 amino acids (524-719) still is bound by HCF. Thus, the *in vitro* translation experiments revealed three direct HCF-interaction domains in Myc. The strongest affinity is mediated by the central part of Myc, whereas the N-terminal and C-terminal interaction sites mediate weaker binding to HCF. These data are largely in accordance with coimmunoprecipitations of overexpressed full length T7-HCF and various N-terminally HA-tagged Myc truncations (Balbi, 2007). Both the strong centrally located interaction site (mapped between amino acids 179 and 403) and the C-terminal site (between aa 524 and 626) were also identified by these experiments. However, the N-terminus (aa 1-179) did not bind to full length T7-HCF. This difference might be explained by *in vivo* conditions that are not conducive for HCF binding to Myc, or the bulk of the full length HCF protein – in the presence of both subunits - might sterically hinder an association with Myc. Alternatively, the addition of a triple HA-tag to the N-terminus of Myc could result in a "non-native" folding pattern of this

short protein stretch. Lastly, the binding of the N-terminus of Myc to HCF seen in the GST-pulldowns could be an artificial interaction that is only seen at very high protein concentrations. However, the broad correlation between the coimmunoprecipitations from S2 cells and the GST-pulldowns, and varying relative binding intensities for different interactors, strongly indicate that the binding between Myc and HCF is indeed physiological.

Taken together, all the data obtained during Mirjam Balbi's Master thesis as well as additional experiments coherently support HCF's role as a novel cofactor of Myc. Biochemical approaches (co-immunoprecipitations and binding studies with i*n vitro* translated HCF) confimed a direct physical interaction of HCF and Myc at three independent sites within the Myc protein. Furthermore, studies in S2 cells revealed that HCF has a direct influence on the expression of known RNA polymerase II-transcribed target genes of Myc and not only the artifical reporter system used for the screen. *In vivo* assays lead to the conclusion that HCF and Myc synergise and that HCF is required for the proper biological activity of Myc.

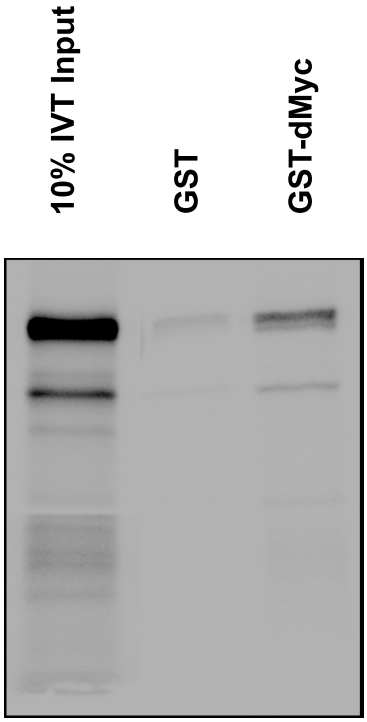

Figure 19

Myc directly binds to HCF.
A GST-coupled Myc fragment (amino acids 46-507) retains in vitro translated ^{35}S labeled-HCF^{1-442} (lane 3). As a control for the specificity of this interaction GST was used (lane2).

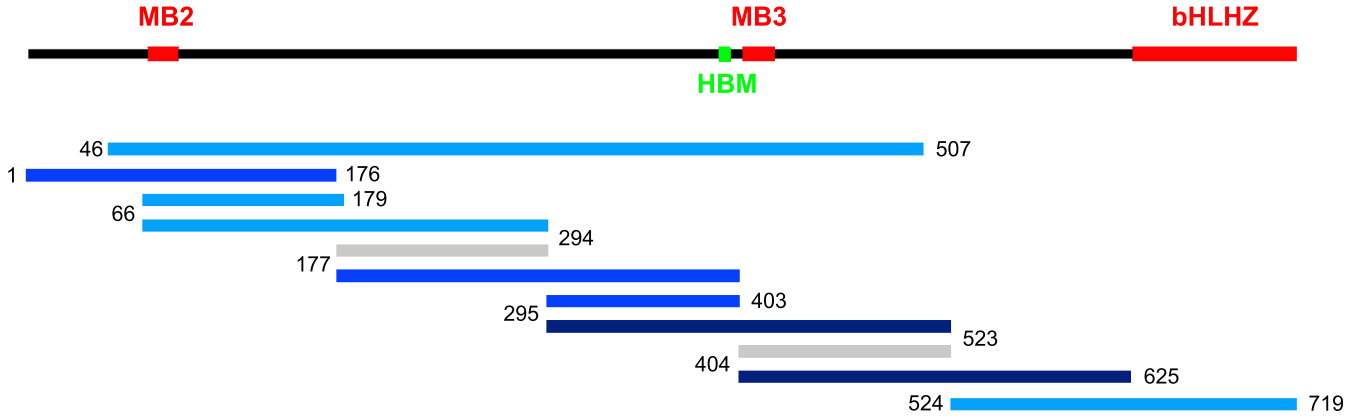

Figure 20a

Schematic overview of the interaction of HCF with various GST-Myc variants.
Depicted are the interactions strengths of various GST-Myc protein fragments with the *in vitro* translated HCF$^{1-442}$ fragment. The darker the colour of the fragments, the stronger the direct interaction with HCF. Fragments shown in grey do not interact with HCF$^{1-442}$. Topmost: schematic drawing of the Myc protein with the conserved motifs MB 2 (Myc Box 2), MB 3 (Myc Box 3), and the basic helix-loop-helix leucine zipper.

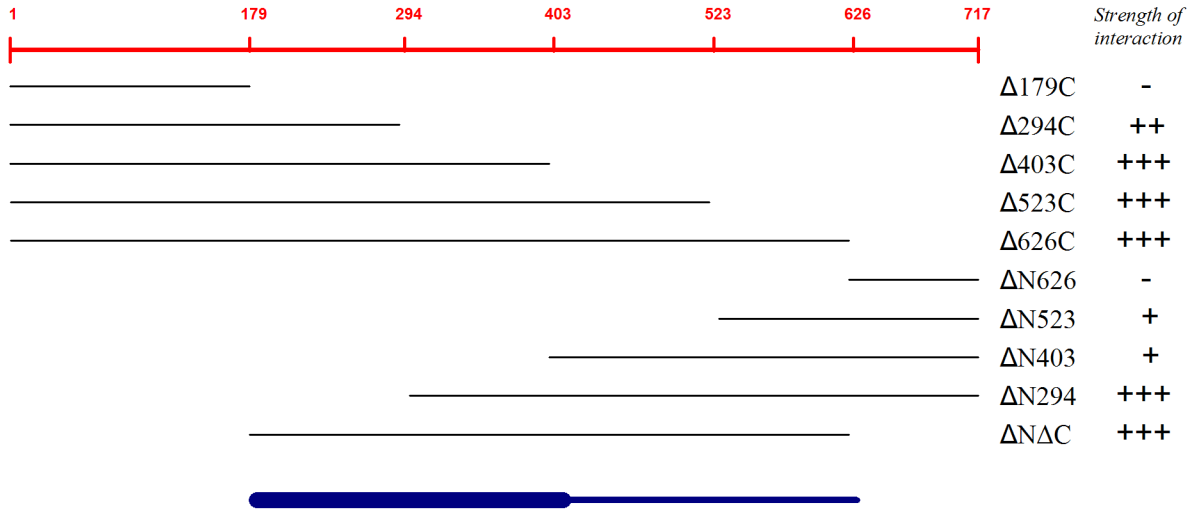

Figure 20b

Schematic representation of the interaction between various Myc deletion mutants and HCF (adapted from Balbi, 2007). Depicted in red are the coordinates of the full-length *Drosophila* Myc protein (aa 1-717). Fragments tested for their ability to physically interact with HCF are shown with their respective interaction strengths ('+++' strong ; '++' intermediate; '+' weak, and '-' no interaction with HCF). The blue bar represents the stretch of the Myc protein that was found to mediate interaction with HCF in tissue culture coimmunoprecipitations.

5. RNA Polymerase II Associated Factor 1 (PAF) complex

In addition to the positive regulators of the luciferase reporters (see Results, Chapters 3 & 4) we have also identified nine repressors of the reporter system. Reduction of the mRNA titre of the corresponding genes led to an increase in expression of the Myc-responsive luciferase variant. Within the group of the nine strongest activator dsRNAs of the reporter system, 3 components of the RNA Polymerase II associated factor 1 complex (PAF complex) (Sims et al., 2004; Adelman et al., 2006) (*hyrax*, *ctr9*, and *atms*) and one PAF complex associated gene *spt6* (Andrulis et al., 2000) were found.

5.1. PAF complex components influence Myc target gene expression

5.1.1. The Myc activity reporter is influenced by both reduction and overexpression of PAF complex components

To confirm the findings of the screen, we repeated the luciferase assay in response to RNA*i* against PAF complex components using the the *CG5033*-Myc activity reporter system. S2 cells were transiently transfected with the wild-type promoter containing *Renilla* reporter, the firefly ΔE-Box reference and dsRNA corresponding to four of the five *Drosophila* PAF complex subunits *hyrax* (*hyx*) (2 independent dsRNA sequences, *hyx1* and *hyx2*; *hyx2* was a kind gift of George Hausmann & Konrad Basler), *atu*, *atms*, and *ctr9*). The cells were harvested 60 hours after transfection and relative luciferase intensities were measured. All values are expressed relative to a *gfp* dsRNA transfection, which serves as a control for unspecific effects of RNA interference. Figure 21 and Table 2 show that downregulation of the individual PAF complex components uniformly leads to an activation of the reporter system between 1.5 fold for *atms* and *atu* and about 3-5 fold for both *hyx* dsRNAs. Therefore, also the fourth subunit tested (Atu), influences the reporter system to a similar extent as the other PAF complex components. Indeed, *atu*-RNA*i* had an activating effect in 2 of the 3 screen runs but was not included in the final candidate list only because it did not comply with the significance criteria in the second screen run. In contrast, downregulation of *rtf1,* which has been reported not to be a stable part of the PAF complex in *Drosophila* (Adelman et al., 2006), did not change the relative luciferase expression.

RNA interference	relative luciferase activity (compared to *gfp* in %)	Standard deviation (in %)
gfp	100	4
myc	14	2
hyx	286	16
hyx 2	493	64
atu	157	19
atms	152	7
ctr9	176	11

Table 2: RNA*i* against Paf complex components activates CG5033-driven Myc activity reporter
S2 cells were subjected to RNA*i* against PAF complex components and luciferase activity was measured. Values are normalised to *gfp* control RNA*i* samples. Standard deviation of two individual measurements.

Since downregulation of PAF complex components led to an activation of the dMyc-dependent luciferase reporter system, we tested whether overexpression of the individual subunits Hyrax and Atu had the opposite effect (Figure 22). Therefore, either a *UAS-HA-Atu* transgene, driven by *tubulin-GAL4*, or *HA-hyx* under the direct control of a *tubulin*-promoter (both kindly provided by Ch. Mosimann) were expressed in S2 cells together with both *CG5033*-controlled Myc activity reporters for 60 hours. Concomitantly, *myc* levels were modulated either by RNA interference or expression of a *UAS-HA-myc* transgene, to test whether the transcription modulating role of the PAF complex is altered by varying Myc levels. *hyx* and *atu* downregulation in response to complementary dsRNAs in cells with endogenous *myc* levels resulted in comparable activation of the reporter system as seen above (264 ± 17% (*hyx*) and 150 ± 17% (*atu*) respectively) compared to non-transfected controls. Overexpression of *hyx* exerted a strong negative effect on the reporter system, as expression levels dropped to 29 ± 2%. In contrast, no changes in luciferase expression could be observed upon elevation of *Atu* levels (104 ± 5%). Modulation of PAF complex component titres had similar effects in cells with reduced *myc* levels. RNA*i* against *myc* reduced luciferase expression levels to 16 ± 2%. This baseline expression could be boosted by about two-fold in response to *hyx*- and *atu*-RNA*i* (31 ± 6% and 37 ± 18%). As in cells with unaltered *myc* abundance, ectopic expression of *hyx* lowered the reporter activity (9 ± 1%), whereas elevated *atu* levels had the opposite effect (38 ± 3%). In the third experimental condition, luciferase intensities were measured in cells that overexpress Myc. An increase in luciferase expression of two-fold is observed upon expression of the *UAS-HA-myc* plasmid (193 ± 4%). This boost in reporter activity is further enhanced to 400 ± 12% or 289 ± 13% by reduced PAF complex levels. It is suppressed to 67 ± 1% in case of Hyx and 163 ± 8% for Atu overexpression.
Taken together, lowering of *hyx* and *atu* titres reproducibly results in an activation of luciferase activity by 1.5-fold for *atu* and at least twofold for *hyx*, irrespective of the Myc content of a cell (as long as there is some Myc protein present). Coherently, upregulation of *hyx* by ectopic expression has a considerable repressive effect on reporter expression. Overexpression of *atu*, however, only results in slightly reduced luciferase activity (from 193 ± 4% to 163 ± 8% in the case of elevated Myc levels). In

cells with endogenous Myc levels it does not influence reporter expression at all, whereas in cells which were treated with *myc* dsRNA, ectopic Atu leads to increased luciferase intensities (16 $\pm$ 2% to 38 $\pm$ 3%).

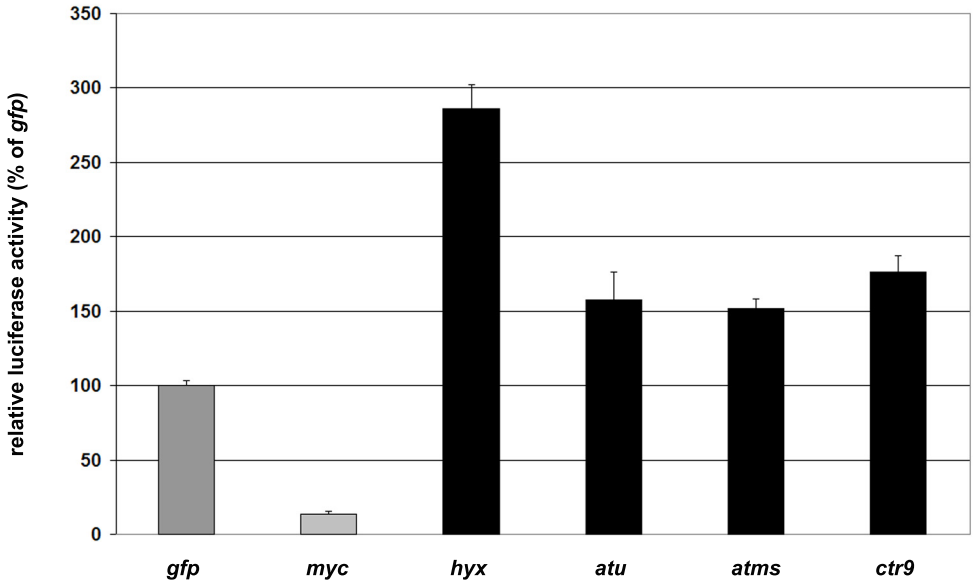

Figure 21

RNA*i*-mediated depletion of PAF complex components results in activation of the Myc activity reporter. S2 cells were transfected with CG5033-driven Myc activity reporter constructs and were subjected to RNA*i* against PAF complex components for 48 hours. Downregulation of PAF complex components leads to an activation of the reporter system. The luciferase activities were normalised to the *gfp* control samples. Error bars indicate standard deviations of two individual experiments.

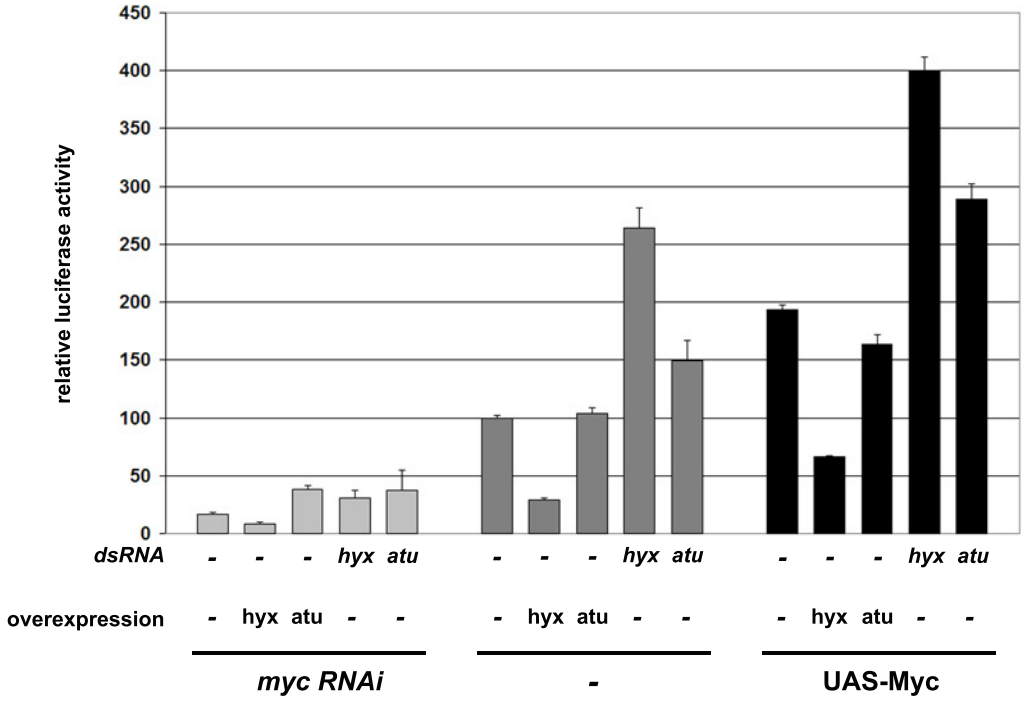

Figure 22

Luciferase assay upon modulation of Hyx and Atu levels.
Relative luciferase activities of the Myc activity reporter (normalised to *gfp* control RNA*i*) were measured upon modulation of Myc and Paf complex components. S2 cells were subjected to RNA*i* against *hyx* or *atu* for 60 hours to downregulate corresponding protein levels. Hyx was ectopically expressed from a *tub-HA-hyx* construct, while a *UAS-HA-Atu* construct was expressed under the control of *tubulin-GAL4*. Error bars indicate standard deviations of two independent measurements. The table below summarises the relative luciferase values depicted in the chart.

dmyc level	RNA interference	overexpression	relative luciferase activity [%]	standard deviation [%]
dmyc RNAi	-	-	16	2
	-	*hyx*	9	1
	-	*atu*	38	3
	hyx	-	31	6
	atu	-	37	18
endogenous	-	-	100	2
	-	*hyx*	29	2
	-	*atu*	104	5
	hyx	-	264	17
	atu	-	150	17
ectopic	-	-	193	4
	-	*hyx*	67	1
	-	*atu*	163	8
	hyx	-	400	12
	atu	-	289	13

5.1.2. The PAF complex is required for the correct expression of endogenous Pol II-transcribed Myc targets

The results from the luciferase assay experiments clearly show that downregulation of the four PAF complex components *hyx*, *atu*, *atms*, and *ctr9* all result in significant activation of the Myc-dependent reporter system in the range of 1.5-fold (in the case of *atu* and *atms*) to five-fold (*hyx*). In order to characterise the influence of PAF complex reduction on endogenous Myc target genes, qRTPCR measurements were performed. Total RNA was extracted from S2 cells that had been treated with dsRNA targeting either *gfp* as a control for unspecific RNA*i* effects, *myc*, or the four PAF complex components mentioned above. After an incubation time of 48 hours cells were lysed, RNA was extracted and analysed for its integrity on a bioanalyzer, cDNA was synthesised, and qRTPCR assays were run. As described in chapter 4.2. of the Results section, RNA polymerase II-transcribed Myc target genes had been identified by microarray analysis (Hulf et al., 2005). In this experimental setup, the levels of two of these targets, *CG5033* and *CG12295*, were determined. Since there are several reports of Myc having a role in transcription by RNA polymerase III (Gomez-Roman et al., 2003; Steiger et al., 2008) assays for the RNA polymerase III-transcribed genes *tRNA(Leu)* and *snoRNA U3* were included. Additionally, we monitored the levels of the Pol II-transcribed Myc targets *Bekka* (*Bka*), which codes for a Trithorax group protein, whose promoter contains a single E-Box at position +33 relative to the transcription start site, and *CG9630*, a predicted RNA-helicase without E-Box in its regulatory region. These two genes were identified as targets which are suppressed by *myc*-RNA*i* and upregulated by *myc* overexpression in the microarray studies mentioned above (Hulf et al., 2005). Furthermore, they are positive targets of the PAF complex component Hyrax (Ch. Mosimann, personal communication).

In Figure 23 the expression levels of *myc*, *CG5033*, *CG12295*, *Bka*, *CG9630*, *tRNA(Leu)*, and *snoRNA U3* are depicted. For each assay two independent RNA extractions were performed. The results were normalised to the reference gene *actin5C* and and plotted relative to their expression level in the sample treated with *gfp* control RNA. Downregulation of *myc* was highly efficient as *myc* mRNA levels are reduced by more than five-fold. However, the depletion of PAF complex components also influences *myc* abundance, as a drop to 75-50% is observed. As expected, the titres of polymerase II-transcribed targets *CG5033*, *CG12295*, *CG9630*, and *Bka* were strongly reduced in response to *myc*-RNA*i*. The polymerase III-transcribed targets *tRNA(Leu)* and *snoRNA U3* were less affected. Downregulation of the three PAF components *hyx*, *Atu* and *atms* also resulted in a drop of Myc target levels to varying extent. Both *CG5033* and *CG12295* were most sensitive to *hyx* reduction as levels dropped to under 50%. For all the other cases only moderate reductions were observed.

In summary, RNA polymerase II-transcribed targets of *myc* are sensitive to changes in PAF complex component abundance. Depletion of *hyx*, *Atu* and *atms* results in reduced expression of selected target genes. The observed reduction, ranges from considerable knockdown in the case of *CG5033* or *CG12295*, as a consequence of *hyx* downregulation, to probably not significant changes of approximately 25% in the majority of the samples. As already seen upon Myc downregulation the polymerase III-transcribed targets are less sensitive to PAF complex reduction; In only two instances there is a significant downregulation (*tRNA(Leu)* upon Atu, and *snoRNA U3* upon Atms depletion). This indicates that polymerase III-dependent targets are generally less affected by reduced PAF

complex levels and a therefore relatively moderate impairment of Myc-activity has no discernable effect on them. Alternatively, the PAF complex might only be involved in RNAP II, but not RNAP III-dependent transcription. Moreover, knockdown of individual PAF complex components has different consequences. While depletion of *ctr9* does not impact on expression of the tested targets, knockdown of *atu*, *atms* and *hyx* generally causes a slight reduction of target levels – with one incident of target gene activation in response to reduced *hyx* levels (*Bka*). This outcome was unexpected as it is in apparent contradiction with the results obtained from the luciferase assays, in which we originally identified the PAF complex components as repressive interactors of the Myc-dependent reporter system (see Discussion section 2.3.1.).

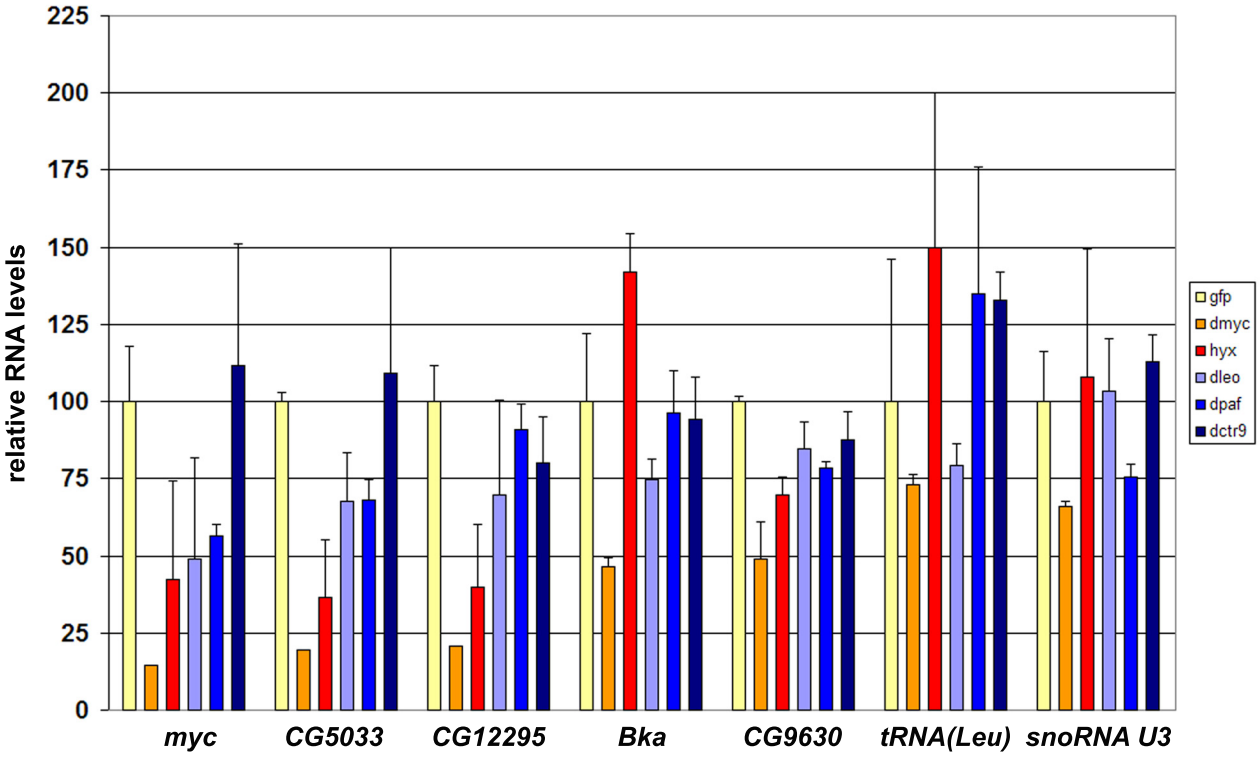

Figure 23

Depletion of PAF complex components leads to a downregulation of RNAP II-transcribed Myc targets. PAF complex components were depleted in S2 cells by RNA*i* for 60 hours. The targeted proteins are listed in the box to the right. Transcript levels of *myc*, the RNAP II-transcribed genes *CG5033*, *CG12295*, *Bka*, and *CG9360*, as well as the RNAP III-transcribed targets *snoRNA U3* and *tRNA(Leu)* were determined by qRTPCR. The chart shows average values and the standard deviations for the indicated transcripts, relative to the reference gene *actin5C*. The values are normalised to *gfp* control RNA*i* samples. For each RNA*i* two samples were measured and three PCR reactions were performed per assayed transcript.

5.2. RNA*i* against PAF complex components does not detectably decrease Myc protein levels

Prompted by the qRTPCR result that depletion of PAF complex components reduces the abundance of *myc* transcript (see Figure 23) we performed Western blot analyses to determine the Myc protein content in response to RNA*i* against all five PAF complex components. As seen in Figure 24, treatment of S2 cells with dsRNA complementary to PAF complex components does not result in obvious changes of Myc protein levels. However, it is possible that reductions by 25-50% (corresponding to the suppression seen in mRNA abundance) are not detectable with our standard enzymatic chemoluminescence detection system. For clarification, thourough quantitation of the band intensities would be necessary. Nevertheless, it is unlikely that reduction of PAF complex levels leads to a decrease in *myc* abundance, as Myc-dependent luciferase assays react to depletion of PAF complex components with a significant activation of the reporter gene. Moreover, this holds true for cells that overexpress *myc* but also in the context of diminished *myc* levels.

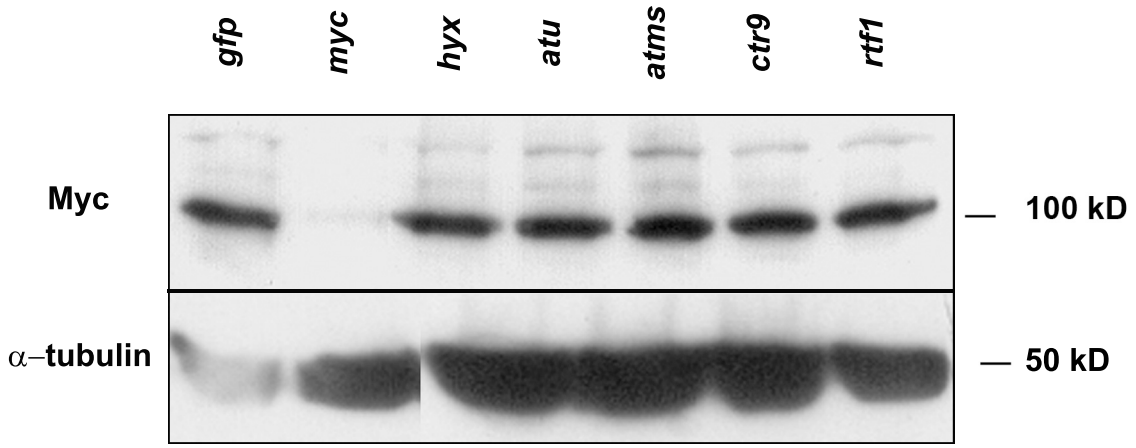

Figure 24

Myc protein levels remain unchanged by RNA*i* against PAF complex components.
S2 whole cell lysates were subjected to RNA*i* against PAF complex components for 48 hours. One lane corresponds to the cell lysate of roughly 2.5 million cells. Myc proteins were detected using a mouse anti-dMyc antibody, while a mouse anti α–tubulin antibody was used as a loading control.

5.3. Myc and the PAF complex subunits Hyrax and Atu interact physically

Despite the fact that modulations of PAF complex levels have diametrically opposed effects on the transactivation of the artificial reporter system and on endogenous Myc targets, both read-outs are reactive to changes in PAF complex abundance. These results indicate a functional link between Myc and the PAF complex. In order to further investigate this connection, we focussed on characterising a potential molecular interaction between the Myc protein and both Atu and Hyx. Since the PAF complex presumably does not (largely) affect Myc protein abundance, it is conceivable that it regulates target gene expression by altering the activity of Myc. Such an effect might involve a physical interaction with Myc. To this end, coimmunoprecipitations between overexpressed forms of Myc and PAF complex subunits were performed. S2 cells were transiently transfected with equal amounts of plasmids, coding for tagged versions of Myc and Atu and/or Hyx. The UAS-constructs (all except *tubulin-HA-hyx*) were driven by co-transfection of a *tubulin-GAL4* plasmid. Lane 1 in the upper panel of Figure 25 reveals a strong physical interaction between Atu, fused to an AU1-tag, and HA-tagged Myc. Figure 26 depicts interactions between both Atu and Hyx and Myc (Lanes 2-4). Cell lysates were incubated with a rabbit anti-HA antibody. 9E10-tagged Myc is precipitated in the samples that contain HA-Atu, HA-Hyx or both, but not from lysates lacking HA-tagged proteins, attesting to the specificity of the anti-HA immunoprecipitation. The interaction between the Atu and Myc proteins is considerably stronger than between Myc and Hyx (compare lanes 2 and 3). Moreover, the strong interaction between Atu and Myc is not abrogated in the presence of overexpressed Hyx protein. This indicates a model in which Myc and Hyx independently associate with Atu without competing with each other, with the association between Hyrax and Myc (faint band in lane 3) being bridged by Atu. Such a model could be tested by immunoprecipitating HA-Hyx and assaying the retrieval of Myc or vice versa in the presence of different levels of Atu. Since we had detected a specific interaction between Myc and the PAF complex component Atu, we raised polyclonal antibodies against the RDKVESQVESAPKEC sequence within the *Drosophila* Atu protein (amino acids 368 to 381). This sequence has been chosen because it was is predicted to be antigenic and because it is not located in a region that is conserved amongst Atu homologues from different species. This suggests that it might not have an important conserved function. A characterisation of the anti-Atu antibody is depicted in Figure 27.

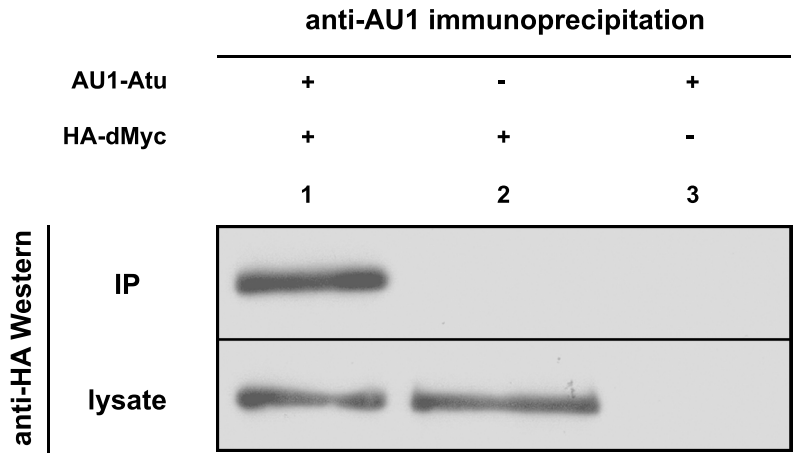

Figure 25

Coimmunoprecipitation of Myc and Atu proteins.
S2 cells overexpressing HA-Myc, and AU1-Atu (driven by *tubulin-GAL4*) were lysed and Atu was immunoprecipitated, using a rabbit anti-AU1 antibody. Myc levels were detected using a mouse anti-HA antibody (upper panel). One lane corresponds to 100% of the lysate from a 3 cm tissue culture dish.

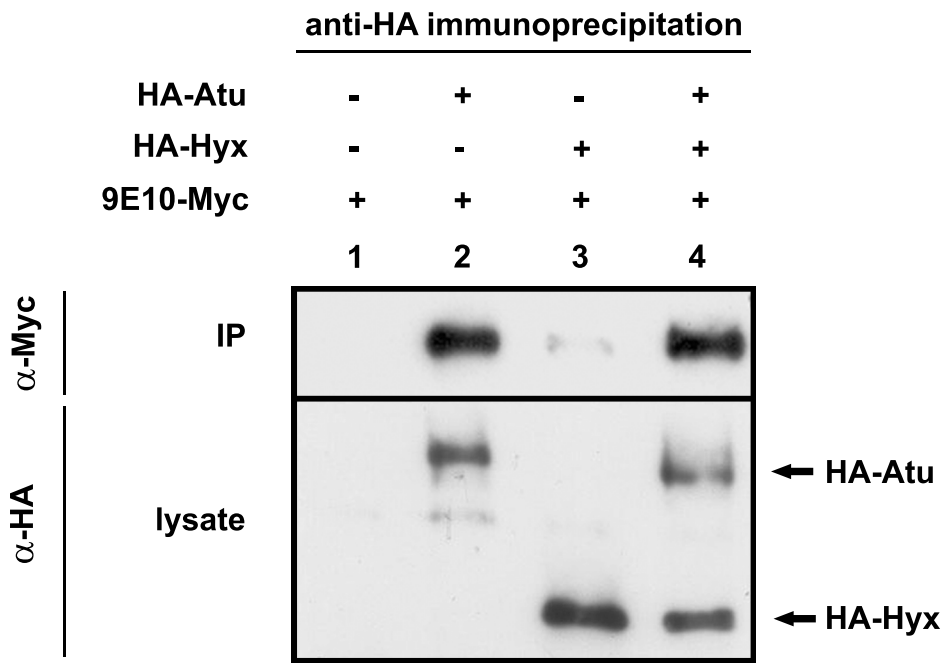

Figure 26

Myc binds the PAF complex components Hyx and Atu
S2 cells were transfected with UAS-9E10-Myc, UAS-HA-Atu and tub-HA-Hyx constructs. UAS-overexpression plasmids were expressed under the control of tub-GAL4. Total DNA concentration was kept constant at 10μg per transfection (a neutral pCaSpeR construct was used to even out differences in DNA content). HA-Hyx and/or HA-Atu were immunoprecipitated with a rabbit anti-HA antibody. Myc levels were detected using a mouse anti-Myc antibody (upper panel), while presence of overexpressed PAF components in the lysate was confirmed by anti-HA Western blotting (lower panel). One lane corresponds to 100% of the lysate from a 3 cm tissue culture dish**.** (approximately 5 million cells).

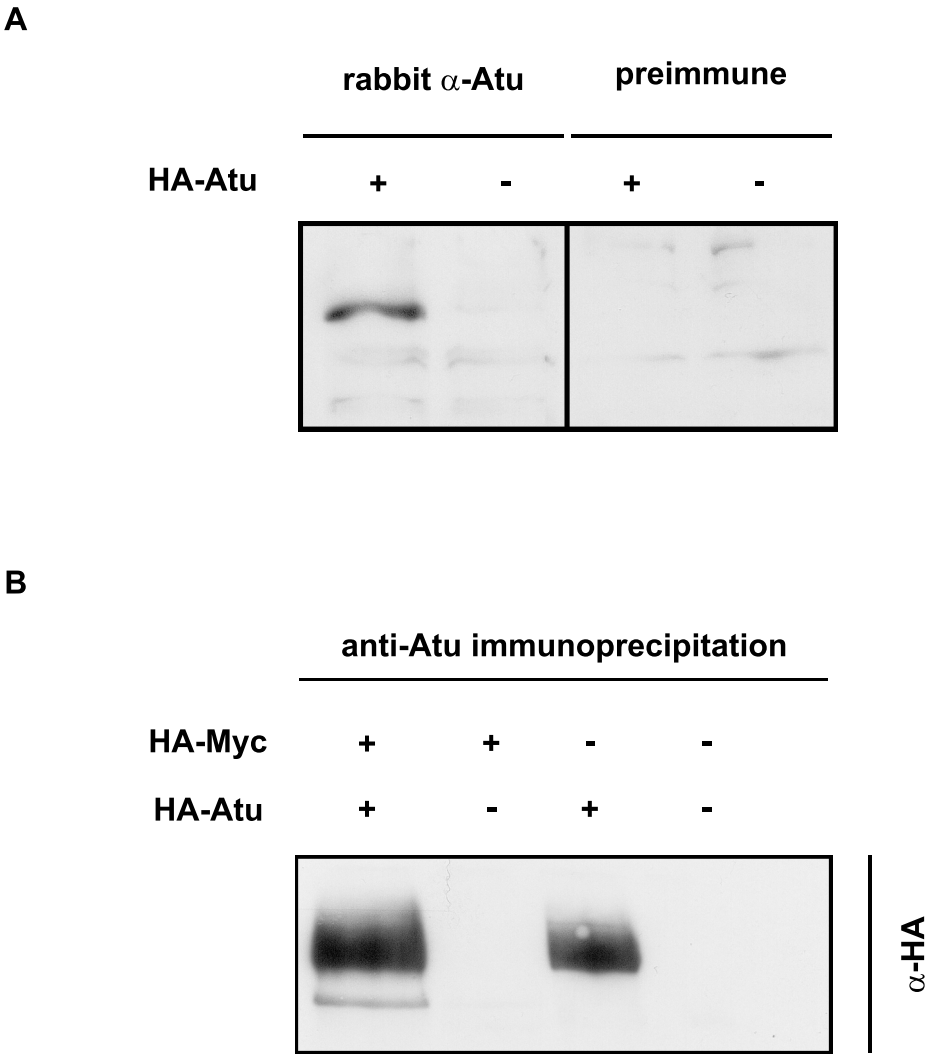

Figure 27

Characterisation of a rabbit anti-Atu polyclonal antibody.
An antibody was raised against the epitope RDKVESQVESAPKEC, wich corresponds to the amino acids 368 to 381 of the *Drosophila* Atu sequence. This sequence stretch is specific to the *Drosophila* Atu protein and not conserved in the vertebrate Atu homologues. **A:** depicts a Western blot of Atu-overexpressing S2 cell lysates (lanes 1 and 3) and non-transfected controls (2 and 4). The left half of the membrane was incubated with rabbit anti-Atu antiserum (1:1000), the right half with preimmune serum from the same animal as a control. A clear band corresponding to the HA-tagged Atu protein of roughly 150 kDa is recognised in lane 1. **B:** coimmunoprecipitations with the rabbit anti-Atu antibody. HA-Myc and HA-Atu proteins were co-overexpressed and immunoprecipitations with the anti-Atu antibody were performed.The membrane was incubated with mouse anti-HA antibody. HA-tagged Myc is specifically recognised in lane 1 (lower band), in which both proteins are present. Lanes 1 and 3 also confirm a specific immunoprecipitation of Atu as visualised by the anti-HA antibody.

5.3.1. Conserved Myc domains are not required for physical interaction with Atu in S2 cells

Coimmunoprecipitations between Atu and Myc have shown that the two proteins interact physically. To map the binding site(s) for Atu in the Myc protein, we performed coimmunoprecipitation experiments using a series of HA-tagged Myc protein mutants. An overview of the mutant Myc variants is presented in Figure 28. Constructs, which expressed Myc variants with individual deletions of the Myc-Boxes 1-3 (ΔMB1-3), the leucine zipper (ΔZ), or the entire bHLH-zipper (ΔC) were tested. Additionally, a variant lacking the N-terminus (ΔN) and a Myc protein lacking both the N-terminus and the bHLH-zipper (ΔNΔC) were included. Individual Myc mutants were transiently co-overexpressed with AU1-Atu in S2 cells. Expression of the constructs was driven by *tubulin-GAL4*. After 48 hours, the cells were harvested and lysates were immunoprecipitated with rabbit anti-AU or rabbit anti-Atu polyclonal antibodies. Anti-HA Western blotting revealed that all the Myc variants with mutations of the conserved domains still retain the ability to physically interact with Atu. Therefore, the well conserved domains of Myc are dispensable for this association. (Figure 29).

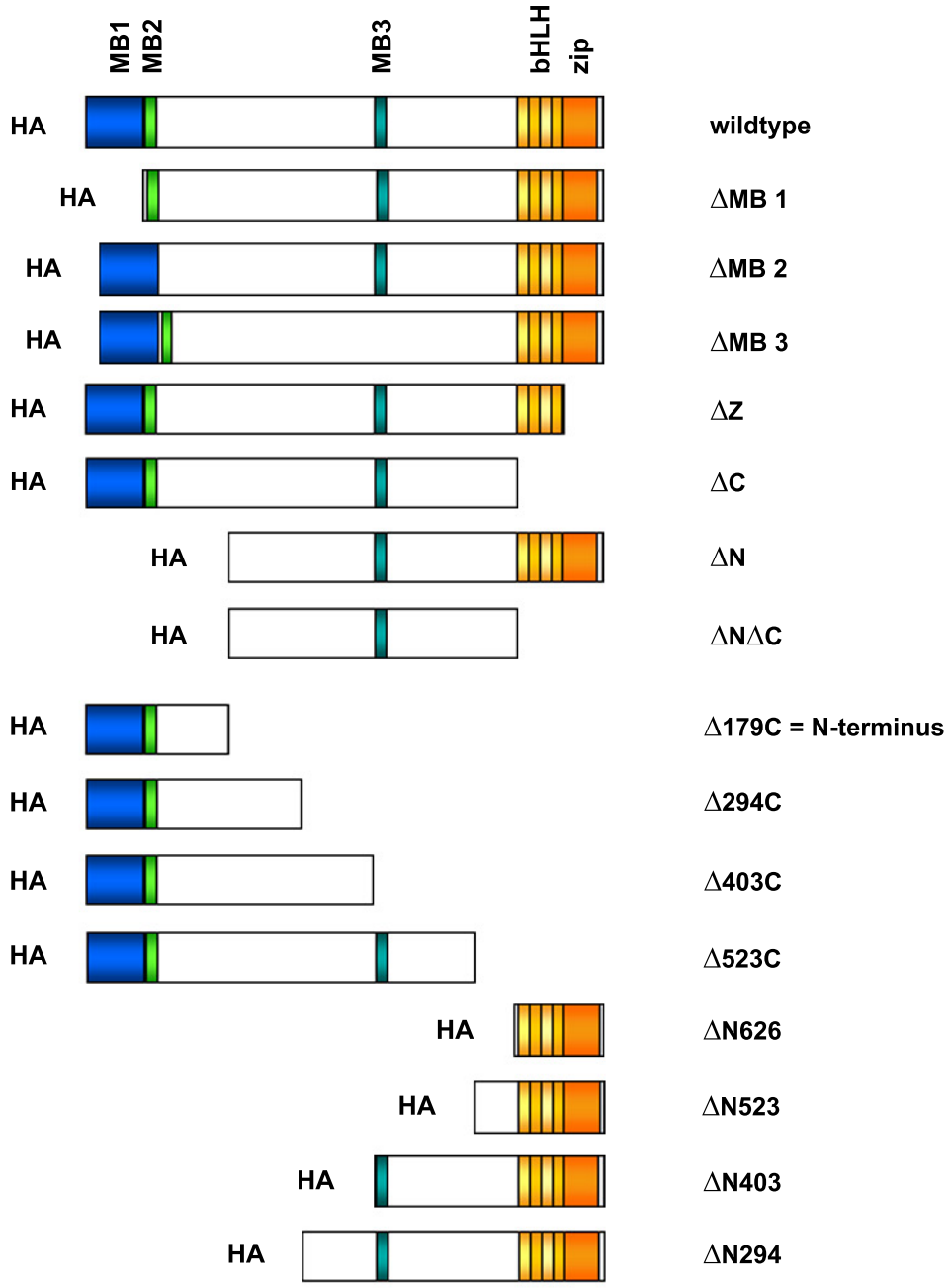

Figure 28

Schematic representation of the various Myc deletion mutants.
ΔMB 1: deletion of Myc-Box 1 (aa 1-65)
ΔMB 2: deletion of Myc- Box 2 (aa 68-84)
ΔMB 3: deletion of Myc-Box 3 (acidic region; aa 405-422)
ΔZ: C-terminal deletion of the leucine zipper motif (aa 678-717)
ΔC: C-terminal deletion of the entire bHLH-zipper motif (aa 620-717)
ΔN: N-terminal deletion of the transactivation domain (aa 1-179)
ΔNΔC: combination of the two truncations ΔN and ΔC (aa 1-179 and 620-717)

The 8 mutants in the lower panel are complementary C- and N-terminal truncations. The terminology is as follows: e.g. Δ179C is a C-terminal truncation lacking aa 179 to the C-terminus ,while ΔN294 is an N-terminal truncation from the start up to aa 294. All the deletion mutants carry an N-terminal triple HA-tag.

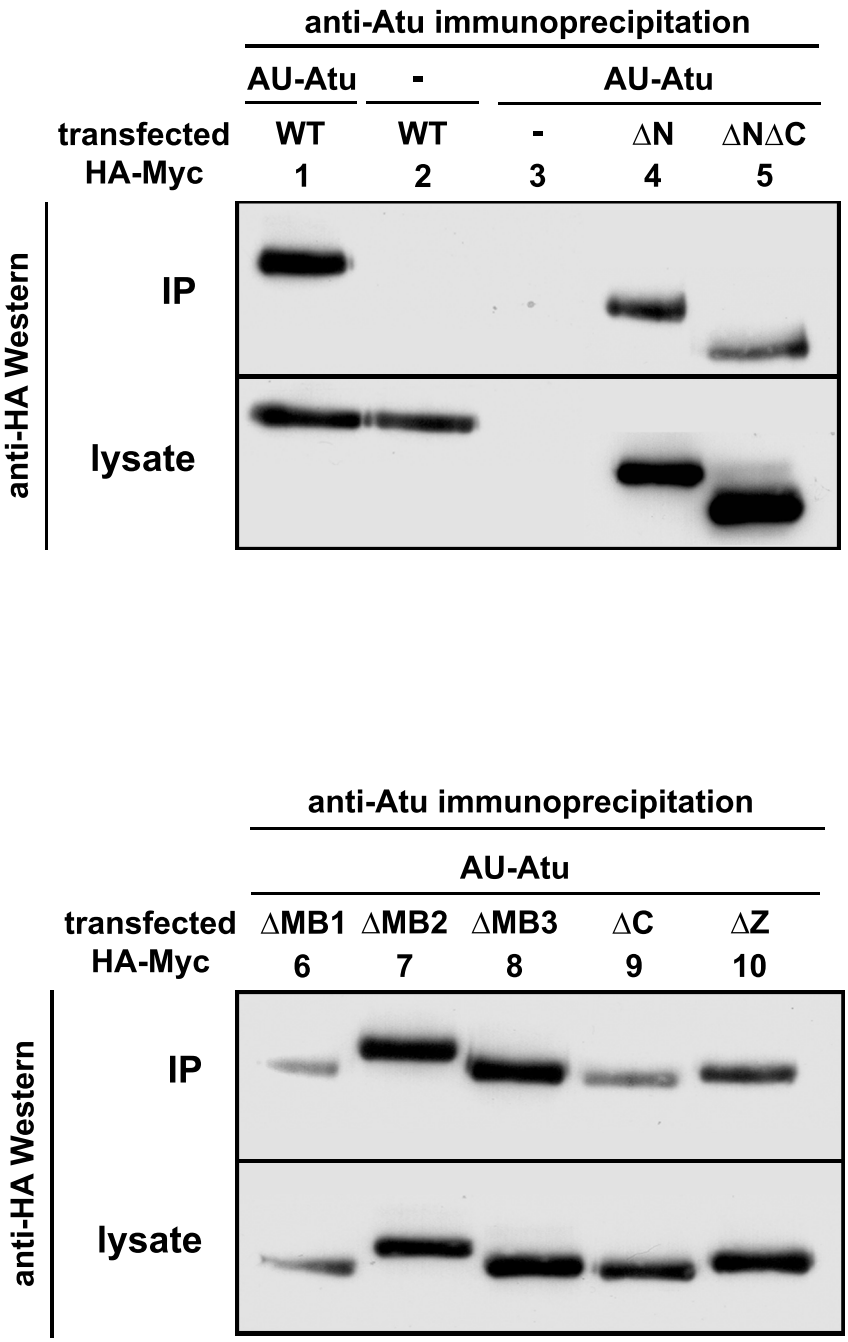

Figure 29

Coimmunoprecipitations of AU1-tagged Atu with various Myc protein deletion mutants. Myc deletion mutants lacking conserved motifs were coimmunoprecipitated with Atu. A schematic of the Myc mutants is depicted in Figure 28. Individual HA-tagged Myc mutants were expressed in S2 cells together with AU1-tagged Atu. Atu was immunoprecipitated using a rabbit anti-Atu antibody. Myc proteins were detected by Western blotting with a mouse anti-HA antibody. One lane corresponds to the lysate of one 3 cm tissue culture dish (approximately 5 million cells).

5.3.2. Atu interacts physically with various Myc protein mutants

Since mutating the conserved domains within Myc did not abrogate the physical interaction with Atu in this first series of interaction experiments, we planned to identify the potential interaction domain by constructing a larger set of additional deletions. For this purpose the Myc protein was simply divided into fragments of roughly equal sizes, for protein alignments between the Myc proteins of twelve *Drosophilid* species and the mosquito *Anopheles gambiae* revealed neither recognisable domains, nor additional regions of higher conservation. Figure 28 shows a schematic depiction of the deletion variants used. During a first series of transfection experiments with the newly produced Myc deletion mutants we observed that the individual constructs were differentially expressed. While the larger fragments were generally well expressed, the shorter fragments, especially the N-terminal truncations, were induced at considerably lower levels. We therefore adjusted the amount of plasmid transfected so as to achieve as uniform an expression as possible. Immunoprecipitations were again performed by transiently expressing *UAS-AU1-Atu* with the individual triple HA-tagged Myc deletion constructs. A polyclonal anti-Atu antibody was used to precipitate AU1-Atu protein and samples were analysed on a Western blot using an anti-HA epitope antibody to detect Myc proteins. All the variants except the short C-terminal fragment ΔN523 and the smallest fragment ΔN626, which was not expressed in S2 cells and therefore could not be assessed, still interact with the Atu protein (Figure 30). Despite adjusting the amount of transfected plasmid DNA to ensure equal expression levels, the protein variants displayed in Figure 30 can be placed in three different groups according to their strength of expression in S2 cells. The strongly expressed C-terminal truncations (Δ294C, Δ403C, and Δ523C) and ΔN294, moreover the three fragments ΔN403, ΔN523, and the N-terminus, which are all expressed at lower levels, and lastly ΔN626 which is not expressed. Of the strongly expressed Myc protein mutants the two fragments Δ523C (lane 3) and ΔN294 (lane 4) clearly interact with Atu as strongly as a wild-type Myc protein (data not shown), while Δ294C and Δ403C display weaker affinities. Within the second group of fragments with reduced expression levels, ΔN523 (lane 6) displays the weakest binding to Atu. As mentioned above ΔN626 could not be assessed as it was not expressed. Taken together, all the protein mutant forms which contain the central domain of the Myc protein, between amino acids 294 and 523 still bind Atu with high affinities. Hereby, the strongest interaction seems to be mediated by the stretch between amino acids 294 and 403 (differences between Δ294C and Δ403C and between ΔN294 and ΔN403). In addition to the central binding site in Myc also an N-terminal interaction is seen, for the N-terminus containing the first 179 amino acids of the Myc protein, is coimmunoprecipitated by Atu.

Even though translation is initiated from identical start sites for all protein mutants, they are expressed at vastly different levels. In general, the shorter fragments are not as strongly expressed as the larger ones. In particular Δ294C-expression is even higher than that of the wild type *myc* protein. However, size seems not to be the only determinant of the expression level, because mutants of similar size are not equally expressed (Δ294C compared to ΔN403). Taking the general size effect into account, this suggests differences in protein stability of the various Myc variants. While the stability of protein truncations could generally be affected by non-native folding, these observations might also indicate the presence of a “destabilizing region” in the central stretch (after residue 403) of the Myc protein, since C-terminal fragments seem to be more abundant or stable. This “destabilizing region” could

correspond to the conserved domain MB 3, since there is data that suggest “destabilising” functions for MB 3 (D. Schwinkendorf, personal communication). This stabilisation effect seen with certain Myc fragments could be due to the loss of binding to components of the proteasome machinery (e.g. ubiquitin-ligases) or binding of factors that negatively influence Myc’s degradation via the ubiquitin-proteasome pathway. Figure 31 shows a schematic overview of the associations seen between the Myc protein mutants and Atu, including their interaction strengths.

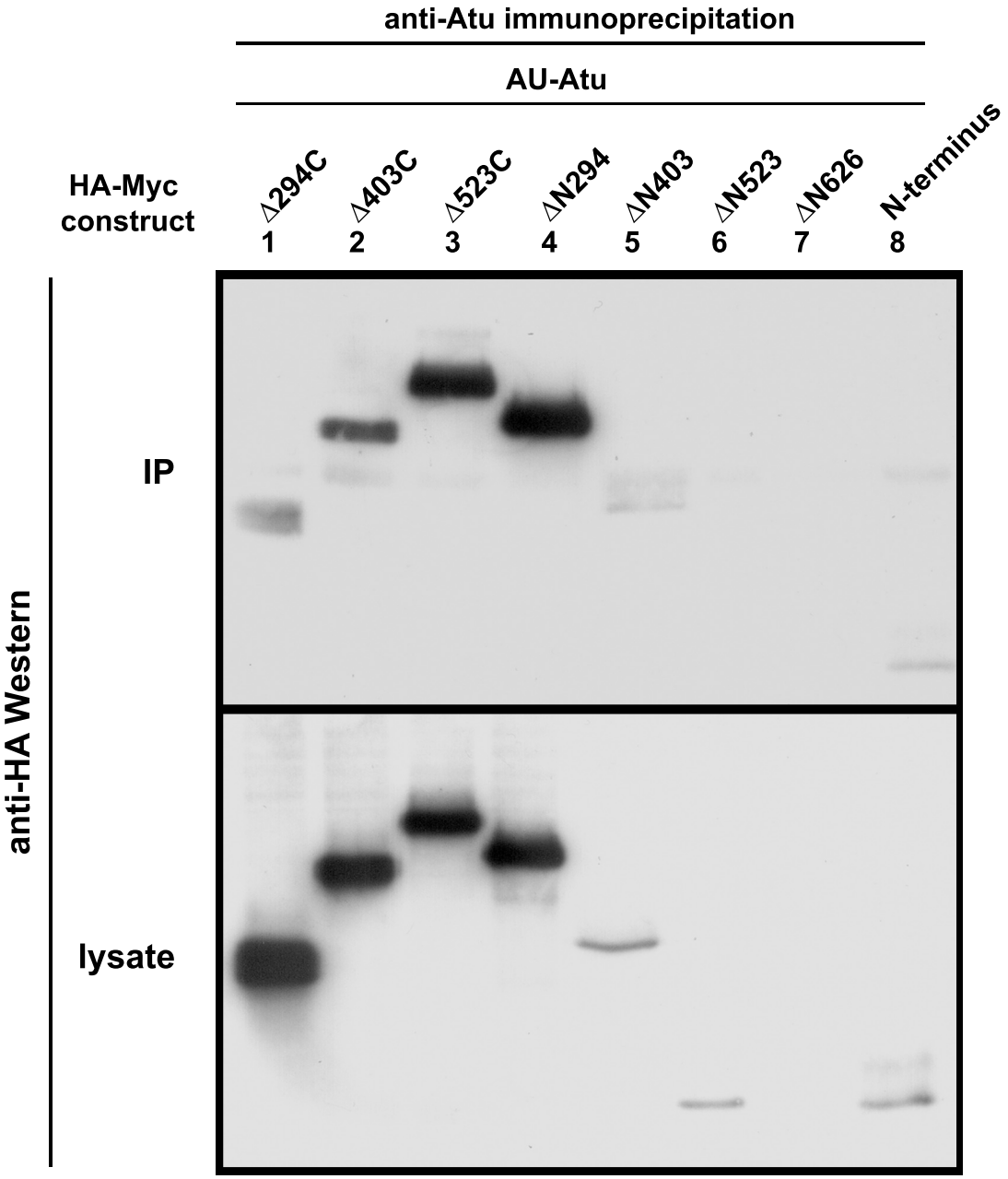

Figure 30

Coimmunoprecipitations between overexpressed Atu and Myc truncation mutants.
S2 cells were transfected with AU1-Atu and HA-Myc deletion mutants. Plasmids were expressed under the control of *tubulin-GAL4*. Total amount of DNA transfected was set to 10μg. Since the expression level of individual Myc truncations varied, transfected DNA amounts were adjusted (see below). Immunoprecipitation was performed with a rabbit anti-Atu antibody, Western blots with mouse anti-HA. One lane corresponds to the lysate of roughly 5 million cells.

Transfection amount	(in μg)
Δ294C	5.0
Δ403C	3.0
Δ523C	1.0
ΔN294	1.0
ΔN403	5.0
ΔN523	7.5
ΔN626	7.5

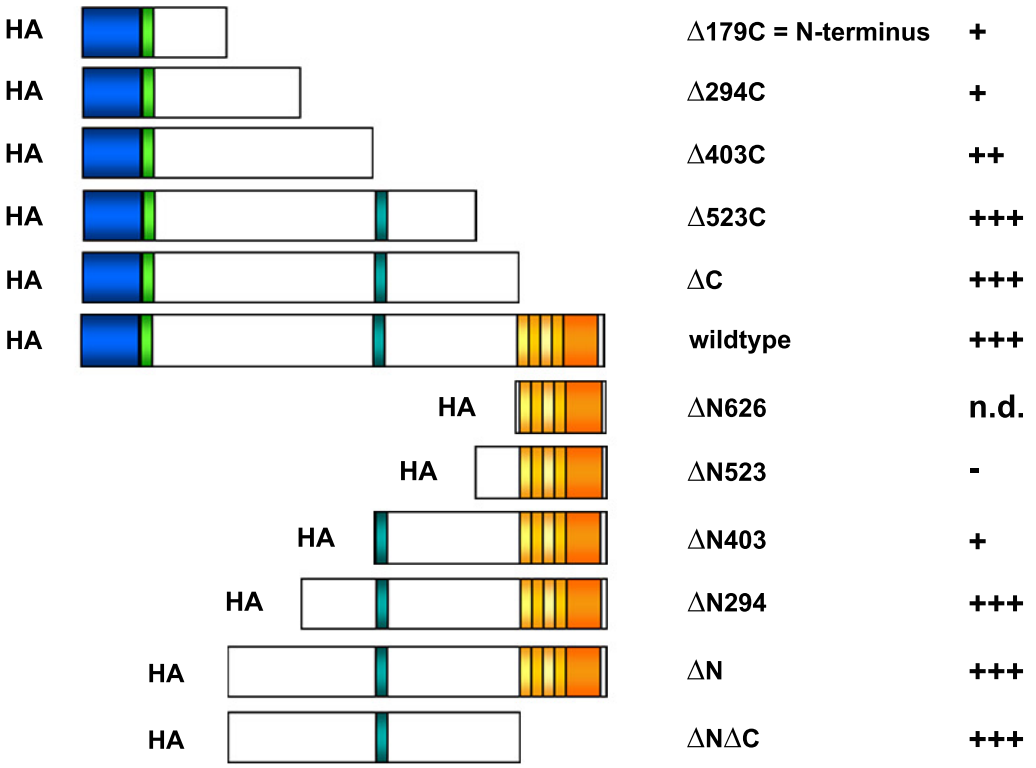

Figure 31

Schematic overview of the interaction between Atu and various Myc mutant protein forms.
To the right the interaction strengths are depicted. '-' no interaction, '+' weak interaction, '++' and '+++' strong and very strong interactions, 'n.d.' not determined.

The interaction studies provided strong evidence that the central part of the Myc protein is important for the physical interaction with Atu. Therefore, three additional mutants with internal deletions were constructed. We combined the C-terminal deletion mutant Δ294C with the N-terminal mutants ΔN403, ΔN523, and ΔN626 respectively. The direct combination of the mutant forms was possible as an Mlu I restriction site was engineered adjacent to the truncation site of all mutants (for cloning procedures see Materials and Methods Section 1). Subsequently, the three resulting Myc proteins with internal deletions were tested for their ability to interact with Atu. As seen in Figure 32, all the three mutant forms still interact very strongly with Atu. This result suggests that the interaction site in the N-terminus of Myc is sufficient to mediate strong physical binding to the Atu protein, even in the absence of the whole central stretch of the protein as seen in the mutant form (Δ294C-626) lane 6.

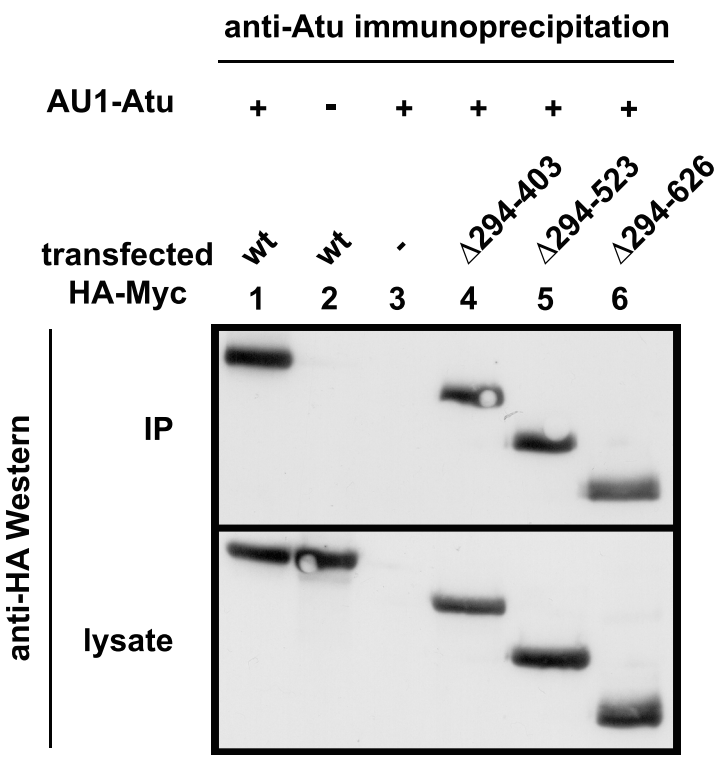

Figure 32

Atu interacts with internal Myc deletion mutants.
S2 cells were transfected with AU1-Atu and HA-Myc deletion mutants. Plasmids were expressed under the control of *tubulin-GAL4*. Total amount of DNA transfected was set to 10μg. Coimmunoprecipitations between overexpressed Atu and Myc truncation mutants were performed with a rabbit anti-Atu antibody, Western blots with mouse anti-HA. One lane corresponds to the lysate of roughly 5 million cells.

5.3.3. The interaction between Myc and Atu is direct

Coimmunoprecipitation experiments with transiently overexpressed Myc and Atu had revealed a strong physical interaction between the two proteins. To address the question if the interaction was direct or mediated by additional proteins in a multimeric complex, recombinant GST-Myc fusion protein variants were expressed in *E. coli* and tested for their ability to interact directly with *in vitro* translated, ^{35}S-labelled Atu. The entire Atu ORF was cloned into pBlueskript SK and expressed from a phage T7 RNA polymerase promoter using a coupled rabbit reticulocyte transcription/translation system. GST pull-downs showed that the Atu protein expressed *in vitro*, is being bound by a glutathione sepharose bead coupled GST-Myc variant that contains amino acids 46 to 507 of Myc (Figure 33). This large Myc fragment includes most of the N-terminal transactivation domain with the conserved Myc Boxes 1-2 (MB1-2), as well as the centrally located Myc Box 3 (MB3). In contrast, GST alone, which is used as a negative control of the binding assay, does not retain Atu in the pull-down assays (compare lanes 2 and 3 of Figure 33), even though it was used in at least equal concentrations as GST-Myc. This experiment shows that the interaction between Myc and Atu is specific and direct.

Since coimmunoprecipitation experiments performed in S2 cells (Results, sections 5.3.1. & 5.3.2.) have revealed two putative Atu-interaction domains in Myc, the corresponding Myc fragments were linked to GST in order to assay whether both these domains mediated direct protein-protein association. Figure 34 represents a schematic overview of the direct interactions between the various GST-Myc fragments and Atu, including the strength of the associations. As shown before, the largest Myc fragment (aa 46-507) binds to Atu with intermediate affinity (dark blue). The N-terminal Myc fragment that spans the region from the translation start to amino acid 176, interacts most strongly with Atu (navy), while the other two N-terminal fragments (aa 66-179 and aa 66-295) display reduced interaction capacity. In addition to the N-terminal portion of the Myc protein, also the centrally located fractions of Myc mediate physical associations with Atu. The three fragments which include MB3 all interact with weak to intermediate affinities. In summary, the *in vitro* translation experiments suggest that Atu directly interacts with Myc at (at least) two sites. These include the N-terminus, the first 180 amino acids, and the central part of the protein in the vicinity of Myc Box 3.

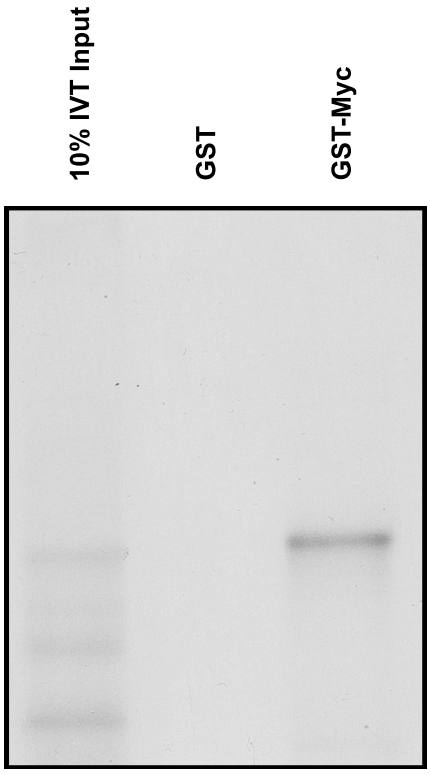

Figure 33

Interaction between *in vitro* translated ^{35}S-labelled Atu and GST-coupled Myc (amino acids 46-507). GST alone was used as a control for the specificity of the interaction.

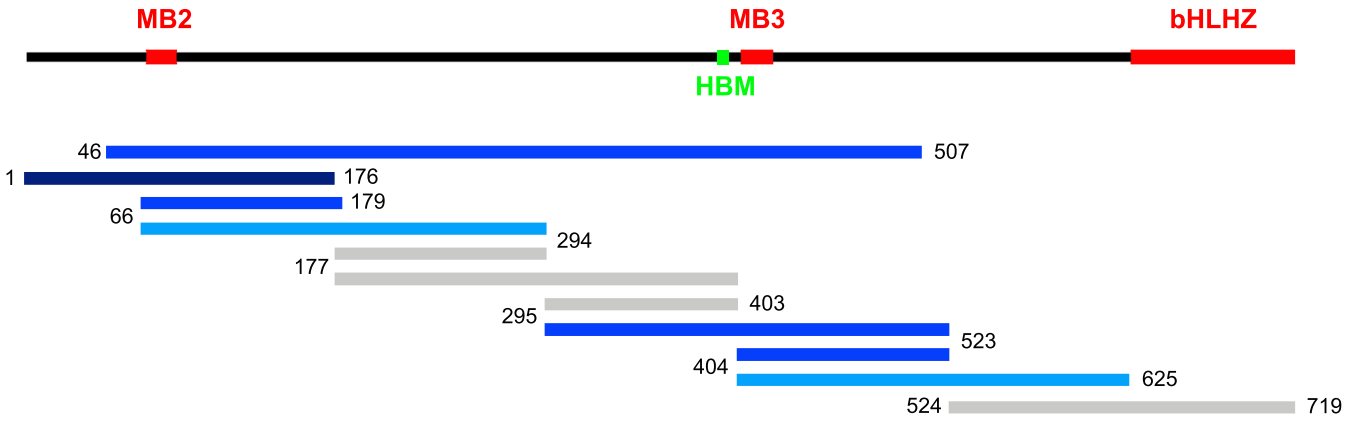

Figure 34

Schematic of the Interaction of Atu with various Myc protein truncations.
Depicted are the interaction strengths of the *in vitro* translated Atu protein with various GST-Myc protein truncations. The darker the shade of blue the stronger the interaction. Fragments shown in grey do no interact. On top: schematic drawing of the Myc protein with the conserved motifs MB 1 (Myc Box 1), MB 3 (Myc Box 3), and the basic helix-loop-helix leucine zipper.

5.4. Functions of the PAF complex *in vivo*

Luciferase assays that confirmed the original screen data, as well as expression profiling of direct Myc target genes and various binding experiments, constitute evidence that several subunits of the RNA Polymerase-associated factor 1 complex are Myc cofactors involved in transcription control. In order to assess the function of the PAF complex components *in vivo*, we examined the effects of PAF complex induction or reduction in various tissues of the adult fly, such as the eye and the wing, but also in larval imaginal discs and fat body.

5.4.1. RNA*i* against individual PAF complex components causes a size reduction of bristles

One of the hallmarks of *myc* hypomorphic mutants in *Drosophila* is a thin bristle phenotype. The macrochaetae are smaller in relation to overall body size than in wild type animals. This phenotype occurs in mutants with defects in protein biosynthesis (e.g. *Minute* mutants) (Schreiber-Agus et al., 1997; Gallant et al., 1996). We tested whether bristles are also sensitive to depletion of PAF complex components, which might indicate a link of Myc and the PAF complex in the control of bristle growth. Indeed, depletion of PAF complex levels also had a clear size effect in scutellar macrochaetae. We expressed *UAS*-hairpin RNA constructs targeting PAF components in bristle progenitor cells with *scabrous-GAL4* (*sca-GAL4*). The size of both anterior and posterior scutellar bristles was measured in flies with reduced PAF complex levels in comparison to control animals that express *lacZ* dsRNA (Figure 35). *atms*-RNA*i* caused a strong reduction of thoracic bristle size by more than 50%. The effects of *rtf1* and *atu* reduction were less pronounced. While *rtf1* depletion caused a slight size reduction of 25-30% in both anterior and posterior scutellar bristles, *atu* knockdown only had a marginal effect in anterior scutellar bristles.

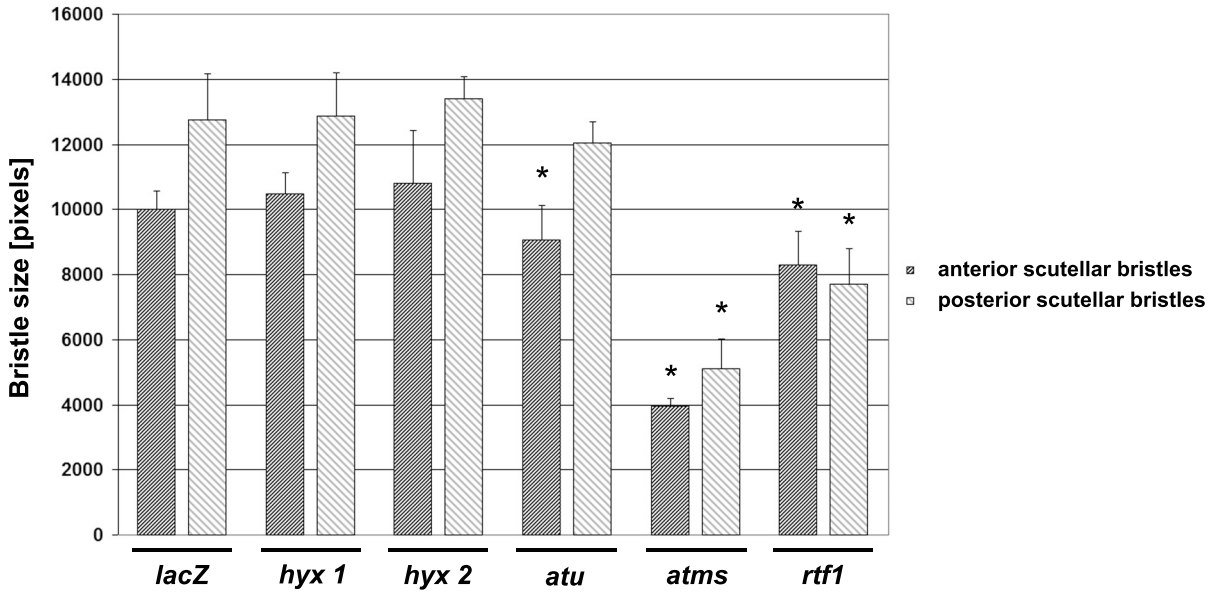

Figure 35

Depletion of the PAF complex components Atu, Atms, and Rtf1 leads to reduction of bristle size. Size of scutellar bristles from male flies expressing hairpin constructs directed against the genes indicated above in the bristle precursor cells by *scabrous-GAL4*. For every genotype, the area of the anterior and posterior scutellar bristles of 5 individual flies was measured. Asterisks indicate significant changes in size compared to *lacZ* controls by the Student's t-test ($p < 0.05$). Error bars indicate standard deviations.

Genotypes

lacZ: *yw/Y; UAS-lacZ-IR M-3i/sca-GAL4*
hyx1: *yw/Y; +/sca-GAL4*; *UAS-hyx1-RNAi/+*
hyx2: *yw/Y; +/sca-GAL4; UAS-hyx2-RNAi/+*
atu: *yw/Y; UAS-atu-RNAi/sca-GAL4*
atms: *yw/Y; +/sca-GAL4; UAS-atms-RNAi/+*
rft1: *yw/Y; +/sca-GAL4; UAS-rtf1-RNAi/+*

5.4.2. *hyx* shows a weak genetic interaction with the hypomorphic *myc* allele *P0*

As described in Chapter 3 of the Result section, the *Drosophila* eye is a particularly sensitive system to changes in Myc activity. Especially the hypomorphic *myc* allele dm^{P0} has previously been used to characterise the strong genetic interaction with the essential Myc cofactor Tip49/Pontin (Pont) (Bellosta et al., 2005). One hallmark of dm^{P0} males carrying a heterozygous mutation in the *pontin* gene, is the occurrence of small, irregularly shaped, and slightly rough eyes. We have used the *ey>*dm^{P0} system (Bellosta et al., 2005) to assay for dominant interactions, since the same phenotype as in dm^{P0}, albeit with a higher penetrance, is seen in this background (Results section 3.1.). Four strains with reduced or elevated *hyx* levels were also tested in the *ey>*dm^{P0} background. The strong hypomorphic *hyrax* allele hyx^{EY6898} which is caused by the EP-element insertion *EY6898* into the 5' UTR of the *hyrax* gene, $hyrax^{P9}$, which contains another EP-element inserted upstream of *hyx* between the two loci *neuralised (neur)* and *hyx*, hyx^{2}, a putative null allele, and the *hyx* overexpression line UAS-$hyx^{1.5}$. These four lines are described in detail in (Mosimann et al., 2006). The offspring from all the experimental crosses showed no aberrance in their eye morphology (data not shown), therefore neither the reduction nor the increase of *hyx* levels led to a phenotype similar to the one observed with *pont*. Since changes in *hyx* levels do not cause obvious phenotypes in the dm^{P0} background (data not shown), the same *hyx* mutant strains were crossed to *ey>*dm^{P0} flies that were in addition heterozygous mutant for *pont*. Indeed, these crosses yield offspring with defective eyes at highly varying frequencies (Figure 36). However, in contrast to *ey>*dm^{P0}*;* $pont^{+/-}$ animals originating from direct crosses, which show an almost complete penetrance of severe eye defects (Bellosta et al., 2005), prolonged propagation of an *ey>*dm^{P0}*;* $pont^{+/-}$ stock causes strong reduction of the frequency of eye defects. This is presumably due to a selective pressure on *ey>*dm^{P0}*;* $pont^{+/-}$ flies. Although the allele hyx^{2} and overexpression with the *UAS-hyx* construct do not cause significantly increased frequencies of eye defects, as compared to control crosses with *yw* (20% and 23%, respectively, of the relevant offspring have eye defects, compared to 16% for crosses with the *yw* control), *UAS-hyx* seems to affect the expressivity. Especially the anterior parts of the eyes show an increased roughness and the eye colour is changed. However, the colouration is affected independently of a lesion in *pont* and could therefore be based on a Myc-independent function of *hyx* or be caused by background mutations. In contrast, the two alleles hyx^{P9} and most potently hyx^{EY6898}, result in eye defects with elevated penetrances of 30% and 58%. The expressivity of the eye defects seen with the EP-insertions varies vastly from eyes displaying a slightly increased roughness to heavily disturbed overall eye morphology. Interestingly, both the overexpression construct *UAS-*$hyx^{1.5}$ and the EP-insertion *EY6898* cause stronger defects in the anterior part of the eye. In addition, a variegation of the eye pigmentation is seen with both alleles. While the anterior part of the eye is orange, the posterior half is dark red in flies carrying the $hyrax^{EY6989}$ allele and pigmentation is almost completely lost in animals containing the *UAS-hyx* transgene.

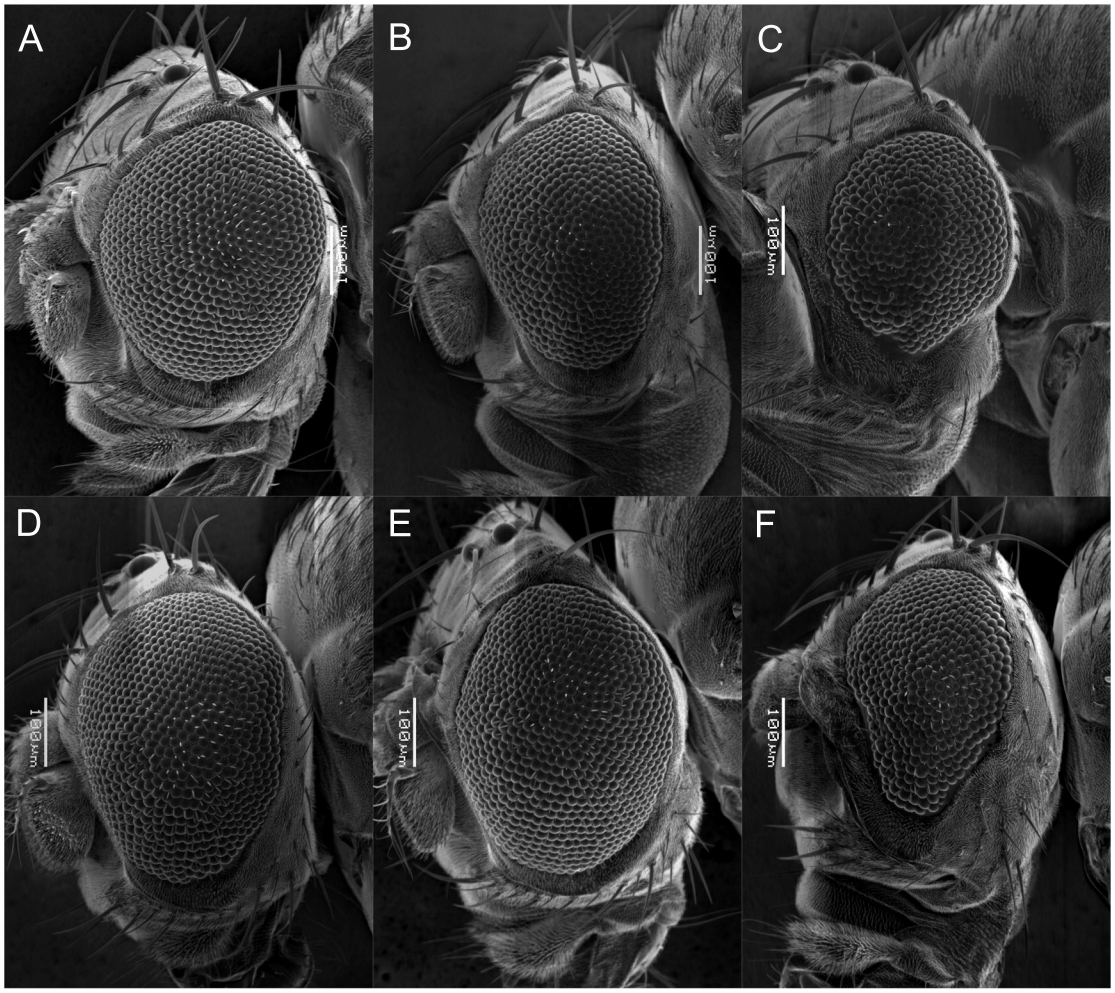

Figure 36

Influence of heterozyogous *hyx* mutants on the eyes of *ey>dmP0/Y; pon* $^{-/+}$ flies. Shown are representative scanning electron micrographs from flies of the genotypes listed below. Genotype A served as a control. *pont*$^{5.1}$ is a putative null allele. Pictures were taken at a magnification of 180x

A: *yw tub>dmyc(y+)>Gal4 eyflp/Y; UAS-lacZ RNAi/+*
B: *yw tub>dmyc(y+)>Gal4 eyflp/Y; +; pont*$^{5.1/+}$
C: *yw tub>dmyc(y+)>Gal4 eyflp/Y; +; pont*$^{5.1}$*/hyx*^{P9}
D: *yw tub>dmyc(y+)>Gal4 eyflp/Y; +; pont*$^{5.1}$*/hyx*^{6898}
E: *yw tub>dmyc(y+)>Gal4 eyflp/Y; +; pont*$^{5.1}$*/hyx*^{2}
F: *yw tub>dmyc(y+)>Gal4 eyflp/Y; UAS-hyx*$^{1.5/+}$*; pont*$^{5.1/+}$

To analyse the observed eye defects in more detail, we examined scanning electron micrographs taken from male *ey>dm^{P0}/Y*; *pon $^{-/+}$* flies that also carried a mutation in one *hyx* allele. The eyes were then analysed with respect to the size of the ommatidia and the number of ommatidia in an individual compound eye. To assess the effects on ommatidial size, the area of 20 centrally located ommatidia of five eyes was measured. While none of the four alleles (*hyx^{P9}*, *hyx^{EY6898}*, *hyx^{2}* and *UAS-hyx$^{1.5}$*) caused any significant change in ommatidial size in an *ey>dm^{P0}*; *pont $^{-/+}$* background (Figure 37), ectopic *hyx* expression by *UAS-hyx* led to a significant reduction of ommatidial number (panel E in Figure 38). Conversely, heterozygosity for the *hyx* null mutation *hyx^{2}* resulted in an increased number of ommatidia within a single compound eye (D in Figure 38).

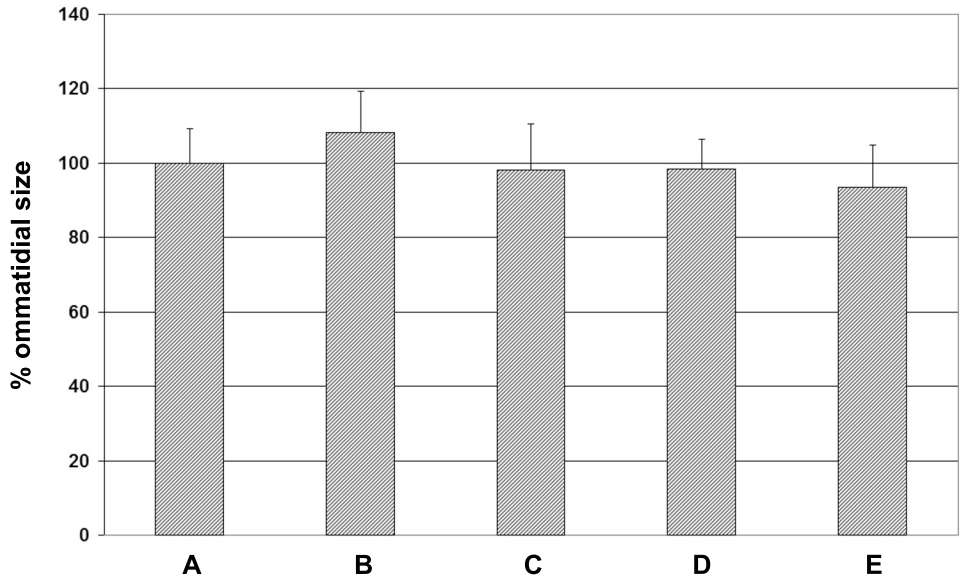

Figure 37

Ommatidial size of *ey>dmP0/Y;+; pont$^{5.1}$* flies, carrying *hyx* heterozygous mutations. For every genotype, the size of 20 centrally located ommatidia of five individual eyes was determined. The ommatidial area of Genotype A was set to 100%. The error bars indicate standard deviations.

Genotypes

A: *yw dm^{P0} tub>dmyc(y+)>Gal4 eyflp/Y; +; pont$^{5.1/+}$*
B: *yw dm^{P0} tub>dmyc(y+)>Gal4 eyflp/Y; +; pont$^{5.1}$/hyx^{P9}*
C: *yw dm^{P0} tub>dmyc(y+)>Gal4 eyflp/Y; +; pont$^{5.1}$/hyx^{EY68989}*
D: *yw dm^{P0} tub>dmyc(y+)>Gal4 eyflp/Y; +; pont$^{5.1}$/hyx^{2}*
E: *yw dm^{P0} tub>dmyc(y+)>Gal4 eyflp/Y; UAS-hyx$^{1.5/+}$; pont$^{5.1/+}$*

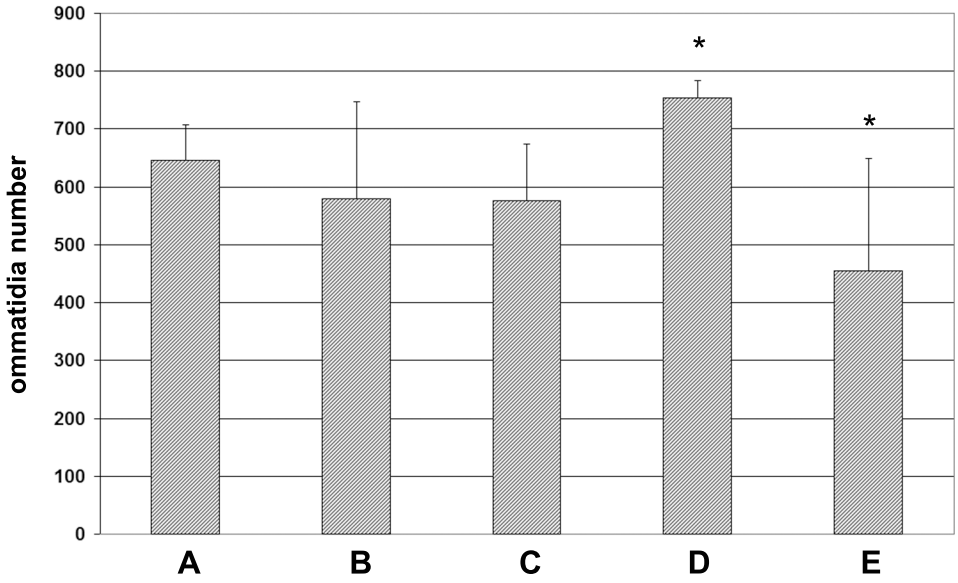

Figure 38

Ommatidial size of *ey>dmP0/Y;+; pont$^{5.1}$* flies, carrying *hyx* heterozygous mutations. For every genotype, the ommatidia number of five individual eyes was counted. The error bars indicate standard deviations. The asterisks depicts significant size changes ($p < 0.05$) after the Student's t-test compared to the control genotype A

Genotypes

A: *yw dm^{P0} tub>dmyc(y+)>Gal4 eyflp/Y; +; pont$^{5.1/+}$*
B: *yw dm^{P0} tub>dmyc(y+)>Gal4 eyflp/Y; +; pont$^{5.1}$/hyx^{P9}*
C: *yw dm^{P0} tub>dmyc(y+)>Gal4 eyflp/Y; +; pont$^{5.1}$/hyx^{EY68989}*
D: *yw dm^{P0} tub>dmyc(y+)>Gal4 eyflp/Y; +; pont$^{5.1}$/hyx^{2}*
E: *yw dm^{P0} tub>dmyc(y+)>Gal4 eyflp/Y; UAS-hyx$^{1.5/+}$; pont$^{5.1/+}$*

Taken together, the data presented in this paragraph are difficult to reconcile with each other, and have to be interpreted cautiously. One source of suspicion is the low incidence of eye defects in the *ey>dm^{P0}; pont$^{+/-}$* stock, as compared to its initial description. Moreover, the high variance of the eye defects in this line further complicates the statistical analyses of ommatidial size and number, as well as the assessment whether eye defects are aggravated by lesions in the *hyx* locus. Nevertheless, there are indications that Hyx acts as a negative cofactor of Myc *in vivo*. We could show that eyes heterozygous for the *hyx* null mutation *hyx^{2}*, contain a significantly higher number of ommatidia. While the overall number of defective eyes is not decreased, individual eyes seem to look more regularly patterned than in control animals. This fact does not necessarily point to a negative genetic interaction between *hyx* and *myc*. However overexpression of *hyx* caused a general aggravation of the eye defects as well as the most strongly defective eyes of all genotypes examined. The loss of large portions of eye-tissue is apparently caused by the significant loss of ommatidia (Figure 38, column E).

5.4.3. Ectopic *hyx* slightly suppresses *myc* overexpression phenotypes in the eye

The cellular consequences of Myc overexpression are increased growth, and at high levels induction of apoptosis. While expression of one copy of *UAS-myc* in the eye leads to larger ommatidia without disruption of the regular ommatidial pattern, further increase of Myc levels (by expressing three copies of *UAS-myc* at 25°C) still causes an enhancement in ommatidial size (up to 20% increase). However, the ommatidial arrangement is disturbed as a consequence of apoptosis. On a macroscopic level this disruption of the ommatidial array is manifested by the rough texture of the eye. At highest levels of ectopic Myc expression (3 copies expressed at temperatures higher than 25°C) the appoptosis overwhelms the growth-promoting effects and the ommatidial size decreases again, while the rougness is even more pronounced. In extreme cases the ommatidial pattern is totally destroyed and the eyes take on a glassy appearance (Steiger, 2007; Montero et al., 2008). We tested if increase or reduction of *hyx* levels influenced Myc activity and the resulting overexpression phenotype. Test crosses to *y w; GMR-GAL4 UAS-myc^{132}/+; UAS-myc^{132} UAS-myc^{42}/+* animals showed that ectopic *hyrax* expression by driving one copy of the *UAS-hyx* transgene slightly suppresses the rough-eye phenotype. This reduced roughness might indicate a reduction of Myc activity. A similar suppression is seen in crosses where *pontin* function is partially disrupted by crossing in the *pontin* null mutant *pont$^{5.1}$*. In contrast, a null mutation in the *hyx* locus (*hyx^{2}*) occasionally leads to a reduction in eye size and a severly affected eye texture. Individual ommatidia cannot be distinguished anymore, and the eye surface becomes smooth with a distinctive glassy appearance, however the relevance of this observation is unclear, since only 5% of a total of 80 flies were affected. This phenotype is commonly seen in eyes with very high levels of Myc. Taken together, increased *hyx* levels seem to suppress the roughness caused by strong overexpression of *myc*, while partial disruption of *hyx* function even aggravates the phenotype seen in cases of very high *myc* levels.

5.4.4. Disruption of *Atu*, but not of *atms*, dominantly influences eye morphology

In addition to *hyx*, other PAF complex subunits were also tested for genetic interaction with *myc*. We examined the influence of two strong *Atu* and *atms* loss of-function alleles respectively. Both alleles are caused by the insertions of transposable elements into the 5' UTR of the corresponding gene, resulting in disruption of their functions and recessive lethality. When crossed to *ey>dm*^{P0} flies, neither *Atu*^{s1938} nor *atms*^{rK509} causes any eye defects that resemble the ones seen with heterozygous *pont* mutations. However, when the system is being sensitised even further by taking away one copy of the *pont* gene as described above, *Atu*^{s1938} aggravates the eye phenotype considerably, as 90% of the offspring show severly disturbed eye morphology. On the other hand, reduction of *atms* levels by *atms*^{rK509} does not have visible consequences. This suggests that Myc-dependent processes in the *Drosophila* eye seem to be more sensitive to the disruption of Atu function than loss of Atms.

5.4.5. Depletion of PAF complex function by RNA*i* causes severe eye phenotypes

All the genetic interaction studies described above were carried out using classic mutations (or overexpression transgenes) in genes coding for PAF complex components. Additionally, we also used fly strains from the Vienna *Drosophila* RNA*i* Center (VDRC). Strains carrying *UAS*-hairpin RNA transgenes targeting PAF complex components were crossed to *ey>dm*^{P0} animals. In the *ey>dm*^{P0} background the rescuing *myc* cDNA is specifically removed in the *eyeless*-expression domain, resulting in a *dm*^{P0} mutant situation in the whole head capsule. However, these flip-out events not only create a *myc* mutant situation but also allow GAL4-driven transgene-overexpression in the eye. As a further control for the dependence on *myc*, the same *UAS*-hairpin RNA transgenes were expressed in an *ey>dm*$^{+}$ wild type background. We used this experimental setup to assess two characteristics of the eyes. On the one hand we examined whether the highly ordered ommatidial pattern was disturbed in response to PAF complex-RNA*i*. On the other hand we measured the RNA*i*-influence on ommatidial size. In contrast to the classic mutations which never showed any dominant interactions in the *ey>dm*^{P0} background, depletion of *atms* and *rtf1* caused by expression of the *UAS*-hairpin construct specifically in the eye, led to distinct eye defects. Disruption of *atms* function caused severe rough-eye phenotypes in 85% of all offspring (55 animals with distinct eye defects /65 total). However, already *rft1*-RNA*i* in the wildtype background resulted in a slight rough-eye phenotype in 66% of all animals. The effect seen upon *rtf1* depletion was less potent as only 55% (37/67) of the animals possessed strongly rough eyes in a *dm*^{P0} mutant situation, and the great majority of the eyes in an *ey>dm*$^{+}$ background displayed slightly increased roughness. In both cases (for *atms*- and *rtf1*-RNA*i* in the *ey>dm*^{P0}) the eye defects resembled the effects seen upon mutating one copy of *pont*. In severely affected eyes a large number of ommatidia at the anterior and ventral edge of the eye were lost, causing indentations in the eye tissue. In most cases, the entire eyes displayed a strong roughness. Additionally, RNA*i* constructs targeting *hyx* and *Atu* were tested but did not cause any eye defects in the ey>*dm*^{P0} and *ey>dm*$^{+}$ backgrounds. As a control for unspecific RNA*i* effects we used the *lacZ*-hairpin line *Z-IR M3i* (Steiger, 2002). These results show a positive genetic interaction of *rtf1* and *atms* with *myc*, whereas the other two PAF complex components, *hyx* and *Atu*, did not genetically interact with *myc*.

In addition to overall defects and texture of the eye, we also examined the effect of PAF complex-RNA*i* on ommatidial size. Figure 39 shows an overview on the RNA*i* effect on ommatidia size. The size difference of the two strains expressing *lacZ*-hairpin RNA (compare column A to A') depicts the published effect of the dm^{P0} allele on ommatidial size. While this reduction of *myc* levels by the allele dm^{P0} results in this significant size reduction, no strong additional size reduction is observed upon further reduction of *myc* levels by *myc*-RNA*i* in an *ey>*dm^{P0} background (column B and B'), suggesting that dm^{P0} already displays strongly reduced Myc activity. Columns A-E depict the size of 20 centrally located ommatidia of five indivdual eyes that express *UAS*-hairpin transgenes in a *myc* wild type background (*ey>*dm^{+}*).* In this situation only knockdown of *myc* leads to a significant reduction of ommatidial size (compare A to B), while RNA*i* against PAF complex components does not significally change ommatidial size. However, the ommatidia seem to be slightly increased in size in response to PAF complex-RNA*i*. Since RNA*i*-mediated knockdown of *Atu* and *atms* in both *ey>*dm^{P0} and *ey>*dm^{+} backgrounds does not result in significant size changes as compared to *lacZ*-RNA*i*, we have to conclude that there is no specific genetic interaction between *myc* and *Atu* or *atms* respectively. However, we observe a negative genetic interaction between *hyx* and *myc* as the downregulation of *hyx* seems to alleviate the requirement for Myc in the dm^{P0} situation (compare columns C and C'). In contrast to the classic mutants, which only showed genetic interaction in the eye in a heavily sensitised background (by mutating one copy of *pont*), expression of *UAS*-hairpin RNA*i* lines have a stronger effect, as they already cause defective eyes in an *ey>*dm^{P0} situation. This suggests that expression of the hairpin-RNA*i* transgenes lead to a stronger downregulation than heterozygosity for a given PAF complex component.

RNA*i*-line	roughness	ommatidial size
hyx	-	+
drtf1	++	-
atu	-	-
atms	+++	-

Table 3 summarises the effects of depletion of PAF complex components by RNA*i* in the *ey>*dm^{P0} situation. While downregulation of *rtf1* and atms results in an increase roughness of the eye texture and loss of ommatidia, *hyx* depletion alleviates the requirement for Myc in the dm^{P0} situation

To characterise the putative genetic interaction between Myc and the components of the PAF complex, we have both tested classic mutants, which disrupt PAF complex function, but also transgenic RNA*i* insertion lines against several PAF complex subunits. Taken together, these interaction studies reveal different properties for individual PAF complex subunits. While *hyx* seems to behave as a negative cofactor of Myc, as seen with the genetic interactions of *UAS-hyx* and hyx^{2} in the eye, the other tested subunits (Rtf1, Atu, and Atms) represent coactivators of Myc in various assays. RNA*i*-mediated depletion of *atms* and *rtf1* strongly reduced bristle growth but also led to severe eye defects in an *ey>*dm^{P0} background. Knockdown of *atu* had milder consequences on bristle size, while the classic mutation Atu^{s1938} caused severe eye malformation with almost complete penetrance.

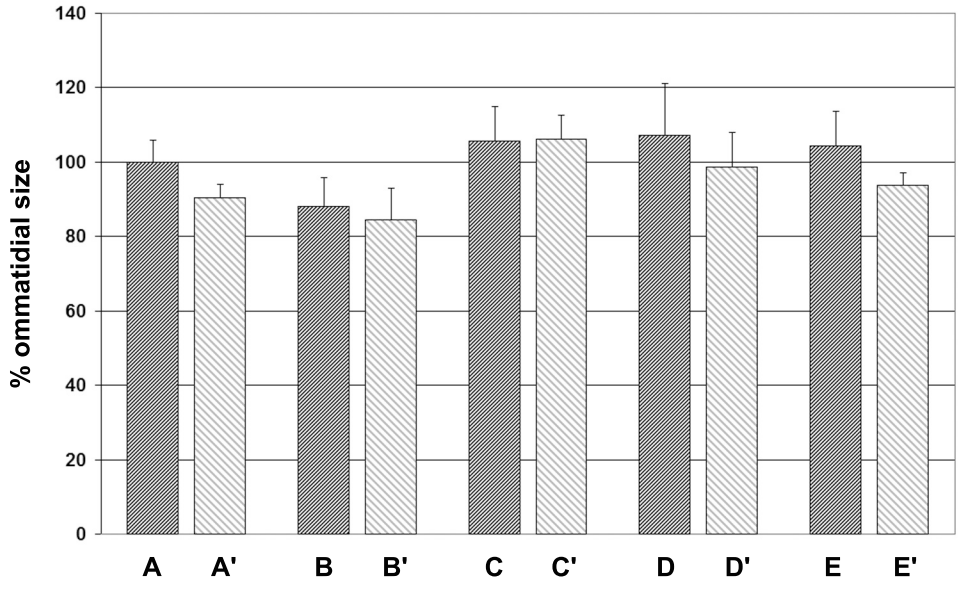

Figure 39

Ommatidial size upon PAF complex RNA*i*.
For every genotype, the size of 20 centrally located ommatidia of five individual eyes was determined. Ommatidia area of genotype A was set to 100%. The size difference between columns A & A' illustrates the published effect of the dm^{P0} allele on ommatidial size. The comparison between columns C & C' reveals a reduced requirement for *hyx* in a *myc* hypomorphic background. The error bars indicate standard deviations.

Genotypes

A: *yw tub>dmyc(y+)>Gal4 eyflp/Y; UAS-lacZ-IR M-3i/+*
A': *yw* dm^{P0} *tub>dmyc(y+)>Gal4 eyflp/Y; UAS-lacZ-IR M-3i/+*
B: *yw tub>dmyc(y+)>Gal4 eyflp/Y; UAS-dmyc-IR/+*
B': *yw* dm^{P0} *tub>dmyc(y+)>Gal4 eyflp/Y; UAS-dmyc-IR/+*
C: *yw tub>dmyc(y+)>Gal4 eyflp/Y; UAS-hyx-IR/+*
C': *yw* dm^{P0} *tub>dmyc(y+)>Gal4 eyflp/Y; UAS-hyx-IR/+*
D: *yw tub>dmyc(y+)>Gal4 eyflp/Y; UAS-atu-IR/+*
D': *yw* dm^{P0} *tub>dmyc(y+)>Gal4 eyflp/Y; UAS-atu-IR/+*
E: *yw tub>dmyc(y+)>Gal4 eyflp/Y; UAS-atms-IR/+*
E': *yw* dm^{P0} *tub>dmyc(y+)>Gal4 eyflp/Y; UAS-atms-IR/+*

5.4.6. RNA*i* against PAF complex components in the wing leads to reduced growth

Slight differences between the sizes of the dorsal and ventral wing epithelia lead to a bent wing phenotype. The overexpression of a cDNA with the strong, dorsal compartment-specific *GAL4* driver *apterous-GAL4* (*ap-GAL4*) therefore reveals growth-promoting or growth-inhibiting abilities of the corresponding protein with high sensitivity (Montagne et al., 1999). In order to assess the influence of PAF complex depletion on wing development, we expressed *UAS*-hairpin RNA constructs targeting the individual PAF complex subunits by *ap-GAL4*. While reduction of *hyx* and *atms* levels did not alter growth of the dorsal wing compartment, a very distinct bent-up wing phenotype was observed upon depletion of *Atu*. This is a strong indication for reduced tissue size in the dorsal wing compartment, where *apterous-GAL4* is expressed. Reduction of *rtf1* levels caused an even more drastic phenotype as wings were almost entirely missing, but these flies were still able to eclose. In contrast, *myc*-RNA*i* was pupal lethal, presumably because adult animals were not able to break out of their pupal case. It is surprising that flies that totally lack adult wings (as caused by *rtf1*-RNA*i*) can still eclose, whereas *myc*-RNA*i* causes pupal lethality without concomitant loss of the wings (as observed by opening several pupae). This discrepancy could be due to leaky expression of *ap*-GAL4, which might reduce *myc* abundance in other tissues, in which Myc function is vitally important. Alternatively, *myc*-RNA*i* still may affect wing morphology to such a degree that eclosion is impeded.

As a second assay, we tested whether RNA*i* against PAF complex subunits could suppress the wing defects caused by Myc overexpression. Elevated Myc abundance in the *apterous* expression domain in a small percentage of the offspring causes overgrowth of the dorsal wing compartment. This is manifested by a slight bent-down phenotype. The majority, however, displays severely disturbed wings. The two wing blade epithelia do not adhere with each other anymore, the interstitium between the epithelial sheets is often filled with fluid and in older flies the wings become necrotic. These phenotypes are presumably largely caused by Myc's growth-promoting activity, but may also by influenced by increased apoptosis and loss of cell-cell adhesion, since both these processes are known to be associated with high Myc levels. This phenotype is clearly *myc*-dependent as depletion of *myc* in response to RNA*i*, suppresses the defects, and the wings are bent upwards. Not only RNA*i* against *myc* itself, but also against *Atu* and *rtf1* leads to a clear bent up wing phenotype and the overall wing defects are rescued. These experiments indicate a positive genetic interaction of the PAF complex components *atu* and *rtf1* with Myc, since depletion of *rtf1* and *atu* causes bent-up wings and more importantly an almost complete suppression of Myc overexpression-induced defects. In contrast, wings in which *hyx* had been depleted in the dorsal compartment still exhibited a clear bent-down phenotype, as observed upon Myc overexpression. In addition, about one third of the wings displayed necrotic patches, which might be due to increased apoptosis rates in response to elevated Myc activity. Therefore, knockdown of *hyx* does not impair growth, however the defects caused by Myc overexpression seemed to be slightly suppressed. Lastly, downregulation of *atms* caused pupal lethality with complete penetrance.

5.4.7. Depletion of PAF complex components modulates growth properties of imaginal disc clones and polyploid fat body nuclei

Experiments in which the abundance of PAF complex components was reduced either by expressing complementary *UAS*-hairpin RNA or introducing classic mutants, suggest a growth promoting role for the Rtf1, Atms, and Atu subunits, while Hyx behaves antagonistically. To characterise the role of the single PAF complex components with respect to cellular growth, we observed growth of wing imaginal disc clones with reduced PAF complex abundance. In contrast to the other tissues examined, here we analyse the role the PAF complex in undifferentiated cells before metamorphosis, with respect to cell size, and in a precisely timed manner. To do so, we used a line carrying an *act>CD2>GAL4* cassette in combination with *UAS-GFP* and *hs-FLP* transgenes. Upon heat-shock, FLP recombinase-mediated recombination takes place in individual cells. Clones descending from these cells concomitantly express the hairpin RNA transgene and GFP. Hence, they can be easily detected by fluorescence microscopy. To assess the dependence on Myc function, crosses were also performed with a line that in addition to the other transgenes expresses Myc from a *UAS-myc* transgene. Crosses with RNA*i* targeting PAF complex subunits were set up and a *lacZ*-hairpin RNA line was included both as a control for non-specific RNA*i* effects but more importantly for possible titration effects of GAL4. Seventy-two hours after egg deposition the larvae were subjected to a heatshock of 8 minutes at 37°C. After another 45 hours, larvae were dissected, wing discs were isolated, and the area of individual clones was assessed in fluorescence micrographs.

Figure 40 depicts the result from one individual clonal analysis and clearly shows that clone growth is enhanced upon concomitant overexpression of Myc. Clones coexpressing Myc were on average twice as large as their counterparts with endogenous *myc* titre (compare panels A and B). This is in agreement with the previous observation that overexpression of Myc in clones in wing imaginal discs strongly enhances growth (Johnston et al., 1999). Moreover, in the Myc overexpression situation, RNA*i* against all the PAF complex components causes significant reduction of the clones' growth potential. This points to a positive genetic interaction between the PAF complex components and Myc. Furthermore, the PAF complex seems to become limiting in the presence of high levels of Myc. In contrast, depletion of PAF complex components in the absence of Myc overexpression leads to rather moderate size changes in clones. Downregulation of some PAF complex components even increases the size of control clones (Figure 40 panel B; compare *hyx*- and *atms*-RNA*i* with *rtf1*-RNA*i*). Taken together, depletion of PAF complex components clearly influences clonal growth potential and has a solid growth limiting effect. Moreover this reduction of clonal growth is far more pronounced in situations with high Myc abundance.

Since Myc has previously been reported to play an important role in endoreplication (Maines et al., 2004), not only imaginal wing discs but also fat bodies from the very same larvae were extracted. Myc overexpressing polyploid cells were reported to contain greatly enlarged nuclei, whereas nuclei in *myc* mutant polyploid tissue are smaller (Pierce et al., 2004). During endoreplicative cycles polyploid fat body nuclei undergo rapid rounds of DNA synthesis without intermittent mitoses. In keeping with this observation, Myc overexpressing fat body cells have enlarged nuclei compared to fat body tissue with physiological Myc levels (Figure 41). However, depletion of PAF complex components had no repressive effect on the nuclear size under these conditions (Figure 41).

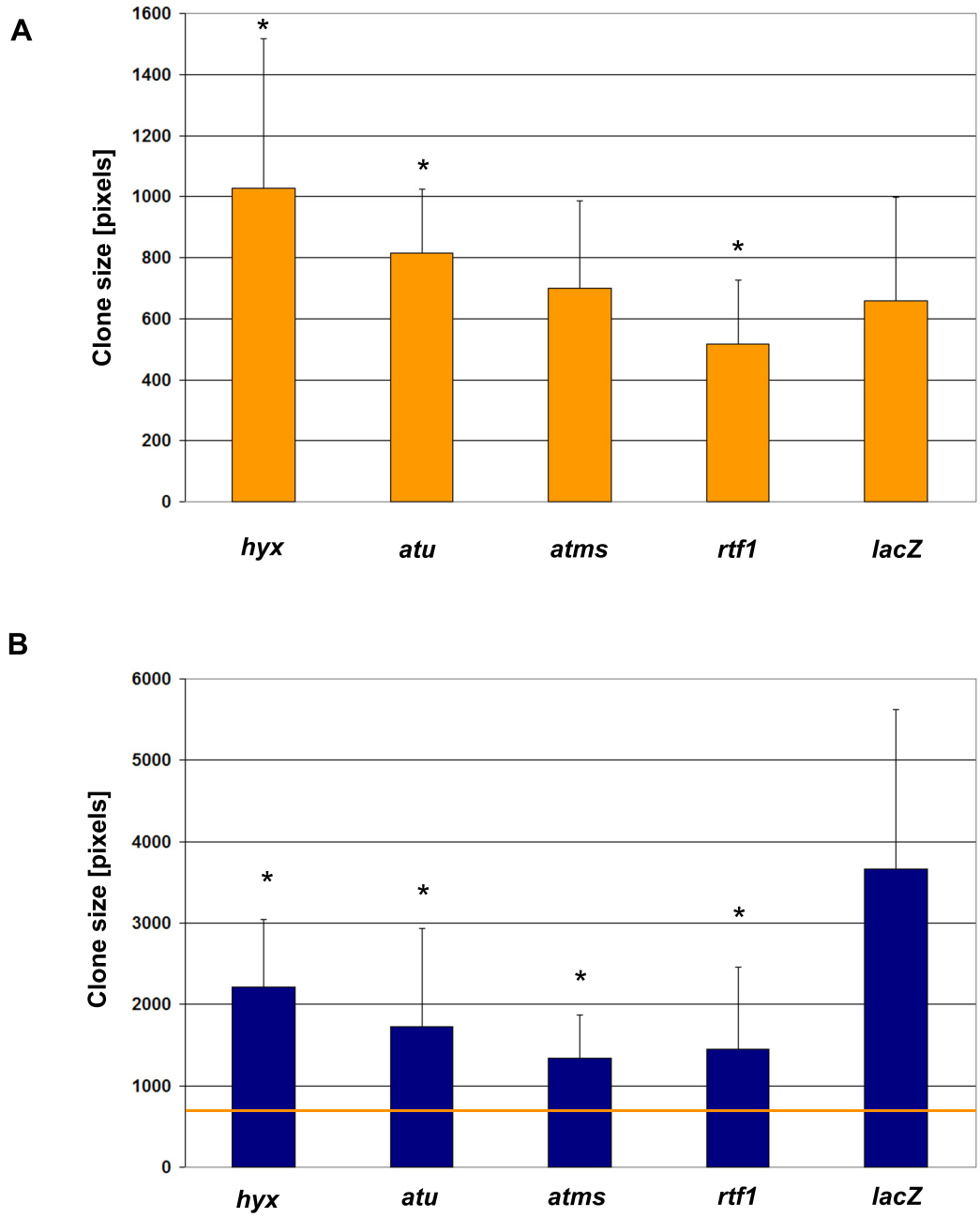

Figure 40

Effect of PAF complex RNA*i* on clone size in imaginal wing discs.
The size of 30-50 clones was measured (5-10 clones per disc). Error bars indicate standard deviations. Asterisks depict significant changes compared to the lacZ control genotype ($p<0.05$) after the Student's t-test. **A:** clone size in endogenous Myc background **B:** clone size in a Myc-overexpression background. The orange line in B indicates the average clone size of *lacZ-RNAi* control clones in A.

Genotypes (Panel A)

y w hs-flp/+; +; act>CD2>GAL4^{w+} UAS-GFP^{w+}/UAS-hyx-RNAi
y w hs-flp/+; UAS-atu-RNAi/+; act>CD2>GAL4^{w+}UAS-GFP^{w+}/+
y w hs-flp/+; +; act>CD2>GAL4^{w+} UAS-GFP^{w+}/UAS-atms-RNAi
y w hs-flp/+; +; act>CD2>GAL4^{w+} UAS-GFP^{w+}/UAS-rtf1-RNAi
y w hs-flp/+; UAS-lacZ-RNAi/+; act>CD2>GAL4^{w+} UAS-GFP^{w+}/+

Panel B: same genotypes except for an additional *UAS-Myc132^{w+}* transgene on the 2nd chromosome.

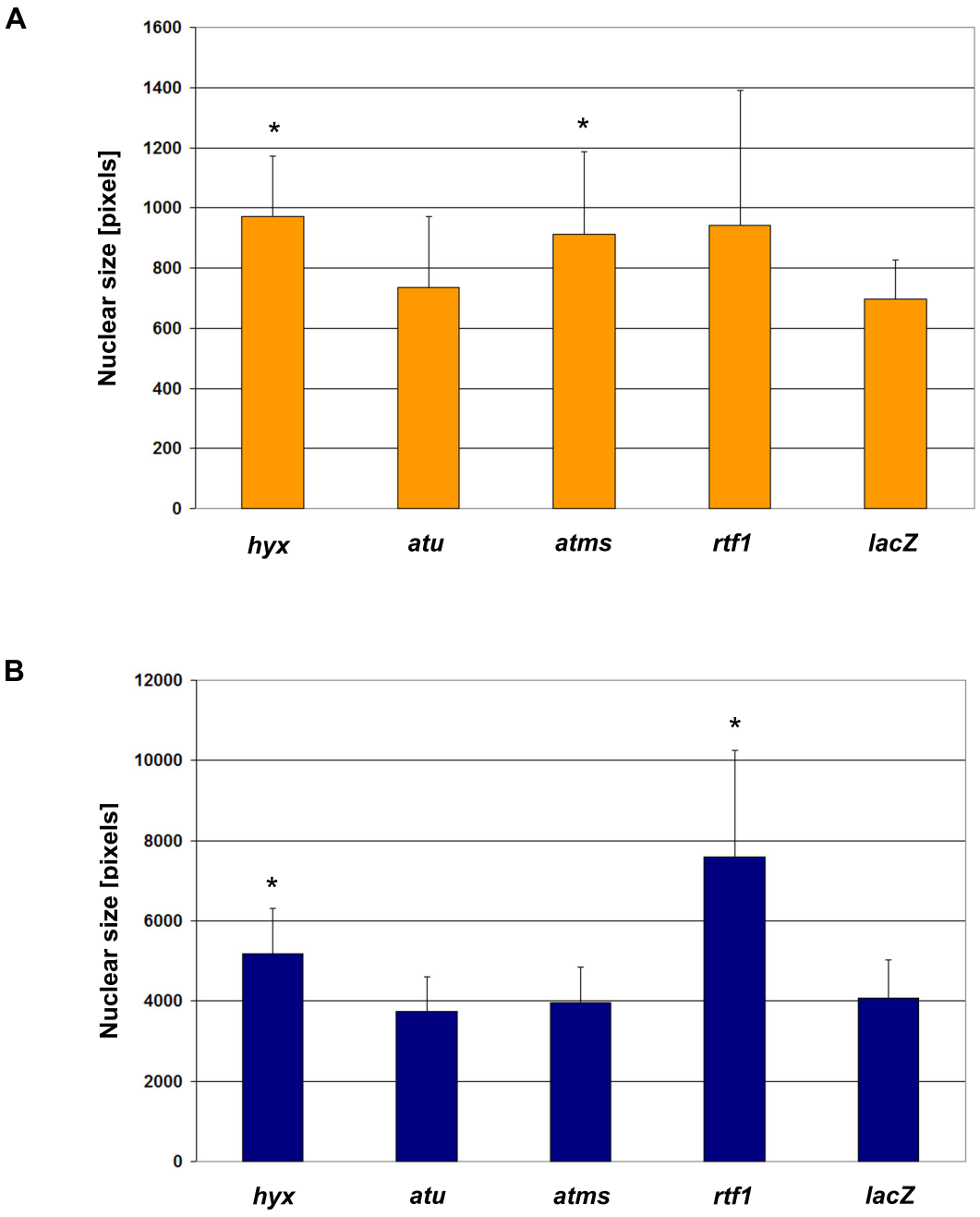

Figure 41

Effect of PAF complex RNA*i* on the size of polyploid fat body nuclei.
The size of 20-50 nuclei was measured. Error bars indicate standard deviations. Asterisks depict significant changes compared to the lacZ control genotype ($p<0.05$) after the Student's t-test. **A:** nuclear size in endogenous Myc background **B:** nuclear size in a Myc-overexpression background.

Genotypes (Panel A)

y w hs-flp/+; +; act>CD2>GAL4^{w+} UAS-GFP^{w+}/UAS-hyx-RNAi
y w hs-flp/+; UAS-atu-RNAi/+; act>CD2>GAL4^{w+}UAS-GFP^{w+}/+
y w hs-flp/+; +; act>CD2>GAL4^{w+} UAS-GFP^{w+}/UAS-atms-RNAi
y w hs-flp/+; +; act>CD2>GAL4^{w+} UAS-GFP^{w+}/UAS-rtf1-RNAi
y w hs-flp/+; UAS-lacZ-RNAi/+; act>CD2>GAL4^{w+} UAS-GFP^{w+}/+

Panel B: same genotypes except for an additional *UAS-Myc132^{w+}* transgene on the 2nd chromosome.

Discussion

In this work, we describe the establishment of a Myc-dependent Dual luciferase reporter system, based on reporter constructs under the control of the Myc target gene promoters. This system allowed us to perform an RNA interference screen in *Drosophila* S2 cells, which led to the identification of several novel cofactors in Myc-dependent transcription regulation. Subsequent to the screen we have analysed three groups of cofactors in more detail. We could show a genetic interaction of subunits of the 19S proteasome regulatory complex with Myc. Furthermore, we give clear evidence for an involvement of the *Drosophila* host cell factor (HCF) and the Polymerase II-associated factor 1 complex (PAF complex) in Myc-dependent transcription regulation.
In the first part of this discussion, the set up of the screen and the resulting candidate list are recapitulated and described. In the following parts we discuss the specific roles of the candidates analysed more thoroughly.

1. RNAi screen for dMyc cofactors

We performed an RNA interference (RNA*i*) screen in embryonic hematopoietic Schneider 2 (S2) cells and identified 33 significant modulators of the system. The screen was based on a directly Myc-dependent Dual luciferase reporter system, in which the reporter genes are under the control of either the *nnp-1* or *CG5033* gene promoters. The ability of *myc* RNA*i* to inhibit wild type *nnp-1* and *CG5033* promoter driven luciferase expression confirms these two genes as targets of Myc. The single E-Box present in both regulatory sequences is important for the transcription of the genes, and hence the reporter, as the mutation of the E-Box leads to a 3 to 4 fold reduction in reporter gene expression in the case of *CG5033* (Figure 6b) and 1.5 to 2.5 fold reduction for the *nnp-1* reporter (Figure 6a). Moreover, Myc's control on *nnp-1* and *CG5033* reporter expression is exclusively mediated via the E-Box, since mutating the E-Box renders the promoters unresponsive to *myc* RNAi (Figures 3a & b). For these reasons we considered the ratio of the luciferase reporters to be strictly dependent on Myc and reflect its overall activity. Since the *CG5033* reporter system is more sensitive to changes of Myc levels it was used as the primary screening reporter pair.
The motivation to conduct an RNAi screen was to identify cofactors that are essential for the physiological regulation of Myc targets (in *Drosophila*). Even though many transcriptional cofactors that physically bind to Myc have been identified - mostly in vertebrate tissue culture systems - the physiological relevance of very few of these proteins has been demonstrated. To minimise the scale of the screen, we chose not to conduct a genome-wide RNA*i* screen but tested a preselection of 752 transcription-associated factors. This selection included factors that had been shown to be involved in Myc-dependent processes in various model organisms. Furthermore, general transcription-associated factors, and as a third group uncharacterised proteins with potential involvement in transcription, as inferred from their gene ontology annotation, were included (see Results, section 1.2.).
The use of the E-Box/ΔE-Box-luciferase system ensured a Myc-dependent readout, as only the input through the E-Box is measured. For this reason – and because their inclusion would have doubled the number of candidates – we did not include sequence-specific transcription factors in the screen. This

strategy excludes the identification of transcription factors that would act together with Myc in the regulation of the Myc activity reporter by binding to DNA cooperatively with Myc. However, we would expect such hypothetical factors only to influence a restricted number of other Myc targets, since the Myc binding sites in Myc targets genes do not share any sequences outside an extended 10 nucleotide E-box (AACACGTGCG) (Hulf et al., 2005), whereas our screen was aimed at identifying more generally acting cofactors of Myc.

Out of the 752 factors tested in the screen, we identified 33 as significant modulators of the Myc-dependent reporter; 19 candidates had a "Myc-like" effect, as their depletion led to a reduction of the relative reporter activity, whereas RNA*i* against 14 other factors led to an activation of the reporter system (Table 1). The fact that only 4.5% of all the candidates were identified as significant modulators of the reporter system suggests a high specificity of the screen, even more so as a biased preselection of candidates was used. As a validation of the targets the final candidate compilation of 33 factors was retested with the *nnp-1*-driven reporter system. All the three PAF complex components identified with the CG5033 reporter (Hyx, Ctr9, and Atms) were also found using the *nnp-1* reporter constructs. Moreover, the PAF-associated factor Spt6 and the HDAC component Sin3A were positively identified with both reporter variants. The activators of the reporter system also had an effect on the *nnp-1* reporters, however it was less signifcant than in the screen and, therefore they were not picked up using the same significance criteria as in the screen. This is probably due to the lower sensitivity of the *nnp-1* reporter pair compared to *CG5033* and the strong variability of the RNA*i* effect for certain factors. However, the dsRNAs causing the strongest downregulation of the reporters (i.e. 19 RC components of the proteasome) reduced *nnp-1* reporter activity to the same extent as *myc*-RNA*i*.

We had previously analysed derivatives of the *nnp1*-luciferase reporter, in which the native E-box had been replaced by an E-box at different positions upstream of the transcription start site (TSS). These experiments had shown that an E-box at position -40 does not mediate transactivation by Myc, whereas an E-box at -320 partially substituted for a native E-box and transactivated the reporter to about 70% of the native E-box; as a transfection control in these experiments we had used a *Renilla* luciferase driven by a *tubulin* promoter (Hulf, 2004; Hulf et al., 2005). RNA*i* against the PAF complex components and *Sin3A* also activated the expression of an *nnp-1* reporter with an E-Box at position -320 to some extent. Typically, the luciferase values are increased by almost two-fold. The luciferase ratios upon PAF complex and sin3A-RNAi were almost identical in both experiments, in which the luciferase ratios between -320 firefly and wild type *Renilla* reporter on one hand, and ΔE firefly and wild type *Renilla* luciferase on the other were compared to *gfp*-RNA*i* controls (data not shown). This might indicate that they are Myc cofactors that are not exclusively recruited to target gene promoters in which the E-Box is located proximally to the transcription start site. However, the influence of RNA*i* against Paf complex components needs to be further addressed in additional experiments, for example in comparison between the -320 reporter with the ΔE-Box variant. As a side, *hcf* knockdown did not show any influence on the -320 reporter, pointing to an exclusive role at downstream E-Boxes. As mentioned above, the position of the E-Box proximal to the TSS can be crucial in order for a Myc regulated gene to achieve the required expression level, since E-Boxes at different positions upstream of TSS cannot recapitulate the full reporter activity. Positioning the E-Box at -40, renders the reporter gene inactive, probably by interfering with the binding of the basal transcription machinery. E-Boxes

positioned distal to TS sites can function to promote gene expression through recruitment of other factors like chromatin remodellers but will be unable to enhance gene expression through molecular interaction with basal transcriptional elements. It has been demonstrated that c-Myc can activate expression of the *cad* gene via a post-RNA polymerase II recruitment mechanism by interacting with P-TEFb (Eberhardy and Farnham, 2001, 2002). It is possible that Myc target genes with an E-Box downstream of the TSS in general are activated by interaction of Myc with the engaged (and possibly paused) RNAP II complex. In addition to the reports from Eberhardy et al., other studies describe that activation of targets by Myc can rely to varying extent the recruitment of different co-factors (e.g. interaction with P-TEFb vs. chromatin remodellers). The three basally expressed genes *CAD*, *CDK4* and *HSP60* do not strictly depend on the recruitment of TRRAP and HAT activity for Myc-dependent induction. Myc variants with mutated MB2 domains are still capable of activating transcription from these loci (Nikiforov et al., 2002b).

Taken together, the factors identified in the primary RNA*i* screen clearly influence the expression of a number of Myc targets. They impact on the expression of two Myc-dependent reporter constructs with downstream E-Boxes, as well as endogenous targets of Myc (shown by qRTPCR experiments).

2. Putative Myc cofactors

In addition to PAF complex components, we have also identifed Spt6, a transcription elongation factor originally identified in yeast (Bortvin and Winston, 1996). Spt6 was shown to mediate chromatin disassembly during transcription elongation and re-establishment of chromatin structure after the polymerase has passed through (Adkins and Tyler, 2006; Hartzog et al., 1998; Saunders et al., 2003). In yeast it has been shown that nucleosome reassembly by Spt6 is involved in trancriptional repression (Kaplan et al., 2003; Adkins and Tyler, 2006).

In *Drosophila* Spt6 is rapidly recruited to sites of active transcription. Spt6 co-purifies with the exosome, a complex of 3' to 5' exoribonucleases that is implicated in the processing of structural RNA and in the degradation of improperly processed pre-mRNA. Immunoprecipitation assays of *Drosophila* nuclear extracts show that the exosome also associates with the elongation factor dSpt5 and RNA polymerase II. A clear link between the PAF complex and Spt6 was revealed in *Drosophila* where depletion of the PAF complex leads to a significant decrease in the recruitment of Spt6 to actively transcribed *hsp70* promoters (Adelman et al., 2006). This suggests that the PAF complex associates with Spt6 to maintain proper chromatin architecture during transription.

2.1. The 19S proteasome RC is an activator of Myc-dependent target expression

Depletion of six out of eight non-ATPase subunits of the 19S proteasome regulatory complex tested, resulted in a marked drop of reporter activity by roughly three-fold compared to GFP control RNA*i* (Figure 8). However, not only the Myc-reporter system proved to be sensitive to downregulation of the proteasome components. *tubulin-GAL4* driven expression of RNA*i* hairpin lines in the *eyeless* expression domain in a Myc hypomorphic background caused severe eye defects. With almost complete penetrance eyes became considerably smaller and most often displayed irregular shapes

due to the loss of a large number of ommatidia. Also the classic P-element insertion mutant Rpn6^{k00103} caused mild eye aberrations similar to the observed RNA*i* phenotype, whereas other Rpn6 mutants and Rpn11 had no effect on the overall eye structure. Moreover, the insertions Rpn6^{k00103} and Rpn11^{BG01694} both suppressed the size increase as well as the disruption of the ommatidial array caused by Myc overexpression. The difference in phenotypic strength between the RNA*i*-mediated downregulation and the classic mutations used is noticeable. While the classic mutations have a rather mild impact on eye morphology, six of seven RNA*i* lines lead to severest eye defects (loss of the majority of ommatidia or even complete loss of eye structures). The mildness of the phenotype seen with the classic mutants is probably due to sufficient levels of gene product in a heterozygous mutant animal to ensure normal eye development. Conversely, RNA*i*-mediated knockdown, although it may not be complete, leads to a stronger reduction of *rpn* levels.

The experiments clearly point to an activating role of the 19S proteasome regulatory complex on Myc activity, since reduction of Rpn levels leads to decreased reporter expression, suppression of Myc overexpression effects, and severe eye defects specifically in *myc* hypomorphic animals. This is surprising since a partial loss of proteasome function leads to a slow-down or loss of protein degradation and presumably a prolonged half-life of its targets, including Myc. Since Myc is a short-lived protein that is rapidly degraded by the proteasome, we would have thought that inhibition of the proteasome increases Myc levels, and hence activity. It is known from *in vitro* studies that the complex consisting of the 19S RC base and the 20S core proteasome can still perform ATP-dependent degradation of unfolded proteins, but it can no longer degrade polyubiquitin-tagged substrates (Pickart and Cohen, 2004; Glickman et al., 1998). As the majority of the Rpn subunits found in the screen are part of the 19S lid subcomplex (all except Rpn2 which forms part of the base subcomplex), RNA*i* against these components may result in impaired substrate recognition and disruption of proteasome function. However, analyses of Myc by Western blots revealed that RNA*i* against proteasome components had no obvious impact on Myc abundance in S2 cells (Figure 9).

Several lines of evidence suggest that disruption of proteasome function leads to reduction of reporter activity and lowered Myc activity. It has been proposed that in order to keep the activity of transcription factors under control, their ability to drive high-level gene expression is tightly coupled to their degradation, i.e. they are only fully active when they have been "marked" for later destruction. One component involved in such a process is the F box protein Skp2, an E3 ubiquitin ligase, which not only regulates the stability of Myc *in vivo*, but also acts as a cofactor that is necessary for full activity of Myc (Muratani and Tansey, 2003). There are reports that monoubiquitination of the artificial activator LexA-VP16 can increase its ability to recruit the elongation factor P-TEFb (Kurosu and Peterlin, 2004). Also the efficiency of posttranscriptional processes, such as recruitment of the RNA processing machinery to produce functional mRNAs, may be stimulated by activator ubiquitination (Muratani et al., 2005). Furthermore, it has been shown for several transcriptional activators that their activation domains closely correspond to the degrons (motifs required for turnover via the ubiquitin-proteasome pathway). This “licensing event” of ubiquitination in order to gain full activity might explain why reduction of proteasome function can oppose Myc activity.

There are two proposed models that try to link activator potential and proteasome activity (Kodadek et al., 2006). These have been termed “timer” or “black widow” mechanisms. While the two models differ

in how ubiquitination and then degradation is triggered, both models incorporate a positive effect of ubiquitination on transcription. In the “timer” mechanism the monoubiquitinated activator is of crucial importance. It is the substrate for the chain extenders – E4 ubiquitin-ligases that add K48-linked ubiquitin molecules – and deubiquitinases that remove ubiquitin moieties to antagonise chain growth. It has been shown that at least four K48-linked ubiquitin molecules are required to promote proteasome-mediated degradation (Thrower et al., 2000). The action of both these types of enzymes, which can work at different rates, provides a “window of opportunity” during which the activator has full activation potential (i.e. the time it takes to stably couple three or more ubiquitins to the substrate). Of central importance for this model is the assumption that the ubiquitinated activators are significantly more active than the non-ubiquitinated form. On the other hand, the “black widow” mechanism suggests that activator polyubiquitination and subsequent destruction are an inevitable consequence of physical interaction with the RNA polymerase holoenzyme. As shown for the yeast activator Gcn4, “mating” with the polymerase leads to phosphorylation by the Mediator component cdk8 and subsquent SCF^{Cdc4}-dependent polyubiquitination (Chi et al., 2001). Thus, by carrying out its function the activator Gcn4 is presented to the protein kinase that triggers its destruction.

Two other implication for the positive role of the 19S proteasome in transcription comes from the observation in *Saccharomyces cerevisiae* that the 19S base subcomplex ATPases Sug1 (also termed Rpt6) and Sug2 (Voges et al., 1999) participate directly in transcription. It was shown in yeast that at least five subunits of the 19S proteasome are recruited to transcriptionally active genes. They stay associated with the polymerase throughout the entire transcribed sequence of the gene (Kim et al., 1994; Gonzalez et al., 2002). Disruption of the 19S RC complex by mutating the Rpt4 or Rpt6 subunits abrogates histone H2B-monoubiquitination and, as a consequence also histone H3K4 and H3K79 methylation (Ezhkova and Tansey, 2004). Moreover, Brower et al. established that ubiquitin-ligase activity is directly linked to the RNAP II holoenzyme by Mediator in vertebrates (Brower et al., 2002). Additionally, it was shown that the lid subcomplex of the 19S proteasome RC can act as a transcription coactivator by directly recruiting the SAGA histone acetyltransferase complex to target promoters (Lee et al., 2005), and that the SAGA complex contains the ubiquitin protease Upb8 that deubiquitylates H2B to allow transcription initiation (Henry et al., 2003).

These data argue that short-lived transcriptional activators, like Myc, only gain their full activity when they are being marked for later degradation and therefore, could explain why depletion of proteasome components leads to reduced transactivation potential of Myc.

2.2. Host cell factor (HCF)

Experiments presented in this study and Mirjam Balbi’s master thesis (Balbi, 2007) identified HCF as a positive cofactor of Myc-dependent transcription control. We showed a direct physical interaction between the HCF and Myc proteins and revealed a requirement for HCF in Myc-dependent gene expression in S2 cells. *In vivo* HCF synergises with Myc in promoting growth in the eye and in wing imaginal discs. HCF depletion by RNA*i* has the potential to partially revert Myc overexpression phenotypes in the wing and in the eye. These data coherently indicate that Myc requires HCF to reach its full transcriptional activity during proliferation and differentiation.

2.2.1. Effect of HCF on the epxression of Myc targets in S2 cells

The original observation from the screen that RNA*i*-mediated depletion of HCF leads to a decrease of Myc-reporter expression was confirmed with additional independent dsRNAs. Knockdown of HCF resulted in a decrease of luciferase expression to about 60%, while RNA*i* against Myc typically reduces reporter expression to 15-30% (Figure 10). This indicates that Myc is dependent on HCF to attain full transcriptional activity. However, this dependence is not complete, since in the situation of HCF depletion Myc still retains reduced activity. Interestingly, *hcf*-RNA*i* only slightly reduces reporter activity in a Myc overexpression situation (from 200% to 180% as compared to *gfp*-RNA*i*), most probably because the HCF-independent activation of Myc-targets is potent enough to ensure strong reporter expression. On the other hand a strong boost in luciferase expression induced by ectopic HCF expression can be reversed by *myc*-RNA*i*, indicating that this activation is Myc-dependent. This could imply that the overexpression effect of Myc on the luciferase reporter is mediated by HCF-independent mechanisms. Thus, *hcf*-RNA*i* would only affect the basal luciferase activity but not the boost resulting from ectopic Myc expression. These assumptions fit with the luciferase expression levels, since *hcf*-RNA*i* causes a reduction in luciferase activity of about 30%, irrespective of the presence of ectopic Myc. Under physiological conditions HCF seems to be limiting in S2 cells, because ectopic HCF expression leads to a four-fold increase of luciferase expression, whereas overexpression of Myc only leads to a doubling of expression levels (Figure 10). Therefore, ectopic HCF could strongly enhance reporter expression in the presence of excess Myc. However, the strong effects seen upon *myc*-RNA*i* on the reporter expression, argues against the presence of excess Myc protein levels. As an alternative explanation for the strong boost of luciferase expression by HCF-overexpression, HCF could be more potent than other hypothetical coactivators for Myc and efficiently compete with these cofactors for Myc binding. Interestingly, co-overexpression of Myc and HCF did not result in a further enhancement of reporter expression but to a decrease from 400 to 250% activity (as compared to HCF overexpression alone), which might be due to a drop in HCF protein abundance in cells that co-overexpress Myc compared to HCF overexpression alone (data not shown). Therefore, the maximal HCF-independent activity of Myc and only basal HCF-dependent activity would be observed in this case. Up to now it is not clear whether this reduction of HCF protein levels is caused by a repression through Myc or simply is an experimental artefact, even though it was seen repeatedly.

A reduction of HCF levels by RNA*i* not only has an influence on the expression of a Myc-dependent reporter gene but also on endogenous RNA polymerase II-transcribed Myc targets (*nnp-1*, *CG5033*, *CG12295*, and *fibrillarin*) (Figure 16). *hcf*-RNA*i* leads to reduced mRNA abundance of established Myc targets by about 30%, a decrease that is comparable to the effect seen on the artificial Myc-reporter. In contrast, the levels of the RNA polymerase III-transcribed targets *5sRNA*, *snoRNA U3*, and *tRNA(Leu)* are not reduced upon *hcf*-RNA*i*, but are slightly elevated (Figure 16). This increase in Pol III target levels might be due to background experimental variability and may not have any biological significance. Potentially, HCF could play a role in recruiting Myc to RNAP II target genes, rather than vice versa. Under such circumstances loss of HCF might be expected to increase the pool of Myc that is available for the activation of RNAP III targets. Therefor, an activation of RNAP III-transcribed Myc targets would be observed. To investigate the influence of Myc on HCF levels or vice versa, we

performed qRTPCR and Western blot experiments. Endogenous *hcf* RNA levels were reduced by 20% in response to *myc*-RNA*i* as seemed to be the abundance of ectopic HCF, although the latter changes were not rigorously quantitated (Figures 16 & data not shown). This slight repressive effect of RNA*i* against *myc* on *hcf* levels stands in contrast to the observation that co-overexpression of Myc and HCF results in markedly lower HCF levels. This repressive effect of ectopic Myc on the abundance of ectopically expressed HCF – but not on endogenous HCF - is unlikely to stem from the saturation of the overexpression system. Myc expression is driven by *tubulin-GAL4*, while ectopic HCF is under the control of an *actin* promoter. On the other hand modulation of HCF titres caused fluctuations in *myc* mRNA levels (to 69% and 130% of control, respectively, for individual experiments). However, Myc target genes did not show such a variable response to *hcf*-RNAi; instead, *hcf*-RNAi decreases the expression of Myc targets in a sample where *myc* levels are elevated (Figure 16). Myc protein levels appear to be constant in response to HCF depletion (Figure 17). This finding could imply that fluctuations of *myc* RNA levels are evened out by some sort of auto-regulation of Myc, or that small changes in protein content (of +/- 30%) are not detected with conventional Western blots.

2.2.2. HCF and Myc interact physically

Coimmunoprecipitations revealed a physical interaction of HCF and Myc in an overexpression system (Figure 12). We could confirm that the association is indeed physiological, since the endogenous proteins were found to be interacting as well (Figure 18). The use of Myc protein mutants (variants with individual deletions of the Myc Boxes 1-3, or of the whole C-terminal bHLHzip domain) showed that the stable interaction between HCF and Myc does not require the characterised conserved motifs within the Myc protein. Furthermore, a truncated Myc protein lacking the entire N-terminus still interacted with HCF. In order to identify putative HCF-interaction domains within the Myc protein sequence, additional Myc truncations were tested for their ability to retain HCF in coimmunoprecipitations. Myc truncations containing the protein stretch between amino acids (aa) 179 and 403 conferred the strongest binding to HCF. However, N-terminal deletion variants that include the region between aa 523 and 626 also interact weakly with HCF (Figure 20b). Therefore we predict two HCF-binding sites within the Myc protein; a strong one in the central portion of the protein between aa 179 and 403 and a weaker one in the C-terminus between aa 523 and 626.

Interestingly, the *Drosophila* Myc protein was found to contain a conserved four amino acid sequence DHSY that conforms to the so-called “HCF-binding motif” (HBM) consensus sequence D/EHxY. The HBM was identified in VP16 and the cellular transcription factor LZIP (Freiman and Herr, 1997), and was also show to be of importance in the E2F-family of transcription factors for binding to HCF (Tyagi et al., 2007). The HBM is contained within the protein stretch interacting most strongly with HCF (amino acids 387-390). However, mutating the HBM did not affect Myc’s ability to interact with HCF. This suggests that additional sequences are sufficient for stable binding of Myc to HCF. In order to characterise the Myc:HCF interaction in more detail, we performed pull-downs of *in vitro* translated HCF with GST-Myc fusion protein variants. First, we could show that the interaction between Myc and HCF is direct and not bridged by other proteins, since a GST-fusion of a large fragment of Myc strongly retains HCF (Figure 19). Second, we could broadly confirm the findings from the coimmunoprecipitations in S2 cells concerning the HCF-interaction domains (Figure 20a): The central

Myc region between aa 295 and 523 interacts most strongly with HCF; additionally, two weaker binding regions between aa 176 and 295, and aa 523 and 626, respectively, were identified with both assays. Therefore, all the interaction sites between Myc and HCF identified in tissue culture cells directly confer association. *In vitro* translation experiments identified one additional HCF-interaction region within Myc. In contrast to the coimmunoprecipitations in S2 cells the very N-terminus is able to bind HCF with intermediate affinity. There are several possible explanations for this discrepancy. The presence of the C-terminal subunit of HCF (HCF-C) in S2 cell lysates might interfere with the physical association with Myc's N-terminus. Furthermore the *in vivo* conditions might not be suitable for HCF binding to the N-terminus - e.g. because of additional proteins competing with HCF for binding to Myc, or because of conditions that do not allow interaction (e.g. by differing buffer composition, ionic strength, pH, etc.). Alternatively, an interaction of HCF with the N-terminus of Myc might be artificial and only be seen at very high protein concentrations, that are never reached in the cell. Moreover, posttranslational modifications of Myc that are absent from the IVT experiments might prevent the binding to HCF.

2.2.3. HCF is required *in vivo* during proliferation and differentiation

To assess the physiological importance of the Myc:HCF interaction *in vivo*, we characterised HCF's influence on wing and eye development as well as the impact on cellular growth during endoreplication and wing disc development. All data obtained from the *in vivo* studies are consistent with the notion that HCF is an important positive cofactor for Myc function.

Induction of *hcf*-RNA*i* in differentiating tissues with physiological Myc levels has relatively mild consequences. Ommatidial size is barely affected by *hcf* depletion, either induced by using the *eyeless*-flp system or driven by a GMR-Gal4 line. Rather mild effects are seen in the wing, as all the individual *hcf*-RNA*i* lines used cause only a slight but distinct aberration of the wing morphology (for a detailed description see Balbi (2007). With high penetrance the longitudinal veins L1 and L2 are merged and additional vein-like structures are present (Figure 13). Also, larval tissues are at most slightly affected by a reduction of HCF levels. RNA*i* induced depletion of HCF in imaginal wing disc clones did not consistently reduce clonal size in a Myc wild type background. Moreover, no significant size reduction of endoreplicating salivary gland nuclei could be observed in response to *hcf*-RNA*i*. These mild consequences of *hcf*-RNA*i* for the development of various tissues suggest only slightly decreased transcriptional activity in the presence of endogenous Myc levels.

HCF depletion in eyes with physiological Myc levels has no significant effect on ommatidia size (see above). However, it leads to a slight but significant size reduction of 10% in a background with reduced *myc* levels; as seen in the hypomorphic background of ey>dm^{P0} (Balbi, 2007). This reduction upon *hcf* depletion is comparable to the effect of *myc*-RNA*i* in an ey>dm^{P0} background. Moreover, reduction of *hcf* and *myc* levels causes a disruption of the regular ommatidial array. Presumably, a reduction of HCF levels further impinges on Myc activity, which – in a hypomorphic *myc* background, but not at physiological *myc* titre – is potent enough to cause further reduction of ommatidia size and increased roughness of the eyes.

Analyses of flies that ectopically express Myc have shown that HCF is needed by Myc for its full functionality. Induction of *hcf*-RNAi in the presence of ectopically expressed Myc significantly

decreases the Myc-induced overgrowth of the ommatidia by 35% and rescues the rough-eye phenotype (Figure 14). HCF depletion also suppresses Myc overexpression phenotypes in the wing (Figure 13). Typically, strong overexpression of Myc under the control of *apterous*-GAL4 leads to severe wing defects. These defects are due to the imbalanced growth of wing compartments, increased apoptosis, and potentially disruption of cell-cell adhesion, which results in dissociation of the two wing blade epithelia. Fluid-filled bubbles are formed between the two wing compartments and very often large parts of the wing become necrotic. While *hcf*-RNA*i* on its own has only mild effects on wing morphology (Figure 13), it can almost completely suppress the phenotypes caused by ectopically expressed Myc. Another piece of evidence that *hcf*-RNA*i* restricts Myc's activation potential stems from measurements of nuclear sizes in endoreplicating tissue. Myc was shown to play a crucial role during endoreplication (Pierce et al., 2004) and ectopic expression of Myc vastly increases the size of endoreplicating nuclei – including salivary gland nuclei. We showed that *hcf*-RNA*i* significantly decreases the size of nuclei in Myc overexpressing cells, indicating that HCF is also needed for full Myc activity during endoreplication. This suggests that Myc retains some activity in the absence of HCF – probably through HCF-independent mechanisms. However, in order to reach its full transcriptional activity Myc needs HCF in differentiating as well as in endoreplicating tissue.

Co-overexpression experiments of both Myc and HCF by GMR-GAL4 indicate a synergism between the two proteins. While overexpression of HCF alone does not change ommatidial size, ectopic Myc expression (using one UAS-Myc transgene) leads to an increase in ommatidia size by about 30%. The concomitant overexpression of HCF and Myc in wing disc clones supports this hypothesis. Analogous to the situation in the eye, ectopically expressed HCF alone does not influence clone size, however it leads to a marked size increase together with elevated Myc levels as compared to Myc-overexpression alone. In contrast, the co-overexpression effects seen in the wing cannot be interpreted as clearly, since individual overexpression of Myc and HCF already cause strong wing defects. However, in this situation ectopic coexpression of Myc and HCF affects wings more severely than expression of either protein alone.

Taken together the data obtained from the *in vivo* experiments indicate that HCF is an important cofactor of Myc. Myc partly functions independently of HCF but depends on HCF presence for full activity, since even excessive levels of Myc cannot bypass the requirement for HCF.

2.2.4. HCF-associated proteins

In order to modulate transcription, Myc and HCF have to recruit additional co-activators, since neither of them possesses intrinsic enzymatic activities. Several chromatin-modifying complexes have been reported to interact with HCF in vertebrates and/or in *Drosophila*. These are the most likely candidates to lend transcription modulating potential to Myc:HCF complexes.

Coimmunoprecipitations confirmed HCF to be a stable subunit of the ATAC-histone-acteyltransferase complex in *Drosophila* (Guelman et al., 2006). However, we have not been able to show a physical interaction between ATAC-components and Myc, which is probably due to technichal problems and does not rule out an association between Myc and ATAC. Induction of RNA*i* against the ATAC components Ada2A, Atac1 and Gcn5 had no influence on the Myc activity reporter in S2 cells, while *dada3*-RNA*i* slightly increased luciferase levels. We have shown that RNA*i* against Ada2A and Atac1

causes a potent reduction of the corresponding protein levels. Therefore, the lack of effect on the Myc activity reporter upon depletion of ATAC components is not due to the inefficiency of RNA*i*. On the other hand, RNA*i* against ATAC components in the dorsal compartment of the wing led to a wide variety of phenotypes. While *atac1*-RNA*i* lines were not available, *dada2*-RNA*i* caused pupal lethality, irrespective of Myc-expression levels. Expression of two RNA*i*-hairpin transgenes against Gcn5 gave conflicting results, since one RNA*i* insertion (Gcn5-T1-IR) resulted in severe wing defects and the second insertion of the same RNA*i*-hairpin construct did not affect wing development (Gcn5-T2-IR). Strikingly, expression of Gcn5-T2-IR, and not Gcn5-T1-IR, by *apterous*-GAL4 led to a strong reversion of the Myc overexpression phenotypes in the wing, as it had already been observed for HCF. The fact that depletion of Gcn5 strongly suppresses Myc overexpression phenotypes, suggests that Gcn5 indeed can specifically influence Myc activity *in vivo*. However, for the lack of data about other complex components, we cannot draw any conclusions whether the ATAC complex could play a role in Myc-dependent transcription regulation. It is possible that downregulation of ATAC components does not affect Myc-dependent readouts for reasons of redundancy. Recently, a second histone-acetyltransferase subunit of the ATAC complex, termed Atac2/KAT14, has been identified by mass spectrometry (Suganuma et al., 2008). Therefore, even knockdown of the catalytic subunit Gcn5 might leave the ATAC complex function partially intact.

As another possibility Gcn5 may influence Myc function independently of the ATAC complex, since it is associated with a number of multisubunit HAT complexes. One of these complexes, the SAGA HAT complex, has been shown to interact with c-Myc via its subunit TRRAP (McMahon et al., 2000). At least part of the transcriptional activation exerted by Myc is dependent on the recruitment of Gcn5 (McMahon et al., 2000; Liu et al., 2003). Therefore, it is well possible that the suppression of Myc overexpression phenotypes by RNA*i*-mediated depletion of Gcn5 is due to the disruption of SAGA-, and not ATAC-function. Still, depletion of another SAGA subunit (Spt3) neither affected luciferase expression nor the Myc overexpression phenotype in wings.

A second complex found to be associated with HCF in vertebrates and *Drosophila*, is the Sin3A-associated histone-deacetylase complex HDAC1. In both the *in vivo* assays and luciferase reporter assays in S2 cells Sin3A functions as an antagonist of Myc function, and RNA*i* against Sin3A leads to strong increase in reporter gene expression, as well as to an overgrowth of the dorsal wing compartment when expressed by *apterous*-GAL4 or the ommatidial cells when driven by GMR-GAL4. However, Sin3A is a negative regulator of the Myc-dependent reporter system, and therefore an HCF:Sin3A complex is not likely to be the link to the growth promoting properties of HCF and Myc. The most obvious explanation for the increase in growth and luciferase expression is the loss of Mnt-dependent target gene repression that is mediated by Sin3A, since Sin3A-associated histone-deacetylases were shown to interact with the Myc antagonist Mnt (Loo et al., 2005). A second explanation for the growth promoting effect of *sin3a*-depletion comes from the observation that HCF is tethered to both the Sin3 HDAC complex and to the Set1/Ash2 HMT complex in a context-dependent manner (Wysocka et al., 2003). While it was shown that HCF-1 can simultaneously bind to the Sin3 HDAC and Set1 H3K4 HMT transcription regulatory complexes and form a “supercomplex”, it is known that the transcriptional activator VP16 preferentially interacts with HMT- but not HDAC-interacting HCF-1 (Wysocka et al., 2003). Also, data from Tyagi et al. demonstrate that HCF-1-E2F1 and HCF-1-

H2F4 complexes display selective association with HMT and HDAC activities. Whereas activator E2F1-bound HCF-1 associates with Set1 H3K4 HMT complexes, repressor E2F4-associated HCF-1 recruits HDAC complexes (Tyagi et al., 2007). Thus, a decrease in Sin3A levels could shift the equilibrium to facilitate the formation of activating HCF:HMT complexes and activation of growth. In a more speculative scenario Sin3A would act as an activator in the context of Myc:HCF:Sin3A complexes and thereby antagonize the known Mnt:Sin3A complex. There is evidence that Sin3-associated HDAC complexes can also lead to gene activation (reviewed in Rottmann and Luscher, 2006). In such a situation, RNA*i* against Sin3A would have different consequences from RNA*i* against HCF, since both the activating Myc:HCF:Sin3A and repressive Mnt:Sin3A functions would be lost upon depletion of Sin3A. The resulting activation would be due to the repressive function in a Mnt:Sin3A complex being more prominent. An experiment to test this hypothesis would be to first eliminate the repressive Mnt:Sin3 complex by *mnt*-RNA*i* and assay the effects on the Myc activity reporter, and then additionally deplete Sin3 (by RNA*i*). We would expect to see a hyperactivation of the reporter system by the depletion of Mnt, since only repression by Sin3 was lost. According to the hypothesis *mnt*-RNA*i* together with *sin3*-RNA*i* would result in lower reporter activity than *mnt*-RNA*i* alone. RNAi-mediated depletion of *mnt*, leads to an activation of the *nnp-1* Myc activity reporter 48 hours after dsRNA addition (Hulf et al., 2005). Therefore, Mnt indeed seems to antagonise Myc function in S2 cells.

As mentioned above HCF is also found in association with Ash2/Set1-histone methyltransferase complexes, which are involved in methylation of histone H3K4 residues – a modification that is correlated with actively transcribed regions. While *ash2*-RNA*i* only causes a slight reduction of Myc-acitvity reporter expression, it potently suppresses the Myc overexpression phenotype in the wing. Conversely, co-overexpressed Ash2 and Myc synergise, causing most strongly defective wings. *ash2*-RNA*i* on its own has no consequences for wing or eye development, nor can it suppress the overgrowth of ommatidia containing high Myc levels. There are reports providing a link between Ash2-containing H3K4 methyltransferase complexes and HCF in *Drosophila* (Beltran et al., 2007). Therefore, it is possible that the growth promoting effects of HCF could be the consequence of its recruiting of an Ash2-containing HMT complex to Myc. A recent report indeed has also demonstrated a physical genetic interaction between Myc and Ash2 in *Drosophila* (Secombe et al., 2007). Myc was found to interact with Ash2 in a complex with the trimethyl histone H3K4 demethylase Little imaginal discs (Lid). However, based on comparisons to biochemical purification experiments in *Schizosaccharomyces pombe*, the authors claim that Ash2:Lid complexes are distinct from Ash2:Set1 HMT complexes. It is not clear yet, whether the genetic interaction between Ash2 and Myc is caused by an Ash:Lid complex. The observation that Ash2 is found both in H3K4 methylating (Set1 in yeast; TAC1 in *Drosophila*) and demethylating complexes suggests that it may be crucial modulator of H3K4 methylation status. It is tempting to speculate that Ash2 also might interact with Myc in a HMT complex.

Taken together, all the three putative chromatin-modifying complexes tested for their genetic interaction with Myc have an influence on certain Myc-dependent processes, and we cannot rule out an involvement of any in linking HCF to Myc-dependent transcriptional regulation. Both HCF and Myc were found in association with Ash2 (Beltran et al., 2007; Secombe et al., 2007), an interaction that is also conserved in mammals (Wysocka et al., 2003); the same holds true for the interaction between

the Sin3A HDAC complex with the Myc antagonist Mnt. A third common interactor between HCF and Myc is the BTB-POZ domain protein Miz-1 (Piluso et al., 2002). Given the diversity of transcriptional targets of Myc it is intriguing to speculate that HCF might link several multisubunit chromatin modifiers to Myc in order to control the expression of target genes. Moreover, Myc has long been shown to apply several distinct modes of interaction with chromatin and with the transcriptional apparatus. However, it is possible that some of the detected interactions do not reflect a physiological requirement. Depending on the biological context (e.g. in different cell types or in different phases of the cell cycle) Myc might recruit different types of cofactors to its target genes. Alternatively, the various complexes might act redundantly at the same target. Our results with HCF have not identified a differential requirement for individual cofactors (at least for the different targets we have looked at). Moreover, the rather mild phenotype of *hcf*-RNA*i* *in vivo* and the limited effect of *hcf* knockdown on overexpressed Myc in S2 cells could be explained by the redundant action of several coactivator complexes at the same target.

2.2.5. Possible mechanisms of an HCF:Myc interaction

We have identified a novel role for HCF as a positive cofactor of Myc-dependent transcription control. This involvement is compatible with previous observations that HCF-1 plays a critical role both in cell growth and division (Julien and Herr, 2003). The growth regulating role of HCF appears largely to be mediated by its chromatin-modifying activities. Thus, HCF influences cell proliferation and growth by regulating chromatin structure. HCF was shown to associate with both HDAC and H3K4 HMT transcription regulatory complexes in a context-dependent manner (Wysocka et al., 2003; Tyagi et al., 2007). Moreover, these interactions are conserved between human HCF-1 and *Drosophila* HCF (Beltran et al., 2007). Intriguingly, some of the components of the chromatin modifying complexes that associate with HCF also interact with the Max network (see Discussion section 2.2.4.).

In addition to the interactions with the chromatin modifiying machinery, HCF was also reported to play a direct role in transcription regulatory complexes formed around several sequence-specific transcription factors, such as Sp1 (Gunther et al., 2000), GABP (Vogel and Kristie, 2000), and E2F proteins (Tyagi et al., 2007; Knez et al., 2006). HCF is a key player in cell proliferation by repressing and activating the transcription of genes required for cell-cycle progression. While the amino-terminal subunit of HCF-1 (HCF-1_N) has been shown to promote passage through G1 phase and thus promotes cell growth, the carboxy-terminal part (HCF-1_C) ensures proper exit from mitosis and faithful cell division (Julien and Herr, 2003). The properly timed transition from G1 to S Phase is dependent the interaction of HCF with E2F transcription factors, namely on the switch from “repressive” HCF-E2F4 complexes to “activating” HCF-E2F1 complexes and subsequent recruitment of MLL H3K4 HMT complexes (Tyagi et al., 2007). One of the characteristics of Myc is to drive the transition from G1 to S phase by promoting growth (Johnston et al., 1999). However, Myc’s ability in *Drosophila* to augment cellular growth but not cell-cycle rates differs markedly from the properties of *Drosophila* E2F, which upon overexpression, accelerates the cell cycle but not cellular growth (Neufeld et al., 1998). Therefore, it is tempting to speculate that concerted regulation of both Myc and E2F target genes by HCF might constitute a means to coordinate proliferation by coupling cell-cycle progression and growth. Indeed, there is evidence that E2F and Myc proteins collaborate in the control of proliferation.

Ectopic c-Myc was shown to contribute to S phase entry by activating the expression of E2F genes (Leone et al., 1997). In contrast, c-Myc is not able to promote S phase entry in the absence of E2F (Leone et al., 2001). Moreover Myc target genes frequently harbour E2F binding sites (Grandori et al., 2000). However, the *CG5033* promoter does not contain a canonical dE2F binding site, and we could not detect such a synergy concerning our Myc activity reporter system, since RNA*i*-mediated depletion of E2F led to a slight (1.8 fold) increase in luciferase expression.

The preceding experiments and discussion points are based on the assumption that HCF is being recruited to target promoters by Myc. This is also the prevailing view from several studies with sequence-specific transcription factors. In case of the HCF-1:E2F interactions it could be shown that *hcf-1* depletion does not lower ChIP signals for E2Fs, and that E2F binding to responsive promoters is a prerequisite for HCF-1 association (Tyagi et al., 2007). However, it might be possible that the recruitment mechanism between HCF and Myc is reversed. In such a concept, Myc would be recruited to target sites by other proteins and not merely via DNA sequence recognition. Such a notion complies with the results from the study of Guccione et al., in which the authors determined that c-Myc binding to target promoters is indeed based on epigenetic features, namely elevated histone H3K4 methylation, and that E-box recognition is secondary to the recognition of specific chromatin states (Guccione et al., 2006). Therefore, Myc cofactor complexes that contain chromatin-binding domains would contribute to chromatin recognition and “lead” Myc to its target promoters. Several chromatin modifying complexes could be plausible candidates for such a Myc recruitment. Especially H3K4 HMT complexes might recruit Myc, since Myc binding sites strongly correlate to chromatin regions with elevated H3K4 methylation levels. Moreover a concerted action of HCF and HCF-associated factors (e.g. E2F) could contribute to Myc binding. Under these circumstances the major function of HCF would be to tether Myc to chromatin and mutations in the catalytic subunits of the HCF-associated complexes would not necessarily affect the functionality of HCF with respect to Myc-dependent processes. However, given the fact that RNA*i*-mediated downregulation of HCF causes reduced expressions of both the endogenous Myc targets and the artificial luciferase reporter system it is probable that HCF not only mediates chromatin-association of Myc. In order to investigate the mechanism by which Myc and HCF act at target gene promoters, chromatin immunoprecipitation experiments will be performed. Depletion of either Myc or HCF would address the question whether the recruitment of Myc to its target promoters is dependent on HCF or vice versa.

2.3. RNA Polymerase II-associated factor complex (PAF complex)

The PAF complex was identified as a negative modulator of the Myc activity reporter in the initial RNA*i* screen. In this work we present evidence that the PAF complex physically interacts with Myc by directly binding it via its Atu subunit. Moreover, it is required for the proper activation of endogenous RNA polymerase II-transcribed Myc target genes. The PAF complex seems to play a dual role in the regulation of a number of *in vivo* processes. While the three subunits Atms, Atu and Rtf1 act as coactivators of Myc, Hyx acts both as an activator and repressor of Myc function depending on the context.

2.3.1. Depletion of PAF complex components activates the Myc activity reporter but represses endogenous Myc target genes

RNA*i*-mediated depletion of the four PAF complex components Hyrax, Atu, Atms, and Ctr9 leads to an activation of the Myc activity reporter in the range of 1.5- to two-fold for *Atu*, *atms*, and *ctr9*, and five-fold for *hyrax* knockdown (Figure 21). These observations confirm the initial RNA-interference screen, in which we identified Hyrax, Atms, and Ctr9 as specific interactors, and present the PAF complex as a negative modulator of Myc-dependent transcription. Nevertheless they were unexpected, since the PAF complex had been described in *Drosophila* as an essential complex that is broadly involved in transcription elongation. Depletion of the fifth PAF complex subunit Rtf1 does not influence reporter gene activity. In contrast to the situation in yeast, Rtf1 is not an integral component of the PAF complex in *Drosophila*. However, it was found to be PAF complex-associated during transcription elongation (Adelman et al., 2006) and to be required in a subset of PAF complex mediated functions (e.g. histone modification) (Tenney et al., 2006). In keeping with the activating effect of *hyx*-RNA*i*, ectopic expression of Hyx represses the Myc activity reporter (Figure 22). This repressive function can partly be suppressed by depleting Myc, indicating its dependence on Myc. In contrast, overexpression of Atu produces ambiguous results (Figure 22). While it does not alter luciferase ratio in cells with endogenous Myc levels, it exerts opposite effects in Myc-depletion and –overexpression situtations; being an activator of the reporter in the presence of low Myc levels and a repressor together with ectopic Myc. So far it is unknown whether the differences seen in behaviour between ectopically expressed Hyx and Atu are due to artificial effects caused by overexpression (e.g. gain-of-function or dominant-negative effects), or if they are really reflecting the biological functions of the two proteins. The varying effects of ectopic Atu could theoretically be explained by Myc-independent activation of the reporter, which is uncovered upon *myc*-RNA*i*. This possibility is rather unlikely, because changes in the luciferase ratio of the Myc activity reporter are largely caused by influencing the E-Box reporter variant. However, the ΔE-Box is not completely inert to increased Atu levels.

The effect of PAF complex depletion on endogenous Myc targets is opposite to the effect on the luciferase reporter system, since depletion of PAF complex components caused a repression of Myc target genes to varying extent (Figure 23). While RNA*i*-mediated knockdown of *ctr9* had no impact on Myc targets, depletion of *Atu*, *atms*, and (most strongly) *hyx*, leads to reduced expressions of RNA polymerase II-transcribed Myc target genes. The strongest effect of Hyx depletion is observed on the expression of *CG5033* and *CG12295*, whose expressions in response to reduced *hyx* levels drop to

below 50%. Less affected is *CG9630*, even though it was identified as a positive target of both Myc and Hyx in microarray studies. Depletion of *Atu* and *atms* typically leads to a reduction of Myc target gene expression by one quarter. Such a limited effect on target gene expression seems to be a characteristic of PAF complex RNA*i*, since Adelman et al. report a maximal reduction of target expression to 75% for *rtf1* depletion and 50% for *atms* knockdown (Adelman et al., 2006). Unlike RNAP II-transcribed targets, RNA polymerase III-transcribed small RNA genes are not sensitive to RNA*i* against PAF complex components. This suggests an RNAP II specific involvement of the PAF complex or a strongly relaxed requirement for PAF complex (and Myc) function for RNAP III-dependent transcription (Figure 23). An alternative explanation might be that both the PAF complex components and the RNAP III targets could be relatively stable. In such a case RNA*i* against PAF complex components would only lead to delayed protein loss and the titre of stable targets would drop even later. In addition to characterised Myc target genes, also the mRNA levels of *myc* itself are reduced to 50-75% by PAF complex RNA*i*. Therefore the slight reduction seen on the targets could be indirect. However, there is evidence that there is a role for the PAF complex is not restricted to the control of *myc* abundance, because neither levels of RNAP III-transcribed genes, nor Myc protein levels are reduced at all by PAF complex depletion (Figure 24). More importantly, the expression of the Myc activity reporter is enhanced upon depletion of PAF complex components.

Taken together depletion of several PAF complex components results in increased expression of the Myc activity reporter. At the same time reduced PAF complex levels have a slight negative effect on the expression of endogenous RNAP II-transcribed Myc targets. These apparently contradictory results might be reconciled by the influence of the chromatin-environment. The PAF complex is essential for processive transcription for the majority of loci embedded in native chromatin. It acts during several phases during transcription initiation and elongation by sequenctially recruiting chromatin modifying complexes, such as Rad6 H2B ubiquitinases (Wood et al., 2003, 2005), the Set1 histone H3-K4 HMT (Dover et al., 2002; Krogan et al., 2003b; Ng et al., 2003), and the Dot1 histone H3-K79 HMT (Krogan et al., 2003b; Krogan et al., 2003a). Loss of the PAF complex leads to defects in transcription elongation that are compatible with the effects we see upon PAF RNA*i* *in vivo*. In contrast, the Myc activity reporter, which is transiently expressed in S2 cells and not embedded in chromatin, is activated in response to PAF complex RNA*i*. Most likely, Myc does not require PAF complex action in order to drive transcription from the artificial reporter. Speculatively, a partial loss of PAF complex function could allocate more Myc protein to the Myc activity reporter, while transcription from endogenous targets is reduced. Such a scenario would imply that Myc is (at least partially) dependent on the PAF complex (or other associated factors) for its recruitment to the target. Alternatively, some of the PAF complex functions might be required for the expression of the Myc activity reporter. While depletion of individual components would be deleterious for the expression of endogenous targets, such a partially defective PAF complex might still be functional in the context of the reporter gene.

2.3.2. Atu and Myc are directly interacting

Myc interacts with the PAF complex by physically binding to the Atu subunit. We detected a strong interaction by coimmunoprecipitating ectopically expressed Myc and Atu (Figure 25). Moreover

overexpressed Hyx is also found in association with Myc, albeit at lower levels than Atu (Figure f, lane 3). Since the interaction between Myc and Atu is not abrogated by the presence of ectopically expressed Hyx (Figure 26, lane 4), this suggests a model in which both Myc and Hyx are independently associated with Atu, without competing with each other. Furthermore, the interaction between the PAF complex component Atu and Myc does not rely on the presence of any of the characterised conserved motifs in Myc, as individual mutants lacking the Myc-Boxes 1-3 (ΔMB1-3), the leucine zipper (ΔZ), or the entire bHLH-zipper (ΔC) still retain the ability to bind to Atu protein. In addition, a variant lacking the N-terminus (ΔN) and a Myc protein lacking both the N-terminus and the bHLH-zipper (ΔNΔC) are still coimmunoprecipitated with Atu (Figure 29). This finding prompted us to construct a larger set of additional deletion mutants of Myc, in order to identify the interaction site(s) within the Myc protein. Further immunoprecipitation experiments showed that the central portion of the Myc protein, ranging from aa 295 to aa 626, exhibits strong binding to Atu, whereby a stretch between aa 295 and 403 seems to confer the strongest affinity (Figure 30). Additionally, we predict a second interaction in the N-terminus because a protein truncation containing only the first 179 amino acids of Myc is coimmunoprecipitated with Atu. This N-terminal interaction domain is potent enough to sustain stable binding to Atu, and a Myc protein deletion lacking the central portion of the protein from aa 295 to 626, still is strongly retained by Atu (Figure 32). As described in Results (section 5.3.2.), individual Myc mutants are not expressed at equal levels which hampers the assessment of the interaction strength (e.g the mutant protein ΔN403 only interacts weakly with Atu, even though it contains parts of the sequence conferring strong binding). Pulldown of *in vitro* translated Atu protein with various GST-Myc fragments revealed the interaction between Myc and Atu to be direct (Figures 33 & 34), and furthermore confirmed the interaction sites identified in the coimmunoprecipitations (Figure 34).

Information gleaned from interaction studies with several proteins (e.g. HCF, Atu, Brf, and Chinmo) revealed physical binding with Myc at multiple interaction sites (P. Gallant & D. Schwinkendorf, personal communication). Even though there are proteins known to interact with several sites within Myc (e.g. Skp2) (Vervoorts et al., 2006), non-specific binding cannot be ruled out for some of the Myc truncations. Especially in the *in vitro* experiments the N-terminal Myc fragments retained the ^{35}S-labelled IVT-proteins, which could suggest non-specific “stickiness” of this domain. Moreover, we have not identified small mutations in Myc that would abrogate interactions with other proteins tested. However varying relative binding intensities for different interactors, indicate that the binding is indeed specific and physiological (compare Figures 20a (HCF) and 34 (Atu)). In addition, more stringent conditions with increased salt concentrations did not abrogate any of the interactions between Atu and internal Myc truncations. However, some interactions are weakened by increased stringency. Still, the fact that binding is retained under stringent conditions implies that the interactions (also with the N-terminal portion of Myc) are specific and not due to general stickiness. We furthermore see a broad correlation between the interaction data obtained from ectopically expressed Myc in S2 cells and from GST-pulldowns; two systems in which buffer conditions and protein concentrations are different, which further suggests that the observed interactions are specific. This especially holds true for endogenous HCF and Myc, for which we have shown an interaction (Figure 18). Taken together, the interaction studies suggest that Atu directly interacts with Myc at (at least) two sites. These include the N-terminus and the central part of the protein in the vicinity of Myc Box 3. To definitely rule out putative

unspecific interactions with Myc further tests using additional negative controls would be needed. For example AU1- or GST-tagged GFP could be used in coimmunoprecipitations or IVTs.

2.3.3. Reduction of Atu, Atms, and Rtf1 levels affects Myc-dependent growth promotion

To characterise the importance of the interaction between Myc and the PAF complex *in vivo*, we downregulated individual components by RNA*i* and assessed the influence on the development of several organs such as macrochaetae, wings and eyes. Moreover, we measured the impact on clonal growth in imaginal wing discs and endoreplication in fat body cells.

When expressing hairpin-RNA*i* constructs by *scabrous*-GAL4 to target *Atu*, *atms* or *rtf1* in bristle precursor cells, growth of bristles is significantly impaired. Scutellar macrochaete size is largely reduced, with *atms*-RNA*i* showing the strongest effect (Figure 35). Since bristle growth is heavily dependent on Myc - small, slender bristles are one of the characteristcs of hypomorphic *myc* mutants; (Johnston et al., 1999) we speculated that the PAF complex cooperates with Myc to promote growth. To address this question, the same hairpin constructs were expressed in the *ey>dm*^{P0} strain (Results, section 5.4.5.). While depletion of *Atu* did not affect eye development, reduction of *atms* and *rtf1* levels caused eye defects of a broad variety, ranging from increased roughness to the loss of a large number of ommatidia, particularly in the arterior half of the eyes. Therefore, depletion of both *myc* and *atms* or *rtf1* leads to disruption of the regular eye pattern due to a reduction of ommatidial number, while in the case of the PAF complex the size of individual ommatidia is not affected. This is an indication that pre-ommatidial proliferation – a process which is known to rely on Myc function - is disturbed. Eye defects upon PAF complex RNA*i* in control flies with endogenous *myc* levels are far less pronounced than in the *ey>dm*^{P0} background. Therefore, we concluded that ommatidial proliferation is synergistically affected by Myc and PAF complex components. In addition to RNA*i*-mediated depletion of PAF complex components, heterozygosity for *Atu*, but not *atms*, also leads to severe eye defects. This is surprising because loss of yLeo1, the yeast homologue of Atu does not affect PAF complex integrity, whereas mutations in yPaf1, the Atms homologue, cause disruption of the complex. If we assume the same to be true in *Drosophila*, the defects seen upon Atu depletion do not reflect a general loss of PAF complex function. Instead, they might by caused by the reduced recruitment of PAF (and possibly other associated factors not present in yeast) to Myc, since Atu constitutes the physical link between Myc and the PAF complex, as inferred from the interaction studies. However the experiment was based on one mutation in the *atms* locus and heterozygosity for *atms*^{rK509} might not result in a sufficient reduction of protein levels to produce a phenotype. When compared to the RNA*i*-hairpin transgenes, the classical mutations only produced an effect in a strongly sensitised background (*ey>dm*^{P0};pont$^{+/-}$). This lack of an observed dominant interaction in case of the classic *Atu* mutation in the *ey>dm*^{P0} background does not rule out a functional relationship, but might indicate that the protein level has not sufficiently been lowered. Therefore, it is likely that RNA*i* leads to a stronger downregulation of *Atu* levels than the loss of one gene copy.

Another process that is affected by PAF complex downregulation is the formation of wings. Knockdown of either *rtf1* or *Atu* severely impairs development of wings, whereas *atms*-RNA*i* has no phenotypic consequences. Expression of *Atu*-RNA*i* in the dorsal wing compartment results in strongly bent-up wings, presumably because of reduced tissue size in comparison to the ventral compartment.

rtf1-RNA*i* seems to affect wing development more severely, since adult wing structures are completely missing. This reduction of growth in the wing still might be independent of Myc action. However, RNA*i* against *Atu* or *rtf1* also suppresses the effects caused by Myc overexpression, indicating a strong positive genetic interaction with Myc.

Not only adult organs are affected by the downregulation of *Atu*, *atms*, and *rtf1*. The size of 48 hour-old Myc overexpressing imaginal wing discs clones is also significantly reduced (Figure 40). In contrast, the effect on clones of the same age containing endogenous *myc* levels is marginal. These data suggest a limiting role for the PAF complex in cells with high *myc* titres and a concomitant reduction of growth upon PAF complex depletion. Interestingly, the size of endoreplicating fat body nuclei is not affected by reduced PAF complex levels. This might be due to elevated PAF complex levels in this polyploid tissue as compared to diploid imaginal disc cells. As a consequence RNA*i* would not reduce PAF complex levels sufficiently to impart a phenotype. However, it is tempting to speculate that Myc controls different target genes in endoreplicating cells. In keeping with such an assumption that proliferating tissue is more sensitive to PAF reduction is the fact that RNA*i*-mediated depletion of PAF complex components in dm^{P0} eyes showed a proliferation defect, whereas growth of the ommatidia was not affected.

Taken together, the three PAF complex components Atu, Atms, and Rtf1 show a positive genetic interaction with Myc in several *in vivo* assays. In addition they also play a role in the correct expression of endogenous Myc target genes. These findings therefore point to a role for these subunits as coactivators in Myc dependent processes. Reduction of individual components leads to a broad variety of phenotypes. This is presumably due to differences in RNA*i* efficiency and varied sensitivity of the single assays to the downregulation of individual components. Additionally, the abundance of PAF complex components might vary in different tissues, which would further increase the variation of RNA*i*. However, the broad variation could also reflect the differential requirement for individual PAF complex components for different processes. While the depletion of *rtf1* consistently yields strong effects in all assays tested, the downregulation of *atms* leads to severe effects in most assays - with exception of the downregulation in the dorsal compartment of the wing, and the lack of phenotype for $atms^{rK509}$. In contrast, the phenotypes resulting from Atu depletion show the broadest variation. While it causes strong effects in both adult wings and larval wing imaginal discs, eye structure is not affected by reduction of Atu levels.

As mentioned above, characterisation of individual mutations of all PAF complex components in yeast revealed large differences in phenotypic strength. While deficiency for yPaf and yCtr9 causes the strongest phenotypes and affects various cellular processes, loss of yRtf1, yLeo1 and Cdc73 has milder consequences (Betz et al., 2002). This is presumably due to the fact that loss of yPaf and yCtr9 causes disruption of the whole PAF complex, whereas mutations in the three other components do not affect PAF complex integrity.

2.3.4. Hyx acts as a negative cofactor of Myc (in a subset of processes) *in vivo*

While the three PAF complex subunits Atu, Atms and Rtf1 presented themselves as coactivators of Myc, there is evidence that the fourth subunit Hyrax has opposite effects. In contrast to the other PAF complex components, expression of *hyx*-hairpin RNA neither caused growth defects in bristles nor did

it interfere with the the development of ommatidia or adult wing structures. This absence of effect might be due to insufficient downregulation of *hyx* levels. However, it could reflect Hyx's biological properties. By comparing the size of ommatidia in both *ey>dm*^{P0} and *ey>dm*^{P0} *;pont*$^{+/-}$ backgrounds, we observed that depletion of *hyx* leads to an alleviation for the need of Myc, indicating a negative genetic interaction between *myc* and *hyx* (Figure 39). Another piece of evidence for such a negative interaction stems from the observation that ectopic expression of Hyx in the eye slightly suppresses the rough-eye phenotype caused by Myc overexpression. There are several reports from the literature that Hyx homologues from yeast and humans have growth inhibiting effects. Both Cdc73 and Parafibromin are known to induce cell cycle arrest in the G1 phase by blocking the expression of cyclin D1 (Zhang et al., 2006; Woodard et al., 2005; Yart et al., 2005).

There is also data that Hyx works as a coactivator of Myc like the other PAF complex components. In imaginal wing disc clones *hyx* depletion reduces growth, albeit to a lesser extent than depletion of the other PAF complex subunits. This is consistent with the results from Mosimann and colleagues who report a clear positive role for Hyx in clonal growth (homozygous mutant *hyx*^{EY6898} clones grow at slower rates than their wild type twinsposts) (Mosimann et al., 2006). Furthermore qRTPCR experiments revealed that RNA polymerase II-transcribed targets of Myc are slightly downregulated in response to *hyx* depletion in S2 cells.

2.3.5. The PAF complex exerts both growth-promoting and –repressing functions

The analysis of the genetic interaction between Myc and the PAF complex produced apparently ambiguous data. Not only did the depletions of individual components vary in their phenotypic strength, they also resulted in converse effects. While the subunits Atu, Atms and Rtf1 generally acted as coactivators of Myc, Hyx behaved contrarily. How can these findings be reconciled?

It is known from studies in yeast with the yPAF complex that deletion mutants of the individual components cause distinct phenotypes (Betz et al., 2002). Even though different organisms are concerned, there is evidence that processes are conversely regulated by individual PAF complex components. The yCtr9 and yPaf1 were shown to be involved in transcriptional activation of G1 phase cyclins (Koch et al., 1999), whereas Cdc73 has the potential to block cell-cyle progression by repressing the expression of cyclin D1 (Zhang et al., 2006). This situation is even more pronounced in metazoan species. It is likely that individual components of the PAF complex have adopted additional functions on top of the general control in transcription elongation. Therefore, the PAF complex could have evolved novel metazoan-specific functions that go beyond the general transcription elongation. This is illustrated by sequence comparisons between the yeast protein Cdc73 and its fly and human homologues Hyx and Parafibromin. While the C-terminus is conserved between all the three species, novel N-terminal sequences were "acquired" in *Drosophila* and humans. It was shown that a confined domain within the N-terminus of both Parafibromin and Hyx interacts with β-catenin/Armadillo and exerts an essential function in Wg/Wnt-signal transduction (Mosimann et al., 2006). Likewise, recruitment to specific targets by Myc might constitute a so far uncharacterised function of the PAF complex.

Strikingly, individual PAF complex subunits are involved in the formation of cancers with opposite roles, since some were characterised as proto-oncogenes, while others seem to work as tumour

suppressors. For instance, the human homologue of Atms, termed hPAF1, was shown to be amplified in pancreatic adenocarcinoma cell lines (Chaudhary et al., 2007) and targeted overexpression has the potential to induce transformation in NIH3T3 cells (Moniaux et al., 2006). Moreover hLeo1, the human homologue of Atu, is involved in the formation of colorectal cancer (Camps et al., 2006), constituting a potential link to Wnt-signalling (which fits with the observation that Atu binds β-catenin in *Drosophila*). In contrast Parafibromin has been shown to act as a tumor suppressor. The gene coding for Parafibromin, termed *HRPT2* for Hyperparathyroidism-Jaw Tumor Syndrome (HTP-JT) tumor suppressor gene, is mutated in hereditary and sporadic forms of parathyroid neoplasias (Carpten et al., 2002). However, Hyx clearly plays a positive role in Wg/Wnt-signalling (Mosimann et al., 2006). These data illustrate that individual PAF complex components can exert independent functions. Therefore the opposing roles observed for Atu, atms, and Rtf1 on one hand and Hyx on the other hand, could reflect physiological properties of the individual components. Depending on the context and the organ that is examined the PAF complex as a whole and its individual subunits may exert various functions. While Atu, Atms, and Rtf1 activate growth - whether by metazoan-specific functions or by facilitating general transcription elongation needs to be addressed – Hyx also exerts growth repressing functions. In order to further elucidate and clarify the role of the PAF complex as a whole, and of the individual subunits in particular, further *in vivo* experiments will be required.

3. Conclusion and Outlook

In this study, we describe the identification and characterisation of two novel physiological cofactors of Myc-dependent transcription control.

We show that the RNA polymerase II-associated factor 1 (PAF) complex is associated with Myc by making direct physical contact with its Atu subunit. Moreover, the PAF complex is required for correct expression of direct Myc target genes and depletion of the PAF complex has strong consequences on Myc-dependent processes *in vivo*. Strikingly, the PAF complex seems to play a dual role in the regulation of a number of *in vivo* processes, since the individual subunits exert differential functions. While Atms, Atu and Rtf1 act as coactivators of Myc in the assays used, there is evidence that Hyx can act both as an activator and repressor of Myc function depending on the context and/or tissue. The further elucidation of the interaction between Myc and the PAF complex could be of great importance since both Myc and the PAF complex are involved in the formation of a variety of human cancers.

Experiments presented in this study and Mirjam Balbi's master thesis (Balbi, 2007) clearly identified HCF as a positive cofactor of Myc-dependent transcription control. We have shown a direct physical interaction between endogenous HCF and Myc proteins and revealed an influence of HCF on expression of Myc target genes in S2 cells. *In vivo* HCF synergises with Myc in the promotion of growth in the eye and wing. HCF depletion by RNA*i* has the potential to revert Myc overexpression phenotypes in the wing and, to a lesser extent, also in the eye. These data coherently indicate that Myc requires HCF to reach its full transcriptional activity during proliferation and differentiation. In order to activate Myc-dependent transcription HCF has to recruit additional complexes with enzymatic activity. The molecular nature of such a mechanism needs to be elucidated.

Taken together, we present evidence that both the PAF complex and HCF are physiologically relevant modulators of Myc-dependent transcription. Further characterisation of the interplay between these proteins will be of importance to understanding the biology of Myc.

Materials and Methods

1. Cloning

1.1. Luciferase reporter constructs

1.1.1. Construction of the *CG5033* and *CG4364* reporters

Promoter sequences from -322 to +61 relative to the transcription start site of *CG5033* (E-box at +21, ATG at +56) and from -561 to +131 relative to the transcription start site of *CG4364* (E-box at –421, ATG at +133), respectively, were fused to the firefly luciferase ORF. Corresponding promoter sequences were PCR amplified with the following primers:
CG5033-upstream: 5'- GTAGAGATCTGAATTTCGCTGAAAATGGTTCGTTG-3' (Bgl II site)
CG5033-downstream: 5'- ATGTTC**CAT**GGGGTCATTTTGAGGTA-3' (Nco I site)
CG4364-upstream: 5'-CCCCAGATCTTCAAGAACACGACACAAG-3' (Bgl II site)
CG4364-downstream: 5'-CCAAC**CAT**GGTGCCGGTTTATGAAAATG-3' (Nco I site)
PCR products were subjected to Bgl II and Nco I restrictions and cloned into the firefly ORF containing vector pGL3-Basic (Promega).

In the ΔE-Box mutants, the sequence "CACGTG" was replaced by "GAATTC". The following oligonucleotides were used:
CG5033-ΔE-Box:
5'-ATCGCTATCGCTGACTGCAA**GAATTC**CGCCGCGTTAGTTTTGTTTTTACC–3';
CG4364-ΔE-Box upstream:
5'-CAATTTGGAACTGGTCACACTTCCTTTC**GAATTC**AAACCAACAAC ACAAAAAACGTGTGTTTTG-3'
CG4364-ΔE-Box downstream:
5'-CAAAACACACGTTTTTTGTGTTGTTGGTTT**GAATTC**GAAAGG AAGTGTGACCAGTTCCAAATTG-3'

For the mutagenesis of the *CG5033* E-Box sequence the GeneEditor in vitro Site-directed Mutagenesis System (Promega), for the *CG4364* E-Box the QuikChange Site-Directed Mutagenesis Kit (Stratagene) was used.

To clone the wild type *CG5033* promoter fragment into the *Renilla* luciferase ORF containing vector pRL (Promega), the promoter was reamplified using the upstream primer from above and the downstream primer CG5033_NheI: 5'-AGTGGCTAG**CAT**TTTGAGGTAAAAACAAAACTAACGCGG CGCAC-3' (Nhe I site)

The sequences printed in bold indicate the beginnings of the luciferase ORF, the underlined sequences the individual restriction sites and the sequences labelled in red mutated E-boxes

1.1.2. Construction of the *mfas* reporter

The promoter sequence from -859 to +503 relative to the transcription start site of *midline fascicline* (*mfas*) (ATG at +504) was fused to the firefly luciferase ORF. Sequences were PCR amplified with the following primer pair:

mfas-upstream: 5'-TCAACGCGTCTCGAGCGGATGATTACGAT-3' (Xho I site)

mfas-downstream: 5'-GAGTC**CAT**GGAGTTTGGTATCACAAT-3' (Nco I site)

The sequences printed in bold indicate the beginning of the luciferase ORF, the underlined sequences the individual restriction sites. After amplification the PCR product was restricted with Xho I and Nco I and cloned into pGL3-Basic (Promega).

1.2. Overexpression constructs

1.2.1. AU1-tagged Atu

For coimmunoprecipitations between overexpressed Atu and HA-tagged dMyc proteins, an AU1-epitope tag was fused to *Atu* ORF with the following two-step strategy. The AU1-epitope tag containing vector pUAST-AU1 was restricted with Bgl II and a short primer hybrid adapter with Bgl II compatible overhangs was inserted to introduce a Nhe I restriction site. These primers were hybridised to form the primer adapter (the Nhe I site is depicted by bold letters. The 5' primer ends were phosphorylated to allow ligation into pUAST-AU1).

BglNhe_f: ^{P}5'-GATCTC**GCTAGC**GT-3'

BglNhe_r: ^{P}5'-GATCAC**GCTAGC**GA-3'

In a second step the complete *Atu* ORF excised from the *UAS-HA-Atu* vector and cloned into the new *UAS-AU1* vector variant, using Nhe I and Xba I restriction enzymes.

1.2.2. HA-tagged Myc deletion mutants

The cloning strategy for the triple HA-tagged Myc deletion mutants is described in detail in (Schwinkendorf, 2008).

The three internal deletion mutants Δ294C-403, Δ294C-523 and Δ294C-626, which lack the central part of the Myc protein, spanning from amino acid 294 to aa 403, 523 and 626 respectively, were cloned as follows. The Mlu I site introduced into the C-terminal deletion Δ294C was used to combine an N-terminal Xba I – Mlu I dMyc fragment with the N-terminally located Mlu I site of the N-terminal deletions ΔN403, ΔN523 and ΔN626. Therefore, an Xba I – Mlu I fragment was introduced into the three N-terminal deletion vectors. To restore the open reading frame a primer adapter was inserted. Primer sequence of Mlu I fillin: ^{P}5'-CGCGAGCCTCGAGGCT-3'

1.2.3. Cloning of pBSK-Atu and pRSet-HCF for *in vitro* expression

The entire *Atu* ORF without the triple HA-tag (3030 bp) was excised from the *UAS-HA-Atu* vector (Städeli, 2006), using Nhe I and Xba I restriction enzymes.Subsequently the fragment was cloned into Xba I linearised pBluescript II SK(+).

The HCF-expression plasmid was cloned as follows. The N-terminal part of the *hcf* ORF, comprising the first 1424 base pairs was PCR amplified using the following primers:
HCF-IVT-Kelch_fwd: 5'-CATCAGATCTACGAAGGCTCAGACTTTGTG-3' (Bgl II site)
HCF-IVT-Kelch_rev: 5'-GTAGCCATGGTCATGCTGCAAAAGTGGTCG-3' (Nco I site)

The PCR product was restricted with Bgl II and Nco I enzymes and cloned Bam HI – Nco I into the pRSetC expression vector.

2. Tissue culture and biochemistry

2.1. Cell culture conditions

Drosophila S2 cells were cultured in 1x Schneider's *Drosophila* medium (Gibco/BRL), supplemented with 10% fetal bovine serum (heat-inactivated), 1% Penicillin/Streptomycin (Invitrogen), at 24°C.

2.2. Synthesis of double stranded RNA

dsRNA was produced by *in vitro* transcription of PCR products of approximately 600 bp in length amplified from the gene of interest. Target sequences were subjected to BLAST analysis to ensure minimal homology with unrelated transcripts. PCR primers each contained a 5' T7 RNA polymerase binding site (TAATACGACTCACTATAGGGAGA) followed by the sequences specific for the targeted genes. The primer sequences were as follows:

dsRNA	primer name	primer sequence (5' → 3')
myc	T7_dmyc_f	CCGGCTCTGATAG
	T7_dmyc_r	TGCTCATCATGGA
gfp	T7_gfp_f	TGAGCAAGGGCGAGG
	T7_gfp_r	GCGGCGGTCACGAAC
hcf2	T7_HCF_fwd2	GACAGTGCCTGGAAGT
	T7_HCF_rev2	TTTTCTGGCACTCAGC
hcf3	T7_HCF_fwd	GAGAGCCCAAAACCTATAG
	T7_HCF_rev	GAAAGATCCTTAAACACACC

hcf1 corresponds to the sequence targeted in the screen and the primary gene specific PCR product was reamplified using the primers complementary to the Eurogentech tag-sequences.

hcf1	S tail 3	TGAGGTACGCGTGGG
	R tail	TGGCGCCCCTAGATG

For all the other RNA*i* experiments dsRNA from the original RNA*i* screen plates was used.

2.3. RNA*i*-mediated depletion of endogenous mRNA

Schneider 2 (S2) cells were cultured as described above. RNA*i* experiments were performed by incubation of 5×10^6 cells in a 3 cm cell-culture dish (6 well plates) with 10µg dsRNA in 1ml serum-free medium for 30 minutes. After addition of 2ml complete medium cells were incubated and harvested at time points indicated.

2.4. Luciferase reporter assays

Luciferase reporter assays were carried out as follows. Schneider 2 (S2) cells were plated out in 24 well culture plates at a density of 2×10^6 cells/ml in 650µl complete medium. The cationic lipid cellfectin (Invitrogen) was used as a transfection reagent at a final concentration of 10µl/ml. Per transfection sample 21µl of a 1:5 cellfectin dilution in serum free medium (SFM) was prepared and incubated for 45 minutes at room temperature. Constant amounts of 1.3µg experimental plasmid DNA were prepared in a volume of 21µl SFM and added to the cellfectin in 1:1 mixture of *wild type-Renilla* luciferase and *ΔEbox*-firefly luciferase reporters (i.e. 0.5µg of each reporter per 10^6 cells). *tubulin-Renilla* luciferase control DNA was used at 0.1 µg/10^6 cells. In case of overexpression studies, 1.3µg of a 1:1 mix *tub-GAL4* and *UAS*-plasmids was added. To ensure equal DNA concentrations between individual samples pCaSpeR4 vector was added where needed. RNA*i* was induced by 40ng of dsRNA. The cellfectin-DNA mixture was incubated for 15 minutes at room temperature and made up to the final transfection volume of 420µl with SFM. Complete growth medium was aspirated from the sample wells and cells were washed once with SFM. After aspirating, the transfection medium was added and the cells were incubated for 16 hours at 24°C. Transfection solution was exchanged with 650µl complete medium and the cells were incubated for the desired time to ensure proper expression of the transgenes and/or efficient RNA*i*. Each experiment was performed in duplicate. To harvest the cells, experimental samples were washed in 1x PBS, lysed for 15 minutes in 100µl 1x Passive Lysis Buffer (Dual-Luciferase Reporter Assay System, Promega). 10µl lysate was transferred to luminometric 96 well plates (Greiner) and relative reporter gene expression was determined on a Wallac luminometer. The luminometer protocol was adjusted to disperse 50µl of each luciferase substrate per measurement. Average of duplicates was calculated and all values are indicated with standard deviations.

2.5. RNA*i* screening process

In order to carry out an RNA interference based reverse genetic screen, to identify specific cofactors of dMyc, a list of putative cofactors was compiled (P. Gallant & K. Basler, personal communication). Specific primer pairs for all the 752 selected candidates were ordered from Eurogentech. Primers were selected to guarantee very high specificity by exclusion of common sequences between *Drosophila melanogaster* genes within the amplicons. This measure was taken to avoid RNA*i* off-target effects. The average amplicon length was set to 400 base pairs. To allow for reamplification of the primary PCR products, universal sequences were added to the primers. All 3'-primers contained the same tag sequence, while 5'-primers contained 9 different sequences. Therefore, the whole set of sequence-specific amplicons could be re-amplified using only 10 primer pairs. The secondary primers used for re-amplification also ontained a 5' 23bp T7 promoter sequence, resulting in PCR products with T7 promoter sequences added to both ends of the amplicons. The primary PCR was performed on genomic *Drosophila* DNA as template and the resulting amplicons were reamplified and T7 ends were introduced. Subsequently, dsRNA was generated. For over 95% of the candidate genes sufficient amounts of dsRNA were obtained and analysed on agarose gels (R. Städeli, personal communication). Tests revealed that unpurified dsRNA showed the best efficiency in knocking down selected luciferase reporter genes (R. Städeli, personal communication). The whole amplification procedure and generation of dsRNAs was performed by Peder Zipperlen in the laboratory of Prof. K. Basler. The dsRNAs were diluted, and an estimated content of 1µg dsRNA in 10µl nuclease-free water was plated out into 96 well plates. The transient transfection protocol described above was adapted as follows: 4.5µl Cellfectin-DNA solution was prepared per sample, containing 50ng of each reporter plasmid and 0.5µl cellfectin. The mixture was incubated for 45 minutes at room temperature to assure association of the plasmid DNA with the cellfectin. The mixture was added to S2 cells in suspension in serum-free medium and plated out. Per well 10^5 cells in a volume of 45.5µl SFM were seeded out and incubated for 12 hours. In contrast to the general protocol, the transfection medium was not removed, but 50µl of full-medium was added to each well and cells were allowed to proliferate for 48 hours before lysis and subsequent luciferase measurements. The screen was performed in duplicate and plates with a clear positional bias in expression levels across the plate were subjected to an additional third run.

2.6. Transient overexpression of tagged proteins in Schneider 2 cells

Drosophila S2 cells were seeded at a density of 5×10^6 cells per well of a 6-well culture plate. Subsequently, cells were transfected in 1ml of serum-free medium containing 10µl cellfectin (Invitrogen) and a constant total amount of 10µg plasmid DNA made up of 3.3µg *tub-GAL4* and 3.3µg of each UAS-plasmid (or *tub-HA-hyx*). In cases of a single overexpressions pCaSpeR4 plasmid DNA was used to top the DNA content up to 10µg. As expression varied for the cloned *UAS-HA-myc* deletion mutants, DNA content was changed to reach level expression. 15-16 hours later, 2ml complete was added for 48 hours, before cells were either directly processed for SDS-PAGE or preceding coimmunoprecipitation.

2.7. Western blotting

Cells were harvested at the indicated time points and washed with 1x PBS, lysed in Laemmli sample buffer by boiling for 5 minutes at 95°C and analysed by SDS-PAGE and immunoblotting. Standard conditions were: Electrophoretic separation of the lysates on 10% SDS-PAGE gels at 120 V for 2 hours, followed by transfer onto nitrocellulose membranes with a constant current of 30 V for 2 hours at 4°C. Subsequently, membranes were blocked with 1x TBS, containing 5% fat free milk powder. Incubation with primary antibodies was performed overnight at 4°C in 1x TBS 5% milk powder. Then the membranes were exposed to the secondary antibodies for 1-2 hours at room temperature. Washing steps were performed with 1x TTBS (TBS + 0.2% Tween-20). Western blots were then either exposed on X-ray films (using multiple exposures for each experiment) or scanned with a CCD camera (Fuji LAS-3000). For detection the enhanced chemiluminescence kit (Amersham) was used.

Primary antibodies used for Western blotting were:

Epitope	Species	Source	Dilution
anti-dMyc hybridoma supernatant	mouse	A. Orian	1:5
anti-α-tubulin	mouse	Sigma	1:25'000
anti-HCF (C-terminal subunit)	rat	J. Workman	1:3000
anti-HA epitope	mouse	BAbCO	1:1000
anti-HA epitope	rabbit	Dunn Labortechnik GmbH	1:10'000
anti-Atu	rabbit	New England Peptide LLC	1:1000

The polyclonal rabbit anti-Atu antibody was raised against the epitope RDKVESQVESAPKEC, wich corresponds to the amino acids 368 to 381 of the *Drosophila* Atu sequence.

Secondary antibodies:

Antibody	Species	Source	Dilution
HRP-coupled anti-mouse	goat	JacksonImmunoResearch	1:10'000
HRP-coupled anti-rat	goat	Amersham	1:3000
HRP-coupled anti-rabbit	donkey	Amersham	1:3000

2.8. Coimmunoprecipitations of overexpressed proteins from cell samples

Transfections were performed as described in (Materials and Methods, sectioin 2.6.) and harvested after 48 hours. Pelleted cells were washed once with cold 1× PBS and lysed on ice for 30 minutes in lysis buffer (250mM NaCl, 50mM Tris-HCl (pH 8.0), 5mM EDTA (pH 8.0), 0.5% (w/v) Nonidet NP-40 (Rozenblatt-Rosen et al., 2005)) containing protease inhibitors (Protease Inhibitor cocktail tablets, Roche). Insoluble contents were precipitated by centrifuging for 10 minutes at 13'000 rpm. The lysates were precleared for 1 hour at 4°C with protein G Sepharose bead suspension (GE Healthcare) and 5% of the lysate was set aside as input control. The incubations with 0.2-1µl of the primary antibodies

were performed at 4°C for 3 hours, followed by a 1 hour precipitation of the epitope antibody complexes with protein G Sepharose beads. The immunoprecipitated material was washed three times for 5 minutes in lysis buffer on ice, SDS sample buffer was added, and the samples were analysed by SDS-PAGE and immunoblotting as described under (2.7.).

2.9. Coimmunoprecipitations of endogenous HCF and Myc from embryos

Overnight collections of 0-18 hour-old *yw* embryos were dechorionated for 1 minute and washed extensively with NaCl-Tx (0,7% (w/v) NaCl, 0,1% (w/v) Triton X-100). The embryos were homogenised at 4°C in 4 volumes 1× LPA lysis buffer (50mM HEPES, pH 7.5, 60mM NaCl, 3mM $MgCl_2$, 1mM $CaCl_2$, 0.2% Triton X-100, 0.2% Nonidet NP-40, 10% glycerol) containing protease inhibitors (Protease Inhibitor cocktail tablets, Roche), using a 1ml glass douncer. The raw extract was centrifuged 15 minutes at 13'000 rpm to pellet cell debris. The clear middle layer was taken out, centrifuged again to get rid of the lipids, and precleared for 90 minutes with protein G Sepharose slurry. In the meantime mouse anti-dMyc hybridoma tissue culture supernatant and control mouse anti-lacZ supernatant were bound to protein G Sepharose beads at room temperature. After having taken out 3% of the whole lysate as input control, lysates were incubated 3 hours with the antibody bound protein G Sepharose beads at 4°C. Beads were washed three times with 1× LPA lysis buffer, followed by 3 washing steps each with WPS salt wash buffer (LPA with 300mM NaCl) and WPD detergent wash buffer (LPA with 0,4% NP-40 and 0,4% Triton X-100). SDS sample buffer was added, and the samples were analysed by SDS-PAGE and immunoblotting. Primary antibody used for Western blotting: rat anti-dHCF (kind gift of J. Workman) and secondary antibody HRP-coupled goat anti-rat antibody (Amersham).

2.10. GST-pulldowns

The original protocol from (Mosimann, 2007) was modified and carried out as follows:

Protein induction: The IPTG-inducable *E. coli* strain BL21 was transformed with the various pGEX-Myc constructs and 50 ml cultures were grown until they reached an OD of 0.5-07. IPTG was added to a final concentration of 1mM and the cultures were incubated for another 3 hours at 37°C to ensure GST-dMyc fusion protein expression.

Lysis: The bacteria were then pelleted for 30 minutes at 4500 rpm and the pellets were lysed in bacterial GST-lysis buffer (10mM Tris-HCl, pH 8.0, 150mM NaCl, 1.5% N-Laurylsarcosine) containing protease inhibitors (Protease Inhibitor cocktail tablets, Roche). After 10 minute incubation on ice, DTT was added to a final concentration of 5mM and the suspension was sonicated until the solution becomes completely transparent (1 minute). Triton X-100 was added to the sonicated lysate to a final concentration of 2%. Cell debris was pelleted and the cleared lysate was bound to Gutathione Sepharose beads overnight at 4°C. The next day, the beads were washed three times in GST Wash Buffer (20mM Tris-HCl, pH 8.0, 200mM NaCl, 1mM EDTA, 1mM DTT, 0.5% Nonidet NP-40) and then resuspended in 250µl GST Binding Buffer (200mM NaCl, 1mM EDTA, 1mM DTT, 0.5% NP-40, 10% glyerol) containing Protease inhibitors.

***In vitro* translation of Atu and HCF**

[^{35}S] methionine labelled in vitro expressed Atu and HCF proteins were produced according to the TNT Coupled Reticulocyte lysate Transcription/Translation System manual (Promega). Expression of the radioactively labelled proteins was performed for 90 minutes at 30°C. 10% of each sample was set aside as a loading control.

GST pulldowns

For the GST pulldowns we used 30µl GST-dMyc coupled Glutathione sepharose beads per reaction. GST-only coupled beads served as a control. Bead-coupled GST-fusion proteins were incubated for 2 hours in GST Binding Buffer in the presence of 0.05% BSA, followed by two-hour's incubation at 4°C with 7.5µl ^{35}S-labelled protein. The samples were washed five times in GST Wash Buffer, taken up in sample buffer and SDS-PAGE gels were run. The acrylamide gels were stained with Coomassie Blue, fixed and dried under vaccum for 2 hours at 80°C. Exposition of the gels was performed on X-ray films for several days or using a Phosphorimager (Fujifilm FLA-7000) screen overnight.

2.11. qRTPCR

Drosophila Schneider 2 cells were treated with dsRNA against PAF complex components or *hcf* as described in (2.3.). The pelleted cells were lysed in 1ml TRIZOL reagent (Invitrogen) and total RNA was extracted and purified according to the protocol supplied with the TRIZOL reagent. After precipitation, RNA was redissolved in 20µl RNase-free water. The concentration of the purified RNA was measured with a Nanodrop ND-1000 spectrophotometer. To remove traces of genomic DNA, 10µg of RNA were subjected to a DNase digestion, using the Ambion TURBO DNA-free-kit. Subsequently, the quality of the purified RNA was analysed using Bioanalyzer chips (Agilent). The Bioanalyzer electropherograms also served as confirmations for the Nanodrop concentration measurements. cDNA was synthesised with the Omniscript Reverse Transcription Kit (Qiagen) using random hexamer primers. 1µg of template RNA was used in the reverse transcription step. Mock RT reactions (containing 1µg of template RNA) were performed in order to control for remaining traces of genomic DNA. qRTPCR reactions were performed on an ABI 7900 Real Time PCR Instrument (Applied Biosystems) using the SYBR GREEN PCR Master Mix (Applied Biosystems). Dissociation curve measurements were included in the PCR run to ascertain the specificity of the amplification reaction. Data were analysed with SDS 2.0 software (Applied Biosystems), subsequent analyses and relative target gene quantification was performed using Microsoft Excel. The amount of target was normalised to *actin5C* for (Paf complex dsRNA Figure 23) and *actin5C* and *Sec24* for (HCF dsRNA Figure 16). Relative expression levels comparded to the *gfp* dsRNA treated samples are given by $2^{-\Delta\Delta Ct}$, where. $\Delta\Delta Ct = \Delta Ct(sample) - \Delta Ct(gfp)$, and ΔCt is the Ct of the target gene subtracted from the Ct of the *actin5C* or the combined *actin5C* and *Sec24* reactions. The following primer pairs were used in the qRTPCR reactions:

Assay/Gene	Primer name	Sequence (5'→3')
actin5C	PG_act5C_F1	GCCCATCTACGAGGGTTATGC
	PG_act5C_R1	AATCGCGACCAGCCAGATC
Sec24	Sec24forw	CCACTCCCCTGCCATCCT
	Sec24rev	ACCCCAAACCCAGCAACA
myc	dmyc_RTPCR_f	GAATCGCGCTCGGTTAGTG
	dmyc_RTPCR_r	CTACGCCGCCGCTTTAAG
nnp1	PG_nnp1_F1	CTATACACACGAAAGTTTCCATGCTATA
	PG_nnp1_R1	CCCTTGCTCTTGGAGAATGG
CG5033	PG_CG5033_F1	TAACCGCTCGGCTTTAATTCA
	PG_CG5033_R1	CCCTTGCTCTTGGAGAATGG
CG12295	CG12295_RTPCR_f	GGCGGAAGATGGATTTAGCTT
	CG12295_RTPCR_r	CCTCGATTGCCCTTCGTATATAA
fibrillarin	fib.Left	ACGACAGTCTCGCATGTGTC
	fib.Right	ATGCGGTACTTGTGTGGATG
hcf	MF_HCF_qPCR_f	AATTCTTGCGGACGAGGAGAA
	MF_HCF_qPCR_r	CCCTCCTTGACATCCTTGGAA
Bka	MF_Bka_fwd	GACCTTAAGAATCGCATCCGG
	MF_Bka_rev	TTGACTCCATACGCTTCTGGC
CG9630	MF_CG9630_fwd	AGGAAATAGGTGCCCTCGTCA
	MF_CG9630_rev	TTCAGGTGCTCCAAGTCTTCG
5sRNA	5sRNA_fw	CGTCCGATCACCGAAATTAAG
	5sRNA_rev	CCAAGCGGTCCCTCATCTAA
snoRNA U3	PG_U3_f	TTTCACACTAGCTGAAAGCCAAGT
	PG_U3_r	CCTCACGCTGCCGAATAGAA
tRNA(Leu)	tRNALeu.L	TAAGGCGCCAGACTCAAGAT
	tRNALeu.R	CCTCAAAGAGGACCAGAAC

3. Fly culture

Flies were kept on standard *Drosophila* medium. Test crosses were performed in climate chambers at 25°C.

3.1. Fly lines

UAS-hairpin-RNAi lines and overexpression constructs for *hcf* and associated factors are described in (Balbi, 2007).

dm^{P0} (Johnston et al., 1999)

y w; dm^{P0} tub>myc $^{y+}$<GAL4 ey-flp/FM7i, act-GFP

y w; tub>myc $^{y+}$<GAL4 ey-flp/FM7i, act-GFP

y w; dm^{P0} tub>myc $^{y+}$<GAL4 ey-flp/FM7i, act-GFP; pont$^{5.1}$/TM6B, Tb

y w; GMR-GAL4^{w+}/CyO, y+

y w; GMR-GAL4^{w+} UAS-Myc^{132w+}/CyO, y+

y w; GMR-GAL4^{w+} UAS-Myc^{132w+}; UAS-Myc^{132w+} UAS-Myc^{42w+}/(SM5^TM6B, Tb)

y w; ap-GAL4^{w+}/CyO, act-GFP

y w; ap-GAL4^{w+} UAS-Myc$^{132\ w+}$/CyO, act-GFP

y w; sca-GAL4/CyO

y w hs-flp; +; act>CD2>GAL4^{w+} UAS-GFP^{w+}/TM6B, Tb

y w hs-flp; UAS-Myc$^{132\ w+}$; act<CD2>GAL4^{w+} UAS-GFP^{w+}/TM6B, Tb

y w; Z-IR M-3i (UAS-lacZ hairpin insertion on the second chromosome. (Steiger, 2007)

w; UAS-lacZ B4-1-2 $^{w+}$

w; +; UAS-hyx-RNAi (VDRC transformant ID 28318)

w;+; UAS-atms RNAi (VDRC transformant ID 20876)

w;+; UAS-rtf1 RNAi (VDRC transformant ID 27341)

w; UAS-atu RNAi (VDRC transformant ID 17490)

w; UAS-rpn6-RNAi (VDRC transformant ID 18021)

w; UAS-rpn6-RNAi (VDRC transformant ID 18022)

w; UAS-rpn5-RNAi (VDRC transformant ID 20104)

w; +; UAS-rpn5-RNAi (VDRC transformant ID 18676)

w; UAS-rpn12-RNAi (VDRC transformant ID 21799)

w; UAS-rpn7-RNAi (VDRC transformant ID 22103)

w; +; UAS-rpn7-RNAi (VDRC transformant ID 22104)

w; Rpn6^{2F}/CyO, P{w+mC =ActGFP}JMR1 (Bloomington Stock Center)

w; Rpn6^{20F}/CyO, P{w+mC =ActGFP}JMR1 (Bloomington Stock Center)

y^{1} w^{67c23}; P{w^{+mC} =lacW}Rpn6^{k00103}/CyO (Bloomington Stock Center)

w^{1118}; P{w+mGT =GT1}Rpn11^{BG01694}/CyO (Bloomington Stock Center)

w^{1118}; P{w^{+mC} =lacW}Atu^{s1938}/TM3, Sb1 (Bloomington Stock Center)

P{ry$^{+t7.2}$=PZ}atms^{rK509} ry^{506}/TM3, Sb^{1} (Bloomington Stock Center)

y w hs-flp;+; FRT82hyx$^{EY6989,\ y+w+}$/TM6B, Tb (Mosimann et al., 2006)

y w hs-flp;+; FRT82 hyx$^{2,\ y+}$/TM6B, Tb (Mosimann et al., 2006)

y w; +; hyx^{P9} (Mosimann et al., 2006)
y w hs-flp; UAS-hyx$^{1.5}$ (Mosimann et al., 2006)

4. Determination of bristle size

Scutella were removed, cleaned from attaching muscle tissue and mounted on glass slides, in glycerol. Pictures were taken with a Zeiss Axiophot microscope (Objective magnification: 5×). Bristle size was determined as the total pixel count a bristle covers in a picture. Pixel counts were determined with Adobe Photoshop.

5. Determination of ommatidial size

Flies were frozen at –20° C for at least one day, slowly defrosted at 0°C and directly used for electron microscopy. The pictures were acquired with a JEOL JSM-6360 LV scanning electron microscope at a magnification of 180×. For determination of ommatidial size, the area of 20 centrally located ommatidia was measured from 5 flies of the same genotype using Adobe Photoshop. The same photomicrographs were also used to determine the total number of ommatidia per eye. Obvious fusions of two ommatidia were counted as two individual ommatidia. The Student's t-test was applied to assess statistical relevance of observed differences.

6. Analysis of clone size in imaginal wing discs and fat body

To analyse the size of clones with downregulated dPaf complex levels in wing discs and fatbody virgin females of the strain *yw hs-flp; +; act>CD2>GAL4*$^{w+}$ *UAS-GFP*$^{w+}$ */TM6B, Tb* were crossed to males from the following *UAS*-hairpin RNA expressing lines:

y w; Z-IR M-3i	(UAS-lacZ hairpin insertion on the second chromosome. (Steiger, 2007)
w; +; UAS-hyx-RNAi	(VDRC transformant ID 28318)
w;+; UAS-atms RNAi	(VDRC transformant ID 20876)
w;+; UAS-rtf1 RNAi	(VDRC transformant ID 27341)
w; UAS-atu RNAi	(VDRC transformant ID 17490)

Crosses with the same *UAS*-hairpin RNA males were performed in a dMyc overexpression background, by using virgin females of the following genotype: *yw hs-flp; UAS-dmyc*$^{132,w+}$*; act>CD2>GAL4*$^{w+}$ *UAS-GFP*$^{w+}$ */TM6B, Tb*

16-24 hour long egglays were performed and the clones were induced by heatshocking the larvae 72 hours AED for 8 minutes in a water bath at 37°C. The wandering third instar larvae were dissected 45 hours after clone induction, fixed in 4% paraformaldehyde for 20 minutes, and washed three times in 1× PBX (1× PBS + 0.1% Triton X-100). During the second washing step 0.5µg/ml of the DNA dye Hoechst 33342 was added to the wash buffer. Subsequently, wing discs and fatbody tissue was extracted and mounted in Vectashield mounting solution (Vector). Pictures were taken with a Leica

DMRA fluorescence microscope (objective Magnification: 10×). Clones were identified by presence of GFP expression and the clone or nuclear size was determined as the total pixel count a clone or nucleus covers in a picture. Pixel counts were determined with Adobe Photoshop. For each genotype 25-50 clones/nuclei were measured. The Student's t-test was applied to assess the statistical significance of the average size changes.

References

Adelman, K., Wei, W., Ardehali, M.B., Werner, J., Zhu, B., Reinberg, D., and Lis, J.T. (2006). Drosophila Paf1 Modulates Chromatin Structure at Actively Transcribed Genes. Mol Cell Biol *26*, 250-260.

Adkins, M.W., and Tyler, J.K. (2006). Transcriptional activators are dispensable for transcription in the absence of Spt6-mediated chromatin reassembly of promoter regions. Mol Cell *21*, 405-416.

Amati, B. (1998). Myc and the cell cycle. Frontiers in Bioscience *3*, 250-268.

Amati, B., Brooks, M.W., Levy, N., Littlewood, T.D., Evan, G.I., and Land, H. (1993a). Oncogenic activity of the c-Myc protein requires dimerization with Max. Cell *72*, 233-245.

Amati, B., Dalton, S., Brooks, M.W., Littlewood, T.D., Evan, G.I., and Land, H. (1992). Transcriptional activation by the human c-Myc oncoprotein in yeast requires interaction with Max. Nature *359*, 423-426.

Amati, B., Littlewood, T.D., Evan, G.I., and Land, H. (1993b). The c-Myc protein induces cell cycle progression and apoptosis through dimerization with Max. EMBO Journal *12*, 5083-5087.

Andrulis, E.D., Guzman, E., Doring, P., Werner, J., and Lis, J.T. (2000). High-resolution localization of Drosophila Spt5 and Spt6 at heat shock genes in vivo: roles in promoter proximal pausing and transcription elongation. Genes Dev *14*, 2635-2649.

Armelin, H.A., Armelin, M.C., Kelly, K., Stewart, T., Leder, P., Cochran, B.H., and Stiles, C.D. (1984). Functional role for c-myc in mitogenic response to platelet-derived growth factor. Nature *310*, 655-660.

Askew, D.S., Ashmun, R.A., Simmons, B.C., and Cleveland, J.L. (1991). Constitutive c-myc expression in an IL-3-dependent myeloid cell line suppresses cell cycle arrest and accelerates apoptosis. Oncogene *6*, 1915-1922.

Ayer, D.E., and Eisenman, R.N. (1993). A switch from Myc:Max to Mad:Max heterocomplexes accompanies monocyte/macrophage differentiation. Genes & Development *7*, 2110-2119.

Ayer, D.E., Kretzner, L., and Eisenman, R.N. (1993). Mad: a heterodimeric partner for Max that antagonizes Myc transcriptional activity. Cell *72*, 211-222.

Balbi, M. (2007). Characterization of dHCF as a Novel Co-Factor of dMyc in *Drosophila melanogaster*. In Zoologisches Institut (Zürich, Universität Zürich), pp. 104.

Barone, M.V., and Courtneidge, S. (1995). Myc but not fos rescue of pdgf signalling block caused by kinase inactive src. Nature *378*, 509-512.

Bellosta, P., Hulf, T., Diop, S.B., Usseglio, F., Pradel, J., Aragnol, D., and Gallant, P. (2005). Myc interacts genetically with Tip48/Reptin and Tip49/Pontin to control growth and proliferation during Drosophila development. Proc Natl Acad Sci U S A *102*, 11799-11804.

Belotserkovskaya, R., Oh, S., Bondarenko, V.A., Orphanides, G., Studitsky, V.M., and Reinberg, D. (2003). FACT facilitates transcription-dependent nucleosome alteration. Science *301*, 1090-1093.

Beltran, S., Angulo, M., Pignatelli, M., Serras, F., and Corominas, M. (2007). Functional dissection of the ash2 and ash1 transcriptomes provides insights into the transcriptional basis of wing phenotypes and reveals conserved protein interactions. Genome Biol *8*, R67.

Benassayag, C., Montero, L., Colombie, N., Gallant, P., Cribbs, D., and Morello, D. (2005). Human c-Myc isoforms differentially regulate cell growth and apoptosis in Drosophila melanogaster. Mol Cell Biol *25*, 9897-9909.

Bernstein, E., Denli, A.M., and Hannon, G.J. (2001). The rest is silence. RNA *7*, 1509-1521.

Betz, J.L., Chang, M., Washburn, T.M., Porter, S.E., Mueller, C.L., and Jaehning, J.A. (2002). Phenotypic analysis of Paf1/RNA polymerase II complex mutations reveals connections to cell cycle regulation, protein synthesis, and lipid and nucleic acid metabolism. Mol Genet Genomics *268*, 272-285.

Blackwell, T.K., Huang, J., Ma, A., Kretzner, L., Alt, F.W., Eisenman, R.N., and Weintraub, H. (1993). Binding of myc proteins to canonical and noncanonical DNA sequences. Molecular & Cellular Biology *13*, 5216-5224.

Blackwood, E.M., and Eisenman, R.N. (1991). Max: a helix-loop-helix zipper protein that forms a sequence-specific DNA-binding complex with Myc. Science *251*, 1211-1217.

Boon, K., Caron, H.N., van Asperen, R., Valentijn, L., Hermus, M.C., van Sluis, P., Roobeek, I., Weis, I., Voute, P.A., Schwab, M.*, et al.* (2001). N-myc enhances the expression of a large set of genes functioning in ribosome biogenesis and protein synthesis. EMBO Journal *20*, 1383-1393.

Bortvin, A., and Winston, F. (1996). Evidence that Spt6p controls chromatin structure by a direct interaction with histones. Science *272*, 1473-1476.

Bouchard, C., Dittrich, O., Kiermaier, A., Dohmann, K., Menkel, A., Eilers, M., and Luscher, B. (2001). Regulation of cyclin D2 gene expression by the Myc/Max/Mad network: Myc-dependent TRRAP recruitment and histone acetylation at the cyclin D2 promoter. Genes Dev *15*, 2042-2047.

Braakhuis, B.J., Brakenhoff, R.H., and Leemans, C.R. (2005). Second field tumors: a new opportunity for cancer prevention? Oncologist *10*, 493-500.

Bray, S., Musisi, H., and Bienz, M. (2005). Bre1 is required for Notch signaling and histone modification. Dev Cell *8*, 279-286.

Bridges, C.B. (1935). Drosophila melanogaster: Legend for symbols, mutants, valuations. Drosophila Information Service *3*, 5-19.

Brower, C.S., Sato, S., Tomomori-Sato, C., Kamura, T., Pause, A., Stearman, R., Klausner, R.D., Malik, S., Lane, W.S., Sorokina, I.*, et al.* (2002). Mammalian mediator subunit mMED8 is an Elongin BC-interacting protein that can assemble with Cul2 and Rbx1 to reconstitute a ubiquitin ligase. Proc Natl Acad Sci U S A *99*, 10353-10358.

Camps, J., Armengol, G., del Rey, J., Lozano, J.J., Vauhkonen, H., Prat, E., Egozcue, J., Sumoy, L., Knuutila, S., and Miro, R. (2006). Genome-wide differences between microsatellite stable and unstable colorectal tumors. Carcinogenesis *27*, 419-428.

Carpten, J.D., Robbins, C.M., Villablanca, A., Forsberg, L., Presciuttini, S., Bailey-Wilson, J., Simonds, W.F., Gillanders, E.M., Kennedy, A.M., Chen, J.D.*, et al.* (2002). HRPT2, encoding parafibromin, is mutated in hyperparathyroidism-jaw tumor syndrome. Nat Genet *32*, 676-680.

Chang, T.-C., Yu, D., Lee, Y.-S., Wentzel, E.A., Arking, D.E., West, K.M., Dang, C.V., Thomas-Tikhonenko, A., and Mendell, J.T. (2008). Widespread microRNA repression by Myc contributes to tumorigenesis. Nat Genet *40*, 43-50.

Chaudhary, K., Deb, S., Moniaux, N., Ponnusamy, M.P., and Batra, S.K. (2007). Human RNA polymerase II-associated factor complex: dysregulation in cancer. Oncogene *Advance Online Publication*, doi:10.1038/sj.onc.1210582.

Cheng, J.Q., Ruggeri, B., Klein, W.M., Sonoda, G., Altomare, D.A., Watson, D.K., and Testa, J.R. (1996). Amplification of AKT2 in human pancreatic cells and inhibition of AKT2 expression and tumorigenicity by antisense RNA. Proc Natl Acad Sci U S A *93*, 3636-3641.

Cheng, S.W., Davies, K.P., Yung, E., Beltran, R.J., Yu, J., and Kalpana, G.V. (1999). c-MYC interacts with INI1/hSNF5 and requires the SWI/SNF complex for transactivation function. Nature Genetics *22*, 102-105.

Chi, Y., Huddleston, M.J., Zhang, X., Young, R.A., Annan, R.S., Carr, S.A., and Deshaies, R.J. (2001). Negative regulation of Gcn4 and Msn2 transcription factors by Srb10 cyclin-dependent kinase. Genes Dev *15*, 1078-1092.

Chin, L., Schreiber-Agus, N., Pellicer, I., Chen, K., Lee, H.W., Dudast, M., Cordon-Cardo, C., and DePinho, R.A. (1995). Contrasting roles for Myc and Mad proteins in cellular growth and differentiation. Proceedings of the National Academy of Sciences of the United States of America *92*, 8488-8492.

Cho, Y., Griswold, A., Campbell, C., and Min, K.T. (2005). Individual histone deacetylases in Drosophila modulate transcription of distinct genes. Genomics *86*, 606-617.

Ciechanover, A. (1998). The ubiquitin-proteasome pathway: on protein death and cell life. EMBO J *17*, 7151-7160.

Cowling, V.H., and Cole, M.D. (2006). Mechanism of transcriptional activation by the Myc oncoproteins. Seminars in Cancer Biology *16*, 242.

Dang, C.V., O'Donnell, K.A., Zeller, K.I., Nguyen, T., Osthus, R.C., and Li, F. (2006). The c-Myc target gene network. Seminars in Cancer Biology *16*, 253.

Davis, A.C., Wims, M., Spotts, G.D., Hann, S.R., and Bradley, A. (1993). A null c-myc mutation causes lethality before 10.5 days of gestation in homozygotes and reduced fertility in heterozygous female mice. Genes & Development *7*, 671-682.

De La Cova, C., Abril, M., Bellosta, P., Gallant, P., and Johnston, L.A. (2004). Drosophila myc regulates organ size by inducing cell competition. Cell *117*, 107-116.

Dezfouli, S., Bakke, A., Huang, J., Wynshaw-Boris, A., and Hurlin, P.J. (2006). Inflammatory Disease and Lymphomagenesis Caused by Deletion of the Myc Antagonist Mnt in T Cells. Mol Cell Biol *26*, 2080-2092.

Dominguez-Sola, D., Ying, C.Y., Grandori, C., Ruggiero, L., Chen, B., Li, M., Galloway, D.A., Gu, W., Gautier, J., and Dalla-Favera, R. (2007). Non-transcriptional control of DNA replication by c-Myc. Nature *448*, 445-451.

Dover, J., Schneider, J., Tawiah-Boateng, M.A., Wood, A., Dean, K., Johnston, M., and Shilatifard, A. (2002). Methylation of histone H3 by COMPASS requires ubiquitination of histone H2B by Rad6. J Biol Chem *277*, 28368-28371.

Dugan, K.A., Wood, M.A., and Cole, M.D. (2002). TIP49, but not TRRAP, modulates c-Myc and E2F1 dependent apoptosis. Oncogene *21*, 5835-5843.

Eberhardy, S.R., and Farnham, P.J. (2001). c-Myc mediates activation of the cad promoter via a post-RNA polymerase II recruitment mechanism. J Biol Chem *276*, 48562-48571.

Eberhardy, S.R., and Farnham, P.J. (2002). Myc recruits P-TEFb to mediate the final step in the transcriptional activation of the cad promoter. J Biol Chem *277*, 40156-40162.

Eilers, M., Picard, D., Yamamoto, K.R., and Bishop, J.M. (1989). Chimaeras of myc oncoprotein and steroid receptors cause hormone-dependent transformation of cells. Nature *340*, 66-68.

Etard, C., Gradl, D., Kunz, M., Eilers, M., and Wedlich, D. (2005). Pontin and Reptin regulate cell proliferation in early Xenopus embryos in collaboration with c-Myc and Miz-1. Mech Dev *122*, 545-556.

Evan, G.I., Wyllie, A.H., Gilbert, C.S., Littlewood, T.D., Land, H., Brooks, M., Waters, C.M., Penn, L.Z., and Hancock, D.C. (1992). Induction of apoptosis in fibroblasts by c-myc protein. Cell *69*, 119-128.

Ezhkova, E., and Tansey, W.P. (2004). Proteasomal ATPases link ubiquitylation of histone H2B to methylation of histone H3. Mol Cell *13*, 435-442.

Fernandez, P.C., Frank, S.R., Wang, L., Schroeder, M., Liu, S., Greene, J., Cocito, A., and Amati, B. (2003). Genomic targets of the human c-Myc protein. Genes Dev *17*, 1115-1129.

Fire, A., Xu, S., Montgomery, M.K., Kostas, S.A., Driver, S.E., and Mello, C.C. (1998). Potent and specific genetic interference by double-stranded RNA in Caenorhabditis elegans. Nature *391*, 806-811.

Frank, S.R., Parisi, T., Taubert, S., Fernandez, P., Fuchs, M., Chan, H.M., Livingston, D.M., and Amati, B. (2003). MYC recruits the TIP60 histone acetyltransferase complex to chromatin. EMBO Rep *4*, 575-580.

Freiman, R.N., and Herr, W. (1997). Viral mimicry: common mode of association with HCF by VP16 and the cellular protein LZIP. Genes Dev *11*, 3122-3127.

Freytag, S.O. (1988). Enforced expression of the c-myc oncogene inhibits cell differentiation by precluding entry into a distinct predifferentiation state in G0/G1. Molecular & Cellular Biology *8*, 1614-1624.

Fuchs, M., Gerber, J., Drapkin, R., Sif, S., Ikura, T., Ogryzko, V., Lane, W.S., Nakatani, Y., and Livingston, D.M. (2001). The p400 complex is an essential E1A transformation target. Cell *106*, 297-307.

Gallant, P. (2006). Myc / Max / Mad in invertebrates - the evolution of the Max network CTMI *302*, 237-254.

Gallant, P., Shiio, Y., Cheng, P.F., Parkhurst, S.M., and Eisenman, R.N. (1996). Myc and Max homologs in Drosophila. Science *274*, 1523-1527.

Glickman, M.H., Rubin, D.M., Coux, O., Wefes, I., Pfeifer, G., Cjeka, Z., Baumeister, W., Fried, V.A., and Finley, D. (1998). A subcomplex of the proteasome regulatory particle required for ubiquitin-conjugate degradation and related to the COP9-signalosome and eIF3. Cell *94*, 615-623.

Gomez-Roman, N., Grandori, C., Eisenman, R.N., and White, R.J. (2003). Direct activation of RNA polymerase III transcription by c-Myc. Nature *421*, 290-294.

Gonzalez, F., Delahodde, A., Kodadek, T., and Johnston, S.A. (2002). Recruitment of a 19S proteasome subcomplex to an activated promoter. Science *296*, 548-550.

Grandori, C., Cowley, S.M., James, L.P., and Eisenman, R.N. (2000). The Myc/Max/Mad network and the transcriptional control of cell behavior. Annu Rev Cell Dev Biol *16*, 653-699.

Grandori, C., Gomez-Roman, N., Felton-Edkins, Z.A., Ngouenet, C., Galloway, D.A., Eisenman, R.N., and White, R.J. (2005). c-Myc binds to human ribosomal DNA and stimulates transcription of rRNA genes by RNA polymerase I. Nat Cell Biol *7*, 311-318.

Grandori, C., Mac, J., Siebelt, F., Ayer, D.E., and Eisenman, R.N. (1996). Myc-Max heterodimers activate a DEAD box gene and interact with multiple E box-related sites in vivo. Embo J *15*, 4344-4357.

Grant, P.A., Duggan, L., Cote, J., Roberts, S.M., Brownell, J.E., Candau, R., Ohba, R., Owen-Hughes, T., Allis, C.D., Winston, F.*, et al.* (1997). Yeast Gcn5 functions in two multisubunit complexes to acetylate nucleosomal histones: characterization of an Ada complex and the SAGA (Spt/Ada) complex. Genes Dev *11*, 1640-1650.

Grant, P.A., Schieltz, D., Pray-Grant, M.G., Yates, J.R., and Workman, J.L. (1998). The ATM-Related Cofactor Tra1 Is a Component of the Purified SAGA Complex. Molecular Cell *2*, 863-867.

Gregory, M.A., and Hann, S.R. (2000). c-Myc Proteolysis by the Ubiquitin-Proteasome Pathway: Stabilization of c-Myc in Burkitt's Lymphoma Cells. Mol Cell Biol *20*, 2423-2435.

Grewal, S.S., Li, L., Orian, A., Eisenman, R.N., and Edgar, B.A. (2005). Myc-dependent regulation of ribosomal RNA synthesis during Drosophila development. Nat Cell Biol *7*, 295-302.

Guccione, E., Martinato, F., Finocchiaro, G., Luzi, L., Tizzoni, L., Dall' Olio, V., Zardo, G., Nervi, C., Bernard, L., and Amati, B. (2006). Myc-binding-site recognition in the human genome is determined by chromatin context. Nat Cell Biol *8*, 764-770.

Guelman, S., Suganuma, T., Florens, L., Swanson, S.K., Kiesecker, C.L., Kusch, T., Anderson, S., Yates, J.R., III, Washburn, M.P., Abmayr, S.M.*, et al.* (2006). Host Cell Factor and an Uncharacterized SANT Domain Protein Are Stable Components of ATAC, a Novel dAda2A/dGcn5-Containing Histone Acetyltransferase Complex in Drosophila. Mol Cell Biol *26*, 871-882.

Gunther, M., Laithier, M., and Brison, O. (2000). A set of proteins interacting with transcription factor Sp1 identified in a two-hybrid screening. Mol Cell Biochem *210*, 131-142.

Guo, S., and Kemphues, K.J. (1995). par-1, a gene required for establishing polarity in C. elegans embryos, encodes a putative Ser/Thr kinase that is asymmetrically distributed. Cell *81*, 611-620.

Hartzog, G.A., Wada, T., Handa, H., and Winston, F. (1998). Evidence that Spt4, Spt5, and Spt6 control transcription elongation by RNA polymerase II in Saccharomyces cerevisiae. Genes Dev *12*, 357-369.

Hassig, C.A., Fleischer, T.C., Billin, A.N., Schreiber, S.L., and Ayer, D.E. (1997). Histone Deacetylase Activity Is Required for Full Transcriptional Repression by mSin3A. Cell *89*, 341-347.

Hatton, K.S., Mahon, K., Chin, L., Chiu, F.C., Lee, H.W., Peng, D.M., Morgenbesser, S.D., Horner, J., and Depinho, R.A. (1996). Expression and activity of l-myc in normal mouse development. Molecular & Cellular Biology *16*, 1794-1804.

Henriksson, M., and Luscher, B. (1996). Proteins of the Myc network: essential regulators of cell growth and differentiation. [Review] [267 refs]. Adv Cancer Res *68*, 109-182.

Henry, K.W., Wyce, A., Lo, W.S., Duggan, L.J., Emre, N.C., Kao, C.F., Pillus, L., Shilatifard, A., Osley, M.A., and Berger, S.L. (2003). Transcriptional activation via sequential histone H2B ubiquitylation and deubiquitylation, mediated by SAGA-associated Ubp8. Genes Dev *17*, 2648-2663.

Hollis, G.F., Mitchell, K.F., Battey, J., Potter, H., Taub, R., Lenoir, G.M., and Leder, P. (1984). A variant translocation places the [lambda] immunoglobulin genes 3[prime] to the c-myc oncogene in Burkitt's lymphoma. Nature *307*, 752-755.

Holzl, H., Kapelari, B., Kellermann, J., Seemuller, E., Sumegi, M., Udvardy, A., Medalia, O., Sperling, J., Muller, S.A., Engel, A.*, et al.* (2000). The Regulatory Complex of Drosophila melanogaster 26S Proteasomes: Subunit Composition and Localization of a Deubiquitylating Enzyme. J Cell Biol *150*, 119-130.

Hulf, T. (2004). dMyc and the Control of Gene Expression. In Zoologisches Institut (Zürich, Universität Zürich), pp. 140.

Hulf, T., Bellosta, P., Furrer, M., Steiger, D., Svensson, D., Barbour, A., and Gallant, P. (2005). Whole-genome analysis reveals a strong positional bias of conserved dMyc-dependent E-boxes. Mol Cell Biol *25*, 3401-3410.

Hurlin, P.J., and Huang, J. (2006). The MAX-interacting transcription factor network. Seminars in Cancer Biology *16*, 265.

Hurlin, P.J., Queva, C., and Eisenman, R.N. (1997). Mnt, a novel Max-interacting protein is coexpressed with Myc in proliferating cells and mediates repression at Myc binding sites. Genes & Development *11*, 44-58.

Hurlin, P.J., Queva, C., Koskinen, P.J., Steingrimsson, E., Ayer, D.E., Copeland, N.G., Jenkins, N.A., and Eisenman, R.N. (1995). Mad3 and Mad4: novel Max-interacting transcriptional repressors that

suppress c-myc dependent transformation and are expressed during neural and epidermal differentiation. EMBO Journal *14*, 5646-5659.

Hurlin, P.J., Steingrimsson, E., Copeland, N.G., Jenkins, N.A., and Eisenman, R.N. (1999). Mga, a dual-specificity transcription factor that interacts with Max and contains a T-domain DNA-binding motif. Embo J *18*, 7019-7028.

Hurlin, P.J., Zhou, Z.Q., Toyo-oka, K., Ota, S., Walker, W.L., Hirotsune, S., and Wynshaw-Boris, A. (2003). Deletion of Mnt leads to disrupted cell cycle control and tumorigenesis. Embo J *22*, 4584-4596. Iritani, B.M., and Eisenman, R.N. (1999). c-Myc enhances protein synthesis and cell size during B lymphocyte development. Proceedings of the National Academy of Sciences of the United States of America *96*, 13180-13185.

Johnston, L.A., Prober, D.A., Edgar, B.A., Eisenman, R.N., and Gallant, P. (1999). Drosophila myc regulates cellular growth during development. Cell *98*, 779-790.

Julien, E., and Herr, W. (2003). Proteolytic processing is necessary to separate and ensure proper cell growth and cytokinesis functions of HCF-1. Embo J *22*, 2360-2369.

Kanazawa, S., Soucek, L., Evan, G., Okamoto, T., and Peterlin, B.M. (2003). c-Myc recruits P-TEFb for transcription, cellular proliferation and apoptosis. Oncogene *22*, 5707-5711.

Kaplan, C.D., Laprade, L., and Winston, F. (2003). Transcription elongation factors repress transcription initiation from cryptic sites. Science *301*, 1096-1099.

Karn, J., Watson, J.V., Lowe, A.D., Green, S.M., and Vedeckis, W. (1989). Regulation of cell cycle duration by c-myc levels. Oncogene *4*, 773-787.

Kato, G.J., Barrett, J., Villa, G.M., and Dang, C.V. (1990). An amino-terminal c-myc domain required for neoplastic transformation activates transcription. Molecular & Cellular Biology *10*, 5914-5920.

Kato, G.J., Lee, W.M., Chen, L.L., and Dang, C.V. (1992). Max: functional domains and interaction with c-Myc. Genes Dev *6*, 81-92.

Kelly, K., Cochran, B.H., Stiles, C.D., and Leder, P. (1983). Cell-specific regulation of the c-myc gene by lymphocyte mitogens and platelet-derived growth factor. Cell *35*, 603-610.

Kim, S.Y., Herbst, A., Tworkowski, K.A., Salghetti, S.E., and Tansey, W.P. (2003). Skp2 regulates Myc protein stability and activity. Mol Cell *11*, 1177-1188.

Kim, Y.J., Bjorklund, S., Li, Y., Sayre, M.H., and Kornberg, R.D. (1994). A multiprotein mediator of transcriptional activation and its interaction with the C-terminal repeat domain of RNA polymerase II. Cell *77*, 599-608.

Kleine-Kohlbrecher, D., Adhikary, S., and Eilers, M. (2006). Mechanisms of transcriptional repression by Myc. Curr Top Microbiol Immunol *302*, 51-62.

Knez, J., Piluso, D., Bilan, P., and Capone, J.P. (2006). Host cell factor-1 and E2F4 interact via multiple determinants in each protein. Mol Cell Biochem *288*, 79-90.

Koch, C., Wollmann, P., Dahl, M., and Lottspeich, F. (1999). A role for Ctr9p and Paf1p in the regulation G1 cyclin expression in yeast. Nucleic Acids Res *27*, 2126-2134.

Kodadek, T., Sikder, D., and Nalley, K. (2006). Keeping Transcriptional Activators under Control. Cell *127*, 261.

Kohl, N.E., Kanda, N., Schreck, R.R., Bruns, G., Latt, S.A., Gilbert, F., and Alt, F.W. (1983). Transposition and amplification of oncogene-related sequences in human neuroblastomas. Cell *35*, 359-367.

Komarnitsky, P., Cho, E.J., and Buratowski, S. (2000). Different phosphorylated forms of RNA polymerase II and associated mRNA processing factors during transcription. Genes Dev *14*, 2452-2460.

Koskinen, P.J., Ayer, D.E., and Eisenman, R.N. (1995). Repression of Myc-Ras cotransformation by Mad is mediated by multiple protein-protein interactions. Cell Growth & Differentiation *6*, 623-629.

Kretzner, L., Blackwood, E.M., and Eisenman, R.N. (1992). Myc and Max proteins possess distinct transcriptional activities. Nature *359*, 426-429.

Kristie, T.M., and Sharp, P.A. (1990). Interactions of the Oct-1 POU subdomains with specific DNA sequences and with the HSV alpha-trans-activator protein. Genes Dev *4*, 2383-2396.

Krogan, N.J., Dover, J., Wood, A., Schneider, J., Heidt, J., Boateng, M.A., Dean, K., Ryan, O.W., Golshani, A., Johnston, M.*, et al.* (2003a). The Paf1 complex is required for histone H3 methylation by COMPASS and Dot1p: linking transcriptional elongation to histone methylation. Mol Cell *11*, 721-729.

Krogan, N.J., Kim, M., Ahn, S.H., Zhong, G., Kobor, M.S., Cagney, G., Emili, A., Shilatifard, A., Buratowski, S., and Greenblatt, J.F. (2002). RNA Polymerase II Elongation Factors of Saccharomyces cerevisiae: a Targeted Proteomics Approach. Mol Cell Biol *22*, 6979-6992.

Krogan, N.J., Kim, M., Tong, A., Golshani, A., Cagney, G., Canadien, V., Richards, D.P., Beattie, B.K., Emili, A., Boone, C.*, et al.* (2003b). Methylation of histone H3 by Set2 in Saccharomyces cerevisiae is linked to transcriptional elongation by RNA polymerase II. Mol Cell Biol *23*, 4207-4218.

Kurosu, T., and Peterlin, B.M. (2004). VP16 and ubiquitin; binding of P-TEFb via its activation domain and ubiquitin facilitates elongation of transcription of target genes. Curr Biol *14*, 1112-1116.

Lee, D., Ezhkova, E., Li, B., Pattenden, S.G., Tansey, W.P., and Workman, J.L. (2005). The proteasome regulatory particle alters the SAGA coactivator to enhance its interactions with transcriptional activators. Cell *123*, 423-436.

Leone, G., Degregori, J., Sears, R., Jakoi, L., and Nevins, J.R. (1997). Myc and ras collaborate in inducing accumulation of active cyclin e/cdk2 and e2f. Nature *387*, 422-426.

Leone, G., Sears, R., Huang, E., Rempel, R., Nuckolls, F., Park, C.H., Giangrande, P., Wu, L., Saavedra, H.I., Field, S.J.*, et al.* (2001). Myc requires distinct E2F activities to induce S phase and apoptosis. Mol Cell *8*, 105-113.

Liu, X., Tesfai, J., Evrard, Y.A., Dent, S.Y., and Martinez, E. (2003). c-Myc transformation domain recruits the human STAGA complex and requires TRRAP and GCN5 acetylase activity for transcription activation. J Biol Chem *278*, 20405-20412.

Loo, L.W., Secombe, J., Little, J.T., Carlos, L.S., Yost, C., Cheng, P.F., Flynn, E.M., Edgar, B.A., and Eisenman, R.N. (2005). The transcriptional repressor dMnt is a regulator of growth in Drosophila melanogaster. Mol Cell Biol *25*, 7078-7091.

Luscher, B., and Larsson, L.G. (1999). The basic region/helix-loop-helix/leucine zipper domain of Myc proto-oncoproteins: Function and regulation [Review]. Oncogene *18*, 2955-2966.

Mahajan, S.S., Johnson, K.M., and Wilson, A.C. (2003). Molecular cloning of Drosophila HCF reveals proteolytic processing and self-association of the encoded protein. J Cell Physiol *194*, 117-126.

Maines, J.Z., Stevens, L.M., Tong, X., and Stein, D. (2004). Drosophila dMyc is required for ovary cell growth and endoreplication. Development *131*, 775-786.

McMahon, S.B., Van, B.H., Dugan, K.A., Copeland, T.D., and Cole, M.D. (1998). The novel ATM-related protein TRRAP is an essential cofactor for the c-Myc and E2F oncoproteins. Cell *94*, 363-374.

McMahon, S.B., Wood, M.A., and Cole, M.D. (2000). The essential cofactor TRRAP recruits the histone acetyltransferase hGCN5 to c-Myc. Molecular & Cellular Biology *20*, 556-562.

Menssen, A., and Hermeking, H. (2002). Characterization of the c-MYC-regulated transcriptome by SAGE: identification and analysis of c-MYC target genes. Proc Natl Acad Sci U S A *99*, 6274-6279.

Meyer, N., Kim, S.S., and Penn, L.Z. (2006). The Oscar-worthy role of Myc in apoptosis. Seminars in Cancer Biology *16*, 275.

Moniaux, N., Nemos, C., Schmied, B.M., Chauhan, S.C., Deb, S., Morikane, K., Choudhury, A., Vanlith, M., Sutherlin, M., Sikela, J.M.*, et al.* (2006). The human homologue of the RNA polymerase II-associated factor 1 (hPaf1), localized on the 19q13 amplicon, is associated with tumorigenesis. Oncogene *25*, 3247-3257.

Montagne, J., Stewart, M.J., Stocker, H., Hafen, E., Kozma, S.C., and Thomas, G. (1999). Drosophila S6 kinase: A regulator of cell size. Science *285*, 2126-2129.

Montero, L., Muller, N., and Gallant, P. (2008). Induction of apoptosis by Drosophila Myc. Genesis *46*, 104-111.

Moreno, E., and Basler, K. (2004). dMyc transforms cells into super-competitors. Cell *117*, 117-129.

Mosimann, C. (2007). The Role of Parafibromin/Hyrax in Nuclear Wnt/Wg and Hedgehog Signal Transduction. In Institut für Molekularbiologie (Zürich, Universität Zürich).

Mosimann, C., Hausmann, G., and Basler, K. (2006). Parafibromin/Hyrax activates Wnt/Wg target gene transcription by direct association with beta-catenin/Armadillo. Cell *125*, 327-341.

Mueller, C.L., Porter, S.E., Hoffman, M.G., and Jaehning, J.A. (2004). The Paf1 complex has functions independent of actively transcribing RNA polymerase II. Mol Cell *14*, 447-456.

Muratani, M., Kung, C., Shokat, K.M., and Tansey, W.P. (2005). The F box protein Dsg1/Mdm30 is a transcriptional coactivator that stimulates Gal4 turnover and cotranscriptional mRNA processing. Cell *120*, 887-899.

Muratani, M., and Tansey, W.P. (2003). How the ubiquitin-proteasome system controls transcription. Nat Rev Mol Cell Biol *4*, 192-201.

Napoli, C., Lemieux, C., and Jorgensen, R. (1990). Introduction of a Chimeric Chalcone Synthase Gene into Petunia Results in Reversible Co-Suppression of Homologous Genes in trans. Plant Cell *2*, 279-289.

Narayanan, A., Ruyechan, W.T., and Kristie, T.M. (2007). The coactivator host cell factor-1 mediates Set1 and MLL1 H3K4 trimethylation at herpesvirus immediate early promoters for initiation of infection. Proc Natl Acad Sci U S A *104*, 10835-10840.

Nau, M.M., Brooks, B.J., Battey, J., Sausville, E., Gazdar, A.F., Kirsch, I.R., McBride, O.W., Bertness, V., Hollis, G.F., and Minna, J.D. (1985). L-myc, a new myc-related gene amplified and expressed in human small cell lung cancer. Nature *318*, 69-73.

Nesbit, C.E., Tersak, J.M., and Prochownik, E.V. (1999). MYC oncogenes and human neoplastic disease [Review]. Oncogene *18*, 3004-3016.

Neufeld, T.P., de la Cruz, A.F., Johnston, L.A., and Edgar, B.A. (1998). Coordination of growth and cell division in the Drosophila wing. Cell *93*, 1183-1193.

Ng, H.H., Robert, F., Young, R.A., and Struhl, K. (2003). Targeted recruitment of Set1 histone methylase by elongating Pol II provides a localized mark and memory of recent transcriptional activity. Mol Cell *11*, 709-719.

Nikiforov, M.A., Chandriani, S., O'Connell, B., Petrenko, O., Kotenko, I., Beavis, A., Sedivy, J.M., and Cole, M.D. (2002a). A functional screen for Myc-responsive genes reveals serine hydroxymethyltransferase, a major source of the one-carbon unit for cell metabolism. Mol Cell Biol *22*, 5793-5800.

Nikiforov, M.A., Chandriani, S., Park, J., Kotenko, I., Matheos, D., Johnsson, A., McMahon, S.B., and Cole, M.D. (2002b). TRRAP-dependent and TRRAP-independent transcriptional activation by Myc family oncoproteins. Mol Cell Biol *22*, 5054-5063.

Nilsson, J.A., and Cleveland, J.L. (2003). Myc pathways provoking cell suicide and cancer. Oncogene *22*, 9007-9021.

Nilsson, J.A., Maclean, K.H., Keller, U.B., Pendeville, H., Baudino, T.A., and Cleveland, J.L. (2004). Mnt loss triggers Myc transcription targets, proliferation, apoptosis, and transformation. Mol Cell Biol *24*, 1560-1569.

O'Connell, B.C., Cheung, A.F., Simkevich, C.P., Tam, W., Ren, X., Mateyak, M.K., and Sedivy, J.M. (2003). A large scale genetic analysis of c-Myc-regulated gene expression patterns. J Biol Chem *278*, 12563-12573.

O'Donnell, K.A., Wentzel, E.A., Zeller, K.I., Dang, C.V., and Mendell, J.T. (2005). c-Myc-regulated microRNAs modulate E2F1 expression. Nature *435*, 839-843.

Ogawa, H., Ishiguro, K., Gaubatz, S., Livingston, D.M., and Nakatani, Y. (2002). A complex with chromatin modifiers that occupies E2F- and Myc-responsive genes in G0 cells. Science *296*, 1132-1136.

Orian, A., Van Steensel, B., Delrow, J., Bussemaker, H.J., Li, L., Sawado, T., Williams, E., Loo, L.W., Cowley, S.M., Yost, C*., et al.* (2003). Genomic binding by the Drosophila Myc, Max, Mad/Mnt transcription factor network. Genes Dev *17*, 1101-1114.

Oster, S.K., Ho, C.S., Soucie, E.L., and Penn, L.Z. (2002). The myc oncogene: MarvelouslY Complex. Adv Cancer Res *84*, 81-154.

Papaioannou, V.E., and Silver, L.M. (1998). The T-box gene family. BioEssays *20*, 9-19.

Parada, L.A., Hallen, M., Tranberg, K.G., Hagerstrand, I., Bondeson, L., Mitelman, F., and Johansson, B. (1998). Frequent rearrangements of chromosomes 1, 7, and 8 in primary liver cancer. Genes Chromosomes Cancer *23*, 26-35.

Patel, J.H., Du, Y., Ard, P.G., Phillips, C., Carella, B., Chen, C.J., Rakowski, C., Chatterjee, C., Lieberman, P.M., Lane, W.S*., et al.* (2004). The c-MYC oncoprotein is a substrate of the acetyltransferases hGCN5/PCAF and TIP60. Mol Cell Biol *24*, 10826-10834.

Pavri, R., Zhu, B., Li, G., Trojer, P., Mandal, S., Shilatifard, A., and Reinberg, D. (2006). Histone H2B Monoubiquitination Functions Cooperatively with FACT to Regulate Elongation by RNA Polymerase II. Cell *125*, 703.

Penheiter, K.L., Washburn, T.M., Porter, S.E., Hoffman, M.G., and Jaehning, J.A. (2005). A posttranscriptional role for the yeast Paf1-RNA polymerase II complex is revealed by identification of primary targets. Mol Cell *20*, 213-223.

Pickart, C.M., and Cohen, R.E. (2004). Proteasomes and their kin: proteases in the machine age. Nat Rev Mol Cell Biol *5*, 177-187.

Pierce, S.B., Yost, C., Britton, J.S., Loo, L.W., Flynn, E.M., Edgar, B.A., and Eisenman, R.N. (2004). dMyc is required for larval growth and endoreplication in Drosophila. Development *131*, 2317-2327.

Piluso, D., Bilan, P., and Capone, J.P. (2002). Host Cell Factor-1 Interacts with and Antagonizes Transactivation by the Cell Cycle Regulatory Factor Miz-1. J Biol Chem %R 101074/jbcM206226200 *277*, 46799-46808.

Prendergast, G.C., Lawe, D., and Ziff, E.B. (1991). Association of Myn, the murine homolog of max, with c-Myc stimulates methylation-sensitive DNA binding and ras cotransformation. Cell *65*, 395-407.

Queva, C., Hurlin, P.J., Foley, K.P., and Eisenman, R.N. (1998). Sequential expression of the MAD family of transcriptional repressors during differentiation and development. Oncogene *16*, 967-977.

Rottmann, S., and Luscher, B. (2006). The Mad side of the Max network: antagonizing the function of Myc and more. Curr Top Microbiol Immunol *302*, 63-122.

Roussel, M.F., Cleveland, J.L., Shurtleff, S.A., and Sherr, C.J. (1991). Myc rescue of a mutant CSF-1 receptor impaired in mitogenic signalling. Nature *353*, 361-363.

Rozenblatt-Rosen, O., Hughes, C.M., Nannepaga, S.J., Shanmugam, K.S., Copeland, T.D., Guszczynski, T., Resau, J.H., and Meyerson, M. (2005). The Parafibromin Tumor Suppressor Protein Is Part of a Human Paf1 Complex. Mol Cell Biol *25*, 612-620.

Saunders, A., Werner, J., Andrulis, E.D., Nakayama, T., Hirose, S., Reinberg, D., and Lis, J.T. (2003). Tracking FACT and the RNA polymerase II elongation complex through chromatin in vivo. Science *301*, 1094-1096.

Sawai, S., Shimono, A., Hanaoka, K., and Kondoh, H. (1991). Embryonic lethality resulting from disruption of both N-myc alleles in mouse zygotes. New Biologist *3*, 861-869.

Sawai, S., Shimono, A., Wakamatsu, Y., Palmes, C., Hanaoka, K., and Kondoh, H. (1993). Defects of embryonic organogenesis resulting from targeted disruption of the N-myc gene in the mouse. Development *117*, 1445-1455.

Schreiber-Agus, N., Chin, L., Chen, K., Torres, R., Rao, G., Guida, P., Skoultchi, A.I., and DePinho, R.A. (1995). An amino-terminal domain of Mxi1 mediates anti-Myc oncogenic activity and interacts with a homolog of the yeast transcriptional repressor SIN3. Cell *80*, 777-786.

Schreiber-Agus, N., Stein, D., Chen, K., Goltz, J.S., Stevens, L., and DePinho, R.A. (1997). Drosophila Myc is oncogenic in mammalian cells and plays a role in the diminutive phenotype. Proc Natl Acad Sci U S A *94*, 1235-1240.

Schuhmacher, M., Staege, M.S., Pajic, A., Polack, A., Weidle, U.H., Bornkamm, G.W., Eick, D., and Kohlhuber, F. (1999). Control of cell growth by c-Myc in the absence of cell division. Current Biology *9*, 1255-1258.

Schwinkendorf, D. (2008). Mutational Identification of cis- and trans-acting Determinants of dMyc Protein Function. In Zoologisches Institut (Zürich, Universität Zürich), pp. 211.

Secombe, J., Li, L., Carlos, L., and Eisenman, R.N. (2007). The Trithorax group protein Lid is a trimethyl histone H3K4 demethylase required for dMyc-induced cell growth. Genes Dev *21*, 537-551.

Sheiness, D., Fanshier, L., and Bishop, J.M. (1978). Identification of nucleotide sequences which may encode the oncogenic capacity of avian retrovirus MC29. J Virol *28*, 600-610.

Sheldon, K.E., Mauger, D.M., and Arndt, K.M. (2005). A Requirement for the Saccharomyces cerevisiae Paf1 complex in snoRNA 3' end formation. Mol Cell *20*, 225-236.

Shen, X., Mizuguchi, G., Hamiche, A., and Wu, C. (2000). A chromatin remodelling complex involved in transcription and DNA processing. Nature *406*, 541-544.

Shibuya, H., Yoneyama, M., Ninomiya, T.J., Matsumoto, K., and Taniguchi, T. (1992). IL-2 and EGF receptors stimulate the hematopoietic cell cycle via different signaling pathways: demonstration of a novel role for c-myc. Cell *70*, 57-67.

Shilatifard, A. (2006). CHROMATIN MODIFICATIONS BY METHYLATION AND UBIQUITINATION: Implications in the Regulation of Gene Expression. Annual Review of Biochemistry *75*, 243-269.

Sierra, J., Yoshida, T., Joazeiro, C.A., and Jones, K.A. (2006). The APC tumor suppressor counteracts beta-catenin activation and H3K4 methylation at Wnt target genes. Genes Dev *20*, 586-600.

Simpson, P., and Morata, G. (1981). Differential mitotic rates and patterns of growth in compartments in the Drosophila wing. Dev Biol *85*, 299-308.

Sims, R.J., III, Belotserkovskaya, R., and Reinberg, D. (2004). Elongation by RNA polymerase II: the short and long of it. Genes Dev *18*, 2437-2468.

Smith, S.T., Petruk, S., Sedkov, Y., Cho, E., Tillib, S., Canaani, E., and Mazo, A. (2004). Modulation of heat shock gene expression by the TAC1 chromatin-modifying complex. Nat Cell Biol *6*, 162-167.

Sontheimer, E.J. (2005). Assembly and function of RNA silencing complexes. Nat Rev Mol Cell Biol *6*, 127-138.

Sorrentino, V., Drozdoff, V., McKinney, M.D., Zeitz, L., and Fleissner, E. (1986). Potentiation of growth factor activity by exogenous c-myc expression. Proceedings of the National Academy of Sciences of the United States of America *83*, 8167-8171.

Staller, P., Peukert, K., Kiermaier, A., Seoane, J., Lukas, J., Karsunky, H., Moroy, T., Bartek, J., Massague, J., Hanel, F.*, et al.* (2001). Repression of p15INK4b expression by Myc through association with Miz-1. Nat Cell Biol *3*, 392-399.

Stange, D.E., Radlwimmer, B., Schubert, F., Traub, F., Pich, A., Toedt, G., Mendrzyk, F., Lehmann, U., Eils, R., Kreipe, H.*, et al.* (2006). High-resolution genomic profiling reveals association of chromosomal aberrations on 1q and 16p with histologic and genetic subgroups of invasive breast cancer. Clin Cancer Res *12*, 345-352.

Steiger, D. (2007). Analysis of the Max Network in *Drosophila*. In Zoologisches Institut (Zürich, Universität Zürich), pp. 173.

Steiger, D., Furrer, M., Schwinkendorf, D., and Gallant, P. (2008). Max-independent functions of Myc in Drosophila melanogaster. Nat Genet *advanced online publication*.

Stern, D.F., Roberts, A.B., Roche, N.S., Sporn, M.B., and Weinberg, R.A. (1986). Differential responsiveness of myc- and ras-transfected cells to growth factors: selective stimulation of myc-transfected cells by epidermal growth factor. Mol Cell Biol *6*, 870-877.

Suganuma, T., Gutierrez, J.L., Li, B., Florens, L., Swanson, S.K., Washburn, M.P., Abmayr, S.M., and Workman, J.L. (2008). ATAC is a double histone acetyltransferase complex that stimulates nucleosome sliding. Nat Struct Mol Biol *15*, 364-372.

Tarkkanen, M., Larramendy, M.L., Bohling, T., Serra, M., Hattinger, C.M., Kivioja, A., Elomaa, I., Picci, P., and Knuutila, S. (2006). Malignant fibrous histiocytoma of bone: analysis of genomic imbalances by comparative genomic hybridisation and C-MYC expression by immunohistochemistry. Eur J Cancer *42*, 1172-1180.

Tenney, K., Gerber, M., Ilvarsonn, A., Schneider, J., Gause, M., Dorsett, D., Eissenberg, J.C., and Shilatifard, A. (2006). Drosophila Rtf1 functions in histone methylation, gene expression, and Notch signaling. Proc Natl Acad Sci U S A *103*, 11970-11974.

Thrower, J.S., Hoffman, L., Rechsteiner, M., and Pickart, C.M. (2000). Recognition of the polyubiquitin proteolytic signal. EMBO J *19*, 94-102.

Toyo-oka, K., Bowen, T.J., Hirotsune, S., Li, Z., Jain, S., Ota, S., Lozach, L.E., Bassett, I.G., Lozach, J., Rosenfeld, M.G.*, et al.* (2006). Mnt-Deficient Mammary Glands Exhibit Impaired Involution and Tumors with Characteristics of Myc Overexpression. Cancer Res *66*, 5565-5573.

Trumpp, A., Refaeli, Y., Oskarsson, T., Gasser, S., Murphy, M., Martin, G.R., and Bishop, J.M. (2001). c-Myc regulates mammalian body size by controlling cell number but not cell size. Nature *414*, 768-773.

Tyagi, S., Chabes, A.L., Wysocka, J., and Herr, W. (2007). E2F Activation of S Phase Promoters via Association with HCF-1 and the MLL Family of Histone H3K4 Methyltransferases. Molecular Cell *27*, 107.

Vennstrom, B., Sheiness, D., Zabielski, J., and Bishop, J.M. (1982). Isolation and characterization of c-myc, a cellular homolog of the oncogene (v-myc) of avian myelocytomatosis virus strain 29. J Virol *42*, 773-779.

Verma, R., Aravind, L., Oania, R., McDonald, W.H., Yates, J.R., 3rd, Koonin, E.V., and Deshaies, R.J. (2002). Role of Rpn11 metalloprotease in deubiquitination and degradation by the 26S proteasome. Science *298*, 611-615.

Vervoorts, J., Luscher-Firzlaff, J., and Luscher, B. (2006). The Ins and Outs of MYC Regulation by Posttranslational Mechanisms. J Biol Chem *281*, 34725-34729.

Vogel, J.L., and Kristie, T.M. (2000). The novel coactivator C1 (HCF) coordinates multiprotein enhancer formation and mediates transcription activation by GABP. EMBO J *19*, 683-690.

Voges, D., Zwickl, P., and Baumeister, W. (1999). The 26S proteasome: a molecular machine designed for controlled proteolysis. Annu Rev Biochem *68*, 1015-1068.

von der Lehr, N., Johansson, S., Wu, S., Bahram, F., Castell, A., Cetinkaya, C., Hydbring, P., Weidung, I., Nakayama, K., Nakayama, K.I.*, et al.* (2003). The F-box protein Skp2 participates in c-Myc proteosomal degradation and acts as a cofactor for c-Myc-regulated transcription. Mol Cell *11*, 1189-1200.

Walker, W., Zhou, Z.Q., Ota, S., Wynshaw-Boris, A., and Hurlin, P.J. (2005). Mnt-Max to Myc-Max complex switching regulates cell cycle entry. J Cell Biol *169*, 405-413.

Wang, P.F., Tan, M.H., Zhang, C., Morreau, H., and Teh, B.T. (2005). HRPT2, a tumor suppressor gene for hyperparathyroidism-jaw tumor syndrome. Horm Metab Res *37*, 380-383.

Wanzel, M., Herold, S., and Eilers, M. (2003). Transcriptional repression by Myc. Trends Cell Biol *13*, 146-150.

Weake, V.M., and Workman, J.L. (2008). Histone Ubiquitination: Triggering Gene Activity. Molecular Cell *29*, 653-663.

Wert, M., Kennedy, S., Palfrey, H.C., and Hay, N. (2001). Myc drives apoptosis in PC12 cells in the absence of Max. Oncogene *20*, 3746-3750.

Wilson, A.C., LaMarco, K., Peterson, M.G., and Herr, W. (1993). The VP16 accessory protein HCF is a family of polypeptides processed from a large precursor protein. Cell *74*, 115-125.

Wood, A., Schneider, J., Dover, J., Johnston, M., and Shilatifard, A. (2003). The Paf1 complex is essential for histone monoubiquitination by the Rad6-Bre1 complex, which signals for histone methylation by COMPASS and Dot1p. J Biol Chem *278*, 34739-34742.

Wood, A., Schneider, J., Dover, J., Johnston, M., and Shilatifard, A. (2005). The Bur1/Bur2 complex is required for histone H2B monoubiquitination by Rad6/Bre1 and histone methylation by COMPASS. Mol Cell *20*, 589-599.

Wood, M.A., McMahon, S.B., and Cole, M.D. (2000). An ATPase/helicase complex is an essential cofactor for oncogenic transformation by c-Myc. Mol Cell *5*, 321-330.

Woodard, G.E., Lin, L., Zhang, J.H., Agarwal, S.K., Marx, S.J., and Simonds, W.F. (2005). Parafibromin, product of the hyperparathyroidism-jaw tumor syndrome gene HRPT2, regulates cyclin D1/PRAD1 expression. Oncogene *24*, 1272-1276.

Wu, S., Cetinkaya, C., Munoz-Alonso, M.J., von der Lehr, N., Bahram, F., Beuger, V., Eilers, M., Leon, J., and Larsson, L.-G. (2003). Myc represses differentiation-induced p21CIP1 expression via Miz-1-dependent interaction with the p21 core promoter. Oncogene *22*, 351-360.

Wysocka, J., and Herr, W. (2003). The herpes simplex virus VP16-induced complex: the makings of a regulatory switch. Trends in Biochemical Sciences *28*, 294.

Wysocka, J., Myers, M.P., Laherty, C.D., Eisenman, R.N., and Herr, W. (2003). Human Sin3 deacetylase and trithorax-related Set1/Ash2 histone H3-K4 methyltransferase are tethered together selectively by the cell-proliferation factor HCF-1. Genes Dev *17*, 896-911.

Yart, A., Gstaiger, M., Wirbelauer, C., Pecnik, M., Anastasiou, D., Hess, D., and Krek, W. (2005). The HRPT2 tumor suppressor gene product parafibromin associates with human PAF1 and RNA polymerase II. Mol Cell Biol *25*, 5052-5060.

Yin, X.Y., Grove, L., and Prochownik, E.V. (1998). Lack of transcriptional repression by max homodimers. Oncogene *16*, 2629-2637.

Yokoyama, A., Wang, Z., Wysocka, J., Sanyal, M., Aufiero, D.J., Kitabayashi, I., Herr, W., and Cleary, M.L. (2004). Leukemia Proto-Oncoprotein MLL Forms a SET1-Like Histone Methyltransferase Complex with Menin To Regulate Hox Gene Expression. Mol Cell Biol *24*, 5639-5649.

Zeller, K.I., Jegga, A.G., Aronow, B.J., O'Donnell, K.A., and Dang, C.V. (2003). An integrated database of genes responsive to the Myc oncogenic transcription factor: identification of direct genomic targets. Genome Biol *4*, R69.

Zervos, A.S., Gyuris, J., and Brent, R. (1993). Mxi1, a protein that specifically interacts with Max to bind Myc-Max recognition sites [published erratum appears in Cell 1994 Oct 21;79(2):following 388]. Cell *72*, 223-232.

Zhang, C., Kong, D., Tan, M.H., Pappas, D.L., Jr., Wang, P.F., Chen, J., Farber, L., Zhang, N., Koo, H.M., Weinreich, M.*, et al.* (2006). Parafibromin inhibits cancer cell growth and causes G1 phase arrest. Biochem Biophys Res Commun *350*, 17-24.

Zhou, Z.Q., and Hurlin, P.J. (2001). The interplay between Mad and Myc in proliferation and differentiation. Trends Cell Biol *11*, S10-14.

Zhu, B., Mandal, S.S., Pham, A.D., Zheng, Y., Erdjument-Bromage, H., Batra, S.K., Tempst, P., and Reinberg, D. (2005). The human PAF complex coordinates transcription with events downstream of RNA synthesis. Genes Dev *19*, 1668-1673.

Zindy, F., Eischen, C.M., Randle, D.H., Kamijo, T., Cleveland, J.L., Sherr, C.J., and Roussel, M.F. (1998). Myc signaling via the ARF tumor suppressor regulates p53-dependent apoptosis and immortalization. Genes & Development *12*, 2424-2433.

Acknowledgements

First of all I want to thank Peter Gallant for his guidance, advice and support during the completion of this work. I would also like to thank the past and present Gallant lab members, who have become more than just colleagues, for always being supportive, for their assistance, and an excellent working athmosphere: Anja Egli, Toby Hulf, Changqing Li, Sonali Mohanty, Nadine Müller, René Oetterli, Regina Pérez, Daniela Schwinkendorf and Dominik Steiger. My very special thanks go to Mirjam Balbi, who conducted a large part of the HCF project included in this study for constantly exceeding my expectations.

For specific support I am very grateful to the following people who made everyday work a lot easier: Anni Strässle, Raymond Grunder, Matthias Bodmer and Martin Moser for sequencing and qRTPCR. In addition, I am indebted to George Hausmann, Christian Mosimann, Reto Städeli and Konrad Basler for generously providing me with fly stocks and other reagents used in this work and for their expertise. I would like to thank Peder Zipperlen for his help during the setup phase of the screen. For discussions and helpful suggestions I acknowledge the members of the Basler, Hafen and Hajnal labs.

Finally, I am extremely thankful for the support of my friends and family, who have always sustained me.

Curriculum vitae

Name	FURRER
Vorname	Michael
Geburtsdatum	27.05.1976
Heimatort	Unterbäch VS

Ausbildung

Maturität Typus C Kantonschule Oerlikon	01/1996
Universität Zürich, Biologie	10/1996–04/2002
Grundstudium Biologie	10/1996–07/1998
Fachstudium Zoologie	10/1998–02/2002
Nebenfachstudium	Molekularbiologie
weiteres Nebenfach	Physikalische Chemie
Diplomarbeit	Maternal Product from the Gene *gomo*, an Inositol Hexakisphosphate Kinase, is Required for the First Mitotic Divisions of *Drosophila* Embryogenesis.
Diplom in Zoologie	04/2002
Doktorat am Zoologischen Institut seit	01.06.2004